Molecular and Cellular Mechanisms of Inflammation- and Age-Related Modulation of Osteogenesis in Osteoporosis

Inaugural-Dissertation

zur Erlangung des Doktorgrades
der Mathematisch-Naturwissenschaftlichen Fakultät
der Heinrich-Heine-Universität Düsseldorf

vorgelegt von

Juliana Franziska Bousch
aus Düsseldorf

Düsseldorf, März 2025

aus der Klinik für Orthopädie und Unfallchirurgie
des Universitätsklinikums Düsseldorf
der Heinrich-Heine-Universität Düsseldorf

Gedruckt mit der Genehmigung der
Mathematisch-Naturwissenschaftlichen Fakultät der
Heinrich-Heine-Universität Düsseldorf

Berichterstatter:

1. Prof. Dr. rer. nat. Christoph Viktor Suschek
   Klinik für Orthopädie und Unfallchirurgie
   Universitätsklinikum Düsseldorf
   Medizinische Fakultät

2. Prof. Dr. rer. nat. Henrike Heise
   Institut für Physikalische Biologie
   Heinrich-Heine-Universität Düsseldorf
   Mathematisch-Naturwissenschaftliche Fakultät

Tag der mündlichen Prüfung:

Danksagung

Diese Arbeit wäre ohne die Unterstützung vieler Menschen nicht möglich gewesen und dafür möchte ich mich herzlich bedanken.

Mein besonderer Dank gilt **Prof. Christoph Suschek**, der mir mit seinen wertvollen Ideen, seiner stetigen Unterstützung und seiner entspannten Art stets zur Seite stand. Ebenso danke ich **Prof. Uwe Maus** für die regelmäßigen hilfreichen Rücksprachen und die Möglichkeit, meine Forschungsergebnisse auf Kongressen präsentieren zu dürfen. **Prof. Henrike Heise** danke ich dafür, dass sie sich dazu bereit erklärt hat, mich als Mentorin zu unterstützen. Außerdem bin ich **Prof. Joachim Windolf** dankbar, dass ich meine Doktorarbeit in der Klinik für Orthopädie und Unfallchirurgie durchführen konnte.

Mein Dank gilt auch meinen Co-Autoren **Dr. Christoph Beyersdorf** und **Dr. Katharina Schultz**, da sie wesentlich zu der Bereitstellung von Patientenmaterial beigetragen haben. Für ihre Unterstützung bei den elektronenmikroskopischen Aufnahmen und im Methodenteil danke ich außerdem **Dr. Ann-Kathrin Bergmann**.

Ein großes Dankeschön geht an die technischen Assistent*innen **Christa Wilkens**, **Jutta Schneider**, **Matthis Schnitker** und **Samira Seghrouchni**. Eure Hilfsbereitschaft und Unterstützung im Labor haben meine Arbeit sehr erleichtert und mir viel Spaß bereitet. Mein besonderer Dank gilt zudem den Studierenden, die mich in dieser Zeit begleitet haben – vor allem **Marina Kondritz**, deren positive Energie ansteckend war und **Greta Brede**, mit der ich viele wertvolle Gespräche geführt habe.

Mein tiefster Dank geht an meine Familie, die mich auf diesem Weg begleitet hat. Meinen Eltern **Martin** und **Birgit** sowie meiner Schwester **Katharina** bin ich sehr dankbar für ihre Unterstützung während meines gesamten Studiums. Zuletzt danke ich meiner Oma **Erika**, die immer an mich geglaubt hat.

Juliana Franziska Bousch, Düsseldorf, den 17.02.2025

Table of Contents

Zusammenfassung

Osteoporose ist eine weit verbreitete Knochenerkrankung, die durch ein Ungleichgewicht zwischen Knochenaufbau und Knochenabbau gekennzeichnet ist. Der daraus resultierende Verlust an Knochenmasse führt zu einer verminderten Knochendichte und einem erhöhten Frakturrisiko. Die Ursachen der Osteoporose sind vielfältig, aber sowohl bei der primären als auch bei der sekundären Form spielt die chronische Inflammation eine entscheidende Rolle. Der Einfluss proinflammatorischer Zytokine auf die knochenaufbauenden Osteoblasten ist jedoch umstritten. Bisherige Studien basieren überwiegend auf mesenchymalen Stammzellen, Tiermodellen oder Zelllinien, während Untersuchungen an primären humanen Osteoblasten (OBs) seltener sind. In dieser Arbeit wird erstmals beschrieben, wie proinflammatorische Zytokine die Differenzierung, Proliferation und metabolische Aktivität dieses klinisch relevanten Zellmodells beeinflussen.

Entgegen der weit verbreiteten Annahme, dass Entzündungen eine hemmende Wirkung auf den Knochenstoffwechsel haben, kann in dieser Studie gezeigt werden, dass proinflammatorische Zytokine die Osteogenese von OBs fördern. Die durch IL-1β und TNF-α gesteigerte Mineralisation korrelierte - im Gegensatz zu der Behandlung mit IL-6, IL-8 und IFNγ - mit einer erhöhten Proliferation und einem gesteigerten Energiemetabolismus. Die durch IL-1β induzierte Glykolyse sowie die durch TNF-α verstärkte oxidative Phosphorylierung könnten mögliche Erklärungen für die stärkere Mineralisation der OBs sein. Interessanterweise unterschieden sich die OBs von Osteoporosepatienten weder in ihrer Aktivität noch in ihrer Zytokinantwort signifikant von denen der Kontrollgruppe. Dies deutet darauf hin, dass Osteoporose weniger durch intrinsische Mechanismen der Osteoblasten als vielmehr durch eine veränderte Signaltransduktion im Knochengewebe gesteuert werden könnte. Darüber hinaus zeigten sich deutliche Unterschiede zwischen OBs und der Osteoblastenzelllinie hFOB 1.19, deren Mineralisation durch Zytokine stark inhibiert wurde. Trotz ihrer osteoblastenspezifischen Eigenschaften lassen diese Ergebnisse Zweifel an der Eignung diese Zelllinie als Modellsystem für Knochenstoffwechselerkrankungen aufkommen und unterstreichen zudem die hohe Relevanz von Untersuchungen an Primärzellen.

Die Ergebnisse stellen das bisherige Verständnis des Einflusses proinflammatorischer Zytokine auf den Knochenstoffwechsel in Frage und verdeutlichen die komplexen Wechselwirkungen zwischen Entzündung und Knochengesundheit. Zukünftige Studien sollten die zugrundeliegenden Signalwege der Zytokin-induzierten Mineralisation identifizieren und deren langfristige Auswirkungen auf die Knochenqualität untersuchen. Darüber hinaus ist es wichtig, die Interaktion zwischen Osteoblasten und anderen Knochenzellen unter entzündlichen Bedingungen genauer zu analysieren. Diese Studie zeigt dabei die Bedeutung der Verwendung klinisch relevanter Zellmodelle, wie den primären humanen Osteoblasten. Der nachgewiesene anabole Effekt auf die Knochensynthese eröffnet neue Perspektiven für die Behandlung entzündungs- und altersbedingter Knochenerkrankungen und könnte zur Entwicklung gezielter Therapien zur Modulation der Osteoblastenaktivität beitragen.

Summary

Osteoporosis is a prevalent bone disease characterized by an imbalance between bone formation and bone resorption. The resulting loss of bone mass leads to reduced bone density and an increased risk of fracture. The causes of osteoporosis are complex, but chronic inflammation plays a major role in both primary and secondary forms. However, the influence of proinflammatory cytokines on bone-forming osteoblasts is controversial. Previous studies have mainly been based on mesenchymal stem cells, animal models or cell lines, while studies on primary human osteoblasts (OBs) are limited. This study is the first to describe how proinflammatory cytokines influence the differentiation, proliferation, and metabolic activity of this clinically relevant cell model.

Contrary to the common understanding that inflammation has an inhibitory effect on bone metabolism, this study demonstrates that proinflammatory cytokine promote osteogenesis in OBs. Increased mineralization induced by IL-1β and TNFα correlated with increased proliferation and energy metabolism, in contrast to treatment with IL-6, IL-8, and IFNγ. Glycolysis induced by IL-1β and oxidative phosphorylation enhanced by TNF-α may explain the increased mineralization of OBs. Interestingly, OBs from osteoporotic patients did not differ significantly from those of the control group, either in their activity or in their cytokine response. This suggests that osteoporosis may be driven less by intrinsic osteoblast mechanisms and more by altered signaling in bone tissue. In addition, there were clear differences between OBs and the osteoblast cell line hFOB 1.19, whose mineralization was strongly inhibited by cytokines. Despite their osteoblast-specific properties, these results cast doubt on the suitability of this cell line as a model system for bone metabolic diseases and emphasize the high relevance of studies on primary cells.

The results in this study challenge the current understanding of the influence of proinflammatory cytokines on bone metabolism and highlight the complex interactions between inflammation and bone health. Future studies should identify the underlying pathways of cytokine-induced mineralization and investigate their long-term effects on bone quality. In addition, it is important to further analyze the

interaction between osteoblasts and other bone cells under inflammatory conditions. This study also demonstrates the importance of using clinically relevant cell models such as primary human osteoblasts. The anabolic effect of the cytokines on bone synthesis opens new perspectives for the treatment of inflammatory and age-related bone diseases and may contribute to the development of targeted therapies to modulate osteoblast activity.

List of Tables

List of Figures

Abbreviations

2-DG	deoxy-D-glucose
ALP	alkaline phosphatase
ATP	adenosine triphosphate
BMD	bone mineral density
BMMs	bone marrow macrophages
BMP	bone morphogenetic proteins
BrdU	bromodeoxyuridine
BSP	bone sialoprotein
C/EBPα	CCAAT/enhancer binding protein alpha
CD	cluster of differentiation
CMST	Seahorse XF Cell Mito Stress Test Kit
Col1	type I collagen
Col1α2	collagen type I α 2 chain
CPC	(1-hexadecyl)pyridinium chloride monohydrate
CRP	C-reactive protein
CSF-1	colony-stimulating factor 1
Ctrl	control
DMEM	Dulbecco's Modified Eagle Medium
DMSO	dimethyl sulfoxide
DXA	dual energy X-ray absorptiometry
ECAR	extracellular acidification rate
ECM	extracellular matrix
EZH2	enhancer of Zeste homology 2
$FADH_2$	flavin adenine dinucleotide
FBS	fetal bovine serum
FCCP	carbonyl cyanide-p-trifluoromethoxyphenyl-hydrazone
FGF	fibroblast growth factor
Fig.	figure
FRAX	Fracture Risk Assessment Tool
GAPDH	glyceraldehyde 3-phosphate dehydrogenase
GluT	glucose transporter

GM	growth medium
GST	Seahorse XF Glycolysis Stress Test Kit
GUSB	β-glucuronidase
hASCs	human adipose stem cells
hBMSCs	human bone marrow-derived mesenchymal stem cells
HEPES	4-(2-hydroxyethyl)-1-piperazineethanesulfonic acid
IFNγ	interferon-gamma
IGF-1	insulin-like growth factor 1
IL-1β	interleukin-1 beta
IL-6	interleukin-6
IL-8/CXCL8	interleukin-8/CXC motif chemokine ligand 8
LPS	lipopolysaccharide
MLBs	multilamellar bodies
MMPs	matrix metalloproteinases
mRNA	messenger ribonucleic acid
MSCs	mesenchymal stem cells
MTT	dimethylthiazolyl blue tetrazolium bromide
NAPH	nicotinamide adenine dinucleotide
ns	not significant
OA	osteoarthritis
OBs	primary human osteoblasts from patients with normal BMD
OCN	osteocalcin
OCR	oxygen consumption rate
OIM	osteogenesis induction medium
oOBs	primary human osteoblasts from osteoporotic patients
OPG	osteoprotegerin
OPN	osteopontin
OSX	osterix
OxPhos	oxidative phosphorylation
p38-MAPK	p38-mitogen-activated protein kinase
PBMCs	peripheral blood mononuclear cells
PBS	phosphate-buffered saline
PDH	pyruvate dehydrogenase

Pen/Strep	penicillin/streptomycin
PHA	phytohemagglutinin
p-p38-MAPK	phosphorylated p38-mitogen-activated protein kinase
PPARγ	peroxisome proliferator-activated receptor gamma
qPCR	quantitative polymerase chain reaction
RA	rheumatoid arthritis
RANKL	receptor activator of NF-κB ligand
ROS	reactive oxygen species
RPLP0	ribosomal protein lateral stalk subunit P0
RT	room temperature
Runx2	runt-related transcription factor 2
S1P	sphingosine 1 phosphate
SD	standard deviation
SEM	scanning electron microscopy
SEMA4D	semaphorin 4D
SOST	sclerostin
TBP	TATA-binding protein
TCA cycle	tricarboxylic acid cycle
TEM	transmission electron microscopy
TFRC	transferrin receptor 1
TGF-β	transforming growth factor beta
TGFβ-RII	transforming growth factor beta – receptor II
TNF-α	tumor necrosis factor-alpha
TRAP	tartrate-resistant acid phosphatase

1. Introduction

1.1. Osteoporosis

Osteoporosis is the most prevalent systemic bone disease defined by microarchitectural deterioration and porous bone tissue, resulting in decreased bone density (Fig. 1.1). This condition leads to increased bone fragility and significantly raises the risk of fractures, with the femoral neck and pertrochanteric region being most commonly affected (Bonjour et al., 1999; DVO Leitlinie Osteoporose, 2023; Riggs & Melton, 1995). In both men and women, advancing age leads to a natural loss of bone density. Additionally, bone resorption in women can significantly increase after the onset of menopause (B. L. Clarke & Khosla, 2010). In 2019, it was estimated that around 25.5 million women and 6.5 million men in Europe suffered from osteoporosis, with 4.3 million fractures occurring that year. Germany has the highest number of people suffering from osteoporosis, with a prevalence of 6.1% (Kanis et al., 2021). Osteoporosis is diagnosed based on bone mineral density (BMD) measured by dual-energy X-ray absorptiometry (DXA) in the femoral neck or spine. A T-score of over -1 is considered normal, between -1 and -2.5 as low (osteopenia), and below -2.5 as osteoporotic (Kanis et al., 2019).

There are two types of osteoporosis: primary and secondary. The primary type of osteoporosis include postmenopausal and senile osteoporosis, which are the most common causes (Dobbs et al., 1999). After the onset of menopause, the rate of bone turnover increases with enhanced bone formation by about 45%, while bone resorption increases by 90%, leading to an imbalance and loss of bone mass over time (Garnero et al., 1996). Senile osteoporosis is becoming increasingly common due to an aging society, and it has been shown that with age, mesenchymal stem cells (MSCs) lose the ability to differentiate into bone-building osteoblasts and are more likely to be directed towards adipogenesis (Infante & Rodríguez, 2018). Secondary osteoporosis is defined as a consequence of other diseases or the use of medications, such as glucocorticoids. The various diseases include endocrine disorders such as

primary hyperparathyroidism or diabetes mellitus type I, neuromuscular or gastrointestinal diseases, as well as chronic inflammatory diseases such as rheumatoid arthritis (Ganesan et al., 2024). A key factor in both primary and secondary osteoporosis is chronic inflammation, which is known to influence bone metabolism.

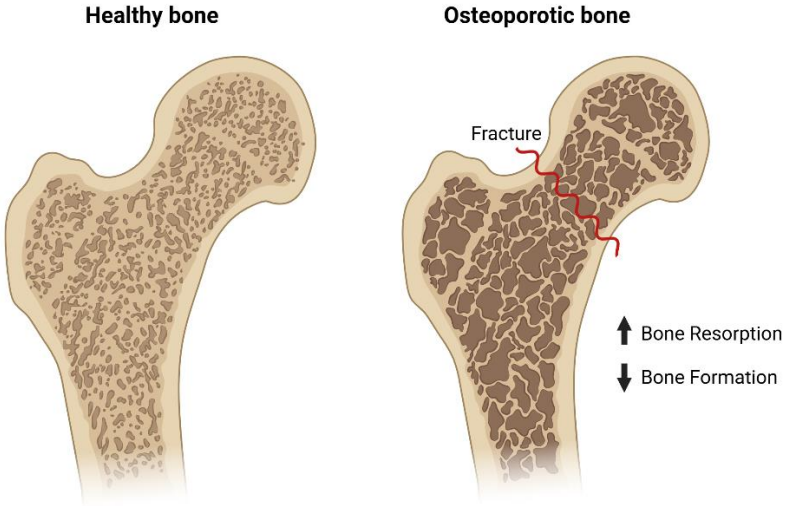

Figure 1.1: Healthy and porous osteoporotic bone structure. Created in BioRender. Bousch, J. (2025) https://BioRender.com/q13e074.

1.2. Bone - a metabolically active organ

1.2.1. Structure of Cortical and Cancellous Bone

Bone is a complex organ with multiple functions. In its function as the skeleton, the bone provides support for the body, protects the internal soft tissue structures from injury, and facilitates the transmission of movement signals from muscles. The bone plays a crucial role in maintaining mineral homeostasis, serves as a reservoir for growth factors and cytokines, and houses the bone marrow, which is the site of hematopoiesis. An analysis of the adult human skeleton reveals that about 80% of the bone is composed of cortical bone, the compact and dense external layer (B. Clarke, 2008). The cortical bone is traversed by blood vessels and is surrounded by the periosteum (Fig. 1.2, A), which plays an important role in fracture healing (Dwek, 2010). Most of the cortical bone mass is located in the shaft of the bone (diaphysis), which encloses the medullary cavity containing the bone marrow. The remaining 20% of the bone comprises cancellous or spongy bone, which is located at the

epiphysis and metaphysis and is surrounded by a thin layer of cortical bone (Syahrom et al., 2017). Cancellous bone is defined by its trabecular bone structure with pores filled with bone marrow and has a lower density than the cortical bone (Fig. 1.2, A, C). The bone matrix mainly consists of type 1 collagen fibers and other proteins such as osteocalcin and is mineralized by the incorporation of hydroxyapatite (Hadjidakis & Androulakis, 2006). The cancellous bone has a higher water and a lower calcium content due to less mineralized structures than the cortical bone (Oftadeh et al., 2015). The red bone marrow is composed of approximately 60% hematopoietic cells and 40% adipocytes. With age, the marrow transforms into 'fatty marrow' with about 95% adipocytes (Griffith, 2017).

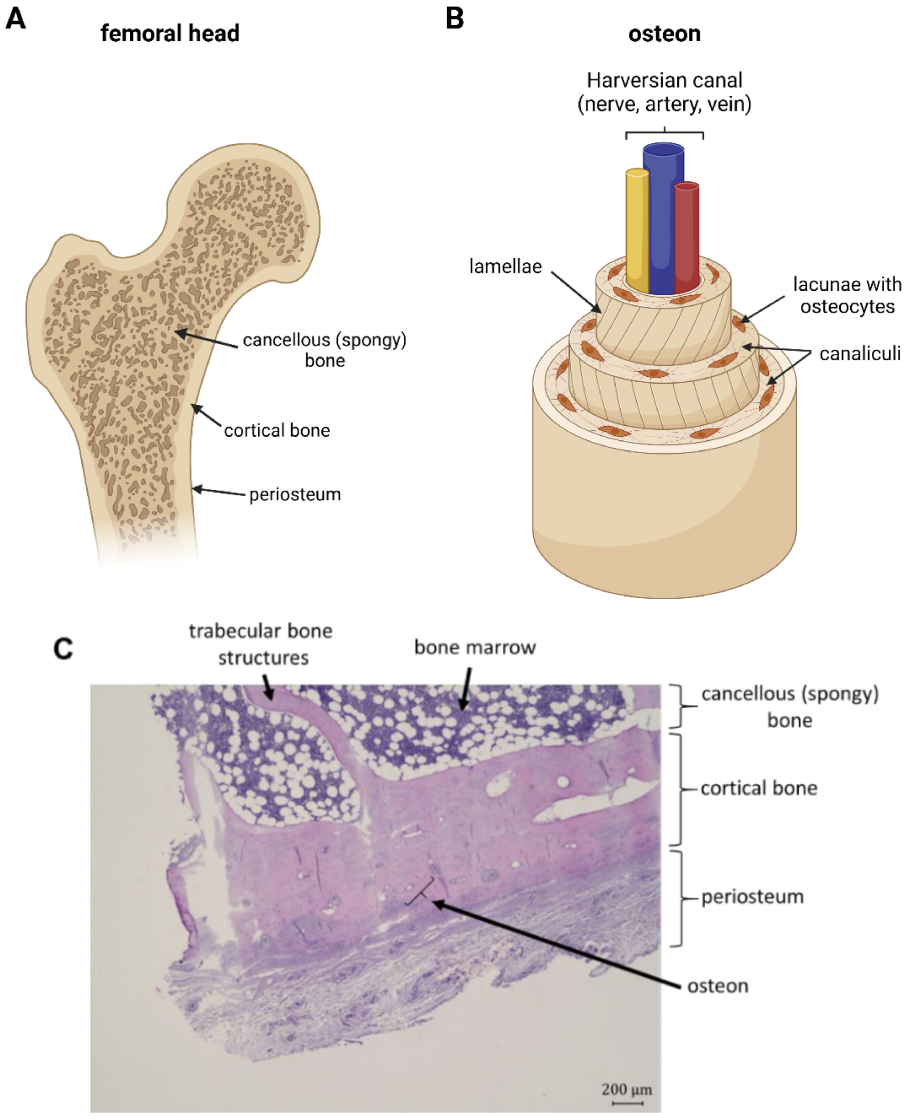

Figure 1.2: Internal bone structure of a human femoral head. (A) The macroscopic location of cortical and cancellous bone in a femoral head, (B) Structure of an osteon,

and (C) microscopic image of a tissue section showing the cortical and cancellous bone (scale: 100 µm). (A) and (B) were created in BioRender. Bousch, J. (2025) https://BioRender.com/r64r080.

The cortical bone is structured in osteons, which can be found as concentric lamellae arranged around a central canal (Fig. 1.2, C). An osteon represents a single functional unit of bone tissue (Baig & Bacha, 2024). The Haversian canal, located at the center of the osteon, houses nerves and blood vessels that provide the bone with essential nutrients and oxygen (Fig. 1.2, B). The lamellae are arranged concentrically around the canal, with osteocytes embedded in the lacunae, which are the spaces between the lamellae. Osteocytes represent the most abundant cell type in bone, with over 90% of the total cell population. Each osteocyte forms about 50–100 canaliculi, which are long dendrites that facilitate the formation of a network with other osteocytes and various cell types and tissues. In this network, the Harversian canals of the individual osteons are also connected via Volkmann's canals (B. Chang & Liu, 2022).

In contrast, the cancellous bone is not constructed with osteons, as the trabecular bone tissue is effectively integrated within the bone marrow through pores, which are perfused with blood, enabling the supply of nutrients and oxygen. A trabecula is comprised of a group of parallel-arranged mineralized collagen fibrils, with osteocytes embedded in their lacunae (Oftadeh et al., 2015). The trabeculae can exhibit diverse architectural arrangements, as they are oriented in the direction of mechanical forces, thereby ensuring the effective force distribution (Gibson, 1985). Cancellous bone also has the advantage of being rebuilt more rapidly than compact bone, enabling it to adapt to variable mechanical loads (Oftadeh et al., 2015). This process is referred to as ‚bone remodeling' and ensures that the bone adapts to given conditions and that old, micro-damaged bone is replaced by new bone tissue. Various bone cells are involved in this process, forming a basic multicellular unit and maintaining the equilibrium between bone resorption and bone formation in a complex system (Florencio-Silva et al., 2015).

1.2.2. The Process of Bone Remodeling

The continuous process of ‚bone remodeling' maintains the structure and stability of the skeleton by repairing microfractures and allowing the skeleton to adapt to changing external forces (Hadjidakis & Androulakis, 2006). The process can be divided into 4 phases: resorption, reversal, formation, and mineralization (Fig. 1.3).

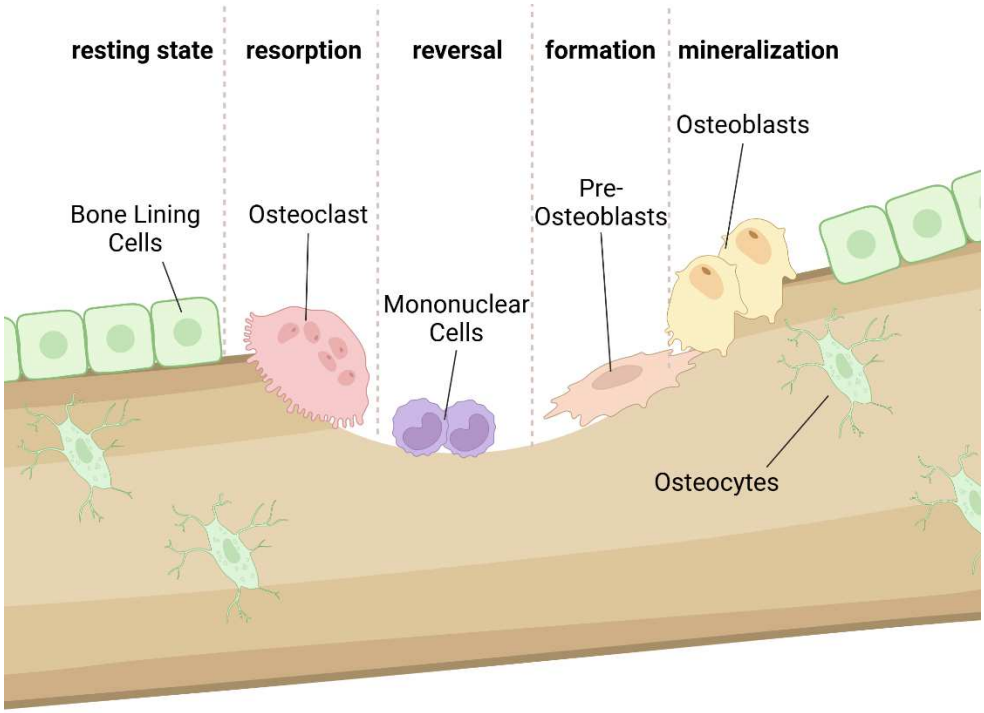

Figure 1.3: The phases of bone remodeling. Created in BioRender. Bousch, J. (2025) https://BioRender.com/d63p607

During the resting state, the bone matrix surface is covered by the so-called bone-lining cells, cells of the osteogenic lineage, which are in contact with the osteocytes embedded in the matrix. The resorption phase can be activated in different ways, for example, when the osteocytes perceive a difference in the physical force of the bone (Raggatt & Partridge, 2010). Mononuclear pre-osteoclasts migrate to the site and differentiate into mature, multinucleated osteoclasts. The osteoclasts secrete lysosomal enzymes on the matrix surface, such as tartrate-resistant acid phosphatase (TRAP) and cathepsin K, as well as hydrochloric acid to dissolve the collagen matrix with embedded hydroxyapatite crystals (Boyce et al., 2009; Hadjidakis & Androulakis, 2006).

Between bone resorption and formation, the reversal phase takes place, in which mononuclear cells migrate to the resorbed site. It is not yet fully known which cells are involved in this phase, but they are probably partly cells of mesenchymal origin and macrophages, such as osteomacs, which secrete matrix metalloproteinases (MMPs) and perform phagocytosis to remove the resorption debris (Delaisse, 2014; Raggatt & Partridge, 2010). The reversal cells prepare the resorbed bone site for the phase of new bone formation, for which osteoblast progenitor cells are recruited to the site. The progenitor cells differentiate into mature osteoblasts and secrete matrix proteins, primarily collagen type I, but also other proteins, including proteoglycans, alkaline phosphatase, and osteocalcin. The matrix is then mineralized by the deposition of hydroxyapatite crystals (Raggatt & Partridge, 2010). Once the mineralization process is over, mature osteoblasts undergo apoptosis, become bone-lining cells, or embed in the matrix by differentiating to osteocytes (Raggatt & Partridge, 2010). Overall, the process of bone remodeling in cancellous bone takes about 200 days, with the resorption and reversal phase lasting about 30-40 days and bone formation about 150 days (Eriksen, 2010; Hadjidakis & Androulakis, 2006).

1.2.3. Regulation of Bone Remodeling

The regulation of bone remodeling is largely based on the regulated cross-talk between the various involved bone cells (Fig. 1.4). The cells involved regulate each other through the secretion of various factors and also through direct contact with each other, the respective precursor cells, osteocytes in the matrix, and immune cells in the bone marrow. In the resting state, osteocytes secrete transforming growth factor β (TGF-β), which inhibits osteoclastogenesis. Damage to the matrix can induce apoptosis of osteocytes, which reduces the TGF-β concentration and can initiate resorption (Heino et al., 2002; Raggatt & Partridge, 2010). In addition, osteocytes secrete sclerostin (SOST), a negative regulator of bone formation that inhibits osteoblast differentiation by suppressing the Wnt signaling pathway (van Bezooijen et al., 2004).

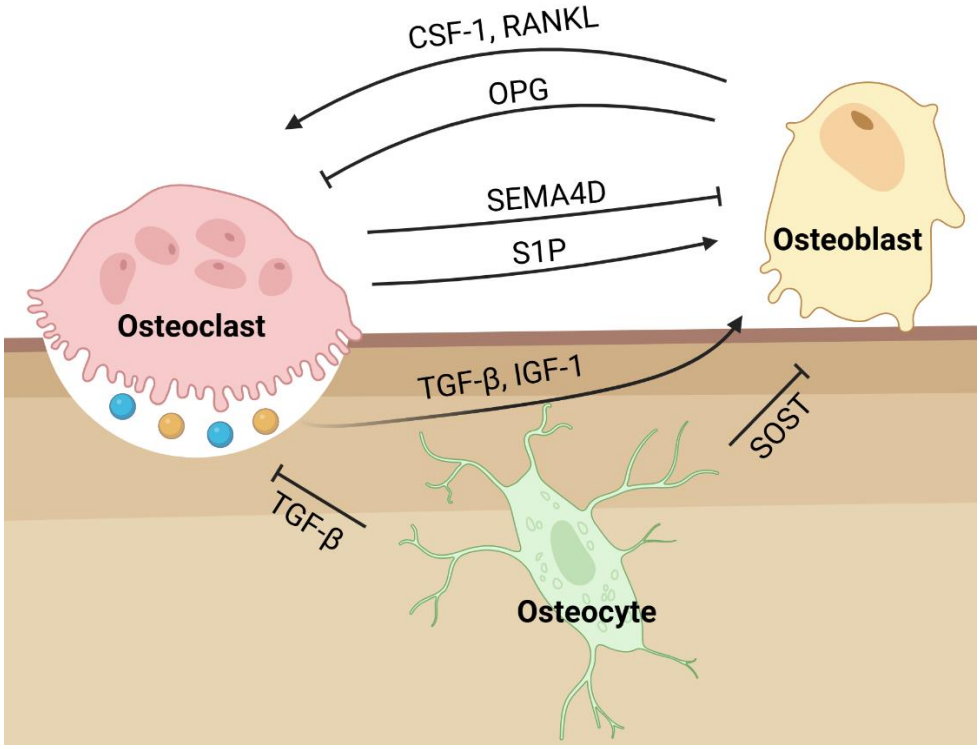

Figure 1.4: Communication between osteoclasts, osteoblasts, and osteocytes to maintain the balance between bone resorption and bone formation. CSF-1 (colony-stimulating factor 1), RANKL (receptor activator of NF-κB ligand), OPG (osteoprotegerin), SEMA4D (semaphorin 4D), S1P (sphingosine 1 phosphate), TGF-β (transforming growth factor β), IGF-1 (insulin-like growth factor 1), SOST (sclerostin). Simplified representation created in BioRender. Bousch, J. (2025) https://BioRender.com/k33x588.

Osteoclasts are in the myeloid lineage of hematopoietic cells and can differentiate *in vitro* from monocytes or macrophages into mature osteoclasts. This requires the addition of two cytokines that are essential for the activity of osteoclasts: colony-stimulating factor 1 (CSF-1) and receptor activator of NF-κB ligand (RANKL), both of which are expressed by cells of the osteoblast lineage (Raggatt & Partridge, 2010). The neutralizer of RANKL is osteoprotegerin (OPG), which acts as a decoy receptor and blocks RANKL (Yasuda et al., 1998). OPG is also secreted by osteoblasts, and the predominant RANKL/OPG ratio determines the influence on osteoclastogenesis. If more RANKL is active, osteoclastogenesis is stimulated; if more OPG is active, this stimulation is blocked (Hadjidakis & Androulakis, 2006).

RANKL stimulation of osteoclasts induces the expression of sphingosine kinase 1 (SPHK1), which leads to the phosphorylation of sphingosine to sphingosine 1 phosphate (S1P). S1P binds to receptors on the osteoblast surface and stimulates their migration and, in turn, their RANKL expression (Ryu et al., 2006). On the other hand, osteoclasts express semaphorin 4D (SEMA4D), which leads to an inhibition of osteoblast differentiation (Kim et al., 2020). During resorption of the bone matrix, TGF-β and insulin-like growth factor 1 (IGF-1) are released, which in turn activate the osteoblasts (Tang et al., 2009; Xian et al., 2012). These are just a few examples of how osteoblasts and osteoclasts influence each other. In direct cell contact, they also communicate via various membrane-bound mediators, for example via ephrin signaling, which can have an inhibitory or activating effect in both directions (Kim et al., 2020).

Immune cells in the bone marrow also play an important role in homeostasis, but the underlying mechanisms are not yet fully understood. It has been found that B cells secrete OPG, and it is assumed that T cells support them in this process. Megakaryocytes also express RANKL and OPG and increase the differentiation of osteoblasts, which influences both bone resorption and formation. It has been shown that without osteomacs, which presumably make up part of the reversal cells, osteogenic differentiation is inhibited *in vitro* (M. K. Chang et al., 2008).

The regulation of bone remodeling is a very complex system involving many different cells at various stages of differentiation. In physiologically healthy bone, these cells maintain the balance between bone resorption and bone formation. However, this can also be upset by disturbed signaling between the cells or by other signal transducers, such as cytokines in the case of inflammation. This can lead to various pathological conditions, such as the most prevalent metabolic bone disease, osteoporosis.

1.3. Osteogenesis

1.3.1. Osteogenic Differentiation Markers

Osteoblasts derive from pluripotent MSCs that have the potential to differentiate into adipocytes, chondrocytes, or osteogenic cells (Bianco et al., 2013). In the osteogenic lineage, they first differentiate into pre-osteoblasts, which secrete a collagen-based extracellular matrix (ECM) as they differentiate into mature osteoblasts. The ECM is mineralized by the mature osteoblasts through the deposition of hydroxyapatite. The osteoblasts then undergo apoptosis or further differentiate into bone lining cells or osteocytes (Fig. 1.5) (Amarasekara et al., 2021). Differentiation into osteoblasts, also named osteogenesis, is divided into an early and a late phase due to the differential expression of proteins and transcription factors that play different roles in ECM formation and subsequent mineralization. However, these phases are not strictly separated and many of the markers of osteogenic differentiation are expressed in both phases, albeit at different levels. Early markers include alkaline phosphatase (ALP), type I collagen (Col1), and bone sialoprotein (BSP), whereas osteopontin (OPN) and osteocalcin (OCN) are expressed in the later phase of osteogenesis (Huang et al., 2007). The best studied and earliest activated transcription factor that modulates osteoblast differentiation is runt-related transcription factor 2 (Runx2) (R. T. Franceschi et al., 2003). Runx2 is a regulator of another early marker, osterix (OSX); both are also essential for the later stages of differentiation (Huang et al., 2007; Nakashima et al., 2002). A number of signaling pathways are involved in osteogenesis, of which the Wnt, TGF-β, bone morphogenetic proteins (BMP), fibroblast growth factor (FGF), and Hedgehog signaling pathways are the best studied in this field (Zhu et al., 2024).

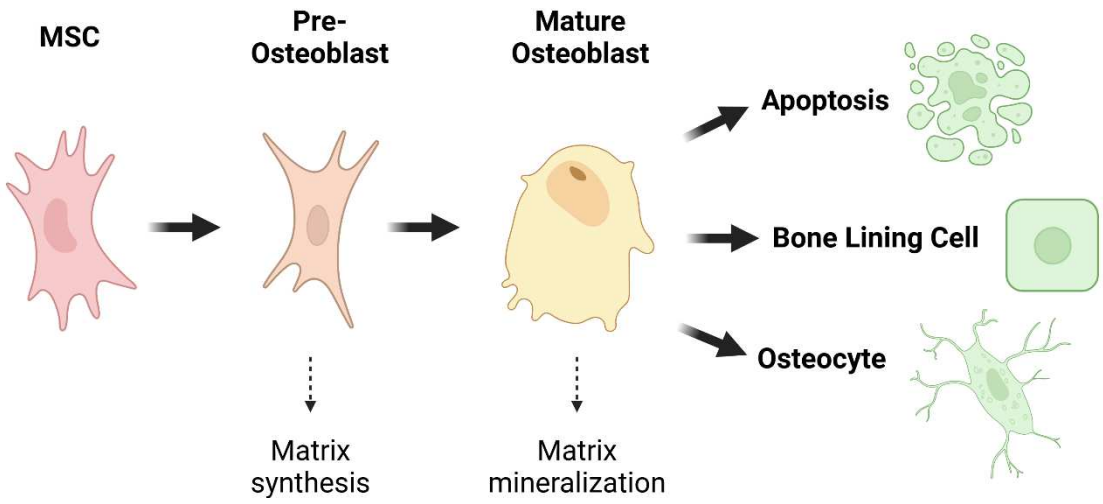

Figure 1.5: Osteogenic differentiation. MSC (mesenchymal stem cell). Image created in BioRender. Bousch, J. (2025) https://BioRender.com/n38v055

To differentiate MSCs into osteogenic lineage *in vitro*, three additives are needed: β-glycerophosphate and ascorbic acid, which are required for the production of a mineralized collagen matrix, and the synthetic glucocorticoid dexamethasone, which is thought to inhibit cell proliferation while inducing osteogenic differentiation (Jaiswal et al., 1997; Langenbach & Handschel, 2013). Ascorbic acid increases the production of Col1, which is essential for the formation of a collagen-based ECM (Langenbach & Handschel, 2013). The binding of cells to the ECM via integrins in turn triggers the activation of Runx2 via mitogen-activated protein kinase (MAPK) signaling, which leads to increased transcription of subsequent osteogenic differentiation markers such as OCN via a signaling cascade (Langenbach & Handschel, 2013; Xiao et al., 1998).

1.3.2. Energy Metabolism During Osteogenic Differentiation

During osteogenic differentiation, cells have an increased energy demand due to the need to produce and secrete large amounts of collagen, other matrix proteins and calcium phosphates (Motyl et al., 2017). To cope with this high energy requirement, cells utilize several metabolic pathways, which are directly interconnected and include glycolysis, tricarboxylic acid (TCA) cycle, and oxidative phosphorylation (OxPhos) (Fig. 1.6). Glucose is transported into the cell by membrane-bound glucose

transporters (GluTs) and converted to pyruvate in the process of glycolysis. Pyruvate is subsequently converted into Acetyl-CoA by pyruvate dehydrogenase (PDH). Acetyl-CoA enters the TCA cycle, generating nicotinamide adenine dinucleotide (NAPH) and flavin adenine dinucleotide ($FADH_2$), which are further processed in the electron transport chain (Esen & Long, 2014; Martínez-Reyes & Chandel, 2020). Energy is generated in the form of adenosine triphosphate (ATP) through glycolysis, the TCA cycle, and the electron transport chain, commonly referred to as OxPhos, producing the majority of ATP molecules. An unavoidable byproduct of OxPhos is the generation of reactive oxygen species (ROS) in the mitochondria, produced through electron transfer reactions (Nolfi-Donegan et al., 2020).

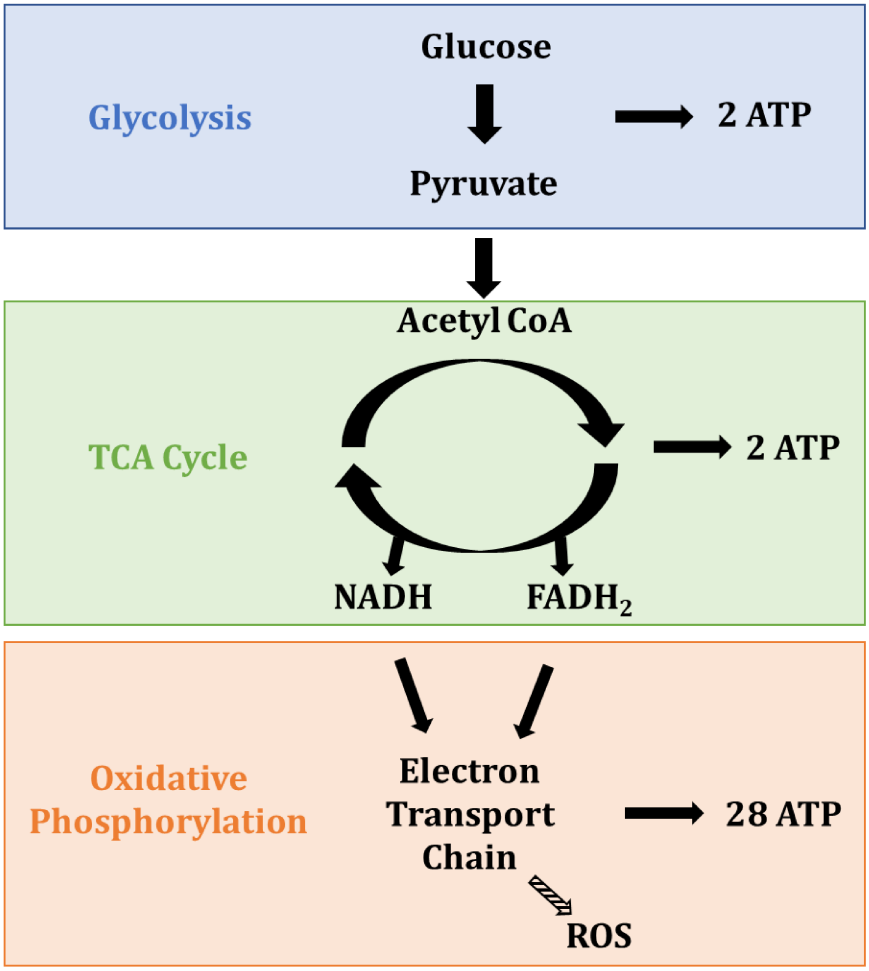

Figure 1.6: Overview of the interconnection and energy production of three main energy metabolic pathways glycolysis, TCA cycle, and oxidative phosphorylation.

ATP (adenosine triphosphate), TCA (tricarboxylic acid) cycle, NADH (nicotinamide adenine dinucleotide), $FADH_2$ (flavin adenine dinucleotide), ROS (reactive oxygen species).

Depending on the cell type and differentiation state studied, an increased rate of glycolysis or OxPhos was measured in differentiated osteoblasts. Osteogenic differentiation of human MSCs led to activation of OxPhos, while the cells rely on glycolysis during proliferation (Shum et al., 2016). Calvarial osteoblasts also activate OxPhos during osteogenesis (Guntur et al., 2014). In contrast, cells of the murine pre-osteoblast cell line MC3T3-E1 and 3T3-L1 adipocytes tend to favor glycolysis compared to undifferentiated cells (Guntur et al., 2018). Activation of the Wnt signaling pathway, one of the key signaling pathways in osteogenic differentiation, has also been shown to induce glycolysis (Esen et al., 2013; Vlashi et al., 2023). Among the glucose transporters GluT1, GluT3, and GluT4 expressed in osteoblasts, GluT4 in particular shows increased expression during osteogenesis (Z. Li et al., 2016). Another study found that silencing of GluT4 suppresses the proliferation and differentiation of pre-osteoblasts (Arponen et al., 2022). Regulation of the glucose metabolism is therefore a critical factor in osteogenesis. Changes in metabolic pathways not only control ATP production, but also gene expression, which in turn regulates the activation of different signaling pathways (Motyl et al., 2017).

1.4. Osteoimmunology – Impact of Cytokines on Bone Health

1.4.1. Association of Bone Loss and Inflammation

The field of osteoimmunology has emerged to investigate the interaction of the immune system and the bone metabolism with later focusing on the impact of inflammatory processes on bone health (Arron & Choi, 2000; Tsukasaki & Takayanagi, 2019). Bone cells have been shown to interact closely with immune cells, partly sharing the same stem cell origin and signaling pathways (Guder et al., 2020). Because of this close interaction, there are a number of chronic inflammatory and autoimmune diseases that lead to increased bone loss. The most common chronic autoimmune disease is rheumatoid arthritis (RA), which causes chronic inflammation of the synovial joints with cartilage damage and loss of bone mass

(Kareem et al., 2021). The risk of fracture is therefore increased in patients with RA (Fardellone et al., 2020). In addition to inflammation in patients with RA, one of the most common treatments is the administration of glucocorticoids, which also increase the risk of osteoporosis (Compston, 2018). Inflammation leads to the production of several cytokines, including tumor necrosis factor (TNF)-α, Interleukin (IL)-1β, and IL-6. TNF appears to be one of the key regulators, as studies have shown that TNF inhibitors reduce bone loss (Haugeberg et al., 2014). TNF-α also plays a critical role in postmenopausal osteoporosis, as it is increased by T cells in the bone marrow when estrogen levels are low (Roggia et al., 2001). Comparing cytokine secretion levels of peripheral blood mononuclear cells (PBMCs) from women with normal or low BMD, the low BMD patients had higher values of proinflammatory cytokines like TNF-α and IL-6 and lower levels of anti-inflammatory cytokines (Azizieh et al., 2017). Also after lipopolysaccharide (LPS) and phytohemagglutinin (PHA) activation of blood cells in cell culture, an enhanced immune response with increased secretion of IL-1β, IL-6, and TNF-α was measured in cells from osteoporosis patients compared to controls (Zheng et al., 1997). A biomarker of systemic inflammation is C-reactive protein (CRP), which is upregulated by IL-1β, IL-6, and TNF-α and high levels of CRP are associated with low bone density (Ginaldi et al., 2005). An increase in cytokines such as TNF-α or IL-6 is also associated with aging (Bruunsgaard, 2002). The chronic inflammation that occurs with age, also known as 'inflamm-aging', has been linked to the loss of bone density in old age (C. Franceschi et al., 2000; Lencel & Magne, 2011).

Postmenopausal osteoporosis results from estrogen deficiency, which leads to activation of RANKL production in osteoblasts, which in turn induces osteoclast recruitment. At the same time, OPG production is less stimulated, leading to a shift in the RANKL/OPG ratio towards bone resorption (B. L. Clarke & Khosla, 2010). Estrogens also suppress the production of cytokines such as IL-1β and TNF-α, which, in turn, can result in increased cytokine production after the cessation of estrogen production following menopause (Charatcharoenwitthaya et al., 2007). Inflammation therefore is an important component of both primary and secondary

osteoporosis, as cytokines can significantly influence bone metabolism and thus alter bone remodeling (Rauner et al., 2007).

1.4.2. Impact of Proinflammatory Cytokines on Bone Cells

The regulation of inflammation is a complex system in which extracellular signaling molecules play an important role. In both acute and chronic inflammation, cytokines are released that can have autocrine, paracrine, and endocrine effects. The release of proinflammatory cytokines leads to an upregulation of inflammatory processes (J.-M. Zhang & An, 2007). The most important proinflammatory cytokines are the interleukins IL-1β and IL-6, and TNF-α. In addition to the best studied chemokine IL-8, interferon (IFN)γ also belongs to the group of proinflammatory cytokines (Borish & Steinke, 2003; Turner et al., 2014). Each of these cytokines can affect bone metabolism in different ways. The current state of research on the partly conflicting effects of these cytokines on osteoclast and osteoblast differentiation, will be summarized in the following section (Fig. 1.7).

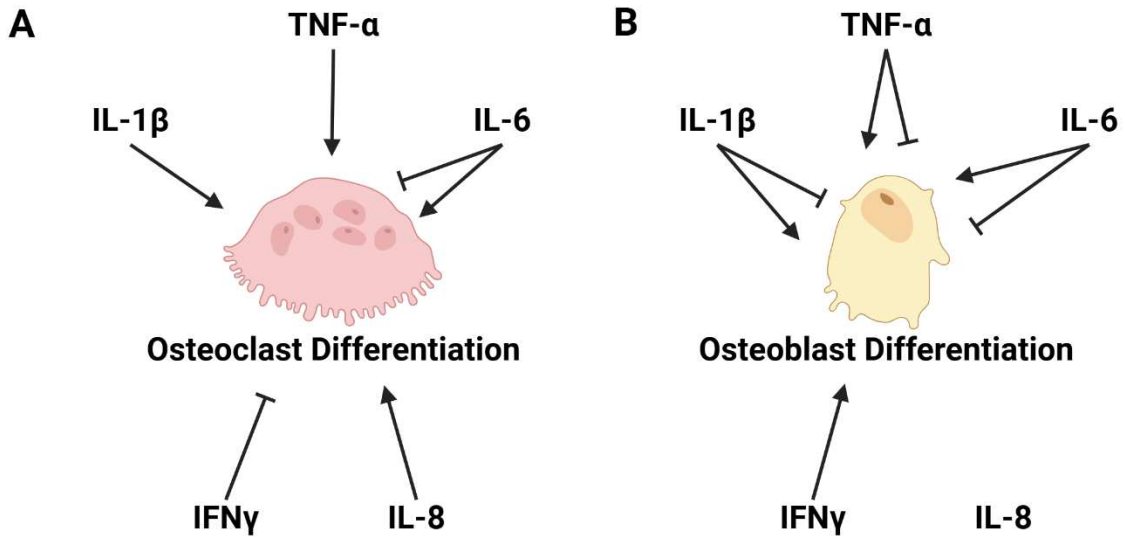

Figure 1.7: Current understanding of the effect of proinflammatory cytokines on the differentiation of bone cells. The figure shows the simplified current status of investigations about the inhibiting (⊤) or activating (↑) effect of IL-1β (Interleukin-1β), IL-6, IL-8, TNF-α (tumor necrosis factor α), and IFNγ (interferon γ)

on the differentiation of (A) osteoclasts and (B) osteoblasts. Created in BioRender. Bousch, J. (2025) https://BioRender.com/l01v138.

1.4.2.1. IL-1β and TNF-α - Pro-Resorptive Mediators in Bone Metabolism

The cytokines IL-1β and TNF-α are generally considered to be mediators of bone resorption (Xu et al., 2023). IL-1β is considered to have a positive effect on osteoclastogenesis by inducing the expression of RANKL (Ruscitti et al., 2015). IL-1β blockers are therefore used as a therapeutic option in patients with RA to reduce both inflammatory cell migration and joint damage (Bresnihan et al., 2004; Dinarello et al., 2012). The effect of TNF-α on osteoclastogenesis has also been well studied and it has been shown several times that TNF-α promotes osteoclastogenesis (Amarasekara et al., 2018).

IL-1β has long been considered an inhibitor of bone formation, albeit with now contradictory observations (Amarasekara et al., 2021; Dr. Stashenko et al., 1987). In murine MSCs, IL-1β inhibited cell proliferation and differentiation (Lacey et al., 2009). Another study using murine MSCs also showed that both IL-1β and TNF-α inhibit osteogenesis while increasing cell migration (Sullivan et al., 2014). In periodontal ligament stem cells, IL-1β showed different effects depending on the used concentration: high concentrations inhibited BMP/Smad signaling and thus osteogenesis, whereas low concentrations activated this pathway and increased osteogenic expression markers (Mao et al., 2016). In human MSCs, IL-1β has also been shown to increase mRNA expression of osteogenic differentiation markers, ALP activity, and ECM mineralization *in vitro*, presumably via the Wnt-5a/Ror2 pathway (Sonomoto et al., 2012). But the presence of IL-1β can also enhance the osteoclastogenic effect of TNF-α (Wei et al., 2005).

However, the influence of TNF-α on osteogenesis remains controversial. TNF-α is mainly classified as an anti-osteoblastogenic factor, although there are also conflicting results in the literature for this proinflammatory cytokine (Amarasekara et al., 2021; Osta et al., 2014). TNF-α inhibits osteogenic differentiation of

spontaneously differentiating primary fetal rat calvarial pre-osteoblasts and in the murine cell line MC3T3-E1-14 by reducing OCN expression and the number of mineralized nodules (Gilbert et al., 2000). Another study also described inhibition of Runx2 expression in these cell models by TNF-α (Gilbert et al., 2002). In a study showing a positive effect of IL-1β on the osteogenic differentiation of human MSCs, a positive effect of TNF-α was also demonstrated, although to a lesser extent (Sonomoto et al., 2012). In contrast, a study of murine MSCs showed the inhibition of differentiation by IL-1β and TNF-α, but only a negative effect on proliferation by IL-1β (Lacey et al., 2009). It is hypothesized that TNF-α stimulates osteogenic differentiation at an early differentiation stage, when MSCs are not yet committed to the osteogenic lineage. In contrast, at later stages, when the cells are already pre-osteoblasts, TNF-α inhibits osteogenesis (Osta et al., 2014).

1.4.2.2. IL-6 - Ambiguous Roles on Bone Metabolism

There is no consensus about the effect of IL-6 on both osteoclasts and osteoblasts, as there are also conflicting studies in this area (Amarasekara et al., 2021; Xu et al., 2023). Early it has been shown, that IL-6 in coculture with osteoblastic cells can induce osteoclastogenesis of murine bone marrow cells (BMMs), presumably via signal transduction of IL-6 receptor on osteoblastic cells (Udagawa et al., 1995). On the other side, direct addition of IL-6 can inhibit the differentiation of mouse bone marrow macrophages (BMMs) into osteoclasts (Yoshitake et al., 2008). The negative effect of TNF-α on BMP-induced osteogenic differentiation of mouse MSCs was partially reversed by IL-6 knockdown. This suggests that IL-6 is an important mediator in the inhibition of osteogenesis by inflammation, presumably through interaction with the Wnt pathway (Malysheva et al., 2016). In primary murine osteoblasts and the murine cell line MC3T3-E1, the addition of IL-6 also reduced mineralization, ALP activity, and the expression of osteogenic markers (Kaneshiro et al., 2014). However, positive effects of IL-6 on osteogenesis have also been shown. For example, IL-6 increased ALP activity and Runx2 expression in periodontal ligament cells, as well as mineralization and ALP activity in human adipose stem cells (hASCs) (Bastidas-Coral et al., 2016; Iwasaki et al., 2008). It is suggested that

the different results depend on the cell model used and its stage of differentiation, and that IL-6 is more likely to activate early osteogenic differentiation (Blanchard et al., 2009).

1.4.2.3. IFNγ - an Anti-Resorptive Proinflammatory Cytokine

The effect of IFNγ is described as anti-osteoclastogenic, as it inhibits RANKL signaling, which leads to inhibition of osteoclastogenesis (Takayanagi et al., 2000). It also inhibits TNF-α-induced osteoclast formation in murine BMMs (Kohara et al., 2011). The production of IFNγ is upregulated of human MSCs during osteogenesis and the inhibition of IFNγ led to a reduction in differentiation. In addition, IFNγ treatment led to increased differentiation (Duque et al., 2009). In a study with murine osteoblasts, IFNγ had a negative effect on calcification, but increased the expression of osteogenic differentiation markers such as ALP and Runx2 (Z. Wang et al., 2018). It is assumed that the effect of IFNγ on osteogenic differentiation is also stage-dependent and that IFNγ tends to positively influence mineralization, which takes place at later stages (Lai et al., 2022).

1.4.2.4. IL-8 - a Largely Unexplored Role in Bone Metabolism

IL-8 (or CXCL8) is a chemokine that recruits inflammatory cells to the site of inflammation (Remick, 2005). IL-8 increases the formation of TRAP-positive multinucleated cells and the RANKL expression in MC3T3-E1 cells (Bendre et al., 2003). During differentiation of human osteoclast precursors, they secrete increased levels of IL-8 via RANKL downstream signaling (Kopesky et al., 2014). IL-8 increases human bone marrow-derived mesenchymal stem cells (hBMSC) migration *in vitro* by binding to its receptor CXCL2 and also contributes to bone regeneration *in vivo* (Yang et al., 2018). Another study also showed that the addition of IL-8 increased the chemotaxis of BMSCs both *in vitro* and *in vivo*. However, it was also shown that both osteogenic and chondrogenic differentiation remained unchanged (Park et al., 2015). In hASCs, IL-8 was shown to inhibit cell mineralization, but without a significant effect on the expression of osteogenic markers (Bastidas-Coral

et al., 2016). Due to the lack of sufficient studies on primary osteoblasts, further studies are needed to determine the effect of IL-8 on osteogenic differentiation.

1.5. Aim and Scope of the Research

Osteoporosis is a multifactorial disease characterized by an imbalance between bone formation and resorption, often exacerbated by inflammatory processes. While the role of proinflammatory cytokines in stimulating osteoclast activity is well documented, their effect on osteoblast function remains controversial. Previous studies have reported conflicting results depending on the cell model, differentiation stage, and cytokine concentration, making a clear interpretation difficult. This study is based on the investigation of primary human osteoblasts (OBs) isolated directly from patients' femoral heads, which significantly increases the clinical relevance of the results. For the first time, the effect of the proinflammatory cytokines IL-1β, IL-6, IL-8, TNF-α, and IFNγ is investigated in primary human osteoblasts.

The first part of the study, which has been largely published, investigates cytokine secretion during osteogenesis by the osteoblasts themselves, and the effect of the cytokines IL-1β, IL-6, IL-8, and TNF-α on cell differentiation and proliferation. A novel aspect is the analysis of cytokine-induced changes in osteoblast energy metabolism, which may contribute to inflammation-related bone diseases. To further analyze the impact of inflammation on bone formation, the second part of this thesis will compare osteoblasts from individuals with normal and osteoporotic bone density (oOBs). This comparison aims to determine whether osteoporotic osteoblasts exhibit intrinsic differences in baseline activity or cytokine responsiveness. Additionally, this study will evaluate the widely used osteoblast cell line hFOB 1.19 as a potential *in vitro* model for inflammatory bone research.

This work aims to improve our understanding of how inflammation affects bone formation and remodeling. The study may contribute to the development of new therapeutic approaches for treatment of inflammation-related bone diseases such as osteoporosis and to promote long-term bone health in aging.

2. Publication

2.1. Declaration of Own Contribution

The project planning was mainly carried out independently in regular exchange with the supervisors Prof. Dr. rer. nat. Christoph V. Suschek and Prof. Dr. med. Uwe Maus. All work steps in the laboratory, the evaluation of the data and the writing of the publication were carried out completely independently.

Confirmation from Prof. Dr. rer. nat. Christoph V. Suschek (supervisor):

Date _____ Signature _____

2.2. Copy of Publication

A copy of the publication is attached below with the reference:

Juliana Franziska Bousch, Christoph Beyersdorf, Katharina Schultz, Joachim Windolf, Christoph Viktor Suschek and Uwe Maus (**2024**): *Proinflammatory Cytokines Enhance the Mineralization, Proliferation, and Metabolic Activity of Primary Human Osteoblast-like Cells.* International Journal of Molecular Sciences, 25, 12358. https://doi.org/10.3390/ijms252212358

International Journal of Molecular Sciences

MDPI

Article

Proinflammatory Cytokines Enhance the Mineralization, Proliferation, and Metabolic Activity of Primary Human Osteoblast-like Cells

Juliana Franziska Bousch, Christoph Beyersdorf, Katharina Schultz, Joachim Windolf, Christoph Viktor Suschek and Uwe Maus *

Department for Orthopedics and Trauma Surgery, Medical Faculty, University Hospital Düsseldorf, Heinrich Heine University Düsseldorf, 40225 Dusseldorf, Germany; julianafranziska.bousch@med.uni-duesseldorf.de (J.F.B.); christoph.beyersdorf@med.uni-duesseldorf.de (C.B.); katharina.schultz@med.uni-duesseldorf.de (K.S.); joachim.windolf@med.uni-duesseldorf.de (J.W.); suschek@hhu.de (C.V.S.)
* Correspondence: uwe.maus@med.uni-duesseldorf.de

Abstract: Osteoporosis is a progressive metabolic bone disease characterized by decreased bone density and microarchitectural deterioration, leading to an increased risk of fracture, particularly in postmenopausal women and the elderly. Increasing evidence suggests that inflammatory processes play a key role in the pathogenesis of osteoporosis and are strongly associated with the activation of osteoclasts, the cells responsible for bone resorption. In the present study, we investigated, for the first time, the influence of proinflammatory cytokines on the osteogenic differentiation, proliferation, and metabolic activity of primary human osteoblast-like cells (OBs) derived from the femoral heads of elderly patients. We found that all the proinflammatory cytokines, IL-1β, TNF-α, IL-6, and IL-8, enhanced the extracellular matrix mineralization of OBs under differentiation-induced cell culture conditions. In the cases of IL-1β and TNF-α, increased mineralization was correlated with increased osteoblast proliferation. Additionally, IL-1β- and TNF-α-increased osteogenesis was accompanied by a rise in energy metabolism due to improved glycolysis or mitochondrial respiration. In conclusion, we show here, for the first time, that, in contrast to findings obtained with cell lines, mesenchymal stem cells, or animal models, human OBs obtained from patients exhibited significantly enhanced osteogenesis upon exposure to proinflammatory cytokines, probably in part via a mechanism involving enhanced cellular energy metabolism. This study significantly contributes to the field of osteoimmunology by examining a clinically relevant cell model that can help to develop treatments for inflammation-related metabolic bone diseases.

Keywords: osteogenesis; osteoblasts; inflammation; proinflammatory cytokines; osteoporosis; proliferation; energy metabolism; osteoimmunology

Citation: Bousch, J.F.; Beyersdorf, C.; Schultz, K.; Windolf, J.; Suschek, C.V.; Maus, U. Proinflammatory Cytokines Enhance the Mineralization, Proliferation, and Metabolic Activity of Primary Human Osteoblast-like Cells. *Int. J. Mol. Sci.* **2024**, *25*, 12358. https://doi.org/10.3390/ijms252212358

Academic Editor: Fernando A. Fierro

Received: 13 September 2024
Revised: 14 November 2024
Accepted: 15 November 2024
Published: 18 November 2024

1. Introduction

Osteoporosis is a metabolic bone disease associated with low bone density due to enhanced bone tissue resorption or insufficient tissue formation, resulting in an increased risk of fracture. It has also been linked to the aging process and to chronic inflammation [1,2]. Chronic inflammatory diseases, such as rheumatoid arthritis and ankylosing spondylitis, can lead to reduced bone density and osteoporosis [3,4]. In metabolically active bone tissue, a continuous process called 'bone remodeling' occurs, in which old, micro-damaged bone is replaced by new, structurally stable bone tissue. Healthy bone requires a balance between the resorption of bone tissue by osteoclasts and the synthesis of new bone mass by osteoblasts [5]. A number of factors, including cytokines released by bone cells themselves, and especially during inflammation, can affect this balance. The interaction between bone metabolism and the immune system is a complex process summarized under the term osteoimmunology [6]. Cytokines can affect bone metabolism in a variety of ways, thereby

disrupting the balance between bone resorption and formation. Inflammation is generally associated with increased bone resorption and metabolic bone diseases [7]. However, the aging process is also associated with chronic inflammation and can disrupt bone remodeling [8]. Mature osteoblasts, which differentiate from mesenchymal stem cells (MSCs), are required for the formation of new bone tissue. During this differentiation, known as osteoblastogenesis, cells secrete and mineralize an extracellular matrix (ECM) before differentiating into osteocytes [9]. Osteoblastogenesis is controlled by several signaling pathways, including Wnt, Notch, Hedgehog, bone morphogenic protein (BMP), and tumor growth factor-beta (TGF-β) [10]. Both proinflammatory and antiinflammatory cytokines can have diverse effects on osteoblastogenesis via different signaling pathways [11].

Proinflammatory cytokines, such as interleukin(IL)-1β and IL-6, as well as the chemokine IL-8 and tumor necrosis factor-alpha (TNF-α), are often described in the literature as promoters of bone resorption, but all show ambiguous roles [11,12]. IL-1β can induce osteoblast differentiation through the Wnt signaling pathway [13] and, conversely, inhibit it [14]. IL-6 triggers osteogenesis but also leads to the inhibition of osteoblastogenesis through downregulation of BMP signaling [11]. TNF-α inhibits the differentiation and proliferation of osteoblasts [11] but has also shown paradoxical results in several studies [15]. Similarly to IL-6, IL-8 is secreted by osteoblasts and is known to have a stimulating effect on the differentiation of osteoclasts [12]. However, IL-8 has also been observed to promote osteogenesis in vivo [16]. Taken together, these conflicting results reveal a complex and essential role of cytokines in bone metabolism. It should be noted that the majority of the studies cited summarize results from different cell models such as human MSCs or adipose stromal cells (ASCs), cell lines such as MC3T3-E1 or C2C12, or primary murine cells. There is a clear lack of results on the clinically relevant cell type, bone-forming osteoblasts from human bone tissue. In our study, we isolated primary human osteoblast-like cells (OBs) from the cancellous bone of human femoral heads to describe, for the first time, the influence of the proinflammatory cytokines IL-1β, IL-6, IL-8, and TNF-α during osteogenesis on the matrix mineralization, proliferation, and energy metabolism of these cells. This study should contribute to a better understanding of the activities of human bone cells under inflammatory conditions, as further research may lead to new therapeutic approaches for inflammation-related bone diseases, such as osteoporosis.

1. Results

First, the morphology of the osteoblast-like cells was observed with a light microscope. The undifferentiated confluent cells predominantly exhibited an elongated shape, although some cells had a more polygonal or roundish shape (Figure 1A). After seven days of osteogenesis, the cell morphology and arrangement in the culture changed notably (Figure 1B). Instead of the observed elongated shape, the cells became more rounded and formed regions of increased cellular density. The arrows in Figure 1 mark some roundish-shaped cells between the elongated-shaped cells as an example.

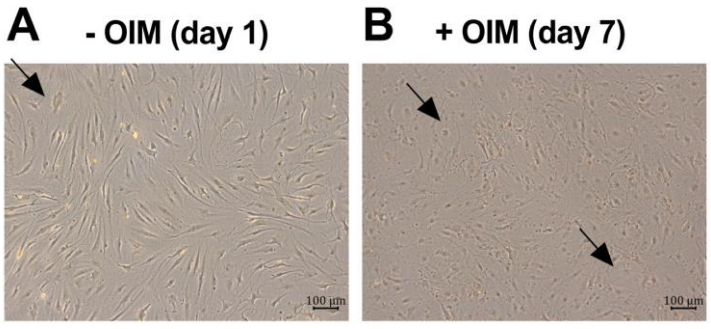

Figure 1. *Cont.*

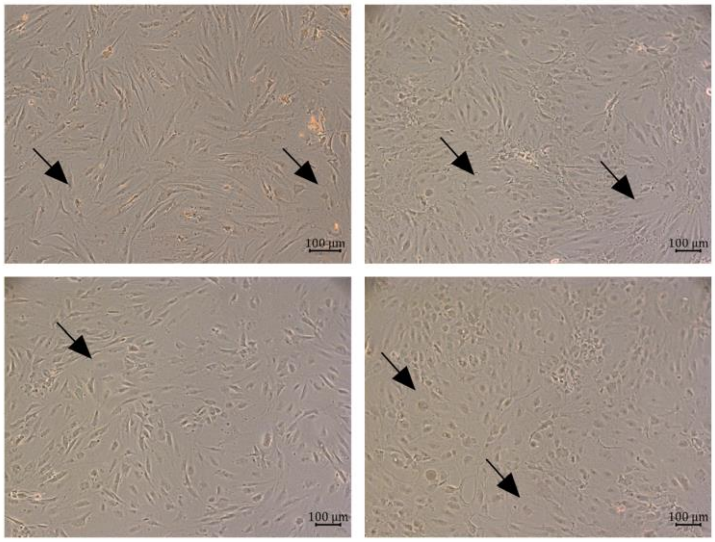

Figure 1. Morphologies of the osteoblast-like cell cultures. Light microscope pictures (100× magnification, scale bars = 100 µm) of OBs from three different donors seeded at confluency (**A**) on day 1 (undifferentiated cells) and (**B**) on day 7 of osteogenesis. The arrows mark roundish-shaped cells as an example.

1.1. OBs Secreted the Proinflammatory Cytokines IL-6 and IL-8 During Osteogenesis

Within the observed period of 35 days, the relative mineralization of ECM by primary human osteoblast-like cells (OBs) increased significantly during treatment with osteogenesis induction medium (OIM) (Figure 2A). Between days 7 and 14, the formation of calcified areas increased, as evidenced by microscopic and macroscopic observations (Figure 2C). The increase in mineralization was continuous until day 35. As shown in Figure 2B, the alkaline phosphatase (ALP) activity of the OBs also increased significantly between day 7 and day 21, and appeared to reach a plateau from this day onwards, until day 35.

During the osteogenesis, we observed a secretion of proinflammatory cytokines (Figure 2D,E). The measuring points represent values of cytokine secretion within one week during incubation in OIM. The undifferentiated cells secreted approximately 534 pg/mL of IL-6 (Figure 2D). A significant decrease in this secretion to about 187 pg/mL was observed on day 7. However, it increased again on day 14 to about the same level as the undifferentiated cells (day 1), with values between 423 and 507 pg/mL, and did not show significant changes until day 35. In contrast, IL-8 was barely secreted by undifferentiated OBs on day 1 (Figure 2E). From day 14 of osteogenesis, IL-8 secretion increased significantly to about 1275 pg/mL and continued to increase to 1947 pg/mL by day 35. No notable correlations were observed between the age or gender of the donors and the mineralization, ALP activity, or IL-6 and IL-8 secretion of the isolated cells (see Supplementary Figures S2 and S3).

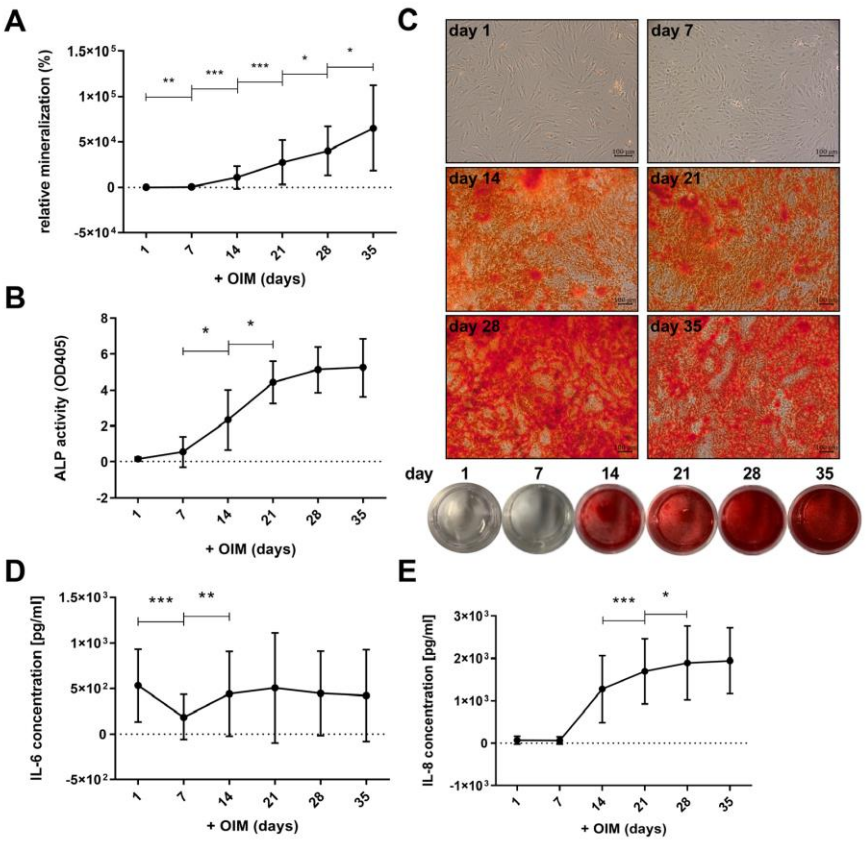

Figure 2. Interleukin (IL)-6 and IL-8 secretion during osteogenesis. The primary human osteoblast-like cells (OBs) were incubated in osteogenesis induction medium (OIM) for 35 days and (**A**) mineralization of the extracellular matrix (ECM) was quantified by Alizarin Red S staining (n = 13, four replicates each), (**C**) accompanied by example images of corresponding microscope images (100× magnification; scale bars = 100 µm) and well plates, and (**B**) alkaline phosphatase (ALP) activity was measured every week (n = 6, 4 replicates each). The protein concentration (pg/mL) of (**D**) IL-6 and (**E**) IL-8 in the supernatant was examined by enzyme-linked immunosorbent assay (ELISA) (n = 11, two replicates). Means with standard deviation (SD) are shown, and all significances were calculated by Wilcoxon signed-rank test ($p \leq 0.05$ (*), $p \leq 0.01$ (**), $p \leq 0.001$ (***)).

1.1. The Proinflammatory Cytokines IL-1β, IL-6, IL-8, and TNF-α Increased the Mineralization of OBs

Treatment with IL-1β significantly induced the mineralization of the ECM by OBs at all concentrations (Figure 3A). The mineralization as a sign of the differentiation of OBs increasing proportionally with increasing concentrations of IL-1β and was already induced 24-fold at 3.125 units/mL IL-1β compared to the control (OIM without cytokines, 0 units/mL). At the highest concentration of 250 units/mL, the mineralization of the cytokine-treated OBs was 3648% stronger than that of the control cells. Treatment with IL-6 and IL-8 also resulted in a trend toward increased cell differentiation independent of the concentration, but at significantly lower values. The induction by IL-6 was about 356%, and that by IL-8 was about 373% higher compared to the control (Figure 3B,C). Only the lowest concentration of IL-6 led to a significant effect. The results with the TNF-α treatment were concentration-dependent, as with IL-1β, and with high concentrations of 50–250 units/mL, a significant induction of mineralization was measured, with up to 1552%

higher values compared to the differentiated osteoblasts without cytokine treatment. The measurement of ALP activity as an early marker of osteogenic differentiation on day 8 and day 10 showed no significant increase, except for a slight trend in the IL-1β-treated cells on day 10. The whiskers and boxplots in Figure 3 reflect the natural variability inherent in the primary cell cultures. Despite this variability, some differences are statistically significant, underscoring the reliability of these results. No reductions in cell count were observed after 7 or 14 days with the cytokines of any tested concentration (Suppl. Figure S1), suggesting that the induction of apoptosis by the inflammatory factors is unlikely.

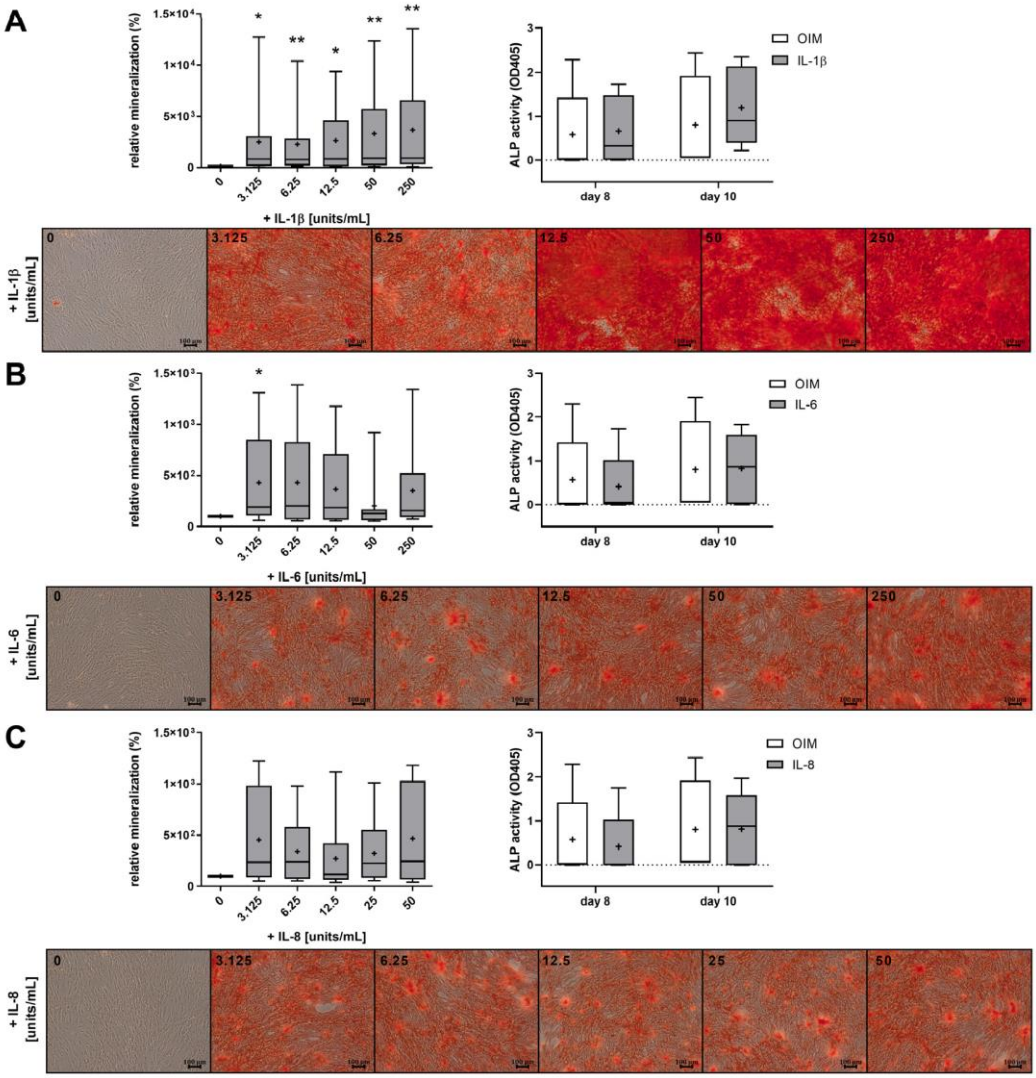

Figure 3. *Cont.*

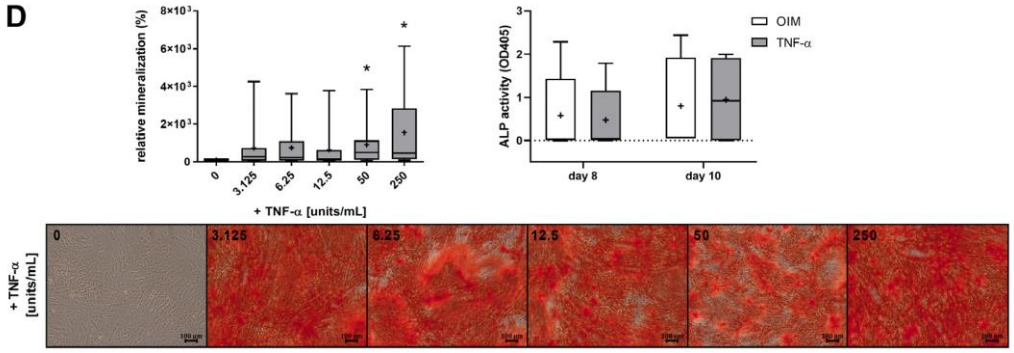

Figure 3. Effects of IL-1β, IL-6, IL-8, and tumor necrosis factor (TNF)-α on the mineralization of OBs. The boxplot diagrams illustrate the relative mineralization quantified by Alizarin Red S staining of OBs (n = 9, four replicates each) incubated for 21 days with the cytokines (**A**) IL-1β, (**B**) IL-6, (**C**) IL-8, and (**D**) TNF-α at concentrations ranging from 3.125 to 250 units/mL in OIM, with the corresponding microscopic images of the calcified nodules (scale bars ≙ 100 µm). Additionally, the ALP activity on day 8 and day 10 with selected concentrations of IL-1β (250 units/mL), IL-6 (12.5 units/mL), IL-8 (12.5 units/mL), and TNF-α (250 units/mL) is shown (n = 5, four replicates each). The whiskers representing the minimum and maximum, the median lines, and the means (+) are shown. The significances refer to the control (0 units/mL) and were calculated by the Wilcoxon signed-rank test ($p \leq 0.05$ (*), $p \leq 0.01$ (**)).

1.1. IL-6 and IL-8 mRNA Expression Were Enhanced by IL-1β and TNF-α

To understand the beneficial impact of cytokines on mineralization, we analyzed whether the cytokines influence each other's reciprocal expression. Since we demonstrated the secretion of IL-6 and IL-8 during osteogenesis (Figure 2), we examined the influence of the cytokines on the mRNA expression of IL-6 and IL-8. The OBs were treated with the cytokines in OIM for 21 days. The highest concentrations (250 units/mL) were chosen for IL-1β and TNF-α, as these induced mineralization with the highest significant levels (Figure 3A,D). IL-6 and IL-8 were used at a concentration of 12.5 units/mL, as the effect on mineralization was independent of the concentration (Figure 3B,C).

Treatment with IL-1β significantly increased the mRNA expression of IL-6 with an 8-fold higher mean value (Figure 4A) and the mRNA expression of IL-8 with a 91-fold higher mean value than the control (Figure 4B). Interestingly, the treatment with TNF-α resulted in an even stronger induction of IL-6 and IL-8. The mRNA expression of IL-6 was increased approximately 26-fold (Figure 4A), and the expression of IL-8 was increased about 104-fold by TNF-α (Figure 4B). Both IL-1β and TNF-α had a stronger impact on IL-8 than on IL-6 mRNA expression. The incubation with IL-6 and IL-8 did not affect their expression.

1.2. IL-1β and TNF-α Enhanced the Cell Count and Proliferation Rate of OBs During Osteogenesis

To analyze the influence of the cytokines on the cell count, the cells were incubated with or without cytokines in OIM for 21 days, and Dimethylthiazolyl Blue Tetrazolium Bromide (MTT) assays were performed. Already on day 7, the cell count of the OBs with IL-1β and TNF-α was significantly higher than the cell count of the control cells (Figure 5A). At day 14 and day 21, the effect of IL-1β remained significant with a cell count that was more than 3-fold higher compared to the control cells, but the cell count of the TNF-α-treated cells tended to be induced at both time points, albeit not significantly (Figure 5B,C). The cell counts of the OBs treated with IL-6 and IL-8 did not differ from the control during the observed period (Figure 5D). The examination of the proliferation rate using a bromodeoxyuridine (BrdU) assay confirmed the results of the MTT assay (Figure 5E). The OBs treated with IL-1β and TNF-α had significant, more than 2-fold higher,

proliferation rates over a 48 h incubation period, while IL-6 and IL-8 had no effect. A comparison of the donors' ages and the cell counts during osteogenesis with and without cytokines did not show a significant correlation (Suppl. Figure S4).

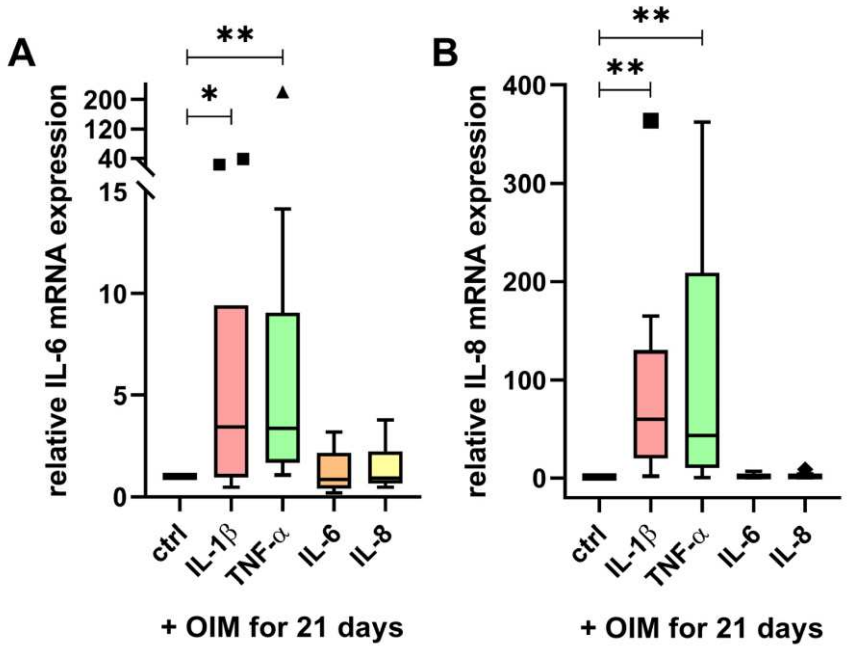

Figure 4. Reciprocal impact of the cytokines on mRNA expression in differentiated OBs. The mRNA expression of (**A**) IL-6 and (**B**) IL-8 was determined upon 21-day incubation of the cytokines IL-1β (250 units/mL), IL-6 (12.5 units/mL), IL-8 (12.5 units/mL), and TNF-α (250 units/mL) in OIM (n = 10, three replicates). The relative mRNA expression was calculated by the 2-ΔΔ Ct method and normalized on the control cells with 21-day OIM incubation without cytokines (ctrl) of each patient. The Tukey boxplot diagrams show the median line, and any values that exceed the threshold of the 75th percentile plus 1.5 times the interquartile range are plotted as statistical outliers (■, ▲). The significances were calculated by the Wilcoxon signed-rank test ($p \leq 0.05$ (*), $p \leq 0.01$ (**)).

1.1. IL-1β and TNF-α Had Effects on Mitochondrial and Glycolytic Metabolism of the OBs

No significant difference in basal respiration, adenosine triphosphate (ATP) production, or maximal respiration could be measured between the undifferentiated (day 1 control) and differentiated (day 14 ctrl) OBs (Figure 6A–C). Nevertheless, the oxygen consumption rate (OCR) of the differentiated OBs (day 14 + OIM) was slightly higher than that of undifferentiated OBs (day 1) throughout the assay (Figure 6D). Notably, treatment with TNF-α resulted in a significant 167% higher induction of basal respiration and significantly higher ATP production, of 166%, in the OBs compared to the day 14 control. However, there was no significant increase in maximum respiration. The treatments with the other cytokines, IL-1β, IL-6, and IL-8, did not result in significant changes (Figure 6A–C). The inductive effect of TNF-α on OCR was observed throughout the course of the assay (Figure 6D).

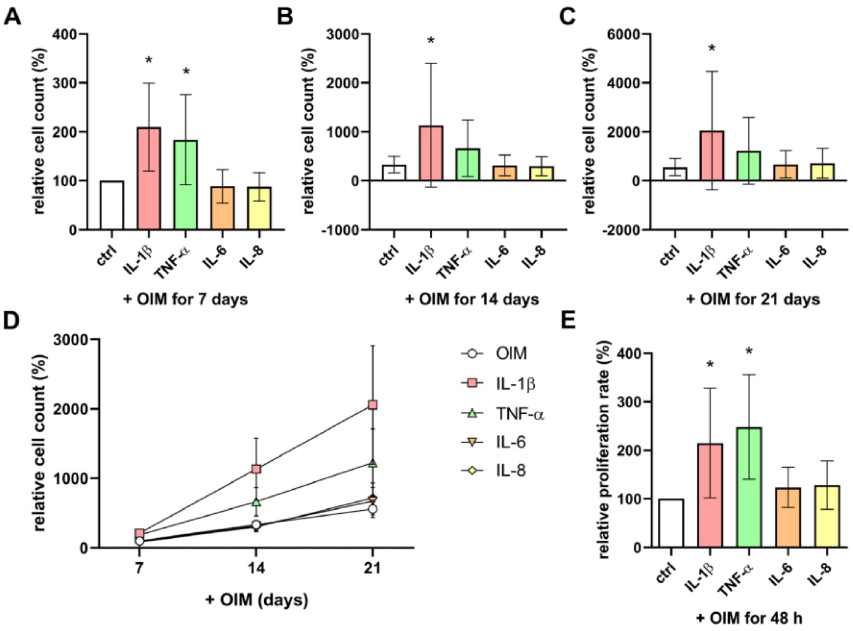

Figure 5. Impact of proinflammatory cytokines on the cell count and proliferation rate. The cell count of OBs incubated with the cytokines IL-1β (250 units/mL), IL-6 (12.5 units/mL), IL-8 (12.5 units/mL), and TNF-α (250 units/mL) in OIM on (**A**) day 7, (**B**) day 14, and (**C**) day 21 of osteogenesis was determined by Dimethylthiazolyl Blue Tetrazolium Bromide (MTT) assay. The mean with SD is shown. The diagram in (**D**) summarizes the observed period from day 7 to day 21 (n = 8, four replicates each); the mean with SEM is shown. All data were normalized for the control (OIM without cytokines) on day 7 from each patient. (**E**) The cell proliferation rate over 48 h was measured by bromodeoxyuridine (BrdU) assay (n = 6, four replicates each). The data were normalized for the control (OIM without cytokines) from each patient, and the mean with SD is shown. The significances were calculated by the Wilcoxon signed-rank test ($p \leq 0.05$ (*)).

The glycolysis of the differentiated OBs (day 14 ctrl) was significantly inhibited by about 60% compared to the undifferentiated OBs (day 1 ctrl). Interestingly, the cells treated with IL-1β showed a tendency to increase glycolysis and glycolytic reserve, although these changes were not statistically significant. The IL-1β-treated cells had a 194% higher glycolytic rate than the differentiated OBs without cytokines. TNF-α, IL-6, and IL-8 did not affect glycolysis compared to the day 14 control, but IL-6 and IL-8 tended to inhibit the glycolytic reserve (Figure 7A,B). This parameter defines the ability of the cell to respond to energy demand and is therefore a parameter of how close the glycolytic rate is to the theoretical maximum of the cell [17]. This is mimicked in the assay by the addition of oligomycin. The treatment with IL-1β induced significantly the non-glycolytic acidification, by 189%, compared to the day 14 control (Figure 7C). The increased basal extracellular acidification rate (ECAR) and the induced response to glucose of the IL-1β-treated OBs are shown in Figure 7D. Over the entire course of the assay, the ECAR of the IL-1β-treated cells was higher than those observed in the differentiated cells without cytokines and in the undifferentiated cells (day 1).

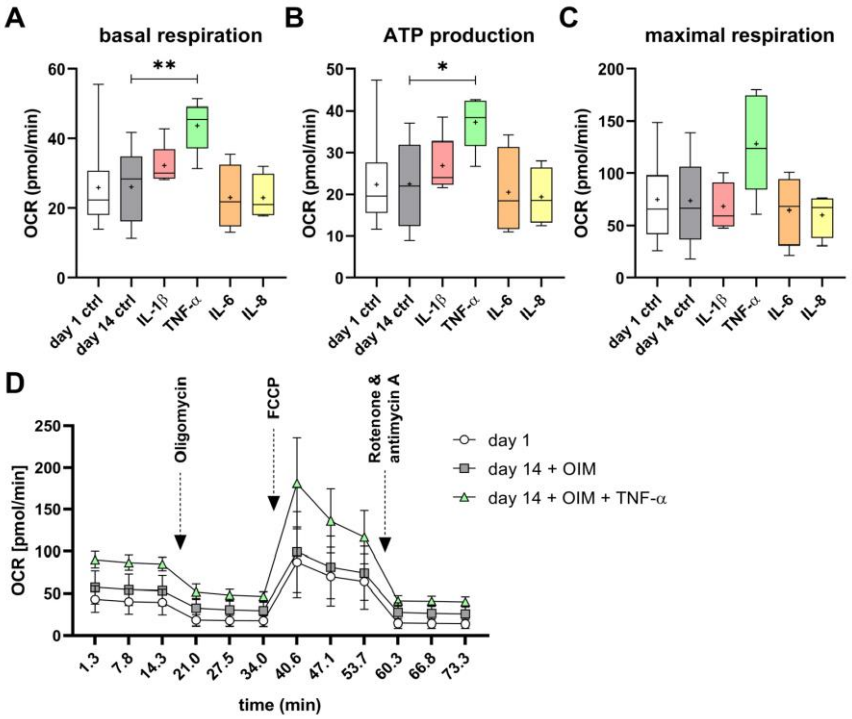

Figure 6. Impact of proinflammatory cytokines on the mitochondrial oxidative phosphorylation during osteogenesis. The (**A**) basal respiration, (**B**) adenosine triphosphate (ATP) production, and (**C**) maximal respiration were determined by Seahorse Cell Mito Stress Tests (Agilent). (**D**) All measurement time points of the assay for day 1, day 14 + OIM, and day 14 with OIM and TNF-α with the injection of assay reagents are shown. The OBs' oxygen consumption rate (OCR) was measured on day 1 of osteogenesis (n = 16), and on day 14 without (n = 9) and with the cytokines IL-1β (250 units/mL; n = 5), IL-6 (12.5 units/mL; n = 4), IL-8 (12.5 units/mL; n = 4), and TNF-α (250 units/mL; n = 5). All experiments were performed with at least 10 technical replicates. The significances were calculated by the Mann–Whitney U test ($p \leq 0.05$ (*), $p \leq 0.01$ (**)).

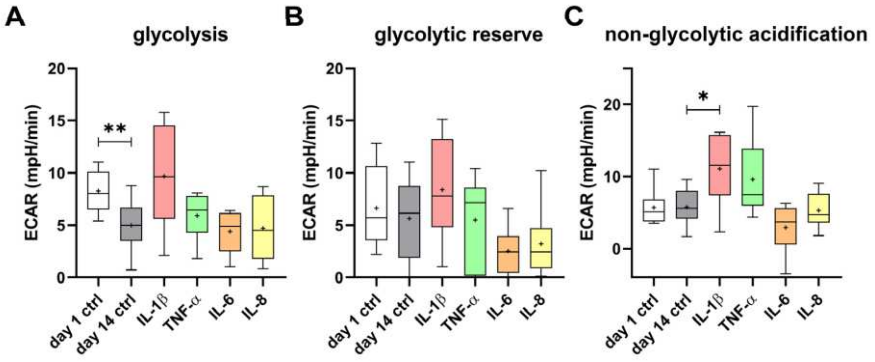

Figure 7. *Cont.*

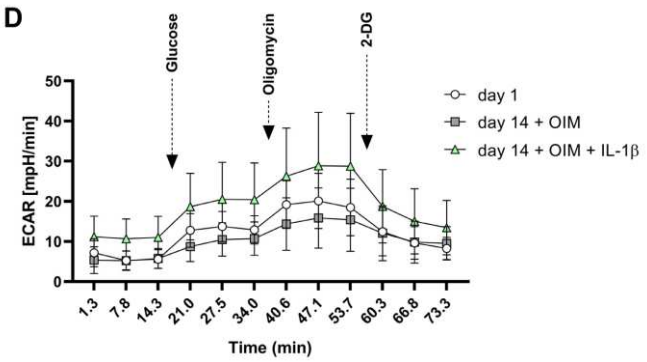

Figure 7. Impact of proinflammatory cytokines on glycolysis during osteogenesis. The (**A**) glycolysis, (**B**) glycolytic reserve, and (**C**) non-glycolytic acidification were determined by the Seahorse Glycolysis Stress Test (Agilent). (**D**) All measurement time points of the assay for day 1, day 14 + OIM, and day 14 with OIM and IL-1β with the injection of assay reagents are shown. The OBs' extracellular acidification rate (ECAR) was measured on day 1 of osteogenesis (n = 8), and on day 14 without (n = 10, and with the cytokines IL-1β (250 units/mL; n = 6), IL-6 (12.5 units/mL; n = 6), IL-8 (12.5 units/mL; n = 6), and TNF-α (250 units/mL; n = 6). All experiments were performed with at least 10 technical replicates. The significances were calculated by the Mann–Whitney U test ($p \leq 0.05$ (*), $p \leq 0.01$ (**)).

1. Discussion

In the present study, we demonstrate, for the first time, the effects of proinflammatory cytokines on mineralization, proliferation, and energy metabolism in primary human osteoblast-like cells as a cell model. We found that the cells secreted IL-6 and IL-8 during the process of osteogenesis and that treatment with IL-1β and TNF-α enhanced the mRNA expression of these cytokines. Interestingly, we observed that all the cytokine treatments for 21 days, especially IL-1β and TNF-α, led to increased osteogenesis. This was demonstrated by increased mineralization of the cells in the presence of ALP activity. At the same time, the cytokines had different effects on the proliferation and energy metabolism of the OBs.

It is known that cytokines significantly influence the differentiation of osteoclasts and osteoblasts. The cytokines TNF-α, IL-1β, IL-6, and IL-8 are generally considered to be osteoclastogenic, as they promote osteoclast differentiation and, thus, contribute to increased bone resorption [18]. However, previous studies on the effect of cytokines on osteoblast activity are ambivalent, and the impact likely depends on the concentration used and the cell model studied [11,12,15,16]. Although TNF-α is predominantly described as an inhibitor of osteogenesis [11], there are studies showing a positive effect on osteogenesis [15]. Similarly, IL-1β and IL-6 have been described as both positive and negative regulators of osteogenesis [11]. IL-8 is known to be produced by both osteoblasts and osteoclasts, but its effect on osteogenesis has not been well studied [12]. To contribute to a better understanding of these contradictory findings in different cell models, such as primary murine cells, cell lines such as MC3T3-E1 or C2C12, and human MSCs or ASCs, we tested the effect of cytokines on the more clinically relevant cell model, primary human OBs isolated from femoral heads of patients without osteoporosis, to investigate the baseline cellular behavior of cells from patients with healthy bone mass.

The observed IL-8 secretion during osteogenesis confirms findings with MSCs, in which IL-8 secretion also increased during differentiation into mature osteoblasts [19]. As observed in bone marrow mesenchymal stromal cells (BMSCs) and other cell types, we also confirmed the induction of IL-8 and IL-6 mRNA expression by TNF-α and IL-1β in OBs [20–22]. IL-8 seems to play an important role in osteogenesis and is significantly induced by other cytokines during inflammation. This could partly explain the observed increase in mineralization by TNF-α and IL-1β if they simultaneously induce other cytokines that promote mineralization, such as IL-8, albeit to a much lower extent. Thus, a combined

cytokine effect could lead to enhanced cell differentiation, as observed with IL-1β and TNF-α. It would be interesting to study the combined effect of different proinflammatory cytokines to see whether an induction of mineralization would occur at an earlier stage. Interestingly, the increase in mineralization by the cytokine treatment did not correlate with an increase in ALP activity. It is conceivable that cytokine-induced mineralization occurs independently of ALP, or that it is indeed ALP-dependent but does not necessitate an increase in ALP activity to sustain this process. Ferreira et al. (2013) showed comparable results following the induction of the mineralization of human MSCs by IL-1β. Furthermore, the inhibition of ALP was shown to reverse the effect of IL-1β, leading to the conclusion that ALP is mandatory for matrix mineralization, but increased ALP activity is not necessary for the induction of enhanced mineralization [23]. Since we measured ALP activity simultaneously with mineralization, we assume enhanced osteogenesis of the cells. Parallel to autocrine effects, IL-8 secretion during osteogenesis could also have paracrine functions in bone cell communication, as it has been described as an osteoclastogenic cytokine [20]. In addition to osteoclasts, osteal macrophages (osteomacs) also play an important role in the bone remodeling process and regulate osteoblast function [24]. Macrophages also have high IL-8 receptor expression, and their proinflammatory cytokine production is enhanced by IL-8 [25]. While we observed a positive effect of cytokines on osteogenesis in an osteoblast culture, the induction of osteoclastogenesis could be mediated by the osteoblasts themselves through IL-8 secretion in vivo, particularly in an inflammatory environment with TNF-α and IL-1β. In future studies, it will be important to investigate whether the increased activity of osteoclasts induced by cytokines impairs the induction of osteoblast activity, as observed here, and whether bone resorption occurs at a faster rate than bone synthesis. The use of osteoblast and osteoclast cocultures could be used to further investigate the communication between bone cells under inflammatory conditions [26].

During differentiation, downregulation of OB proliferation would be expected, with mature osteoblasts secreting the ECM and subsequently initiating mineralization [9,11]. However, our findings show that IL-1β and TNF-α significantly induce both cell proliferation and mineralization. Despite generally negative effects on osteogenic differentiation, these cytokines have previously been shown to have positive effects on the proliferation of osteogenic lineage cells [27–29]. The observed increase in proliferation rate due to IL-1β and TNF-α treatment is a possible explanation for the stronger induced mineralization compared to IL-6 and IL-8 treatment, as the higher cell count on day 21 could contribute to this effect.

Due to hormonal differences in donor sex and physical changes with age, we analyzed whether there were differences in osteogenesis or cytokine expression in OB cultures. When analyzing the correlation between age and the observed results, the cells of the middle age group (60–70 years) showed a decreased rate of mineralization during late osteogenesis compared to the oldest group (>70 years), while the other age groups (<60 years and >70 years) showed no statistically significant differences (Suppl. Figure S2). However, there was no effect on ALP activity. In addition, the cells from the middle age group had the lowest levels of IL-6 and IL-8 secretion, albeit not to a significant degree, and showed the least influence of cytokines on cell count during osteogenesis (Suppl. Figures S3 and S4). To confirm these observations, it would be necessary to include more donors in the study, thus increasing the size of the groups. The same applies to the comparison of donor sex, in which a slight but non-significant tendency towards higher mineralization and ALP activity in cells from female donors compared to male donors, as well as higher IL-6 and IL-8 secretion during osteogenesis, was observed (Suppl. Figures S2 and S3).

During osteogenesis and the formation and mineralization of the ECM, osteoblasts have an increased energy demand, which is provided at various stages of osteogenic differentiation through different metabolic pathways. Therefore, metabolic changes occur during osteogenesis, primarily involving oxidative phosphorylation (OXPHOS), glycolysis, or the tricarboxylic acid (TCA) cycle [30,31]. These changes depend on the cell model studied and the timing of measurements during differentiation, with multiple switches between

the major energy sources likely occurring throughout this process. Undifferentiated MSCs prefer glycolysis and increase the rate of oxygen consumption by activated OXPHOS after 14 days of differentiation, whereas in murine calvarial osteoblasts, both pathways increase during early differentiation [32,33]. In the murine osteoblast cell line MC3T3-E1, an increase in glycolysis was observed at day 21 of differentiation, while OXPHOS was decreased compared to undifferentiated cells [34]. The present study did not detect any changes in OXPHOS at day 14 of differentiation in the OBs, but glycolysis was significantly inhibited compared to the undifferentiated control. Furthermore, treatment with IL-1β and TNF-α, both significant inducers of osteogenesis in OBs, also altered energy metabolism by increasing the ATP demand of the cells. The significant increase in OXPHOS by TNF-α suggests a slightly more mature differentiation phase compared to control cells not treated with cytokines. A significant increase in OXPHOS could also lead to the generation of excessive reactive oxygen species, possibly mitigated by a subsequent switch to glycolysis during the late matrix mineralization phase [33]. IL-1β, on the other hand, tended to increase glycolysis and significantly increased non-glycolytic acidification, which could indicate the use of the TCA cycle or glycogenesis [35]. This may suggest an even later differentiation phase of OBs, aligning with the increased mineralization observed with IL-1β treatment.

The partially divergent effects of these cytokines on osteoblast ATP production may activate distinct signaling pathways, despite the fact that they all lead to increased cell differentiation. A key signaling pathway involved is the p38 MAPK pathway, which mediates the increase in IL-6 production in osteoblasts and chondrocytes in response to IL-1β and TNF-α [36]. In human MSCs, it has also been shown that IL-1β can induce their osteogenic differentiation after 10 days via the Wnt-5a/Ror2 signaling pathway, but it can also induce specific miRNA, which in turn leads to the repression of β-catenin expression, thus inhibiting Wnt-driven osteogenesis [13,14]. These are just a few examples of cytokine-induced signaling pathways that target osteogenic differentiation. Future studies should prioritize the investigation of the underlying signaling pathways that regulate mineralization under inflammatory conditions. This may clarify the discrepancies observed in the current research and facilitate a deeper understanding of the mechanisms underlying inflammatory bone diseases such as osteoporosis. This study shows that energy metabolism and increased ATP production may play an important role in cytokine signaling and osteogenesis.

The differences in the effects of IL-1β, TNF-α, and IL-6 on the OBs' differentiation could be relevant regarding anti-cytokine therapies, which are commonly used in the treatment of chronic inflammatory diseases such as RA. IL-1β, TNF-α, and IL-6 have stimulatory effects on osteoclast differentiation and bone resorption [18]. This observation aligns with the effectiveness of anti-TNF-α and anti-IL-6 therapies. Monotherapy with tocilizumab, an antibody against the IL-6 receptor, as well as an antibody against IL-1Ra, has been shown to inhibit the progression of structural joint damage in RA patients [37]. Similarly, treatment with anti-TNF-α (infliximab) in RA patients led to the arrest of spine and hip bone loss with a decrease in bone resorption markers like RANKL [38]. Additionally, Infliximab has also been shown to inhibit IL-1β and IL-6 gene expression in the human osteosarcoma cell line MG-63 [39]. Based on the findings in this study, blocking cytokines, particularly IL-1β and TNF-α, may not only inhibit osteoclastogenesis, but could also potentially limit osteoblast-driven matrix mineralization. To address this, combination therapies with bone anabolic agents that promote bone formation may be beneficial, reducing bone resorption without inhibiting bone formation.

It is acknowledged that this study is not without limitations. Measuring energy metabolism or mRNA expression at specific time points during osteogenesis might miss important changes in cells. Although working with human primary cells is valuable, these cells are derived from patients who have suffered a fracture or had coxarthrosis prior to isolation, implying an inflammatory preload and increasing the risk of sampling bias. It should be noted that osteoarthritis (OA) has a significant impact on bone health. Increased expression of cytokines in chondrocytes, along with the degradation of cartilage

matrix proteins and other factors, also has an influential impact on bone cells [40]. This could potentially affect the results obtained with primary cells from OA patients, possibly leading to the observed variability between donor cells. It is also noteworthy that among the OA donors, there were a few cell cultures with a low response to cytokines on ECM mineralization. However, due to the relatively small number of donors, it was not possible to identify a pattern that could be attributed to donor OA status. The variability observed could have been due to individual differences between the patients' medical histories, which requires further investigation. Moreover, it is important to recognize that OA and fractures involve disparate inflammatory responses, with OA being marked by a chronic low-grade inflammatory process, whereas fractures trigger an acute inflammatory reaction that reaches its peak within the initial 24 h following the injury [41,42]. This temporal and qualitative difference in inflammation may lead to phenotypic and functional differences in cells derived from these patients. However, due to relatively small sample sizes and inherent variability between patients, including age and medication use, it remains challenging to investigate the effects of chronic versus acute inflammation on human osteoblast function. To minimize the potential for bias related to pathological bone conditions, patients with normal bone density, as determined by DXA, indicating a normal balance of bone remodeling, were selected for inclusion in this study. Further studies comparing osteoblasts from OA and fracture patients would be necessary to better understand the specific impact of different inflammatory conditions. Individual variations among patients due to previous illnesses, age, and medication intake can also occur and cannot be avoided with a relatively small patient sample size. Despite using an established isolation method for primary osteoblast cultures, contamination by other bone cells and their precursors, such as osteomacs, cannot be entirely ruled out and could influence osteoblast activity [24]. To maintain a pure cell population, only low-passage cells were used. Finally, it is important to note that these were in vitro studies with 2D cell cultures. In vivo, cells interact with a matrix and other cells that are not present in cell culture. They are also exposed to mechanical loading in vivo, which can alter their response to cytokines. It was shown that IL-1 coupled with mechanical load caused less ECM degradation of bovine articular cartilage than IL-1 alone [43]. The nitric oxide release induced by IL-1β in primary chondrocytes was also suppressed by additional mechanical loading [44]. Thus, the results observed here cannot be directly transferred to 3D systems, and follow-up studies are required. Although the cells were treated with cytokines for 21 days, this period may not be sufficient to mimic the chronic inflammation seen in patients with osteoporosis. Future studies should compare OBs from the non-osteoporotic patients studied here with cells from osteoporotic patients exposed to a chronic inflammatory environment.

The partly contradictory results in the literature show the complexity of the regulation of bone remodeling and the necessary communication of bone cells, and probably depend on the cell model investigated and the experimental conditions. While most studies report negative effects of proinflammatory cytokines on hMSCs' differentiation to osteoblasts, our results show that cytokines can promote the osteogenesis of mature osteoblasts under the selected conditions. Primary human OBs provide a realistic and clinically relevant model to study the effects of cytokines on bone metabolism. This study improves our understanding of the complex interplay between inflammation and the development of osteoporosis. Further research in this area could pave the way for new therapeutic strategies to prevent and treat inflammation-related metabolic bone diseases.

1. Materials and Methods

1.1. Materials

The cell culture materials were obtained from Sarstedt AG & Co. KG (Nümbrecht, Germany). Unless otherwise specified, all other materials and reagents were obtained from Merck KGaA (Darmstadt, Germany).

1.1. Bone Material, Ethics Approval, and Patient Information

The isolation and use of primary human osteoblast-like cells (OBs) was approved by the local Research Ethics Committee of the Heinrich Heine University Düsseldorf (Study No. 5585R). The patients had given written consent and had undergone arthroplasty due to osteoarthritis or fracture at the Clinic for Orthopedic and Trauma Surgery at the University Hospital of Düsseldorf (Germany). The bone density of each patient's spine (L1–L4) and proximal femur was quantified by dual-energy X-ray absorptiometry (DXA). Femoral heads from patients with t-scores > −2.5 (non-osteoporotic) [45], acquired during surgery, were included in this study and stored in phosphate-buffered saline (PBS) with 1% penicillin/streptomycin (Pen/Strep) by PAN-Biotech GmbH (Aidenbach, Germany). A total of 28 patients (20 female, 8 male) with a mean age of 66 years (SD = 12.4) and a range of 31 to 88 years were included in this study. A detailed list of age, sex, condition, medications, and experiments in which the donor cells were used is provided in the Supplementary Materials (Supplementary Table S1).

1.2. Isolation of Human Osteoblast-like Cells

In order to isolate the OBs from the femoral heads, the cancellous bone was scraped out. The bone pieces were thoroughly rinsed with Dulbecco's Modified Eagle Medium (DMEM), high-glucose (Gibco® by Life Technologies™, Carlsbad, CA, USA), and 1% Pen/Strep. They were then placed in a Falcon tube with 2.5 mg/mL collagenase type IV (Gibco® by Life Technologies™, Carlsbad, CA, USA), dissolved in OB growth medium. The bone pieces were digested for 2.5 h at 37 °C and the supernatant containing the cells was transferred to a new Falcon tube. After centrifugation at 400 × *g* for 5 min, the supernatant was discarded and the cells were resuspended in OB growth medium and seeded into a T75 cell culture flask [46,47].

1.3. Cell Culture

The OB growth medium was composed of DMEM, high-glucose, with 10% fetal bovine serum (FBS), 1% Pen/Step, and 1% 4-(2-hydroxyethyl)-1-piperazineethanesulfonic acid (HEPES) solution. The osteogenesis induction medium (OIM) consisted of DMEM, high-glucose, 10% FBS, and 1% Pen/Strep, with the addition of 50 µM L-ascorbic acid 2-phosphate, 10 mM β-glycerophosphate disodium salt hydrate, and 500 nM dexamethasone [47,48]. The recombinant human cytokines IL-1β (1 unit/mL = 1 pg/mL), IL-6 (1 unit/mL = 100 pg/mL), IL-8 (1 unit/mL = 10 ng/mL), and TNF-α (1 unit/mL = 50 pg/mL) were obtained from Peprotech (Hamburg, Germany). The cells were maintained in a humidified chamber at 37 °C with 5% CO_2.

1.4. Alizarin Red S Staining

The Alizarin Red S staining method was employed to quantify the calcium phosphates present in the mineralized ECM [49]. In 24- or 48-well plates, OBs were seeded at confluency and were treated with OIM for up to 35 days and with cytokines for 21 days to induce differentiation. For the Alizarin Red S stain, the cells were fixed with 4% formaldehyde for 15 min, followed by two washes with PBS. Subsequently, the cells were incubated with the 2% Alizarin Red S mono sodium salt staining solution for 20 min at 37 °C. Following several washes with deionized water, images of the wells were captured. The stain was redissolved with 10% (1-Hexadecyl)pyridinium chloride monohydrate (CPC; Thermo Fisher Scientific GmbH, Karlsruhe, Germany) for approximately 1 h in a shaker. The absorption of the dye, indicative of the mineralized ECM, was determined photometrically (OD600).

1.5. Extracellular ALP Activity

To determine the extracellular activity of alkaline phosphatase (ALP), the OBs were seeded in confluency in 48-well plates. The cells were treated with OIM for a period of up to 35 days or with cytokines for 10 days. To remove any residual medium, the cells were washed with PBS. This was followed by the addition of 750 µL of the ALP substrate

p-nitrophenyl phosphate, and the plates were incubated at 37 °C for 10 min. The substrate's conversion to yellowish p-nitrophenol by active ALP was determined in a photometer at a wavelength of 405 nm [50].

1.1. Quantification of Cytokines in Cell Supernatants by Enzyme-Linked Immunosorbent Assay (ELISA)

For the quantification of secreted cytokines, the OBs were seeded in 6-well plates. Upon reaching confluency, the medium was first replaced with OB growth medium, which was collected after 6 days for the 'day 1' sample. This was followed by starting the induction of the OB differentiation by incubation in OIM for up to 35 days. The supernatant containing the secreted proteins was collected every week and replaced with fresh OIM. The cytokine concentrations were determined by photometric measurement using the sandwich ELISA DuoSet® Human IL-6 ELISA and DuoSet® Human IL-8/CXCL8 ELISA with the DuoSet® Ancillary Reagent Kit 2 by R&D Systems (Minneapolis, MN, USA). The tests were performed according to the manufacturer's instructions.

1.2. Real-Time qPCR

In 6-well plates, the OBs were seeded at confluency and incubated in OIM with and without cytokines for 21 days. Total cell RNA was isolated after lysing the cells using the RNeasy® Mini Kits (QIAGEN N.V., Hilden, Germany). The RNA was converted into cDNA using the Omniscript® RT Kits (QIAGEN N.V., Hilden, Germany). RT-qPCR was performed in triplicates using the Power SYBR® Green PCR Master Mix (Thermo Fisher Scientific GmbH, Karlsruhe, Germany) with 10 ng cDNA for IL-6 and 1 ng cDNA for IL-8 in a 25 µL PCR reaction with a 7300 Real-Time PCR System (Applied Biosystems, Waltham, MA, USA). For the determination of mRNA expression, primer concentrations of 0.2 µM for IL-6 and 0.4 µM for IL-8 were used. Transferrin receptor 1 (TFRC) was used as the reference gene for normalization. The forward and reverse primer sequences are listed in Table 1. The 2-ΔΔ Ct method was employed for the calculation of relative mRNA expression [51].

Table 1. List of RT-qPCR Primers.

Target Gene	Forward Primer (5´->3´)	Reverse Primer (5´->3´)	Product Length
IL-6	TCCAGTTCCTGCAGAAAAAGGCAA	TGGTTCTGTGCCTGCAGCTT	100
IL-8	CCACCGGAAGGAACCATCTCAC	CCTTGGCAAAACTGCACCTTCAC	114
TFRC	TTCAGGTCAAAGACAGCGCTCA	CTATACGCCACATAACCCCCAGG	100

1.3. MTT Assay for Cell Count Quantification

Dimethylthiazolyl Blue Tetrazolium Bromide (MTT) assays were performed to quantify cell count, with a starting cell number of 7.5×10^2 OBs per well in 96-well plates. After 24 h, the cells were treated with and without the cytokines in OIM for up to 21 days. On days 1, 7, 14, and 21, the yellowish MTT was added to the cells in growth medium (0.5 mg/mL) and incubated at 37 °C for 2 h. Viable cells converted the MTT into purple formazan, which was redissolved with dimethyl sulfoxide (DMSO) [52]. The absorbance was measured photometrically at 540 nm.

1.4. BrdU Assay for Cell Proliferation Rate

The proliferation rate of the cells was examined using the colorimetric bromodeoxyuridine (BrdU) kit, manufactured by Roche Holding AG (Basel, Switzerland). In total, 2×10^4 OBs per well were seeded in a 48-well plate. After 48 h of resting time, the cells were treated with OIM in the presence or absence of cytokines with the addition of 10 µM BrdU labeling solution. Following a 48 h incubation period with the cells at 37 °C, the cells were fixed by incubation in FixDenat™ for 30 min. Subsequently, the anti-BrdU-POD working solution was incubated for 90 min. After 15 min of TMB substrate incubation, its

conversion was stopped by adding 1 M sulphuric acid, followed by the measurement in the photometer at 450 nm.

1.1. Seahorse Assay: Evaluation of Oxygen Consumption Rate (OCR) and Extracellular Acidification Rate (ECAR)

For the metabolic assays, all materials were purchased from Agilent Technologies, Inc. (Santa Clara, CA, USA), and the tests were performed according to the manufacturer's instructions, unless otherwise noted. In total, 1.5×10^4 OBs per well were seeded in a 96-well cell culture microplate and after 24 h, the treatment with and without cytokines in OIM was started for 14 days. Oxidative phosphorylation (OXPHOS) was quantified using the Seahorse XF Cell Mito Stress Test Kit (CMST), and glycolysis was quantified using the Seahorse XF Glycolysis Stress Test Kit (GST). Before measurement, cells were incubated in Seahorse XF Base Medium with 2 mM L-glutamine (Gibco® by Life Technologies, Carlsbad, CA, USA) for 30–60 min without CO_2 at 37 °C. The following concentrations of the reagents were used: 1 µM oligomycin, 1 µM carbonyl cyanide-p-trifluoromethoxyphenyl-hydrazone (FCCP), and 1 µM rotenone/antimycin A for the CMST, and 10 mM glucose, 1 µM oligomycin, and 50 mM 2 deoxy-D-glucose (2-DG) for the GST. The oxygen consumption rate (OCR) and the extracellular acidification rate (ECAR) were measured using a Seahorse XFe96 analyzer, and Seahorse Wave Desktop Software (Version 2.6.3) by Agilent Technologies, Inc. (Santa Clara, CA, USA) was used to evaluate the data. After the measurement, the cells were stained for 5 min with 1:1000 diluted Hoechst, and the fluorescence intensity was measured (excitation: 361 nm, emission: 486 nm) to normalize the data to the cell count.

1.2. Microscopic Images

The microscopic images in Figure 1 were taken with the BZ-X810 microscope by Keyence Corporation (Osaka, Japan), and the images in Figures 2 and 3 were taken with the Axiovert 2000 microscope by Carl Zeiss AG (Oberkochen, Germany) at 100× magnification.

1.3. Statistics

The statistical analyses were performed using the GraphPad PRISM 8 software (Boston, MA, USA). The data were treated as non-parametric. Therefore, the Wilcoxon signed-rank test was used for the statistical analysis of paired data, and the Mann–Whitney U test was used for unpaired data. *p*-values lower than 0.05 were considered statistically significant. Details on the respective biological and technical replicates performed are provided in the corresponding figure caption.

Supplementary Materials: The following supporting information can be downloaded at: https://www.mdpi.com/article/10.3390/ijms252212358/s1.

Author Contributions: Conceptualization, J.F.B., C.V.S. and U.M.; Methodology, C.V.S. and J.F.B.; Validation, C.V.S. and J.F.B.; Formal analysis, J.F.B.; Investigation, J.F.B.; Resources, C.B., K.S. and U.M.; Data curation, J.F.B.; Writing—original draft preparation, J.F.B.; Writing—review and editing, C.B., K.S., C.V.S. and U.M.; Visualization, J.F.B.; Supervision, U.M. and C.V.S.; Project administration, U.M. and C.V.S.; Funding acquisition, J.W., U.M. and C.V.S. All authors have read and agreed to the published version of the manuscript.

Funding: This study was not subject to third-party funding and was financed by the Department of Orthopedics and Trauma Surgery, Faculty of Medicine at the University Hospital Düsseldorf, Germany. Christoph Beyersdorf is funded by the FUTURE program of the Deutsche Forschungsgemeinschaft (DFG, German Research Foundation)–493659010.

Institutional Review Board Statement: The study was conducted in accordance with the Declaration of Helsinki, and approved by the local Research Ethics Committee of the Heinrich Heine University Düsseldorf (Study No. 5585R).

Informed Consent Statement: Informed consent was obtained from all subjects involved in the study.

Data Availability Statement: The raw data supporting the conclusions of this article will be made available by the authors on request.

Acknowledgments: Andreas Reichert, Institute for Biochemistry and Molecular Biology I, Medical Faculty, University Hospital Düsseldorf, Heinrich Heine University Düsseldorf, Germany, for providing the Agilent Seahorse XFE96 analyzer.

Conflicts of Interest: The authors declare no conflicts of interest.

References

1. Livshits, G.; Kalinkovich, A. Targeting chronic inflammation as a potential adjuvant therapy for osteoporosis. *Life Sci.* **2022**, *306*, 120847. [CrossRef] [PubMed]
2. Kaur, M.; Nagpal, M.; Singh, M. Osteoblast-n-Osteoclast: Making Headway to Osteoporosis Treatment. *Curr. Drug Targets* **2020**, *21*, 1640–1651. [CrossRef] [PubMed]
3. Ashai, S.; Harvey, N.C. Rheumatoid arthritis and bone health. *Clin. Med.* **2020**, *20*, 565–567. [CrossRef] [PubMed]
4. Magrey, M.; Khan, M.A. Osteoporosis in Ankylosing Spondylitis. *Curr. Rheumatol. Rep.* **2010**, *12*, 332–336. [CrossRef] [PubMed]
5. Hadjidakis, D.J.; Androulakis, I.I. Bone remodeling. *Ann. N. Y. Acad. Sci.* **2006**, *1092*, 385–396. [CrossRef]
6. Okamoto, K.; Takayanagi, H. Osteoimmunology. *Cold Spring Harb. Perspect. Med.* **2019**, *9*, a031245. [CrossRef] [PubMed]
7. Epsley, S.; Tadros, S.; Farid, A.; Kargilis, D.; Mehta, S.; Rajapakse, C.S. The Effect of Inflammation on Bone. *Front. Physiol.* **2021**, *11*, 511799. [CrossRef]
8. Kushioka, J.; Chow, S.K.-H.; Toya, M.; Tsubosaka, M.; Shen, H.; Gao, Q.; Li, X.; Zhang, N.; Goodman, S.B. Bone regeneration in inflammation with aging and cell-based immunomodulatory therapy. *Inflamm. Regen.* **2023**, *43*, 29. [CrossRef]
9. Rutkovskiy, A.; Stensløkken, K.-O.; Vaage, I.J. Osteoblast Differentiation at a Glance. *Med. Sci. Monit. Basic Res.* **2016**, *22*, 95–106. [CrossRef]
10. Hojo, H.; Ohba, S.; Chung, U.-I. Signaling pathways regulating the specification and differentiation of the osteoblast lineage. *Regen. Ther.* **2015**, *1*, 57–62. [CrossRef]
11. Amarasekara, D.S.; Kim, S.; Rho, J. Regulation of Osteoblast Differentiation by Cytokine Networks. *Int. J. Mol. Sci.* **2021**, *22*, 2851. [CrossRef] [PubMed]
12. Xu, J.; Yu, L.; Liu, F.; Wan, L.; Deng, Z. The effect of cytokines on osteoblasts and osteoclasts in bone remodeling in osteoporosis: A review. *Front. Immunol.* **2023**, *14*, 1222129. [CrossRef]
13. Sonomoto, K.; Yamaoka, K.; Oshita, K.; Fukuyo, S.; Zhang, X.; Nakano, K.; Okada, Y.; Tanaka, Y. Interleukin-1β induces differentiation of human mesenchymal stem cells into osteoblasts via the Wnt-5a/receptor tyrosine kinase–like orphan receptor 2 pathway. *Arthritis Rheum.* **2012**, *64*, 3355–3363. [CrossRef]
14. Huang, J.; Chen, L. IL-1β inhibits osteogenesis of human bone marrow-derived mesenchymal stem cells by activating FoxD3/microRNA-496 to repress wnt signaling. *Genesis* **2017**, *55*, e23040. [CrossRef] [PubMed]
15. Osta, B.; Benedetti, G.; Miossec, P. Classical and Paradoxical Effects of TNF-α on Bone Homeostasis. Front. *Immunol.* **2014**, *5*, 48. [CrossRef]
16. Yang, A.; Lu, Y.; Xing, J.; Li, Z.; Yin, X.; Dou, C.; Dong, S.; Luo, F.; Xie, Z.; Hou, T.; et al. IL-8 Enhances Therapeutic Effects of BMSCs on Bone Regeneration via CXCR2-Mediated PI3k/Akt Signaling Pathway. Cell. Physiol. Biochem. *Int. J. Exp. Cell Physiol. Biochem. Pharmacol.* **2018**, *48*, 361–370. [CrossRef] [PubMed]
17. Agilent Technologies, Inc. Seahorse XF Glycolysis Stress Test Kit User Guide. Published online October 2019. Available online: https://www.agilent.com/cs/library/usermanuals/public/XF_Glycolysis_Stress_Test_Kit_User_Guide.pdf (accessed on 4 April 2024).
18. Amarasekara, D.S.; Yun, H.; Kim, S.; Lee, N.; Kim, H.; Rho, J. Regulation of Osteoclast Differentiation by Cytokine Networks. *Immune Netw.* **2018**, *18*, e8. [CrossRef]
19. Ye, F.; Li, J.; Xu, P.; Xie, Z.; Zheng, G.; Liu, W.; Ye, G.; Yu, W.; Lin, J.; Su, Z.; et al. Osteogenic differentiation of mesenchymal stem cells promotes c-Jun-dependent secretion of interleukin 8 and mediates the migration and differentiation of CD4+ T cells. *Stem Cell Res. Ther.* **2022**, *13*, 58. [CrossRef]
20. Liu, X.; Chen, Z.; Lan, T.; Liang, P.; Tao, Q. Upregulation of interleukin-8 and activin A induces osteoclastogenesis in ameloblastoma. *Int. J. Mol. Med.* **2019**, *43*, 2329–2340. [CrossRef]
21. Mukaida, N.; Mahe, Y.; Matsushima, K. Cooperative interaction of nuclear factor-kappa B- and cis-regulatory enhancer binding protein-like factor binding elements in activating the interleukin-8 gene by pro-inflammatory cytokines. *J. Biol. Chem.* **1990**, *265*, 21128–21133. [CrossRef]
22. Choi, H.M.; Oh, D.H.; Bang, J.S.; Yang, H.-I.; Yoo, M.C.; Kim, K.S. Differential effect of IL-1β and TNF-α on the production of IL-6, IL-8 and PGE2 in fibroblast-like synoviocytes and THP-1 macrophages. *Rheumatol. Int.* **2010**, *30*, 1025–1033. [CrossRef] [PubMed]
23. Ferreira, E.; Porter, R.M.; Wehling, N.; O'Sullivan, R.P.; Liu, F.; Boskey, A.; Estok, D.M.; Harris, M.B.; Vrahas, M.S.; Evans, C.H.; et al. Inflammatory Cytokines Induce a Unique Mineralizing Phenotype in Mesenchymal Stem Cells Derived from Human Bone Marrow. *J. Biol. Chem.* **2013**, *288*, 29494–29505. [CrossRef] [PubMed]

24. Chang, M.K.; Raggatt, L.-J.; Alexander, K.A.; Kuliwaba, J.S.; Fazzalari, N.L.; Schroder, K.; Maylin, E.R.; Ripoll, V.M.; Hume, D.A.; Pettit, A.R. Osteal Tissue Macrophages Are Intercalated throughout Human and Mouse Bone Lining Tissues and Regulate Osteoblast Function In Vitro and In Vivo. *J. Immunol.* **2008**, *181*, 1232–1244. [CrossRef]
25. Meniailo, M.E.; Malashchenko, V.V.; Shmarov, V.A.; Gazatova, N.D.; Melashchenko, O.B.; Goncharov, A.G.; Seledtsova, G.V.; Seledtsov, V.I. Interleukin-8 favors pro-inflammatory activity of human monocytes/macrophages. *Int. Immunopharmacol.* **2018**, *56*, 217–221. [CrossRef]
26. Borciani, G.; Montalbano, G.; Baldini, N.; Cerqueni, G.; Vitale-Brovarone, C.; Ciapetti, G. Co–culture systems of osteoblasts and osteoclasts: Simulating in vitro bone remodeling in regenerative approaches. *Acta Biomater.* **2020**, *108*, 22–45. [CrossRef]
27. Frost, A.; Jonsson, K.B.; Nilsson, O.; Ljunggren, Ö. Inflammatory cytokines regulate proliferation of cultured human osteoblasts. *Acta Orthop. Scand.* **1997**, *68*, 91–96. [CrossRef] [PubMed]
28. Ghali, O.; Chauveau, C.; Hardouin, P.; Broux, O.; Devedjian, J.-C. TNF-α's effects on proliferation and apoptosis in human mesenchymal stem cells depend on RUNX2 expression. *J. Bone Miner. Res.* **2010**, *25*, 1616–1626. [CrossRef] [PubMed]
29. Lange, J.; Sapozhnikova, A.; Lu, C.; Hu, D.; Li, X.; Miclau, T.; Marcucio, R.S. Action of IL-1β during fracture healing. *J. Orthop. Res.* **2010**, *28*, 778–784. [CrossRef]
30. Shen, L.; Hu, G.; Karner, C.M. Bioenergetic Metabolism in Osteoblast Differentiation. *Curr. Osteoporos. Rep.* **2022**, *20*, 53–64. [CrossRef] [PubMed]
31. Shum, L.C.; White, N.S.; Mills, B.N.; de Mesy Bentley, K.L.; Eliseev, R.A. Energy Metabolism in Mesenchymal Stem Cells During Osteogenic Differentiation. *Stem Cells Dev.* **2016**, *25*, 114–122. [CrossRef]
32. Chen, C.-T.; Shih, Y.-R.V.; Kuo, T.K.; Lee, O.K.; Wei, Y.-H. Coordinated Changes of Mitochondrial Biogenesis and Antioxidant Enzymes During Osteogenic Differentiation of Human Mesenchymal Stem Cells. *Stem Cells* **2008**, *26*, 960–968. [CrossRef] [PubMed]
33. Guntur, A.R.; Le, P.T.; Farber, C.R.; Rosen, C.J. Bioenergetics During Calvarial Osteoblast Differentiation Reflect Strain Differences in Bone Mass. *Endocrinology* **2014**, *155*, 1589–1595. [CrossRef] [PubMed]
34. Guntur, A.R.; Gerencser, A.A.; Le, P.T.; DeMambro, V.E.; Bornstein, S.A.; Mookerjee, S.A.; Maridas, D.E.; Clemmons, D.E.; Brand, M.D.; Rosen, C.J. Osteoblast-like MC3T3-E1 Cells Prefer Glycolysis for ATP Production but Adipocyte-like 3T3-L1 Cells Prefer Oxidative Phosphorylation. *J. Bone Miner. Res.* **2018**, *33*, 1052–1065. [CrossRef] [PubMed]
35. Pike Winer, L.S.; Wu, M. Rapid Analysis of Glycolytic and Oxidative Substrate Flux of Cancer Cells in a Microplate. *PLoS ONE* **2014**, *9*, e109916. [CrossRef]
36. Kumar, S.; Votta, B.J.; Rieman, D.J.; Badger, A.M.; Gowen, M.; Lee, J.C. IL-1- and TNF-induced bone resorption is mediated by p38 mitogen activated protein kinase. *J. Cell. Physiol.* **2001**, *187*, 294–303. [CrossRef]
37. Nishimoto, N.; Hashimoto, J.; Miyasaka, N.; Yamamoto, K.; Kawai, S.; Takeuchi, T.; Murata, N.; van der Heijde, D.; Kishimoto, T. Study of active controlled monotherapy used for rheumatoid arthritis, an IL-6 inhibitor (SAMURAI): Evidence of clinical and radiographic benefit from an x ray reader-blinded randomised controlled trial of tocilizumab. *Ann. Rheum. Dis.* **2007**, *66*, 1162–1167. [CrossRef]
38. Vis, M.M.; Havaardsholm, A.E.; Haugeberg, G.; Uhlig, T.; Voskuyl, A.E.; Van De Stadt, R.J.; Dijkmans, B.A.C.; Woolf, A.; Kvien, T.K.; Lems, W.F. Evaluation of bone mineral density, bone metabolism, osteoprotegerin and receptor activator of the NF B ligand serum levels during treatment with infliximab in patients with rheumatoid arthritis. *Ann. Rheum. Dis.* **2006**, *65*, 1495–1499. [CrossRef]
39. Musacchio, E.; Valvason, C.; Botsios, C.; Ostuni, F.; Furlan, A.; Ramonda, R.; Modesti, V.; Sartori, L.; Punzi, L. The Tumor Necrosis Factor-α-blocking Agent Infliximab Inhibits Interleukin 1ß (IL-1ß) and IL-6 Gene Expression in Human Osteoblastic Cells. *J. Rheumatol.* **2009**, *36*, 1575–1579. [CrossRef]
40. Loeser, R.F.; Goldring, S.R.; Scanzello, C.R.; Goldring, M.B. Osteoarthritis: A Disease of the Joint as an Organ. *Arthritis Rheum.* **2013**, *64*, 1697–1707. [CrossRef]
41. Mountziaris, P.M.; Mikos, A.G. Modulation of the Inflammatory Response for Enhanced Bone Tissue Regeneration. *Tissue Eng. Part B Rev.* **2008**, *14*, 179–186. [CrossRef]
42. Sokolove, J.; Lepus, C.M. Role of inflammation in the pathogenesis of osteoarthritis: Latest findings and interpretations. *Ther. Adv. Musculoskelet. Dis.* **2013**, *5*, 77–94. [CrossRef] [PubMed]
43. Torzilli, P.A.; Bhargava, M.; Park, S.; Chen, C.T.C. Mechanical load inhibits IL-1 induced matrix degradation in articular car-tilage. *Osteoarthritis Cartilage.* **2010**, *18*, 97–105. [CrossRef] [PubMed]
44. Fu, S.; Thompson, C.L.; Ali, A.; Wang, W.; Chapple, J.P.; Mitchison, H.M.; Beales, P.L.; Wann, A.K.T.; Knight, M.M. Mechanical loading inhibits cartilage inflammatory signalling via an HDAC6 and IFT-dependent mechanism regulating primary cilia elongation. *Osteoarthritis Cartilage.* **2019**, *27*, 1064–1074. [CrossRef] [PubMed]
45. Kanis, J.A. Diagnosis of osteoporosis and assessment of fracture risk. *Lancet Lond. Engl.* **2002**, *359*, 1929–1936. [CrossRef]
46. Neidlinger-Wilke, C.; Stalla, I.; Claes, L.; Brand, R.; Hoellen, I.; Rübenacker, S.; Arand, M.; Kinzl, L. Human osteoblasts from younger normal and osteoporotic donors show differences in proliferation and TGFβ-release in response to cyclic strain. *J. Biomech.* **1995**, *28*, 1411–1418. [CrossRef]
47. Robey, P.G.; Termine, J.D. Human bone cells in vitro. *Calcif. Tissue Int.* **1985**, *37*, 453–460. [CrossRef]
48. Jaiswal, N.; Haynesworth, S.E.; Caplan, A.I.; Bruder, S.P. Osteogenic differentiation of purified, culture-expanded human mesenchymal stem cells in vitro. *J. Cell. Biochem.* **1997**, *64*, 295–312. [CrossRef]

49. Puchtler, H.; Meloan, S.N.; Terry, M.S. On the history and mechanism of alizarin and alizarin red s stains for calcium. J. Histochem. *Cytochem. Off. J. Histochem. Soc.* **1969**, *17*, 110–124. [CrossRef]
50. Sabokbar, A.; Millett, P.J.; Myer, B.; Rushton, N. A rapid, quantitative assay for measuring alkaline phosphatase activity in osteoblastic cells in vitro. *Bone Miner.* **1994**, *27*, 57–67. [CrossRef]
51. Livak, K.J.; Schmittgen, T.D. Analysis of relative gene expression data using real-time quantitative PCR and the $2-\Delta\Delta CT$ Method. *Methods* **2001**, *25*, 402–408. [CrossRef]
52. Van Merloo, J.; Kaspers, G.J.; Cloos, J. Cell sensitivity assays: The MTT assay. *Methods Mol. Biol.* **2011**, *731*, 237–245. [CrossRef]

2.3. Supplementary Materials of the Publication

Supplements

List of Tables:

Supplementary Table S1: Information about the donors involved in the study, including age, sex, condition, medications, and the list of the experiments in which the donor cells were used.

List of Figures:

Supplementary Figure S1: Influence of the applied concentrations of the cytokines (A) IL-1β, (B) IL-6, (C) IL-8, and (D) TNF-α (see Figure 2) on the cell count (n = 3), determined by MTT assay.

Supplementary Figure S2: Influence of donor age and sex on mineralization and ALP activity of osteoblast-like cells *in vitro*.

Supplementary Figure S3: Influence of donor age and sex on IL-6 and IL-8 secretion of osteoblast-like cells *in vitro*.

Supplementary Figure S4: Influence of donor age on the cell count during osteogenesis with and without cytokine treatment of osteoblast-like cells *in vitro*.

Supplementary Table S1: Information about the donors involved in the study, including age, sex, condition, medications, and the list of the experiments in which the donor cells were used.

	age	sex	condition	medication	experiments
1	70	f	coxarthrosis	Cotrimoxazol, Carvedilol, Pantoprazol, Torasemid, Digitoxin, Xipamid, ASS, Prednisolon, Trospiumchlorid, Sevelamer, Levemir	A, C, D, S
2	83	f	coxarthrosis	Allopurinol, Ferrosanol, Estradiol, Lansoprazol, Metformin, Doxepin, Gabapentin, Circadin, Atorvastatin, Folsäure, Torasemid, Doxazosin, Eliquis	A, C, D, H
3	78	f	coxarthrosis	ASS, Atorvastatin, Metoprolol, Ramipril, HVT, Lercanidipin, Pantoprazol	A, D, H
4	77	f	fracture	Amiodaron, Candecor, Nebivolol, Nexium, L-Thyroxin, Simvastatin, Spiolto, Eliquis, Torasemid	A. H
5	54	f	coxarthrosis	ASS, Omeprazol, Zanipress	A, C, D, E, H
6	56	m	coxarthrosis		A, B, C, E, H
7	88	m	fracture	Marcumar, Ferrosanol, Allopurinol, Amlodipin, Xipamid, Bicanorm	A, C, D, E, H
8	70	m	coxarthrosis		A, C, D, E, H
9	78	m	fracture	L-Thyroxin, Ramipril, Atorvastatin, Metohexal, Dostinex, Pantoprazol, Mirtazapin, Ergenyl Chrono, Amlodipin, Hydrocortison, Tamsublock, Duo, Spasmex, Macrogol, Restex	A, E
10	77	f	coxarthrosis	Lercanidipin, Metohexal, Opipramol, Simvahexal, Candesartan, Torem	A, D, E, F, G, H, I
11	55	f	coxarthrosis	Amlodipin, Doxepin, Pantozol, Lisihexal	A, C, E
12	60	f	coxarthrosis		A, B, C, F, G, H, I, J
13	79	m	fracture	Amiodaron, Atorvastatin, Metoprolol, Apixaban, ASS, Torasemid, Spironolacton, Foster Spray, Tamsulosin, Allopurinol, Zopiclon, EPO	A, B, D, F, H, I
14	66	f	coxarthrosis	Ramipril, Amlodipin, Triamtorem/HCT	B, F
15	57	f	coxarthrosis		B, G, H, J
16	57	f	coxarthrosis		C, E, H
17	67	m	coxarthrosis	Enalapril	C, D, H, S
18	50	f	coxarthrosis	Pantoprazol, Venlaflaxin, Ramipril, Metoprolol, HCT, L-Thyroxin, Hydromophon	C, F, G, H, I
19	64	m	coxarthrosis		E
20	77	f	fracture	Amiodaron, Candecor, Nebivolol, Nexium, L-Thyroxin, Simvastatin, Spiolto, Eliquis, Torasemid	E
21	69	f	coxarthrosis	Pantoprazol, L-Thyroxin, Valsartan, Spasmex	F, H, I
22	31	f	coxarthrosis		G, H, I, J
23	55	f	coxarthrosis	Amlodipin, Doxepin, Pantozol, Lisihexal	B, F, I
24	77	f	fracture	Marcumar, ASS, Amiodaron, Bisoprolol, Pantozol, Rosuvastatin, Ezetimib, Azopt	F, G, H, I
25	63	m	fracture	Xarelto, ASS, Metoprolol, Ramipril, Torem, Simvastatin, Citalopram, Mirtazaptin, Foster Spray	I

26	53	f	coxarthrosis	ASS, Ramipril, Pantozol, Torasemid, Spironolacton, Metoprolol, Digitoxin, Lercanidipin, Atorvastatin	I
27	65	f	coxarthrosis	N.A.	J
28	81	f	coxarthrosis	N.A.	J
Only included in supplemental results (Fig. 2)					
29	97	f	coxarthrosis	Amlodipin, Folsan, Novalgin, Ramipril, Tilidin, Torasemid, Zopiclon, Paracetamol, Tinzaparin	S

Experiment legend:

A mineralization (Fig. 2 A)

B ALP activity (Fig. 2 B)

C IL-6/IL-8 secretion (Fig. 2 D/E)

D mineralization with cytokines (Fig. 3)

E IL-6/IL-8 mRNA expression (Fig. 4)

F cell count with cytokines during osteogenesis (Fig. 5 A-D)

G proliferation rate with cytokines (Fig. 5 E)

H oxidative phosphorylation (Fig. 6)

I glycolysis (Fig. 7)

J ALP activity with cytokines (Fig. 3)

S cell count with cytokine concentrations in Supplements (Suppl. Fig. 1)

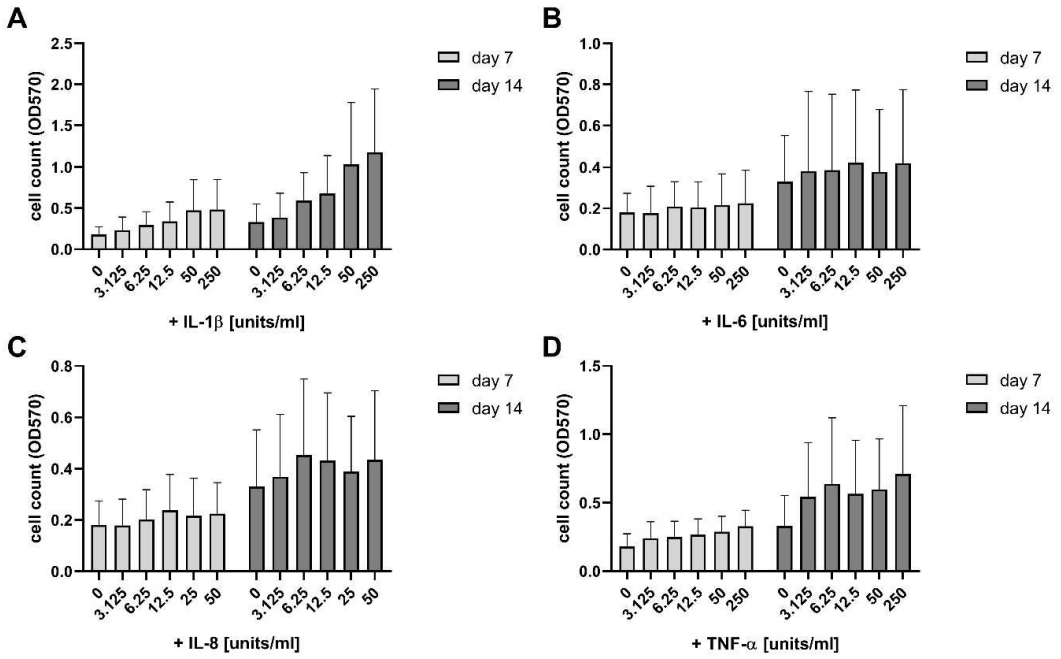

Supplementary Figure S1: Influence of the applied concentrations of the cytokines (A) IL-1β, (B) IL-6, (C) IL-8, and (D) TNF-α (see Figure 2) on the cell count (n = 3), determined by MTT assay.

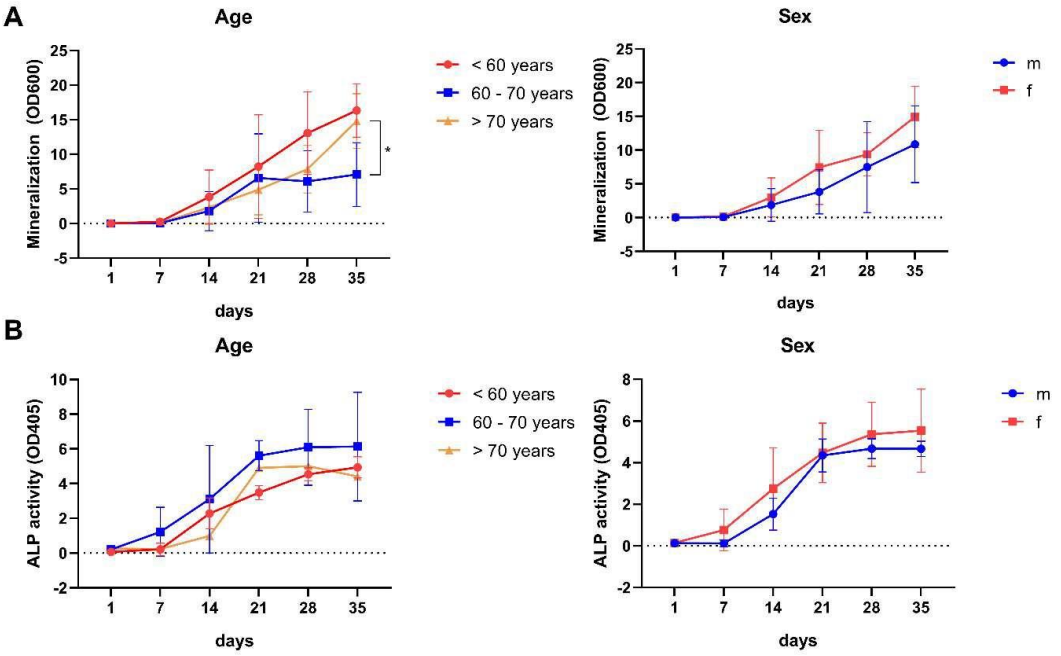

Supplementary Figure S2: Influence of donor age and sex on mineralization and ALP activity of osteoblast-like cells *in vitro*. (A) The results of Fig. 2 A were divided into three age

and female (n = 8). (B) The results of Figure 2 B were divided into three age groups, < 60 years (n = 3), 60 – 70 years (n = 2), and > 70 years (n = 1), and by sex: male (n = 2) and female (n = 4). Mean with SD is shown and Mann-Whitney U tests were performed ($p \leq 0.05$ (*)).

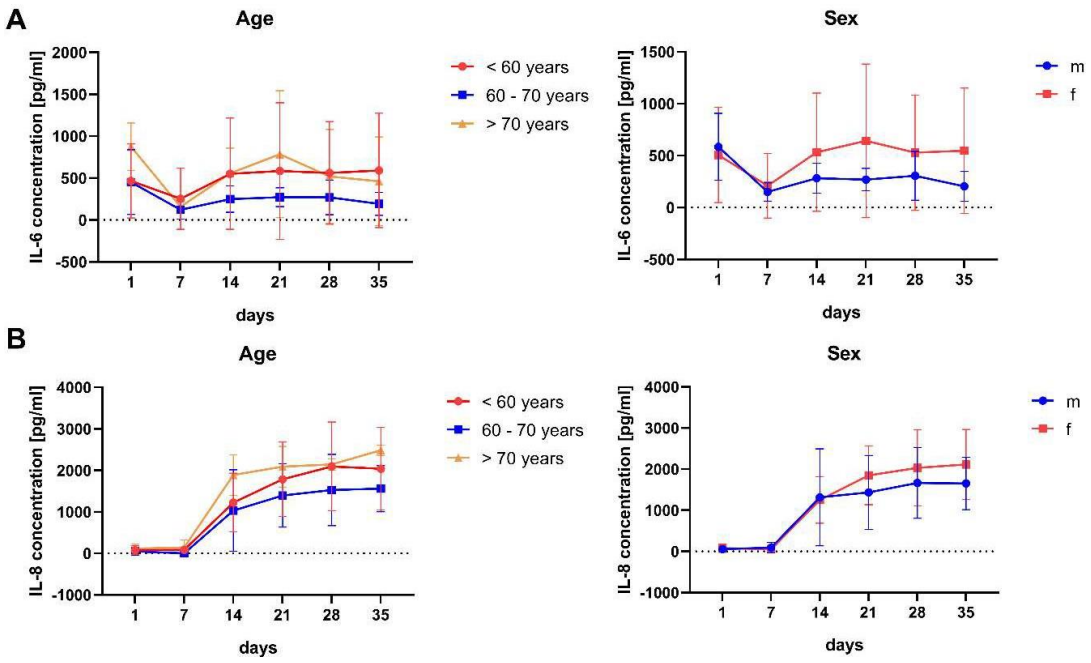

Supplementary Figure S3: Influence of donor age and sex on IL-6 and IL-8 secretion of osteoblast-like cells *in vitro*. The results of (A) IL-6 secretion in Fig. 2 D and (B) IL-8 secretion in Fig. 2 E were divided into three age groups, < 60 years (n = 5), 60 – 70 years (n = 4), and > 70 years (n = 2), and by sex: male (n = 4) and female (n = 7).

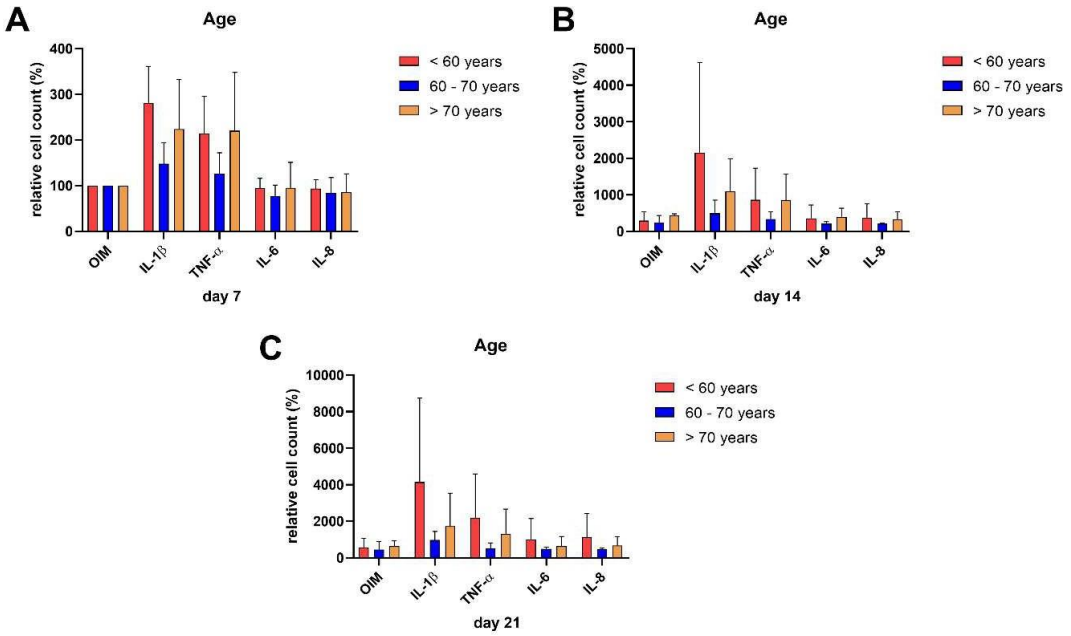

Supplementary Figure S4: Influence of donor age on the cell count during osteogenesis with and without cytokine treatment of osteoblast-like cells *in vitro*. The results of Fig. 5 A-C were divided into three age groups, < 60 years (n = 2), 60 – 70 years (n = 3), and > 70 years (n = 3).

3. Supplementary Material and Methods and Results

3.1. Supplementary Materials and Methods

3.1.1. Materials

3.1.1.1. Cells

The human BMSCs used in this work were purchased from the Unfallchirurgische Klinik at the Medizinische Hochschule Hannover (Univ.-Prof. Dr. med. Christian Krettek). All BMSCs used in this work were classified by FACS and tested positive for osteogenic, adipogenic, and chondrogenic differentiation potential.

The human fetal osteoblast cell line hFOB 1.19 (CRL-3602™) was purchased from ATCC® (Manassas, VA, USA). The cells were immortalized by the transfection with a temperature sensitive expression vector (pUCSVtsA58) with the SV40 large T antigen and a neomycin (G418) resistance expression vector (pSV2-neo). The cells are characterized by the expression of alkaline phosphatase.

3.1.1.2. Oligonucleotides for qPCR

Except for *Col1α2* (Collagen type I α 2 chain), which was purchased by OriGene Technologies, Inc. (Rockville, MD, USA), the primer sequences were self-designed. The web-based tool Primer-BLAST by NCBI (Bethesda, MD, USA) was used to find suitable primers for the target genes (see Table 3.1). Primers were then selected to be as comparable as possible in terms of PCR product length (between 100 – 130 bp) and melting temperature (62 – 64 °C). In addition, exon-exon junction spanning primers with low GC content (< 60%) were selected if possible. Each primer pair was then tested for non-specific binding in the agarose gel and the most efficient concentration of primers and cDNA for each was tested in qPCR. All qPCR analyses were performed in triplicates and outliers (deviation > 0.5) were removed from the analysis.

Table 3.1: List of primers used for qPCR.

Target Gene	***Forward Primer (5'->3')***	***Reverse Primer (5'->3')***	***Product Length***
ALP (Alkaline phosphatase)	GCAGGCAGCTTGAC CTCCTC	GCATGGGGGCCAG ACCAAAG	121
Col1α2 (Collagen type I α 2 chain)	CCTGGTGCTAAAGG AGAAAGAGG	ATCACCACGACTT CCAGCAGGA	135
Runx2 (Runt-related transcription factor 2)	AGTGGACGAGGCAA GAGTTT	TGTCTGTGCCTTC TGGGTTC	125
OPN (Osteopontin)	CACTCCAGTTGTCC CCACAGTAG	TCTGTAGCATCAG GGTACTGGATGT	120
OCN (Osteocalcin)	CTCCTCGCCCTATT GGCCCT	CTGCTTGGACACA AAGGCTGC	105
OSX (Osterix)	TGGGGAAGGCTTTC TCTAGGATCA	TCTCAGGGCTTCT AGGCACCAG	100
TGFβ-RII (Transforming Growth Factor β – receptor II)	AGCACCCCTGTGTC GAAAGC	CACACCATCTGGA TGCCCTGG	103
IL-6 (Interleukin-6)	TCCAGTTCCTGCAG AAAAAGGCAA	TGGTTCTGTGCCT GCAGCTT	100
IL-8 (Interleukin-8)	CCACCGGAAGGAAC CATCTCAC	CCTTGGCAAAACT GCACCTTCAC	114

Good reference genes are characterized by their stable expression in the respective cell type and the treatments used. The expression stability (M value) of five different candidate genes (see Table 3.2) were tested for OBs and hFOB 1.19 cells during osteogenesis. The web-based tool RefFinder was used, which summarizes the results of four different methods to find the best reference gene (BestKeeper, NormFinder, Genorm, and the comparative delta-Ct method). If the M value is < 1.5, the gene can be assumed to be a good reference gene (Yu et al., 2019). Based on the

resulting recommendations (see Fig. 3.1), *TFRC* (transferrin receptor 1) was used as a reference gene for the qPCR analysis of OBs and *RPLP0* (ribosomal protein lateral stalk subunit P0) was used for the analysis of hFOB 1.19 cells.

A

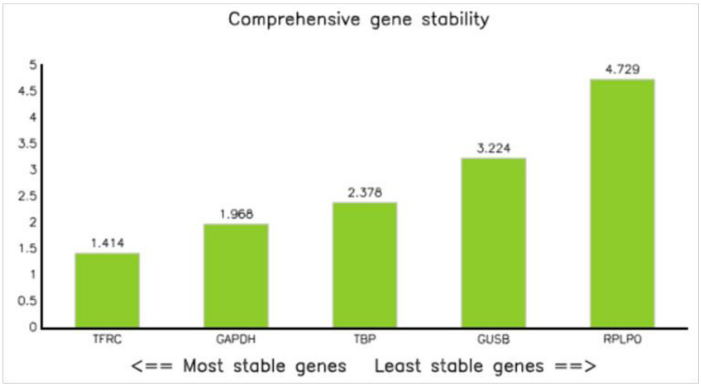

Method	1	2	3	4	5
Delta CT	GAPDH	TFRC	GUSB	TBP	RPLP0
BestKeeper	TFRC	TBP	GUSB	RPLP0	GAPDH
Normfinder	GAPDH	TFRC	GUSB	TBP	RPLP0
Genorm	TBP/TFRC		GAPDH	GUSB	RPLP0
Recommended	**TFRC**	GAPDH	TBP	GUSB	RPLP0

B

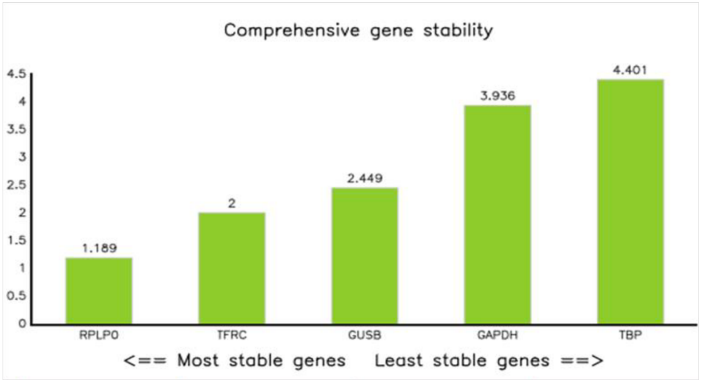

Method	1	2	3	4	5
Delta CT	RPLP0	TFRC	GUSB	GAPDH	TBP
BestKeeper	TFRC	RPLP0	TBP	GUSB	GAPDH
Normfinder	RPLP0	TFRC	GUSB	GAPDH	TBP
Genorm	RPLP0/GUSB		GAPDH	RFRC	TBP
Recommended	**RPLP0**	TFRC	GUSB	GAPDH	TBP

Figure 3.1: Recommended reference genes von dem web-based tool RefFinder. Based on the qPCR results the RefFinder tool recommends the reference genes (A) *TFRC* for OBs and (B) *RPLP0* for hFOB 1.19 cells, based on the M value < 1.5. Source: https://blooge.cn/RefFinder/

Table 3.2: List of tested reference genes for qPCR.

Target Gene	*Forward Primer (5'->3')*	*Reverse Primer (5'->3')*	*Product Length*
TFRC (Transferrin-receptor 1)	TTCAGGTCAAAGACAGCGCTCA	CTATACGCCACATAACCCCCAGG	100
RPLP0 (Ribosomal protein lateral stalk subunit P0)	TTCTCGCTTCCTGGAGGGTGT	CCAGGACTCGTTTGTACCCGT	113
GUSB (β-glucuronidase)	CGAACGGGAGGTGATCCTGC	CGACCCCATTCACCCACACG	110
GAPDH (Glyceraldehyde 3-phosphate dehydrogenase)	GAAGGCTGGGGCTCATTTG	CAGGAGGCATTGCTGATGATC	138
TBP (TATA-binding protein)	TGTATCCACAGTGAATCTTGGTTG	GGTTCGTGGCTCTCTTATCCTC	124

3.1.1.3. Antibodies

Table 3.3: List of primary antibodies used for Western Blot.

Protein	*Host*	*Company*	*Ref. No.*
β-catenin	Rabbit	Abcam	Ab16051
p38 MAPK (Mitogen activated protein kinase)	Rabbit	Cell Signaling	9212
p-p38 MAPK (Phospho-MAPK)	Rabbit	Cell Signaling	9211

Merck (Darmstadt, Germany), Cell Signaling Technology (Cambridge, UK), Abcam (Cambridge, UK), Invitrogen (Waltham, MA, USA).

Table 3.4: List of secondary antibodies used for Western Blot.

Product	*Host/Reactivity*	*Company*	*Ref. No.*
Polyclonal Immunoglobulins/HRP	Goat Anti-Rabbit	Dako	P0448
Polyclonal Immunoglobulins/HRP	Goat Anti-Mouse	Dako	P0447

Dako by Agilent Technologies (Santa Clara, CA, USA).

3.1.1.4. Recombinant Proteins

Protein Name	*Company*	*Ref. No.*
Human IL-1β	PeproTech	200-01B
Human IL-6	PeproTech	200-06
Human IL-8	PeproTech	200-08M
Human TNF-α	PeproTech	300-01A
Human IFNγ	PeproTech	300-02

PeproTech GmbH by Thermo Fisher Scientific (Waltham, MA, USA).

3.1.1.5. Kits

Product	*Company*	*Ref. No.*
Omniascript® RT Kit	QIAGEN	205113
RNeasy® Mini Kit	QIAGEN	74106
QIAshredder	QIAGEN	79656
Cell Proliferation ELISA, BrdU	Roche	11647229001
PCR Kit	QIAGEN	201225
RNAse-free DNAse Set	QIAGEN	79254
Seahorse (SH) XF Glycolysis Stress Test Kit	Agilent	103020-100
SH XF Cell Mito Stress Test Kit	Agilent	103015-100

SH XF DMEM Medium, pH 7.4	Agilent	103575-100
SH XFe96/XF Pro Pro FluxPak	Agilent	103792-100
SH XFe96/XF Pro Cell Culture Microplates	Agilent	103794-100
SH XF Calibrant (pH 7.4)	Agilent	100840-000
Pierce™ BCA Protein Assay Kit	Thermo Scientific	23227

QIAGEN (Hilden, Germany), Roche (Basel, Switzerland), Agilent Technologies (Santa Clara, CA, USA), Thermo Fisher Scientific (Waltham, MA, USA).

3.1.1.6. Media and Additives for Eukaryotic Cell Culture

Product	*Company*	*Ref. No.*
Dulbecco's Modified Eagle Medium (DMEM)	Gibco	41965
FBS Superior	Sigma	S0615
Dulbecco's Phosphate Buffered Saline (PBS)	Sigma	D8537
Penicillin-Streptomycin	Gibco	P06-07100
Dexamethasone	Sigma	D2915
L-Ascorbic-2-Phosphate	Sigma	A8960
β-Glycerophosphate	Sigma	G9422
HEPES solution	Sigma	H0887
Trypsin-EDTA Solution	Sigma	T4174
DMEM/F-12 (1:1), -Phenol Red	Gibco	21041-025
Fibroblast growth factor 2 (FGF2)	PeproTech	100-18B
G 418 disulfate salt solution	Sigma	G8168
Collagenase Type IV	Gibco	17104-019
L-Glutamine 200 mM	Gibco	25030-024

Sigma-Aldrich (St. Louis, MO, USA), Gibco® by Life Technologies™ (Carlsbad, CA, USA), PeproTech GmbH by Thermo Fisher Scientific (Waltham, MA, USA).

3.1.1.7. Media and Buffer Composition

Table 3.5: Composition of Media and Buffer.

Media/Buffer	***Composition***
OB Growth Medium	500 mL DMEM (4,5 g/L Glucose, 1% Glutamine), 10% (v/v) FCS, 1% (v/v) Pen/Strep, 1% (v/v) HEPES
BMSC Growth Medium	500 mL DMEM (4,5 g/L Glucose, 1% Glutamine), 10% (v/v) FCS, 1% (v/v) Pen/Strep, 1% (v/v) HEPES, 2 ng/mL FGF2
hFOB 1.19 Growth Medium	500 mL F-12, 10% (v/v) FCS, 0.3 mg/mL G184
OB and BMSC Osteogenesis induction medium (OIM)	500 mL DMEM (4,5 g/L Glucose, 1% Glutamine), 10% (v/v) FCS, 1% (v/v) Pen/Strep, 500 nM Dexamethasone, 50 µM L-Ascorbin-2-Phosphate, 10 mM β-Glycerophosphate
hFOB 1.19 OIM	500 mL F-12, 10% (v/v) FCS, 0.3 mg/mL G184, 500 nM Dexamethasone, 50 µM L-Ascorbin-2-Phosphate, 10 mM β-Glycerophosphate
RIPA Lysis Buffer	50 mM Tris, 150 mM NaCl, 1% (w/v) NP-40, 0.5% (w/v) Na-Deoxycholate, 0.1% (w/v) SDS in H_2O
4 x Laemmli Buffer	252 mM Tris-HCl, 40% (v/v) Glycerol, 8% (w/v) SDS, 0.01% (w/v) Bromophenol blue in H_2O
SDS-PAGE Running Buffer	25 mM Tris, 192 mM Glycine, 0.1% (w/v) SDS in H_2O (pH = 8.3 - 8.8)
Tris-Glycine Transfer Buffer	12 mM Tris-Base, 96 mM Glycine in H_2O
TBS-T Buffer	7.7 mM Tris, 150 mM NaCl (pH = 7.5)

3.1.1.8. Additional Material

Product	*Company*	*Ref. No.*
Alizarin Red S mono sodium salt	Sigma	1.06278.0100
Cetylpyridinium Chlorid Monohydrate (CPC)	Santa Cruz	sc-239495B
ROTI®-Histofix 4%	Roth	P087.5
CellTiter-Blue® Cell Viability Assay	Promega	G8081
Thiazolyl Blue Tetrazolium Bromide (MTT)	Sigma	M2128
Dimethyl sulfoxide (DMSO)	Sigma	D8418
4-Nitrophenol solution	Sigma	N7660
Power SYBR® Green PCR Master Mix	Invitrogen	4368702
dNTP-Mix	QIAGEN	201901
Blotting membrane	Invitrogen	LC2010
Immobilon Forte Western HRP Substrate	Sigma	WBLUF0100
Hoechst 33342	Invitrogen	H3570
Loading Dye	Invitrogen	R0621
ROTIMark Western Plus	Roth	2245.2
Milk Powder	Roth	T145.2
Blotting Filter Paper	Invitrogen	LC2010
Bovines Serumalbumin (BSA) Fraktion V	Roth	8076.3
TWEEN®20	Sigma	P9416
Triton™ X-100	Sigma	T8787
TRIS PUFFERAN®	Roth	AE15.2
Mini-PROTEAN TGX Stain-Free Gels 4-20%	BIO-RAD	4568096
Mini-PROTEAN TGX Stain-Free Gels 4-15%	BIO-RAD	4568083
cOmplete™ Protease-Inhibitor Cocktail	Roche	4693159001

Sigma-Aldrich (St. Louis, MO, USA), Santa Cruz Biotechnology (Dallas, TX, USA), Carl Roth (Karlsruhe, Germany), Promega (Madison, WI, USA), Invitrogen (Waltham, MA,

USA), QIAGEN (Hilden, Germany), Bio-Rad (Hercules, CA, USA), Roche (Basel, Switzerland).

3.1.1.9. Instruments

instrument	*company*
7300 Real Time PCR System	Applied Biosystems
Infinite M Plex Photometer	TECAN
ChemiDoc™ MP Imaging System	BIO-RAD
Fine Scale	Sartorius
T100™ Thermal Cycler	BIO-RAD
Victor™ X3 Multimode Plate Reader	PerkinElmer
Trans-Blot®Turbo™ Transfer System	BIO-RAD
PowerPac™ Basic	BIO-RAD
Mini PROTEAN® Tetra Cell	BIO-RAD
Seahorse XFE96 analyzer	Agilent

Applied Biosystems (Waltham, MA, USA), Tecan Group (Männedorf, Switzerland), Bio-Rad (Hercules, CA, USA), Sartorius (Göttingen, Germany), PerkinElmer (Waltham, MA, USA), Agilent Technologies (Santa Clara, CA, USA).

3.1.2. Methods

3.1.2.1. Cell Culture of the Cell Line hFOB 1.19

Due to the temperature-sensitive vector of the hFOB 1.19 cell line, the cells were incubated at 34 °C with 5% CO_2 in DMEM/F-12, without phenol red with 10% FCS and 0.3 mg/mL neomycin (G184), as the cells proliferate best at low temperatures. During differentiation with OIM treatment (addition of 500 mM dexamethasone, 50 µM L-ascorbin-2-phosphate, and 10 mM β-glycerophosphate to the proliferation medium), the cells were also incubated in 34 °C with 5% CO_2, as there were no differences in the mineralization between incubation at 34 °C and 37 °C with osteogenic additives (data not shown).

3.1.2.2. Divergence in the Methods Working with the hFOB 1.19 Cells

To quantify the mineralization of an ECM, 1.5 x 10^5 hFOB 1.19 cells per well were seeded in 24-well cell culture plates and the experiment was started by adding OIM after 48 h. To resolve the Alizarin Red S staining, 500 µL CPC per well was added.

To measure ALP activity, cell numbers were also measured by MTT at the time points analyzed. The hFOB 1.19 cells were also seeded at 1.5 x 10^5 cells per well in a 24-well cell culture plate and the experiment started after 48 hours of incubation. 1.4 mL/well of ALP substrate (4-nitrophenol solution) was incubated on the cells for 10 minutes.

For qPCR samples, 7.5 x 10^5 cells per well were seeded in 6-well culture plates and the experiment was also started after 48 hours.

For BrdU, 6 x 10^4 hFOB 1.19 cells were seeded per well in 48-well cell culture plates and treated with the respective treatments and BrdU labelling after 48 h to start the experiment. After a total proliferation time of 24 hours, the BrdU assay was analyzed to determine the proliferation rate.

3.1.2.3. Preparation of Cell Lysates and Protein Determination

Cell lysates were prepared for Western blot analysis and protein levels were determined. The cells were scraped from 6-well cell culture plates and transferred to a falcon for centrifugation (5 min, 400 x g, RT) with PBS. The supernatant was then aspirated and the cells resuspended in an appropriate volume (30 – 100 µL) of RIPA Lysis Buffer containing protease inhibitor. After thorough vortexing and sonification (10 strokes, 80%, 0.5 sec), the lysate was centrifuged again for 5 min at 15,000 x g and the supernatant was transferred to a new tube. The amount of protein was determined according to the manufacturer's instructions for the Pierce™ BCA Protein Assay Kit by Thermo Fisher Scientific. The samples are measured in duplicate by incubating 10 µl of the samples with 200 µl BCA Working Reagent™ (50 parts of Reagent A + 1 part of Reagent B) for 30 min at 37 °C. The

absorbance (562 nm) was determined photometrically and the amount of protein was calculated using a BSA standard series.

3.1.2.4. SDS-PAGE

The proteins in cell lysates were separated by size on a gel using the sodium dodecyl-sulfate polyacrylamide gel electrophoresis (SDS-PAGE) method. For sample preparation, 20 – 30 µg of total protein was adjusted to a volume of 10 µL by the addition of ddH_2O. To denature the proteins, 5 µL of 4 x Laemmli buffer containing 20% (v/v) β-mercaptoethanol was added and the samples were incubated for 5 min at 95 °C on the heating block. The Mini-PROTEAN® TGX Stain-Free Protein Gel™ (Bio-Rad) was clamped into the Mini-PROTEAN® Tetra Vertical Electrophoresis Chamber (Bio-Rad) and the chamber was filled with SDS-PAGE Running Buffer. The SDS gel was then loaded with the prepared samples and a protein ladder (ROTI®Mark Western Plus by Carl Roth). The chamber was connected to a power supply and the gel was run at 100 V for 10 min and then at 160 V for approximately 45 min. Once the Laemmli Buffer had passed through the gel, the power was switched off and the Stain-Free Gel was then imaged in the ChemiDoc™ MP Imaging System to visualize the total protein of each lane.

3.1.2.5. Western Blot

Using the Western Blot method, the proteins in the gel, separated according to size, were transferred to a membrane and the amount of the protein of interest was determined using specific antibodies. The Trans-Blot®Turbo™ Transfer System (Bio-Rad) was used to perform the semi-dry Western blot method. A filter paper soaked in WB Transfer Buffer was placed in the chamber. On top of the filter paper, a piece of nitrocellulose membrane cut to the size of the gel and activated in WB transfer buffer was placed. The gel was applied to the membrane avoiding air bubbles and was covered with a second piece of soaked filter paper. The chamber was tightly sealed and connected to the power supply (2.5 A/25 V). The proteins were then transferred from the gel to the membrane by the flowing from the cathode (upper filter paper) to the anode (lower filter paper) for 5 min. The membrane was

blocked in 5% BSA in TBS-T Buffer for 1 h at RT. After blocking, the primary antibody for a specific protein was diluted in 5% BSA in TBS-T Buffer and incubated for 2 h at RT or overnight at 4 °C. After three 5-minute washes with TBS-T Buffer, the peroxidase-conjugated secondary antibody was added to the membrane and incubated for 1 h at RT. The membrane was then washed three more times for 5 min each with TBS-T Buffer. After addition of Immobilon Forte Western HRP substrate to the membrane, the specific protein bands were visualized by chemiluminescence detection in the ChemiDoc™ MP Imaging System. Analysis was performed using Bio-Rad Image Lab Software (Version 6.1) with normalization to total protein amount.

3.1.2.6. Scanning Electron Microscopy (SEM)

For scanning electron microscopy analyses (SEM), OBs were seeded on acetone-resistant plastic plates in 24-well cell culture plates. After reaching confluence, the cells were treated with the cytokines IL-1β (250 units/mL) or IL-8 (12.5 units/mL) in OIM for 21 days. On day 1 and day 21, the cells were fixed by adding 500 µL fixative (4% paraformaldehyde with 2.5% glutaraldehyde in 0.1 M sodium cacodylate buffer (pH 7.4)) and incubated overnight at 4 °C. The next day, the platelets were washed three times with ddH_2O for 10 minutes. For dehydration, the samples were incubated in 50% acetone for 20 minutes, 70% acetone overnight at 4 °C, and then twice in 90% acetone for 20 minutes and twice in 100% acetone for 20 minutes with gentle shaking.

The critical point drying was done using a Leica EM CPD 030 (Leica Biosystems, Wetzlar, Germany) and the surfaces of the samples were coated with a 20-25 nm thick gold layer using a Cressington 108 auto (Cressington Scientific Instruments, Watford, UK) sputter coater. Both steps were performed at the Core Facility Electron Microscopy (CFEM) under the direction of Dr. Ann Kathrin Bergmann. The samples were imaged with a FIB-SEM (Crossbeam 550, Carl Zeiss AG) at an accelerating voltage of 2 kV/2nA, at a working distance of 5 mm with a SE2 detector and the software package SmartSEM (version 6.07, Carl Zeiss AG).

3.1.2.7. Transmission electron microscopy (TEM)

For sample preparation for transmission electron microscopy analyses (TEM), 21-days differentiated OBs were detached from a 6-well cell culture plate with a cell scraper, resuspended with PBS and centrifuged to form a cell pellet (5 min, 400 x g, RT). The cell pellet was covered with fixative (4% paraformaldehyde with 2.5% glutaraldehyde in 0.1 M sodium cacodylate buffer (pH 7.4)) and stored at 4 °C until embedding in resin.

All samples which tend to fall apart were pre-embedded in agarose. The supernatant was aspirated and a volume of approximately 10 µL was left. Low melting agarose (3% in aqua bi-dest.) was dissolved at 40 °C in a water bath and used to layer the pellets. All following steps were performed at RT. After centrifugation at 4,000 x g for 2 min, the samples were incubated in 1% OsO_4 in 0.1 M sodium cacodylate buffer for 2 hours. The samples were washed three times with aqua dest. for 10 min, once with 50% acetone for 30 min and once with 70% acetone for 20 min. Block contrast was applied using freshly made and filtered 0.5% uranyl acetate/1% phosphotungstic acid in 70% EtOH for 1 hour. Dehydration was completed using 90% acetone twice for 30 min and 100% acetone twice for 30 min. The pellets were embedded in SPURR epoxy resin (Serva, 21050) and cured at 70 °C for 48 hours. Ultra-thin sections of 70 nm were cut using a Ultracut EM UC7 (Leica, Wetzlar, Germany) and stained with 1.5% uranyl-acetate for 25 min and lead-citrate for 8 min (according to Reynolds, 1963). Images were captured using a JEOL JEM-2100plus TEM (JEOL, Tokyo, Japan) at an accelerating voltage of 200 kV equipped with a Matataki Flash camera (JEOL, Tokyo, Japan).

3.1.2.8. Statistics

For all statistical analyses a combination of Microsoft Excel (Microsoft Corporation, Redmond, WA, USA) and GraphPad PRISM 8 software (Boston, MA, USA) was used. The results of the primary cells were treated as non-parametric values, as a normal distribution cannot be assumed. Therefore, the Wilcoxon signed rank test was used to calculate significances for paired data and the Mann-Whitney U test for unpaired

data. The results of the hFOB 1.19 cell line were considered as parametric data, as a normal distribution can be assumed due to the stability of cell lines. The paired t-test was used for paired data.

3.2. Supplementary Results

3.2.1. A Comparison of Osteoblasts from Donors with Normal (OBs) and Osteoporotic (oOBs) Bone Mineral Density

To compare osteoblasts from healthy and osteoporotic donors, the cells were categorized into two groups based on DXA measurements. Cells from donors with a T-score ≤ -2.5 were assigned to the osteoporotic group (oOBs) due to their low BMD and compared to OBs from patients with a T-score ≥ -2.5. The aim was to analyze potential differences in cytokine secretion, proliferation, differentiation, and energy metabolism during osteogenesis. Additionally, the response of OBs and oOBs to proinflammatory cytokines was investigated.

3.2.1.1. Comparison of the Mineralization of OBs and oOBs

The mineralization of OBs and oOBs was induced by treatment with osteogenic induction medium (OIM) for 35 days (Fig. 3.2). Although no statistically significant differences were observed between the groups, several trends emerged. On day 7, oOBs exhibited slightly faster mineralization compared to OBs, but their mineralization remained lower on days 14 and 21. While the mineralization of OBs continued to increase exponentially until day 35, oOBs reached a maximum on day 28, followed by a slight decline by day 35.

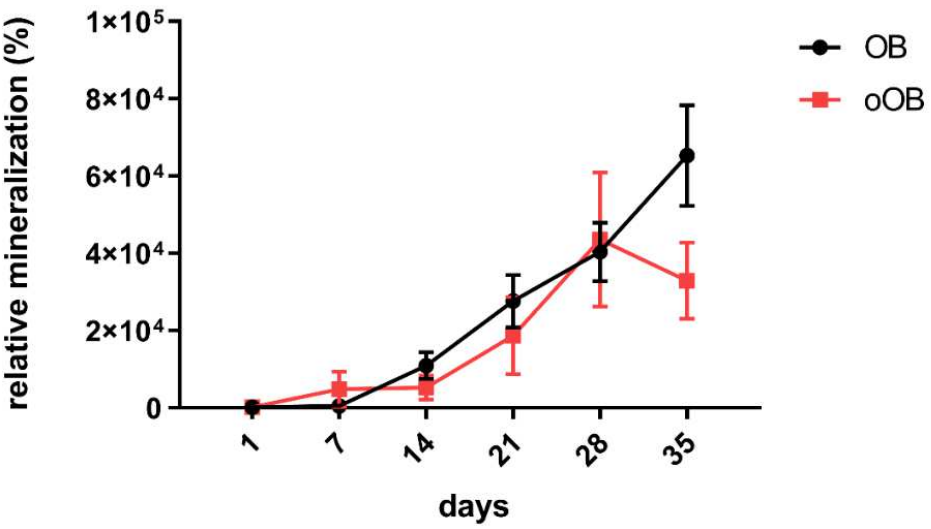

Figure 3.2: Mineralization of OBs and oOBs over 35 days. OBs (n = 13) and oOBs (n = 7) were incubated in osteogenic induction medium (OIM) in 24-well plates (6 replicates per donor). Mineralization was quantified using alizarin red S staining on days 1, 7, 14, 21, 28, and 35. The data were normalized to day 1 for each donor. Statistical significance was calculated using the Mann-Whitney U test (ns). Data are presented as the mean ± SD.

3.2.1.2. Comparison of the Cytokine Secretion of OBs and oOBs

The secretion of IL-6 during osteogenesis did not differ significantly between OBs and oOBs (Fig. 3.3, A). Both groups had similar IL-6 levels in undifferentiated cells on day 1, followed by a decrease on day 7. Afterward, IL-6 secretion showed some fluctuations but remained comparable between the two groups throughout the treatment period.

The secretion of IL-8 showed no statistically significant differences between OBs and oOBs (Fig. 3.3, B). On days 1 and 7, both groups secreted very little or no detectable IL-8. From day 14 onward, an increase in IL-8 secretion was observed in both groups, with OBs showing a tendency toward higher secretion compared to oOBs. This trend persisted until day 35 but did not reach statistical significance.

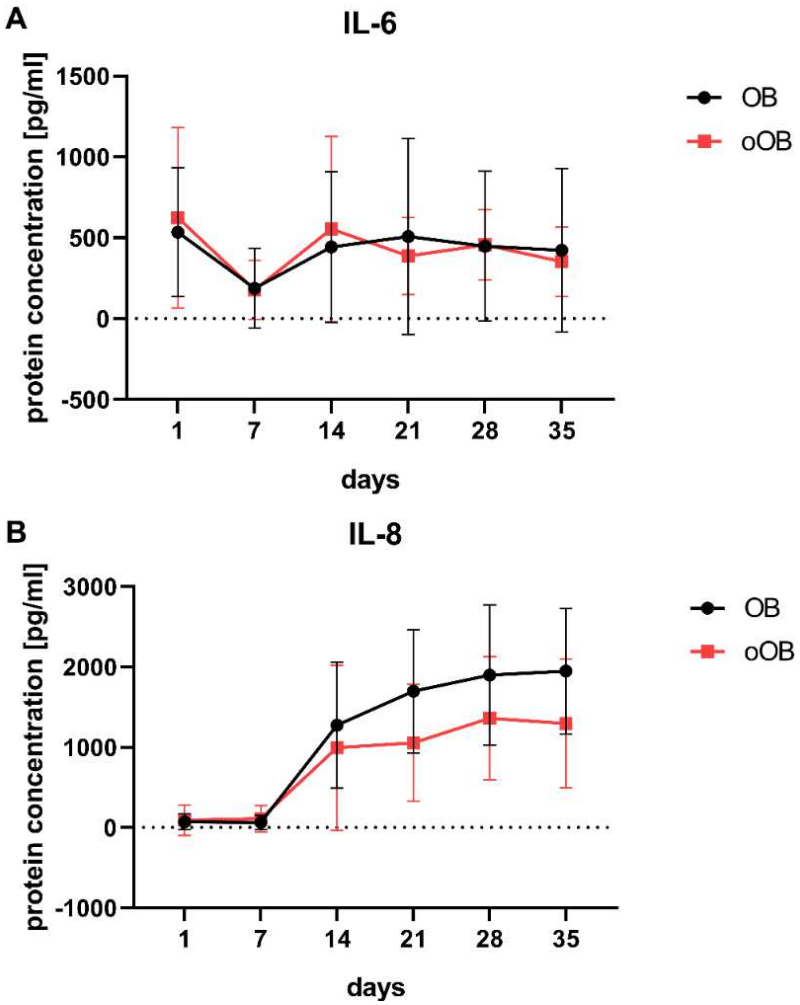

Figure 3.3: Cytokine secretion of OBs and oOBs during osteogenesis. The protein concentration [pg/mL] of (A) Interleukin (IL)-6 and (B) IL-8 were measured in the supernatant of OIM-treated OBs (n = 11) and oOBs (n = 6 for days 1 - 21; n = 5 for days 28 – 35) by ELISA. Statistical significance was calculated using the Mann-Whitney U test (ns). Data are presented as the mean ± SD.

3.2.1.3. Comparison of the Proliferation of OBs and oOBs

The proliferation of OBs and oOBs was analyzed in both growth medium (GM) and OIM over 21 days (Fig. 3.4). While cells cultured in OIM tended to show higher proliferation compared to those in GM, no statistically significant differences were observed. Similarly, no significant differences were found between the proliferation rates of OBs and oOBs. However, there was a slight tendency for OBs to proliferate faster than oOBs under both conditions.

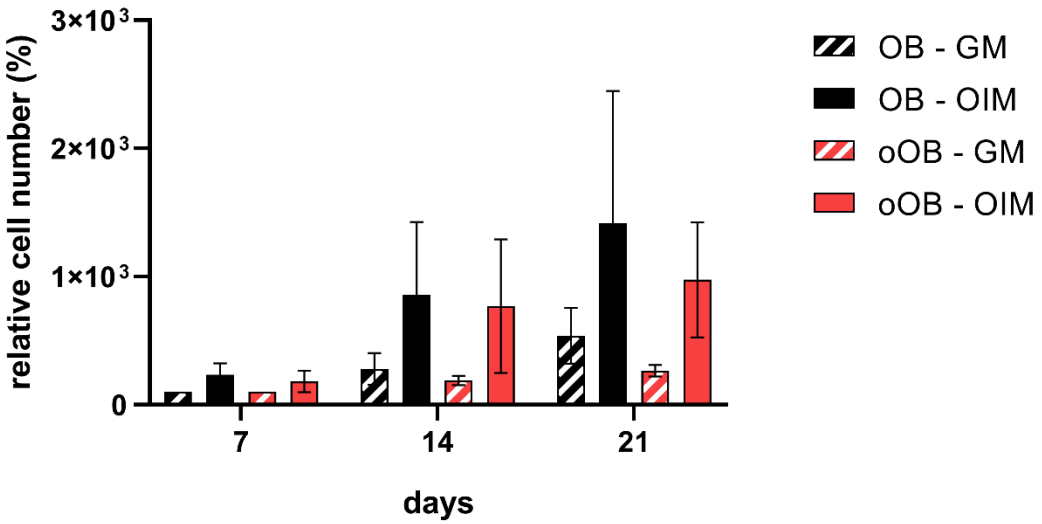

Figure 3.4: Proliferation of OBs and oOBs in GM and OIM. OBs (n = 8) and oOBs (n = 5) were cultured in growth medium (GM) and osteogenic induction medium (OIM) for 21 days. The relative cell number was assessed on days 7, 14, and 21 using the MTT assay. No statistically significant differences were observed between OBs and oOBs (Mann-Whitney U test) or between OIM and GM treatments (Wilcoxon signed rank test). Data are presented as mean ± SD.

3.2.1.4. Comparison of the Energy Metabolism of OBs and oOBs

The energy metabolism of untreated OBs and oOBs was analyzed by assessing OxPhos and glycolysis parameters.

For OxPhos, several parameters were measured, including basal respiration, proton leak, maximal respiration, spare respiratory capacity, non-mitochondrial oxygen consumption, and ATP production (Fig. 3.5). There were no significant differences between the two groups measured. Across all parameters, no statistically significant differences were observed between OBs and oOBs. OBs and OBs showed similar distribution, but with slightly higher variability in OBs.

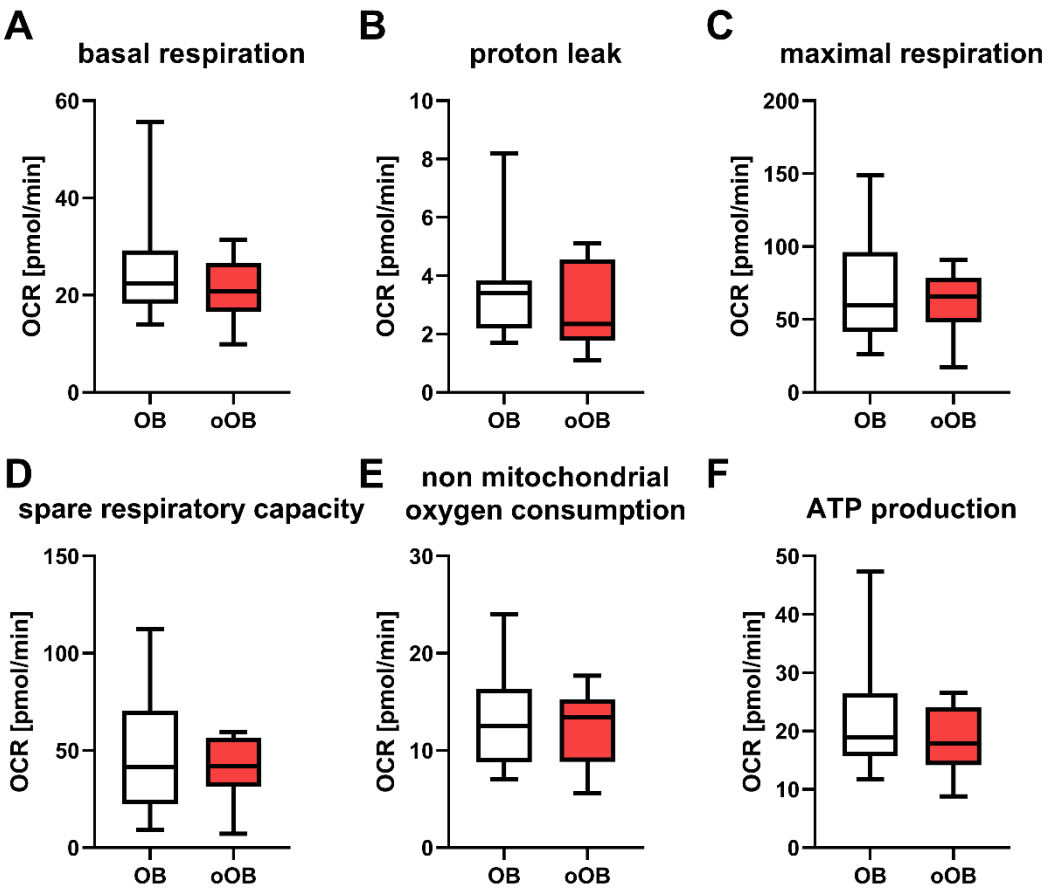

Figure 3.5: OxPhos parameters of untreated OBs and oOBs. Boxplots show the oxygen consumption rates (OCR) of (A) basal respiration, (B) proton leak, (C) maximal respiration, (D) spare respiratory capacity, (E) non-mitochondrial oxygen consumption, and (F) ATP production from OBs (n = 17) and oOBs (n = 8). Across all parameters, no significant differences were observed between the groups (Mann-Whitney U test, ns).

In addition to OxPhos, glycolysis parameters were measured to provide an overview of the energy metabolism (Fig. 3.6). Parameters analyzed included glycolysis, non-glycolytic acidification, glycolytic capacity, and glycolytic reserve. Similar to the OxPhos results, no significant differences were found between OBs and oOBs. Glycolysis and non-glycolytic acidification were slightly higher in oOBs compared to OBs, but the variability within each group led to overlapping distributions.

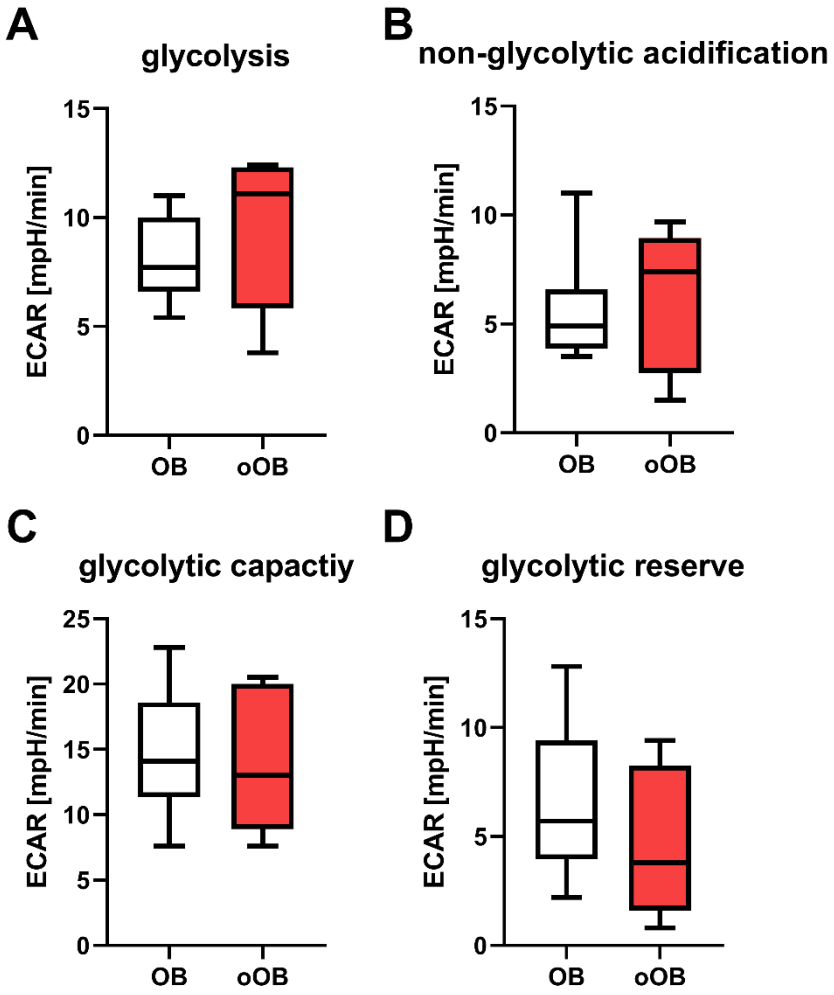

Figure 3.6: Glycolysis parameters of untreated OBs and oOBs. Boxplots show the extracellular acidification rate (ECAR) of (A) glycolysis, (B) non-glycolytic acidification, (C) glycolytic capacity, and (D) glycolytic reserve in OBs (n = 9) and oOBs (n = 5). Statistical analysis revealed no significant differences between the groups (Mann-Whitney U test, ns).

3.2.1.5. Comparison of the Influence of Proinflammatory Cytokines on OBs and oOBs

The effect of proinflammatory cytokines on OBs and oOBs was analyzed to determine whether cells from donors with normal BMD showed a different response compared to osteoporotic donors. The cytokines IL-1β, IL-6, IL-8, TNF-α, and IFNγ were used to assess their impact on cell activity parameters including proliferation, differentiation, and energy metabolism in both cell types.

3.2.1.5.1. Influence of Proinflammatory Cytokines on the Proliferation of OBs and oOBs

To evaluate the influence of cytokines on proliferation, OBs and oOBs were treated with cytokines over a period of 21 days in OIM. The relative cell number was determined using MTT assay on days 7, 14, and 21 (Fig. 3.7) Both OBs and oOBs showed an increase in proliferation when treated with IL-1β and TNF-α. No significant differences in cytokine-induced proliferation were observed between OBs and oOBs across all measurement time points.

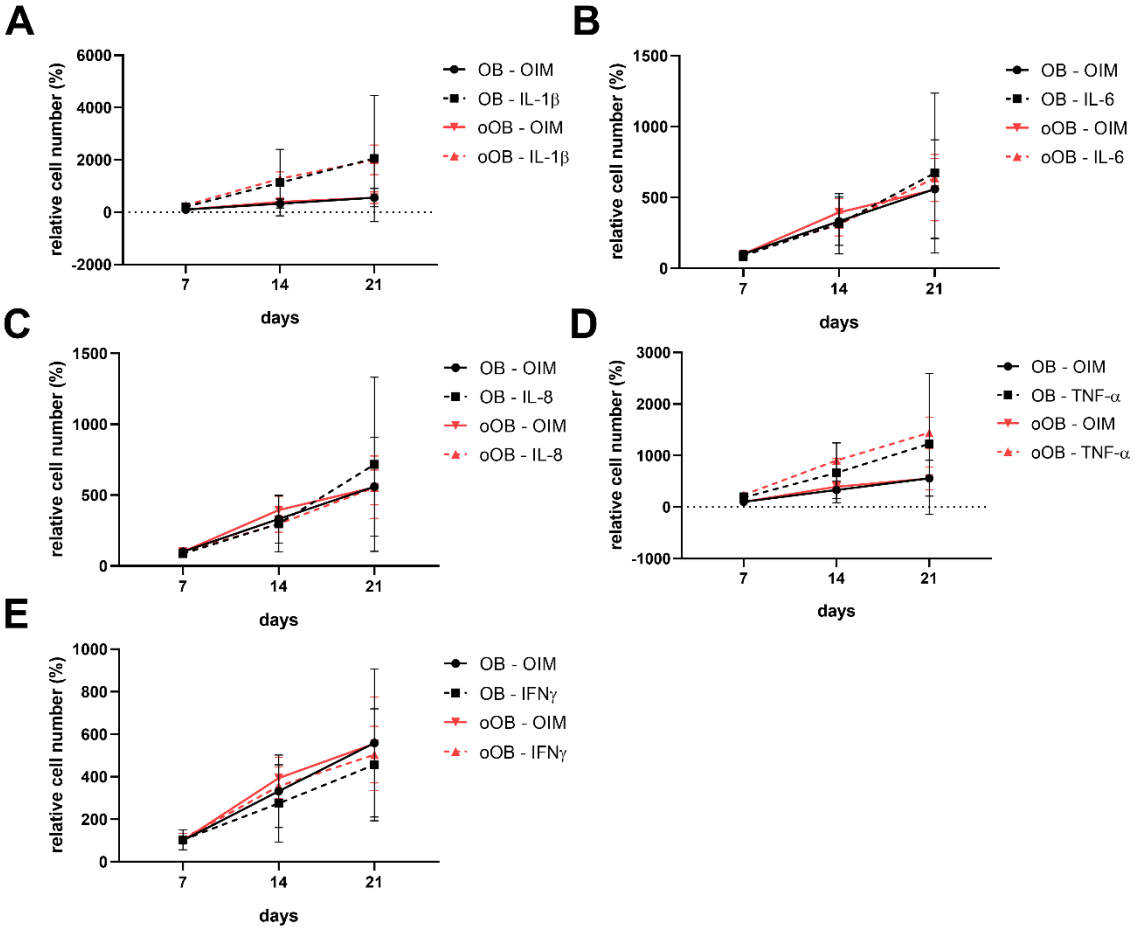

Figure 3.7: Influence of proinflammatory cytokines on the proliferation of OBs and oOBs during osteogenesis. The relative cell number of OBs (n = 8) and oOBs (n = 5) was determined using the MTT assay on days 7, 14, and 21. Cells were treated with the cytokines (A) IL-1β (250 units/mL), (B) IL-6 (12.5 units/mL), (C) IL-8 (12.5 units/mL), (D) TNF-α (250 units/mL), and (E) IFNγ (3.125 units/mL) in OIM. Statistical analysis using the Mann-Whitney U test revealed no significant differences between OBs and oOBs. Data are presented as the mean ± SD.

In addition to long-term treatments, short-term effects of cytokines on proliferation were analyzed using BrdU assays after 48 hours of treatment in GM and OIM (Fig. 3.8). In GM, both OBs and oOBs showed a slight but non-significant increase in proliferation when treated with TNF-α, while IL-1β did not alter proliferation significantly. IL-6 and IL-8 led to a slight, non-significant inhibition of proliferation in oOBs compared to OBs. In OIM, a significant proliferation-promoting response to IL-1β and TNF-α was observed in OBs, whereas oOBs showed a similar trend without reaching significance (Fig. 3.8, B). The short-term proliferation responses observed in the BrdU assay were consistent with the long-term results obtained using the MTT assay.

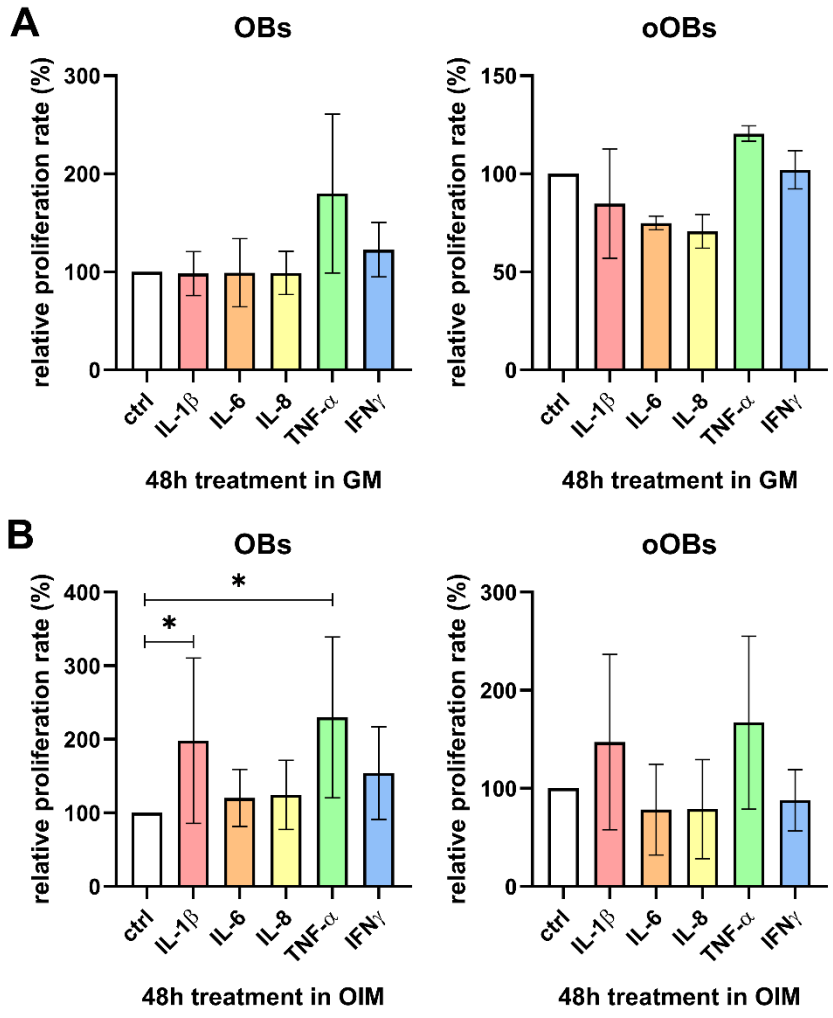

Figure 3.8: Influence of proinflammatory cytokines on the proliferation rate of OB and oOB in GM and OIM. Cells (2 x 10^4 per well) were seeded in 48-well plates

and treated with cytokines after 48 h of initial culture in GM. The BrdU assays were performed after an additional 48 hours of cytokine treatment in (A) GM (OBs: n = 4; oOBs: n = 3) and (B) OIM (OBs: n = 7, oOBs: n = 5) with IL-1β (250 units/mL), IL-6 (12.5 units/mL), IL-8 (12.5 units/mL), TNF-α (250 units/mL), and IFNγ (3.125 units/mL). Data were normalized to untreated controls (GM or OIM without cytokines) and presented as the mean ± SD. Statistical significance was calculated using the Wilcoxon signed-rank test ($p \leq 0.05$ (*)).

3.2.1.5.2. Influence of Proinflammatory Cytokines on the Osteogenesis of OBs and oOBs

The differentiation of OBs and oOBs was assessed by quantifying ECM mineralization. No significant differences were observed between OBs and oOBs in response to any of the cytokines examined (Fig. 3.9). In both groups, the cytokines IL-1β, IL-6, IL-8, TNF-α, and IFNγ had a promoting effect on mineralization compared to the control (OIM without cytokines). Across all concentrations tested, the mineralization trends remained comparable between OBs and oOBs, with overlapping variability ranges.

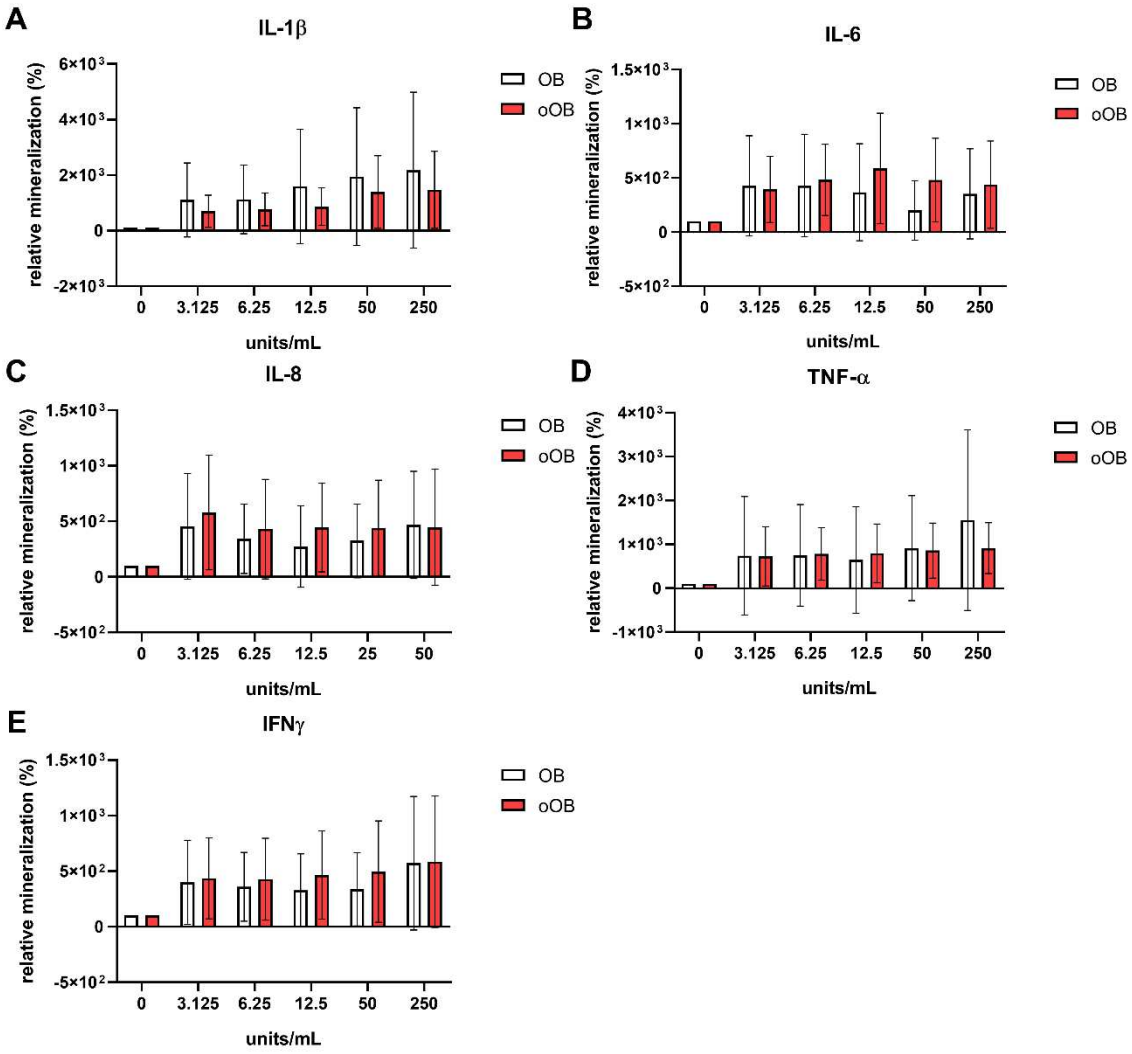

Figure 3.9: Influence of proinflammatory cytokines on the mineralization of OBs and oOBs. OBs (n = 9) and oOBs (n = 7) were incubated with different concentrations of the cytokines (A) IL-1β, (B) IL-6, (C) IL-8, (D) TNF-α, and (E) IFNγ in OIM for 21 days. Mineralization was quantified by alizarin red S staining, and the data were normalized to the control (0 units/mL, OIM without cytokines). Statistical differences between OBs and oOBs were calculated using Mann-Whitney U tests (ns). Data are presented as mean ± SD.

In addition to ECM mineralization, ALP activity was analyzed as an additional osteogenic marker. Measurements on days 8 and 10 of cytokine treatment revealed no significant differences between OBs and oOBs (Fig. 3.10). However, oOBs exhibited a tendency toward higher ALP activity in response to IL-1β treatment compared to the control, although this increase was not statistically significant. The

distribution of ALP values was more variable in OBs, suggesting donor-dependent effects.

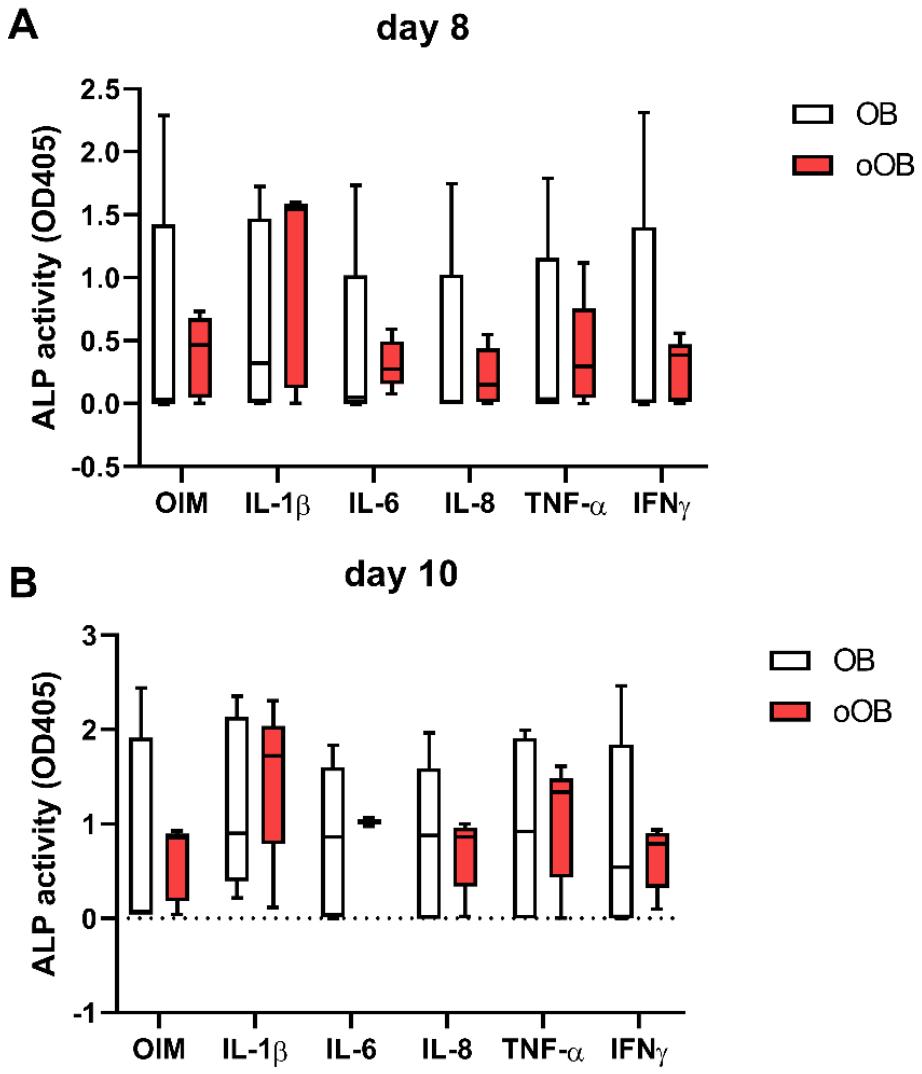

Figure 3.10: Impact of proinflammatory cytokines on ALP activity in OBs and oOBs. ALP activity was measured in OBs (n = 5) and oOBs (n = 5) on (A) day 8 and (B) day 10 of incubation in OIM, with or without the cytokines IL-1β (250 units/mL), IL-6 (12.5 units/mL), IL-8 (12.5 units/mL), TNF-α (250 units/mL), and IFNγ (3.125 units/mL). Statistical differences between cytokine-treated and control cells were analyzed using Wilcoxon signed-rank tests (ns), and differences between OBs and oOBs were calculated with Mann-Whitney U tests (ns). Data are presented as mean ± SD.

3.2.1.5.3. Influence of Proinflammatory Cytokines on the Energy Metabolism of OBs and oOBs

The effect of proinflammatory cytokines on the energy metabolism of OBs and oOBs was analyzed by measuring OxPhos and glycolysis parameters.

The OxPhos parameters of cytokine-treated OBs and oOBs showed a few notable differences (Fig. 3.11). TNF-α treatment significantly increased basal respiration, proton leak, maximal respiration, non-mitochondrial oxygen consumption, and ATP production in OBs, with similar trends observed in oOBs but without reaching statistical significance. IL-1β treatment revealed significant differences between OBs and oOBs in basal respiration, proton leak, and ATP production, with all parameters being higher in oOBs compared to OBs. However, these values were not significantly different from untreated differentiated OBs (OIM). In general, the variability in oOBs was greater than in OBs, as indicated by larger standard deviations.

Figure 3.11 shows the comparison of OxPhos parameters of cytokine-treated OBs and oOBs. At first sight, there are few differences between these two groups, with the oOBs showing larger standard deviations than the OBs. The significant increase in basal respiration, proton leak, maximal respiration, non-mitochondrial oxygen consumption, and ATP production due to TNF-α treatment in the OBs can also been seen tendentially in the oOBs, but not significantly. In contrast, there are significant differences between OBs and oOBs treated with IL-1β in basal respiration, proton leak, and ATP production. All parameters are higher in oOBs, but not significantly different from untreated differentiated OBs (OIM).

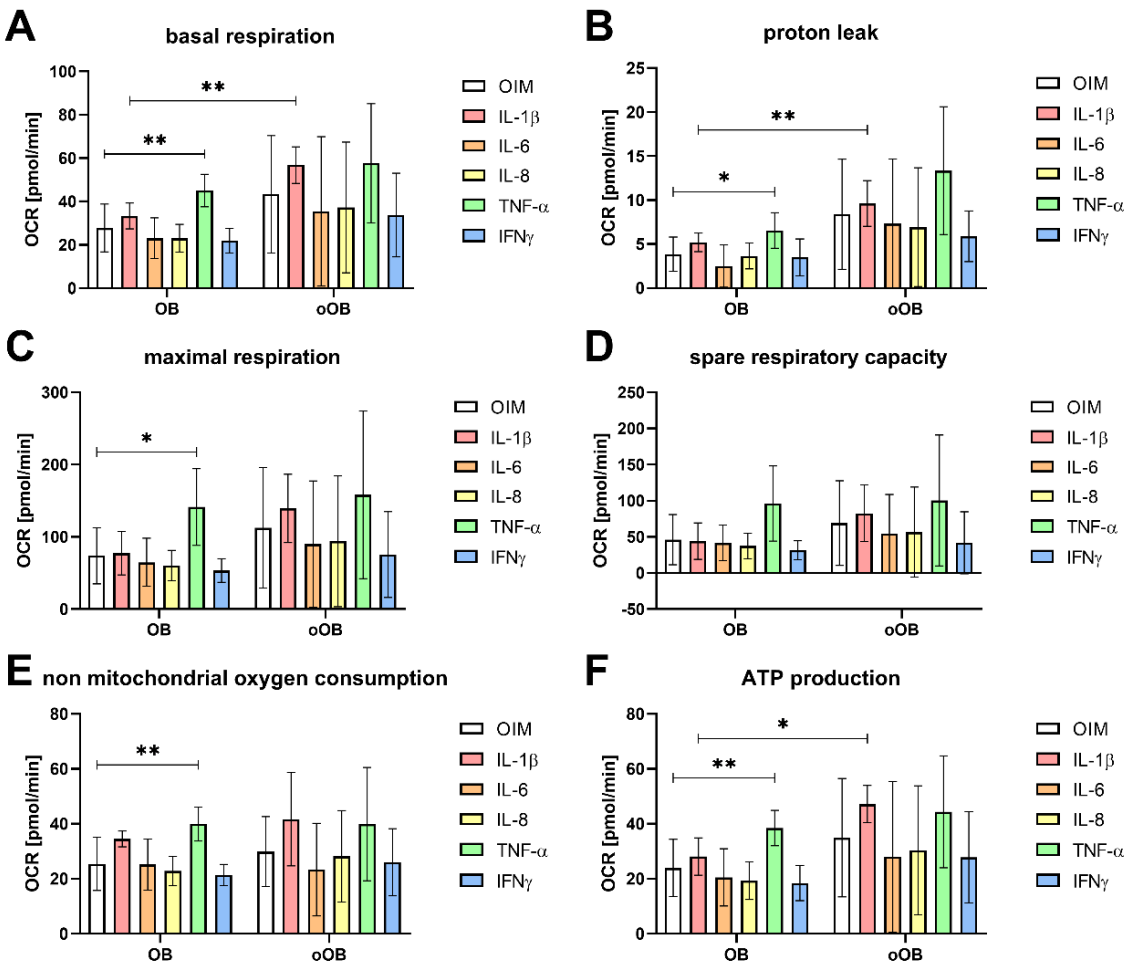

Figure 3.11: OxPhos parameters of cytokine-treated OBs and oOBs. The OCR of the parameters (A) basal respiration, (B) proton leak, (C) maximal respiration, (D) spare respiratory capacity, (E) non mitochondrial oxygen consumption, and (F) ATP production was measured on day 14 of treatments in OBs and oOBs. Treatments included OIM without cytokines (OBs: n = 10; oOBs: n = 5), with IL-1β (250 units/mL) (OBs: n = 6; oOBs: n = 4), IL-6 (12.5 units/mL) (OBs: n = 4; oOBs: n = 5), IL-8 (12.5 units/mL) (OBs: n = 4; oOBs: n = 4), TNF-α (250 units/mL) (OBs: n = 6; oOBs: n = 4), or IFNγ (3.125 units/mL) (OBs: n = 4; oOBs: n = 4). Statistical analysis was performed using Mann-Whitney U tests ($p \leq 0.05$ (*), $p \leq 0.01$ (**)). Data are presented as mean ± SD.

The glycolysis parameters showed similar patterns between OBs and oOBs (Fig. 3.12). Both groups had an increase in glycolysis and glycolytic capacity upon IL-1β treatment, though these increases were not statistically significant. Non-glycolytic acidification was significantly higher in both groups under IL-1β treatment

compared to the control (OIM). Glycolytic reserve showed significant differences between OBs and oOBs under TNF-α treatment, with oOBs displaying significantly lower values compared to OBs. However, no significant differences were observed when compared to the respective controls (OIM). As with OxPhos, the variability in oOBs tended to be greater than in OBs.

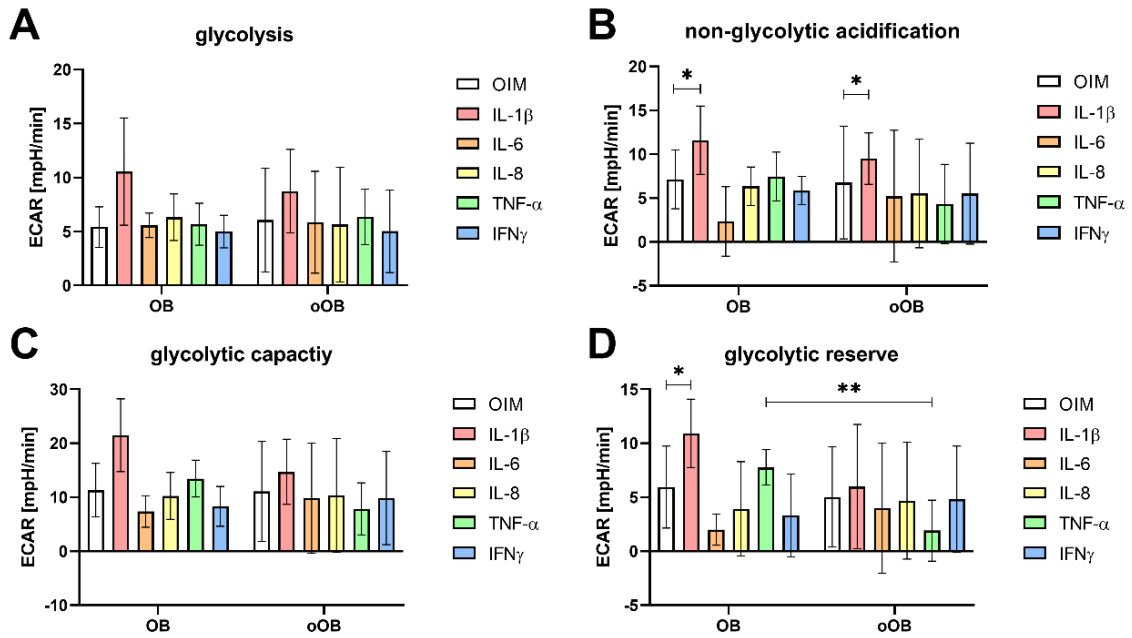

Figure 3.12: Glycolysis parameters of cytokine-treated OBs and oOBs. The ECAR of the parameters (A) glycolysis, (B) non-glycolytic acidification, (C) glycolytic capacity, and (D) glycolytic reserve was measured on day 14 in OBs and oOBs. Treatments included OIM without cytokines (OBs: n = 9; oOBs: n = 8), with IL-1β (250 units/mL) (OBs: n = 5; oOBs: n = 5), IL-6 (12.5 units/mL) (OBs: n = 4; oOBs: n = 7), IL-8 (12.5 units/mL) (OBs: n = 4; oOBs: n = 6), TNF-α (250 units/mL) (OBs: n = 5; oOBs: n = 6), or IFNγ (3.125 units/mL) (OBs: n = 4; oOBs: n = 6). Statistical analysis was performed using Mann-Whitney U tests ($p \leq 0.05$ (*), $p \leq 0.01$ (**)). Data are presented as mean ± SD.

3.2.2. A Comparison of Primary Osteoblasts (OBs) and the Cell Line hFOB 1.19

In addition to primary osteoblasts, the effect of proinflammatory cytokine treatment on proliferation and osteogenesis was investigated in the human fetal osteoblast cell line hFOB 1.19. The cells were compared morphologically, and the mRNA expression of IL-6 and IL-8 was analyzed in hFOB 1.19 cells during osteogenesis and after cytokine treatments. To identify differences in cell activity between the cell line and primary cells, parameters like proliferation and differentiation were analyzed. To further understand the differences in cellular responses, the expression of well-known osteogenic differentiation markers was analyzed using qPCR.

3.2.2.1. Cell Morphology of hFOB 1.19 cells and OBs

Morphological differences between the cell line hFOB 1.19 and OBs were observed microscopically (Fig. 3.13). The hFOB 1.19 cells were generally smaller in size with a homogeneous spindle-shaped morphology. In contrast, OBs exhibited a greater degree of heterogeneity in both shape and size, with some cells having a polygonal or spindle-shaped appearance.

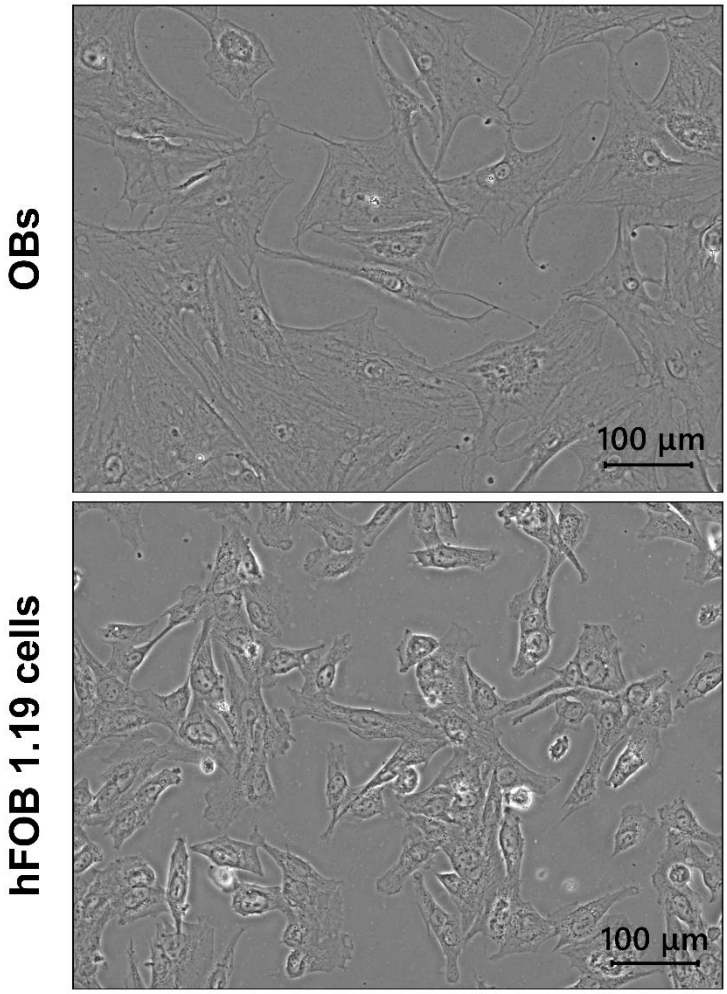

Figure 3.13: Morphological differences between hFOB 1.19 cells and the OBs. Representative images of OBs and hFOB 1.19 cells cultured in 24-well plates.

3.2.2.2. Cytokine Expression of IL-6 and IL-8 in hFOB 1.19 Cells

The mRNA expression of *IL-6* and *IL-8* during osteogenesis in hFOB 1.19 cells revealed distinct patterns. *IL-6* expression was highest in undifferentiated cells (day 1), decreased significantly by day 7, and showed a small second peak on day 14 before remaining low until day 35 (Fig. 3.14, A). Treatment with cytokines for 21 days did not significantly alter *IL-6* expression levels.

In contrast, *IL-8* expression peaked on day 14 of differentiation, with low levels before and after this time point (Fig. 3.14, B). Similarly, 21-day cytokine treatments did not significantly impact *IL-8* mRNA expression in hFOB 1.19 cells.

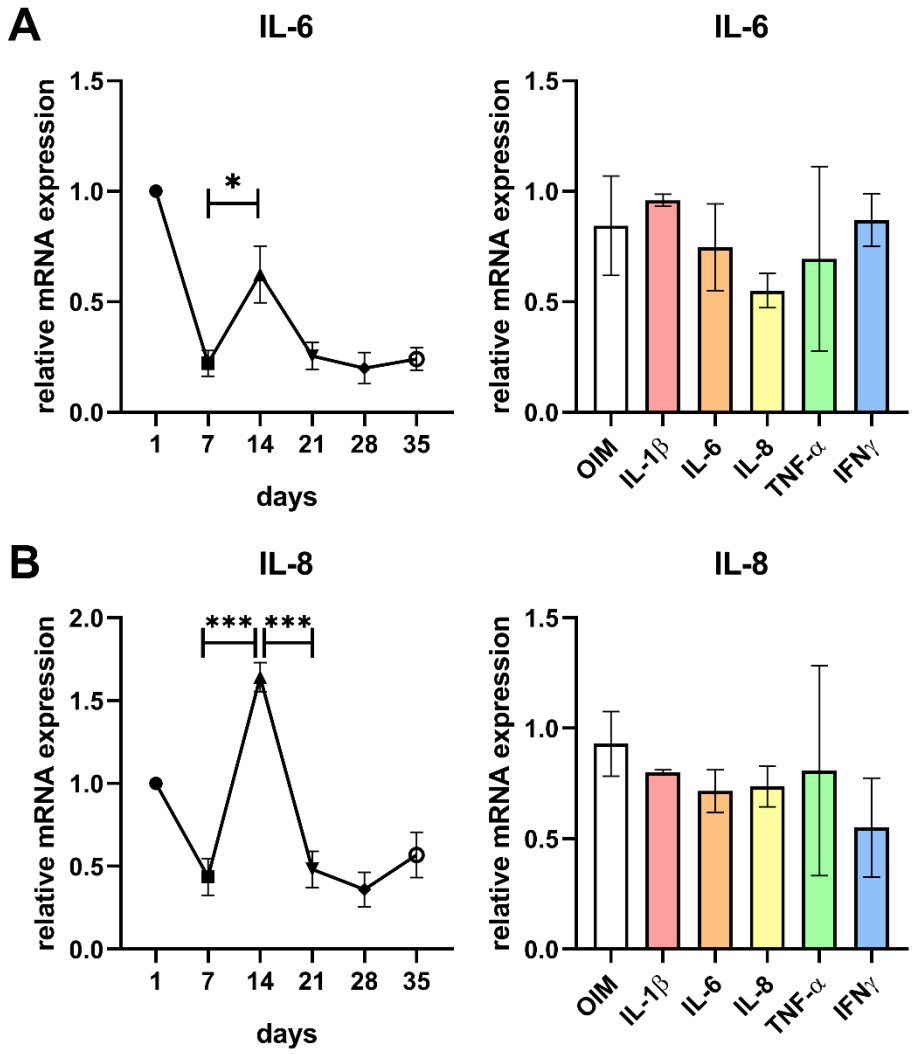

Figure 3.14: *IL-6* and *IL-8* mRNA expression in hFOB 1.19 cells. The mRNA expression of (A) *IL-6* and (B) *IL-8* was measured by qPCR during osteogenesis and after 21-day cytokine treatment with IL-1β (6.25 units/mL), IL-6 (12.5 units/mL), IL-8 (3.125 units/mL), TNF-α (6.25 units/mL), and IFNγ (6.25 units/mL) in hFOB 1.19 cells (n = 3). Statistical significance was calculated using paired t-test ($p \leq 0.05$ (*), $p \leq 0.01$ (**), $p \leq 0.001$ (***)). Data are presented as mean ± SD. Relative mRNA levels were normalized using the 2-ΔΔ Ct method against *RPLP0* as the reference gene and day 1 and OIM as the control.

3.2.2.3. Influence of Proinflammatory Cytokines on the Proliferation of hFOB 1.19 Cells

To determine the influence of proinflammatory cytokines on the proliferation of hFOB 1.19 cells, BrdU and MTT assays were performed. The BrdU assays showed

that the proliferation rate of cells cultured in GM or OIM was not significantly affected by any of the cytokines analyzed (Fig. 3.15, A and B).

The MTT assays, performed after 14 and 21 days of incubation, revealed that the relative cell number in OIM-treated cells was significantly higher on day 14 compared to cells cultured in GM (Fig. 3.15, C). Furthermore, on day 14, cells treated with IL-8 in OIM showed a significantly higher cell number compared to the untreated OIM control. However, these differences were no longer statistically significance on day 21.

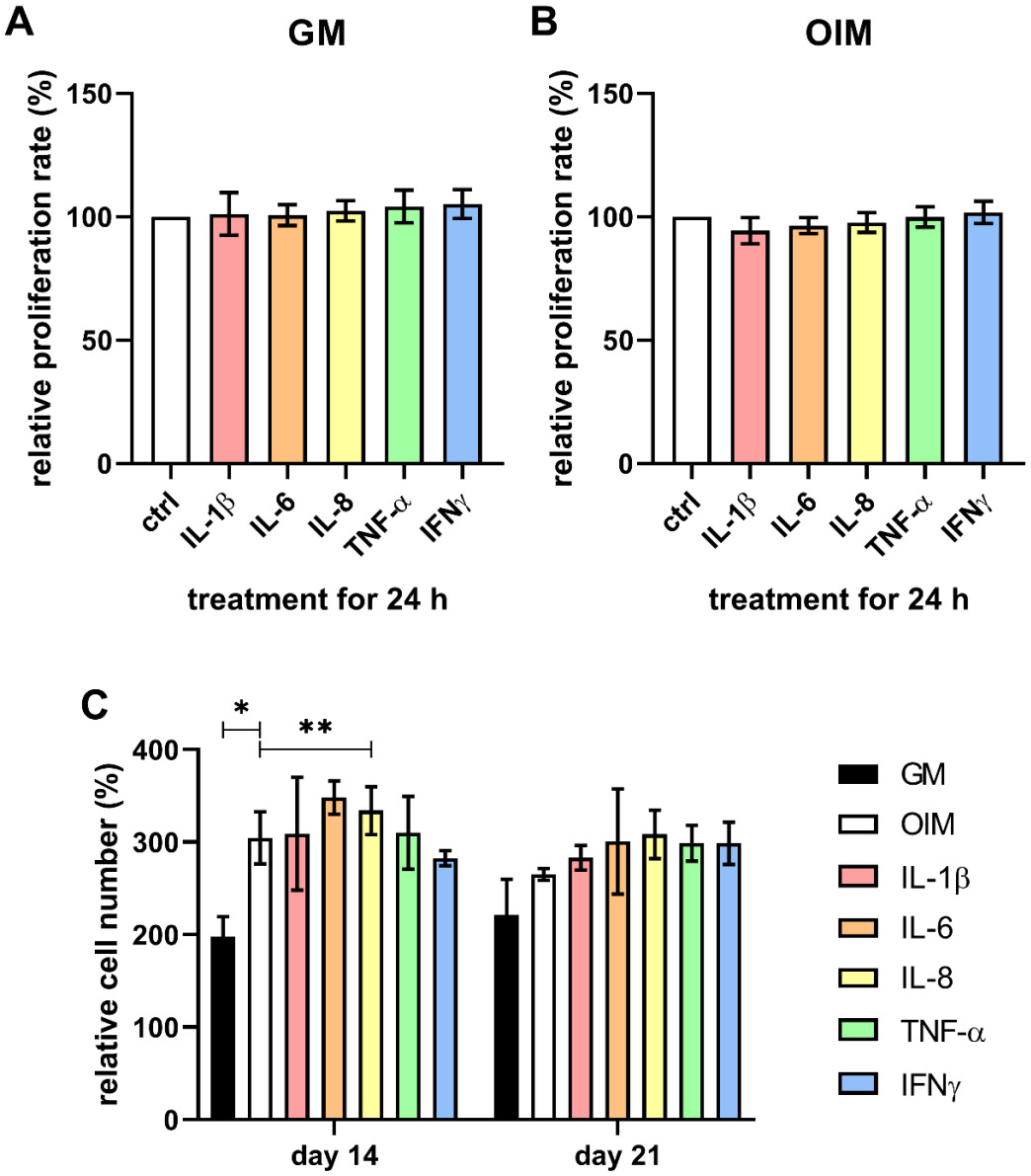

Figure 3.15: Impact of proinflammatory cytokines on the proliferation rate and cell number of hFOB 1.19 cells. The proliferation rate was measured by BrdU assays

after 24 hours of treatment with or without IL-1β (6.25 units/mL), IL-6 (12.5 units/mL), IL-8 (3.125 units/mL), TNF-α (6.25 units/mL), and IFNγ (6.25 units/mL) in (A) GM (n = 3) and (B) OIM (n = 4). Data were normalized to the untreated control (GM or OIM). (C) relative cell number was determined by MTT assays on day 14 and 21 of treatment of confluent cells with OIM with and without cytokine and GM. Data were normalized to day 1. Data are presented as mean ± SD, and statistical significance was calculated using paired t-tests ($p \leq 0.05$ (*), $p \leq 0.01$ (**)).

3.2.2.4. Comparison of Osteogenic Parameters of OBs and hFOB 1.19 Cells

3.2.2.4.1. Mineralization

During osteogenesis, hFOB 1.19 cells had the most pronounced increase in mineralization between days 14 and 21, followed by a plateau that persisted until day 35 (Fig. 3.16, A). In contrast, the mineralization of OBs progressed more gradually, with a steady increase observed from day 7 to day 35, without reaching a visible plateau (Fig. 3.16, B).

A direct comparison between hFOB 1.19 cells and OBs showed significantly higher mineralization levels in OBs on days 28 and 45 (Fig. 3.16, C). However, it should be noted that these experiments were conducted using different culture formats: OBs were cultured in 48-well plates, while hFOB 1.19 cells were cultured in 24-well plates due to better adherence, both with the same volume of alizarin red S dissolution solution (CPC) for quantification. This methodological difference leads to the suggestion, that hFOB 1.19 cells could have an even lower mineralization level if they were cultured in 48-well plates.

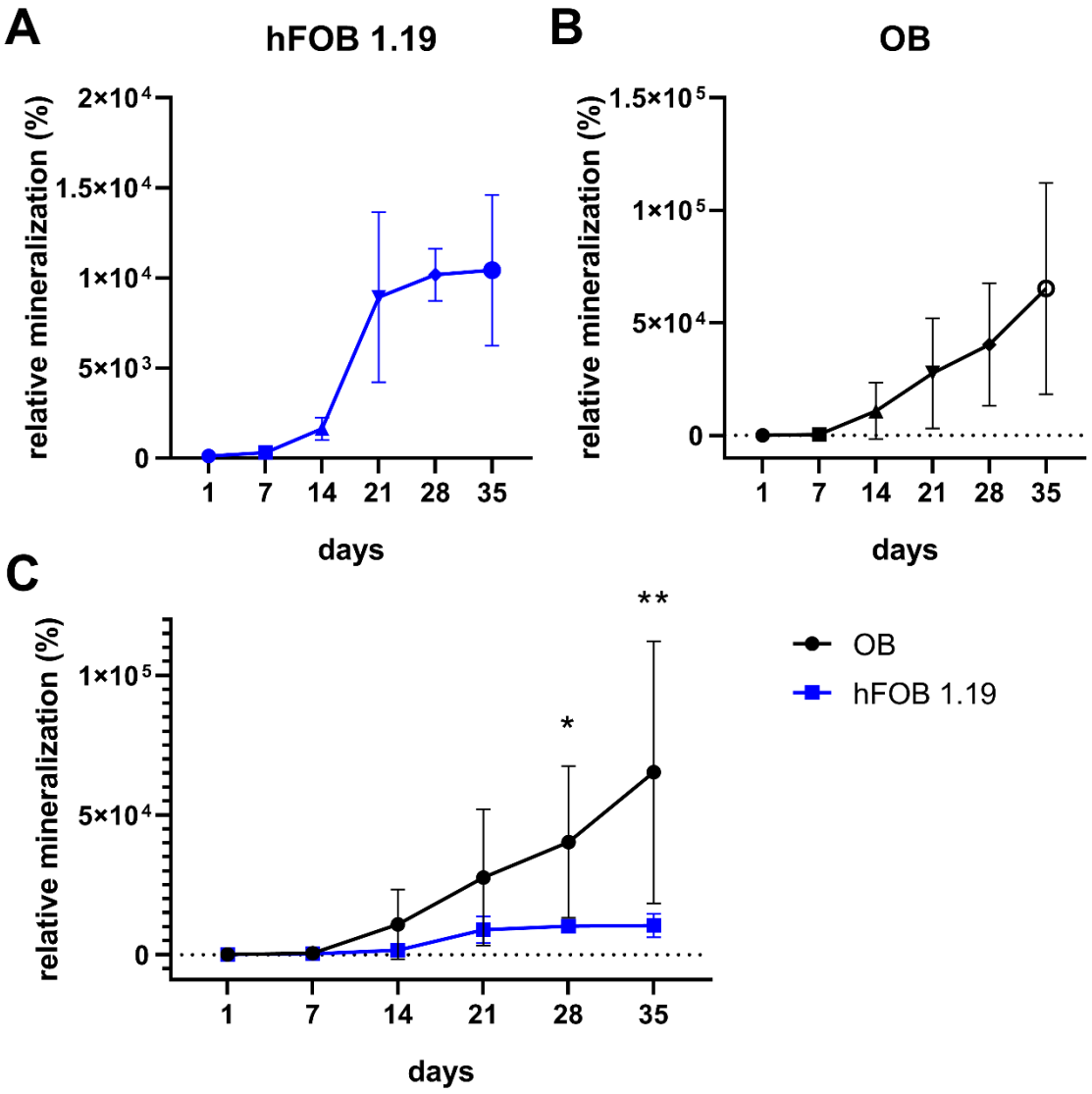

Figure 3.16: Mineralization of hFOB 1.19 cells compared to OBs during osteogenesis. Relative mineralization (quantified via alizarin red S staining) of (A) hFOB 1.19 cells (n = 3) and (B) OBs (n = 13) with OIM treatment over 35 days. (C) Direct comparison of the relative mineralization of hFOB 1.19 cells and OBs over time, normalized to day 1. Data are presented as mean ± SD, and statistical significance was calculated using Mann-Whitney U test ($p \leq 0.05$ (*), $p \leq 0.01$ (**)).

The quantitative differences in mineralization between OBs and hFOB 1.19 cells, as shown in Figure 3.16, are also evident in the microscopic observations of the alizarin red S staining.

In OBs, a network of mineralized nodules begins to form spontaneously between days 14 and 21, with visible gaps where no calcium phosphate is deposited in the matrix until at least day 28 (Fig. 3.17). By day 25, the mineralization appears more homogeneous, and the dark red color suggests that multiple layers of mineralized nodules have formed, indicating an advanced stage of osteogenesis.

In hFOB 1.19 cells, the mineralization process appears different. A yellowish hue becomes visible over the compacted cells at day 7, preceding the formation of calcified nodules (Fig. 3.18). Similar to OBs, red-colored nodules of calcified matrix start forming between days 14 and 21. However, these nodules appear more patchy and less interconnected compared to the reticular structures observed in OBs. By day 35, nearly the entire well shows red staining, although small gaps without mineralization remain.

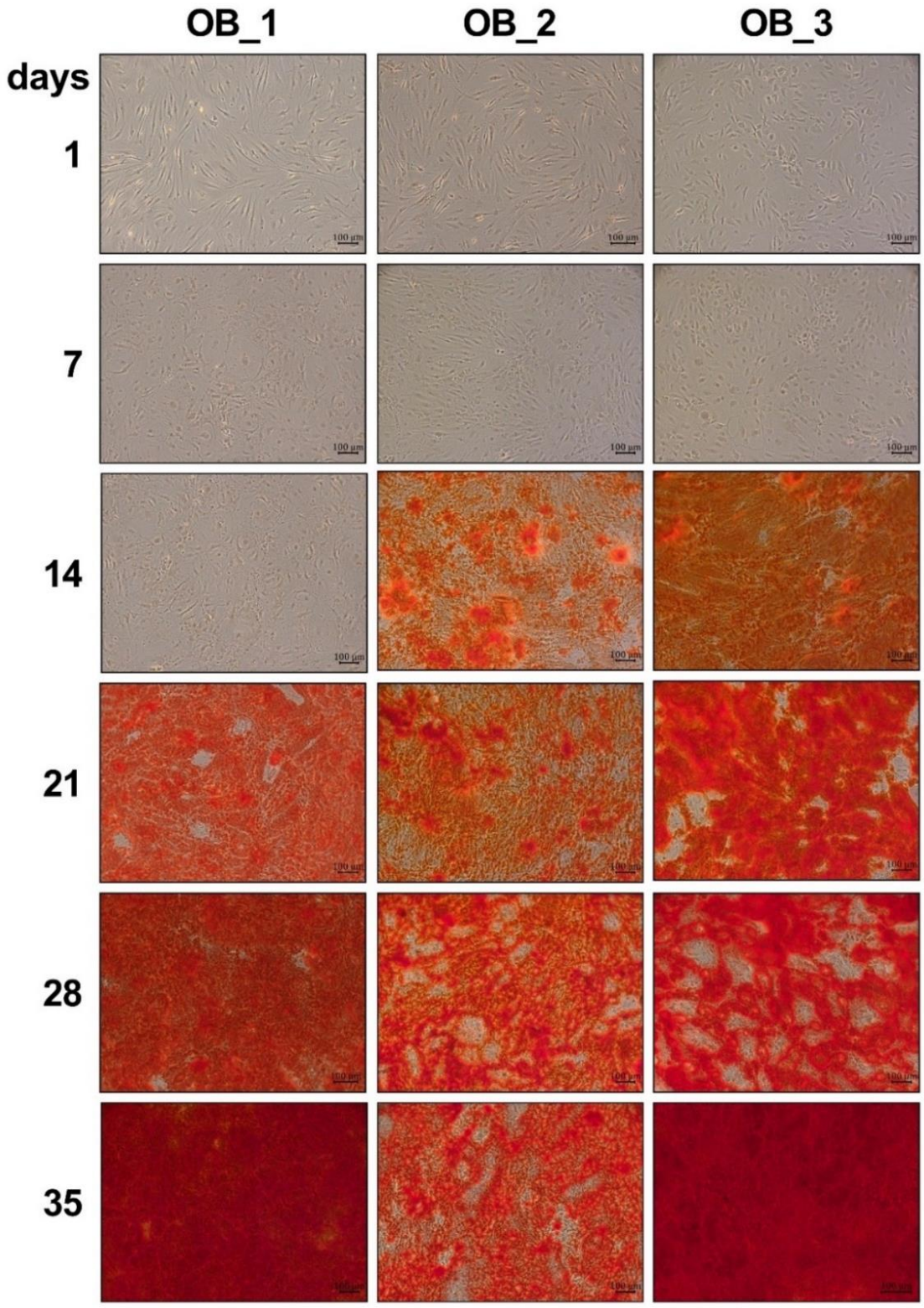

Figure 3.17: Morphology of OBs during osteogenesis and the formation of calcified nodules. Representative microscopically images of primary OBs from three different donors (OB_1, OB_2, and OB_3) during the incubation in OIM after alizarin red S staining on days 1, 7, 14, 21, 28, and 35. Scale bar = 100 µm.

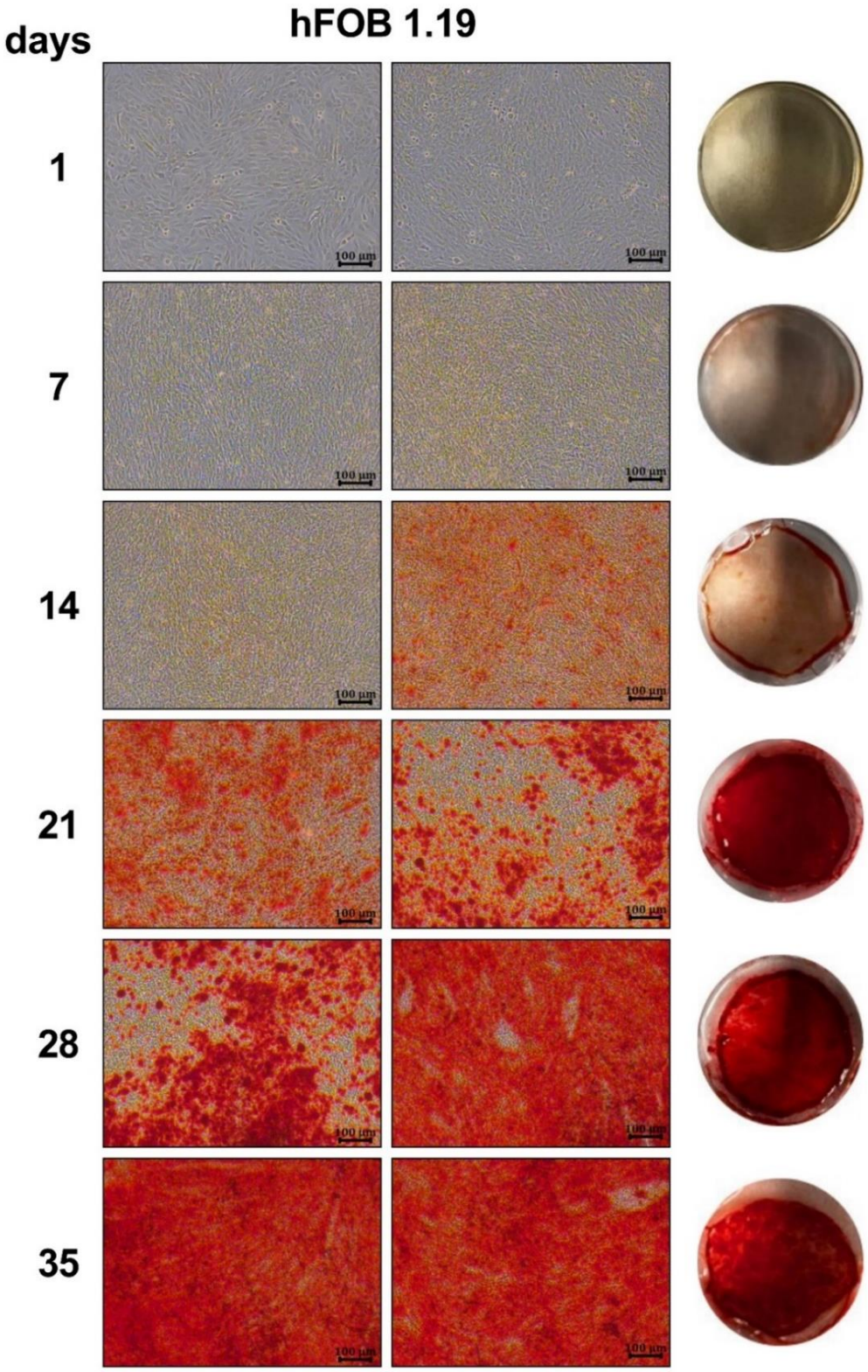

Figure 3.18: Morphology of hFOB 1.19 cells during osteogenesis and the formation of calcified nodules. Representative microscopically images of hFOB 1.19 cells during incubation in OIM after alizarin red S staining on days 1, 7, 14, 21, 28, and 35. Scale bar = 100 µm.

The effects of proinflammatory cytokines on the mineralization of hFOB 1.19 cells were compared to OBs and human bone marrow-derived mesenchymal stem cells (BMSCs).

IL-1β significantly increased the mineralization of OBs and BMSCs in a concentration-dependent manner, with the highest effect observed at 250 units/mL (Fig. 3.19). In contrast, IL-1β had a strong and significant inhibitory effect on the mineralization of hFOB 1.19 cells at all concentrations tested.

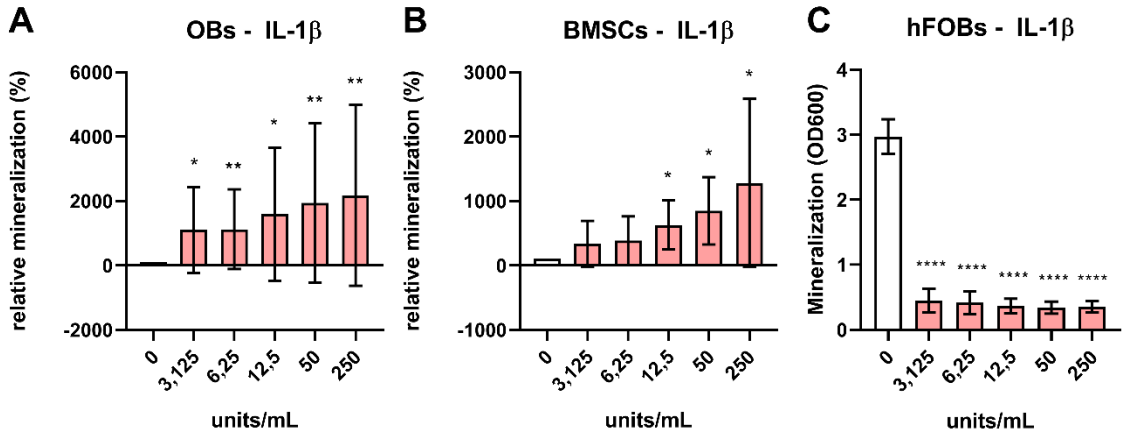

Figure 3.19: Effect of IL-1β on mineralization in OBs, BMSCs, and hFOB 1.19 cells. (A) OBs (n = 9) were cultured for 21 days, (B) BMSCs (n = 6) for 14 days, and (C) hFOB 1.19 cells (n = 5) for 21 days in OIM with different concentrations of IL-1β (3.125 – 250 units/mL). Mineralization was quantified using alizarin red S staining. Data were normalized to the control (0 units/mL) of each experiment. Statistical significance was calculated using the Wilcoxon signed rank test for (A, B) and paired t-tests for (C) ($p \leq 0.05$ (*), $p \leq 0.01$ (**), $p \leq 0.001$ (***)). Data are presented as mean ± SD.

Similar to IL-1β, treatment with IL-6 and IL-8 promoted mineralization in OBs and BMSCs (Fig. 3.20 and 3.21). However, both cytokines significantly inhibited mineralization in hFOB 1.19 cells, although their inhibitory effects were slightly less pronounced than of IL-1β (Fig. 3.19).

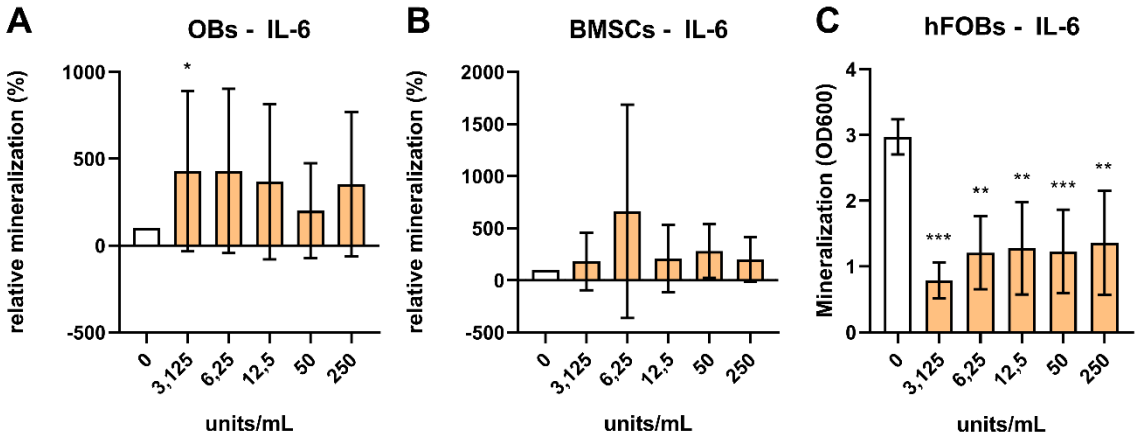

Figure 3.20: Effect of IL-6 on mineralization in OBs, BMSCs, and hFOB 1.19 cells. Similar conditions and analyses were applied as described in Fig. 5.21.

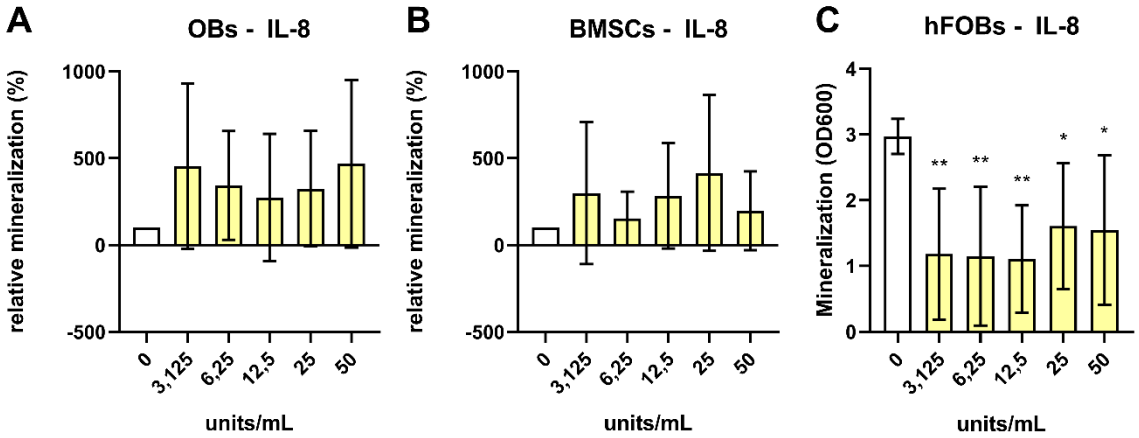

Figure 3.21: Effect of IL-8 on mineralization in OBs, BMSCs, and hFOB 1.19 cells. Similar conditions and analyses were applied as described in Fig. 5.21.

TNF-α showed a strong mineralization-promoting effect in OBs and BMSCs, with significant increases observed in a concentration-dependent manner (Fig. 3.22). Conversely, TNF-α significantly reduced the mineralization of hFOB 1.19 cells at all tested concentrations.

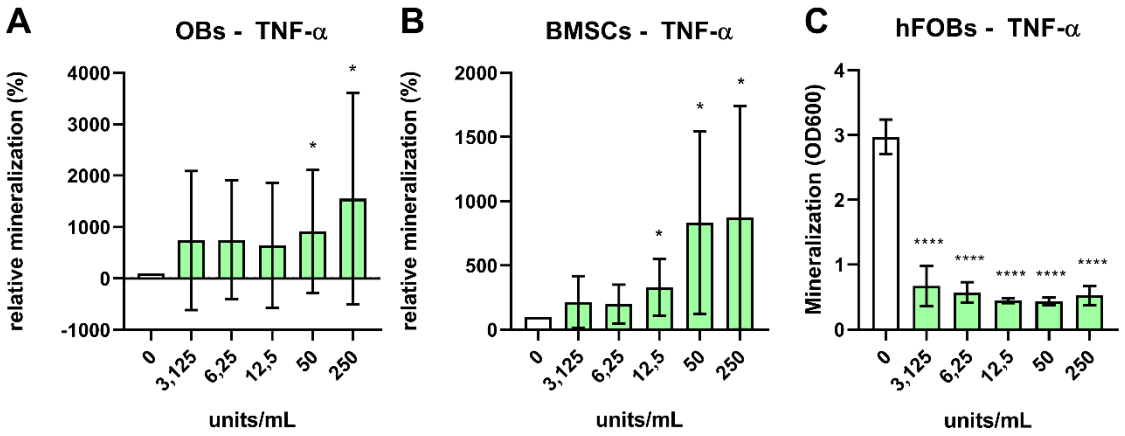

Figure 3.22: Effect of TNF-α on mineralization in OBs, BMSCs, and hFOB 1.19 cells. Similar conditions and analyses were applied as described in Fig. 5.21.

IFNγ significantly enhanced mineralization in OBs at all concentrations but had a significant inhibitory effect on hFOB 1.19 cells at concentrations ≤ 6.25 units/mL (Fig. 3.23). Interestingly, IFNγ appeared to have a tendentially positive effect on BMSC mineralization but with large variability. In hFOB 1.19 cells, higher concentrations of IFNγ also showed signs of toxicity, indicated by increased variability in the data.

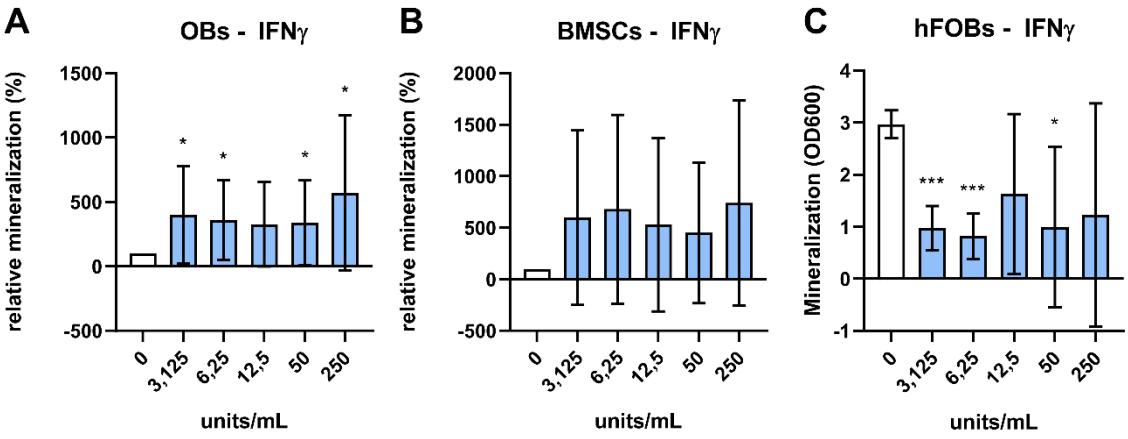

Figure 3.23: Effect of IFNγ on mineralization in OBs, BMSCs, and hFOB 1.19 cells. Similar conditions and analyses were applied as described in Fig. 5.21.

3.2.2.4.2. ALP Activity

The ALP activity in hFOB 1.19 cells increased steadily during osteogenic differentiation in OIM from day 1 to day 35 (Fig. 3.24). The activity was normalized to the respective cell numbers, determined by MTT assays, demonstrating a consistent enhancement of osteogenic activity over the differentiation period.

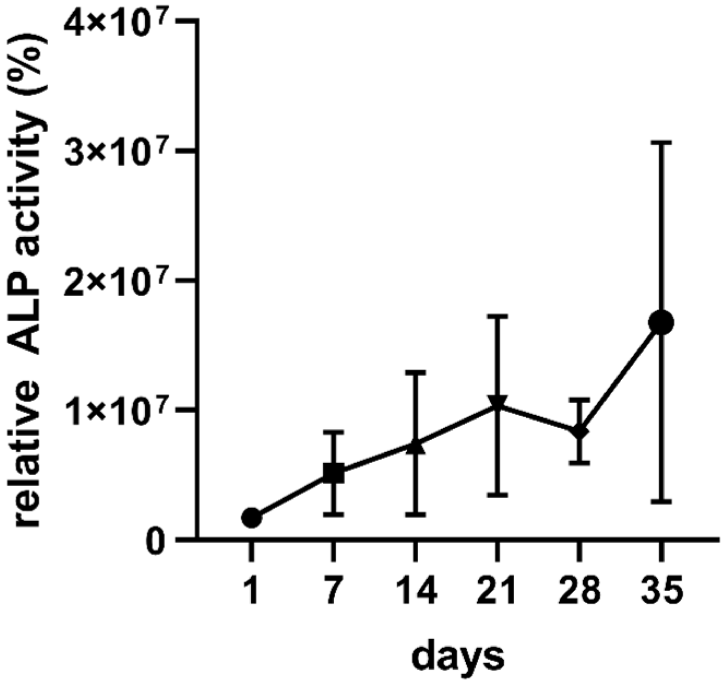

Figure 3.24: ALP activity of hFOB 1.19 cells during osteogenesis. The alkaline phosphatase (ALP) activity of hFOB 1.19 cells was measured weekly from day 1 to 35 during incubation in OIM. The activity was normalized to the respective cell numbers determined by MTT assay on each day and further normalized to the control (day 1) for each experiment (n = 3). The data are presented as mean ± SD.

The addition of proinflammatory cytokines during osteogenesis had varying effects on the ALP activity of hFOB 1.19 cells (Fig. 3.25). Treatment with IL-1β significantly reduced ALP activity on both days 14 and 21 compared to the control (OIM), correlating with its inhibitory effect on mineralization. TNF-α treatment also tended to reduce ALP activity, although the decrease was not statistically significant. Conversely, treatments with IL-6, IL-8, and IFNγ had no measurable impact on ALP activity despite their observed inhibitory effects on mineralization.

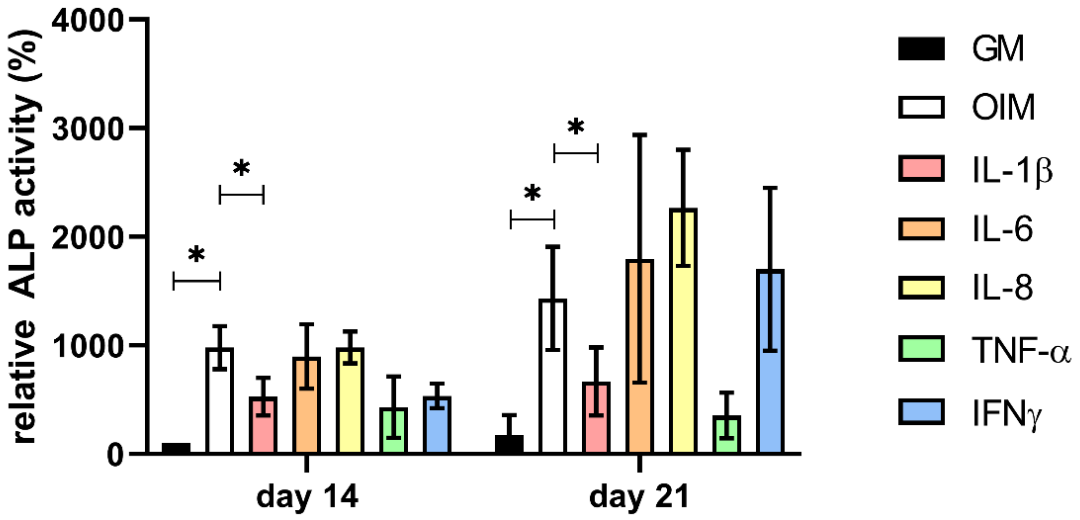

Figure 3.25: Effect of proinflammatory cytokines on the ALP activity of hFOB 1.19 cells during osteogenesis. hFOB 1.19 cells were incubated with the cytokines IL-1β (6.25 units/mL), IL-6 (12.5 units/mL), IL-8 (3.125 units/mL), TNF-α (6.25 units/mL), and IFNγ (6.25 units/mL) in OIM for 14 and 21 days (n = 3). ALP activity was normalized to the respective cell numbers determined by MTT assay on each day. Mean ± SD is shown, and significances were calculated by paired t-tests ($p \leq 0.05$ (*)).

3.2.2.4.3. Expression of Osteogenic Differentiation Markers

To evaluate the impact of cytokines on osteogenic differentiation, the mRNA expression of seven key markers during osteogenesis (days 1 - 35) was analyzed in hFOB 1.19 cells (Fig. 3.26).

The expression of *ALP* increased significantly during the initial seven days and remained on the same level until day 28, with a slight increase observed on day 35. Similarly, *TGFβ-RII* followed a comparable trend, peaking early and stabilizing, with another sharp increase on day 35. The *Col1α2* mRNA expression peaked on day 7 but fell back to baseline levels by day 14 and remained unchanged until a slight increase on day 35. The expression of *Runx2* shows a dynamic pattern, increasing slightly by day 14, significantly dropping on day 21, peaking strongly on day 28, and then dropping again significantly on day 35. *OPN* peaked early at day 14 and returned to baseline by day 35, whereas *OCN* expression only began to rise significantly after day 21, peaking at day 35. Notably, *OSX* displayed peaks at days 14 and 35, with high variability on these days.

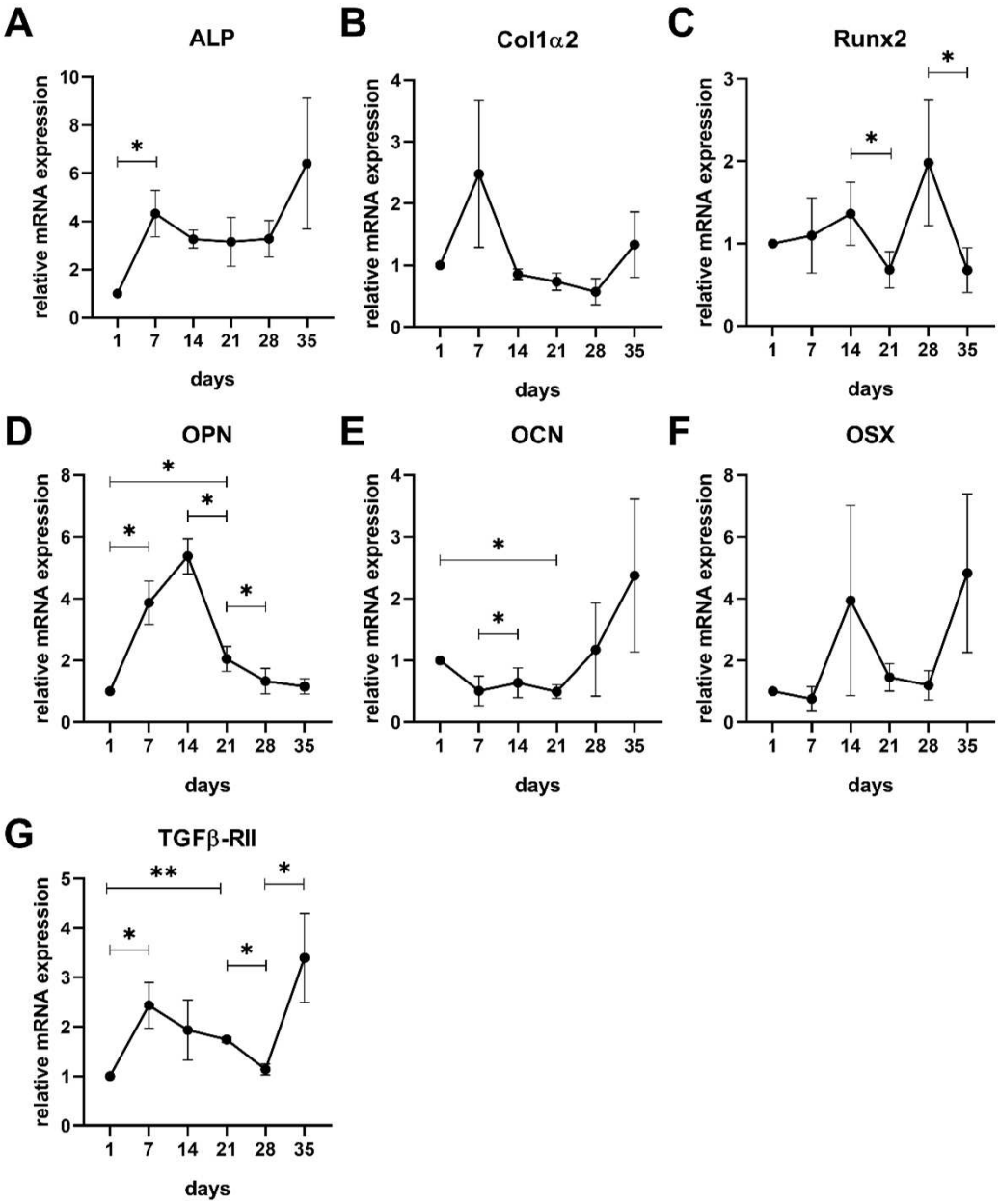

Figure 3.26: Osteogenic marker expression during osteogenesis in hFOB 1.19 cells. The mRNA levels of osteogenic differentiation markers (A) *ALP*, (B) *collagen type 1 alpha 2* (*Col1α2*), (C) *runt-related transcription factor 2* (*Runx2*), (D) *osteopontin* (*OPN*), (E) *osteocalcin* (*OCN*), (F) *osterix* (*OSX*), and (G) *transforming growth factor beta receptor II* (*TGFβ-RII*) were quantified via qPCR from day 1 to 35 in OIM-treated hFOB 1.19 cells (n = 3). Relative mRNA levels were normalized using the 2-ΔΔ Ct method against *RPLP0* as the reference gene and day 1 as the control. Data are presented as mean ± SD, with significances calculated using paired t-tests ($p \leq 0.05$ (*)).

Subsequent analysis investigated the effects of cytokine treatments on these osteogenic markers on day 21 of osteogenesis (Fig. 3.27). IL-6 was the most notable cytokine, significantly increasing *ALP* and *OPN* expression, while also showing a tendency to enhance *Col1α2* and *Runx2* expression. IL-8 led to a significant increase in *Runx2* and *OPN*, but concurrently inhibited *OSX* expression. TNF-α and IL-1β, which strongly inhibited mineralization (Fig. 3.19 and 3.22), did not significantly affect marker expression except for a non-significant inhibitory effect of *OSX*. Treatment with IFNγ also activated *OPN* expression while significantly suppressing *OSX*. Among all cytokines, IL-6 was the only one that increased *ALP* expression while not effecting *OSX* negatively, showing its unique impact on hFOB 1.19 cells.

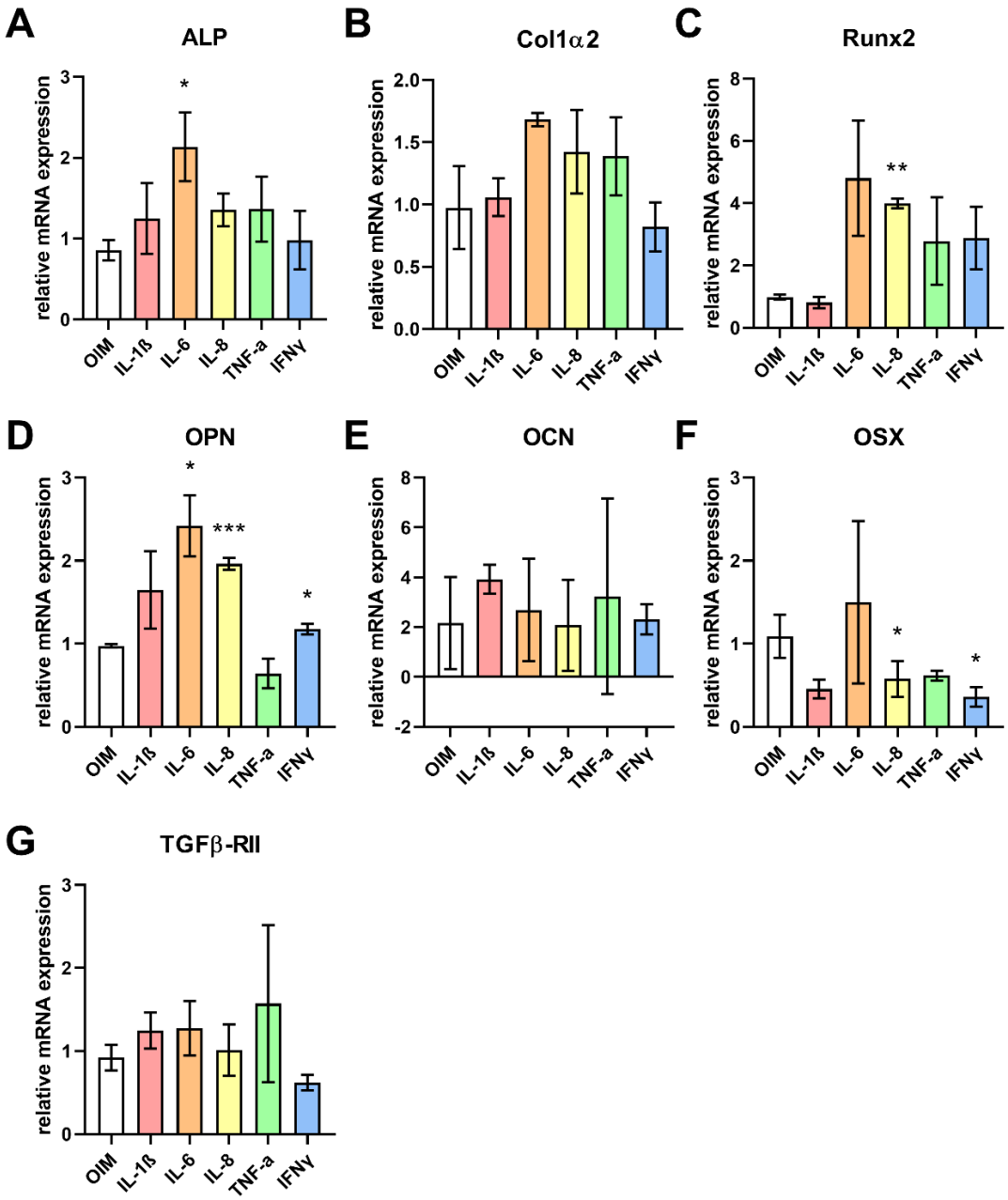

Figure 3.27: Impact of proinflammatory cytokines on the expression of osteogenic markers in hFOB 1.19 cells. The mRNA expression of the osteogenic differentiation markers (A) *ALP*, (B) *Col1α2*, (C) *Runx2*, (D) *OPN*, (E) *OCN*, (F) *OSX*, and (G) *TGFβ-RII* were determined by qPCR on day 21 of treatment with the cytokines IL-1β (6.25 units/mL), IL-6 (12.5 units/mL), IL-8 (3.125 units/mL), TNF-α (6.25 units/mL), and IFNγ (6.25 units/mL) in OIM of hFOB 1.19 cells (n = 3). Relative mRNA levels were normalized using the 2-ΔΔ Ct method against *RPLP0* as the reference gene and OIM as the control. Data are presented as mean ± SD, with significances calculated using paired t-tests ($p \leq 0.05$ (*), $p \leq 0.01$ (**), $p \leq 0.001$ (***)).

The expression of osteogenic differentiation markers was also analyzed in OBs, focusing on *ALP*, *Col1α2*, *Runx2*, *OPN*, and *OSX*. Compared to the hFOB 1.19 cell line, mRNA expression in OBs exhibited greater variability, as reflected by the high standard deviations (Fig. 3.28). A distinct increase in *ALP* mRNA expression was observed during the early stages of osteogenesis, reaching its peak on day 14, followed by a gradual decline until day 35. *Col1α2* expression peaked early on day 7, maintaining a steady level until day 28 before decreasing by day 35. *Runx2* expression exhibited a continuous rise from day 1 through day 28. Interestingly, *OPN* mRNA expression was predominantly detected at later stages of osteogenesis, with a strong increase between days 21 and 35. Similarly, *OCN* expression showed an initial modest increase, followed by a marked rise starting from day 21, suggesting its involvement in the late stages of differentiation.

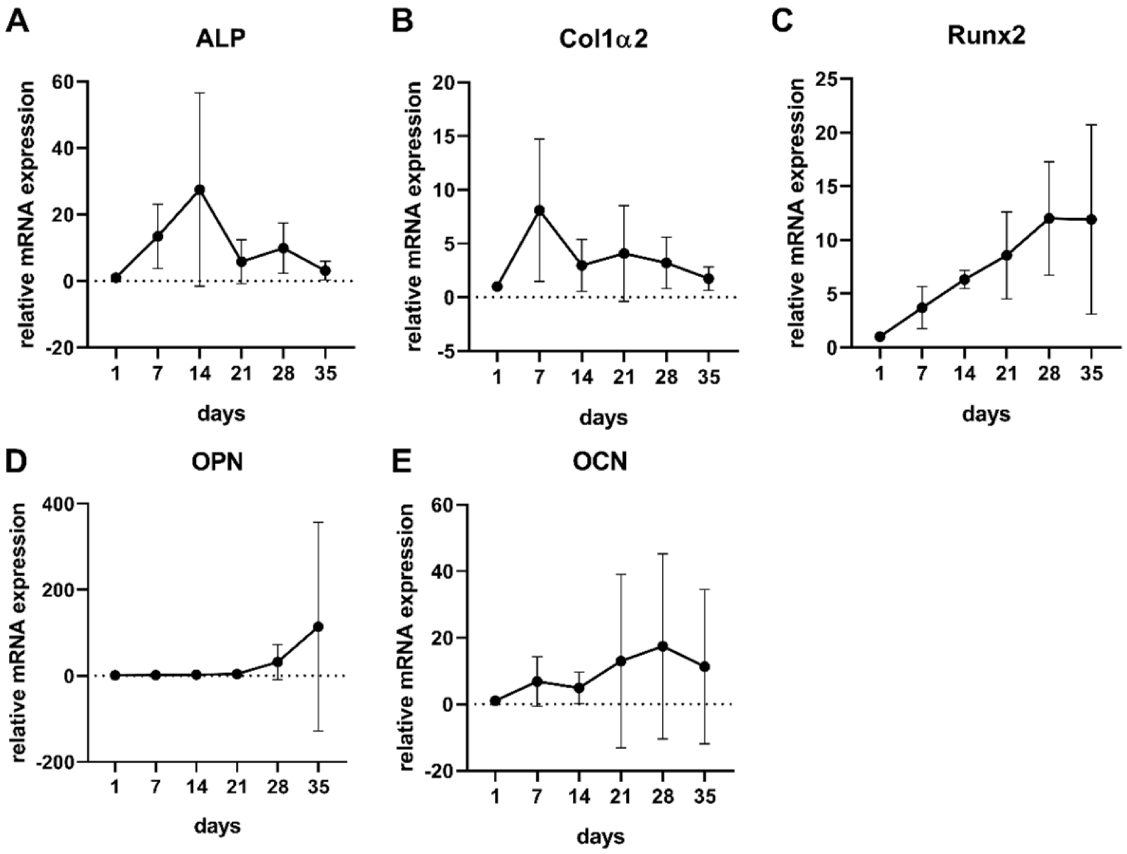

Figure 3.28: mRNA expression of osteogenic markers in OBs during osteogenesis. The mRNA expression levels of the osteogenic differentiation markers (A) *ALP*, (B) *Col1α2*, (C) *Runx2*, (D) *OPN*, and (E) *OCN* were quantified by qPCR on days 1, 7, 14, 21, 28, and 35 of OIM-treated OBs (n = 5). Relative mRNA levels were normalized using the 2-ΔΔ Ct method against *TFRC* as the reference gene and day 1 as the control. Data

are presented as mean ± SD, with significances calculated using Wilcoxon-signed rank test (ns).

The observed variability in mRNA expression among OBs likely reflects donor-specific differences. Further insights into these variations are provided in the individual donor analysis presented in the subsequent section.

In the individual analysis of *ALP* expression, clear differences between the five OBs from different donors were observed (Fig. 3.29). Four of the OBs displayed distinct peaks of *ALP* expression at specific time points during differentiation. For OB_4 and OB_5, the maximum expression was observed on day 14. OB_2 had an earlier peak on day 1, while OB_1 reached its maximum on day 28, with a slight increase on days 7 and 14. OB_3 presented a unique pattern, with the highest expression recorded on day 7, which remained elevated until day 28. Followed by a decrease on day 35.

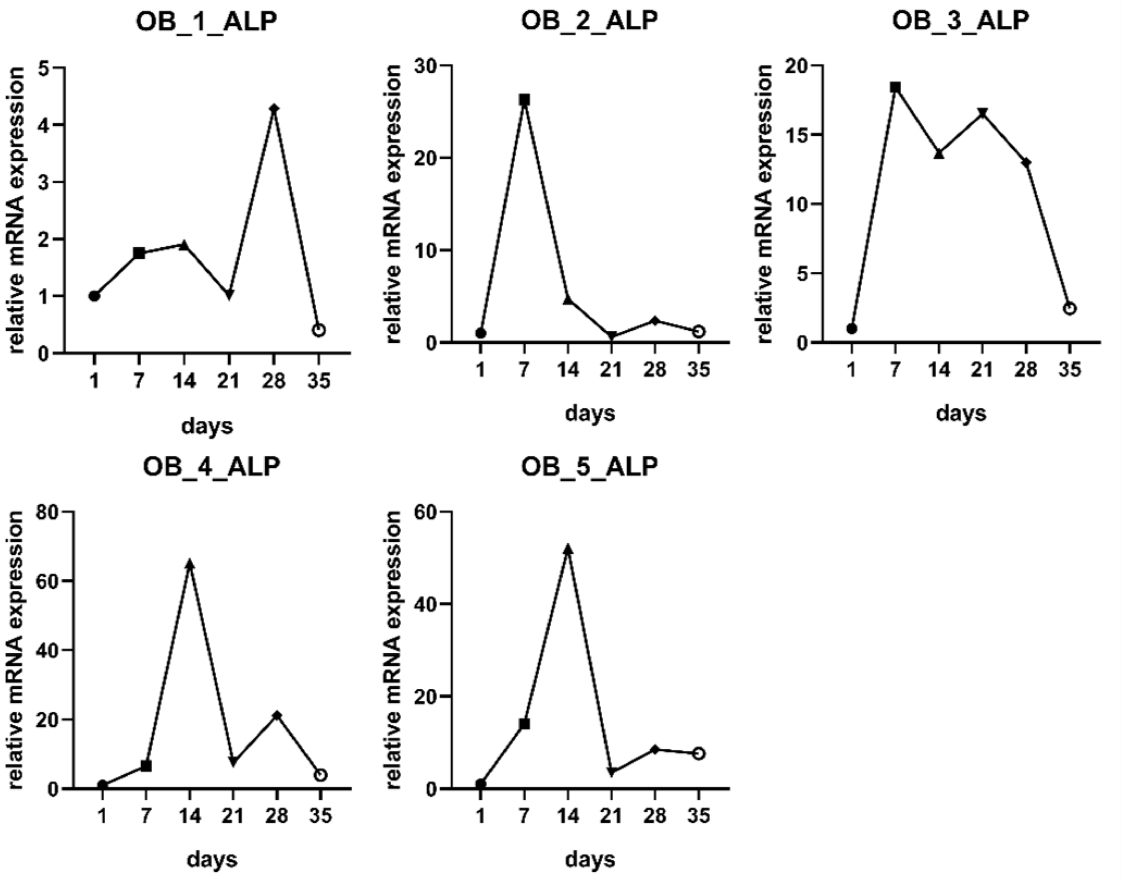

Figure 3.29: Individual evaluation of *ALP* mRNA expression across five different OBs during osteogenesis. The mRNA expression of the osteogenic differentiation

marker *ALP* was analyzed by qPCR on days 1, 7, 14, 21, 28, and 35 of OIM-treated OBs (n = 5). Relative mRNA expression was calculated by the 2-ΔΔCt method and normalized to the control (day 1) of each experiment using the reference gene *TFRC*.

The analysis of *Col1α2* mRNA expression also revealed variability among the donors, but also with similarities (Fig. 3.30). OB_1, OB_2, OB_3, and OB_5 had a maximum peak on day 7, with OB_1, OB_2, and OB_3 showing a secondary, smaller peak at later stages of differentiation (between days 21 and 28). In contrast, OB_4 demonstrated its smaller peak on day 7 and reached its maximum *Col1α2* expression on day 28.

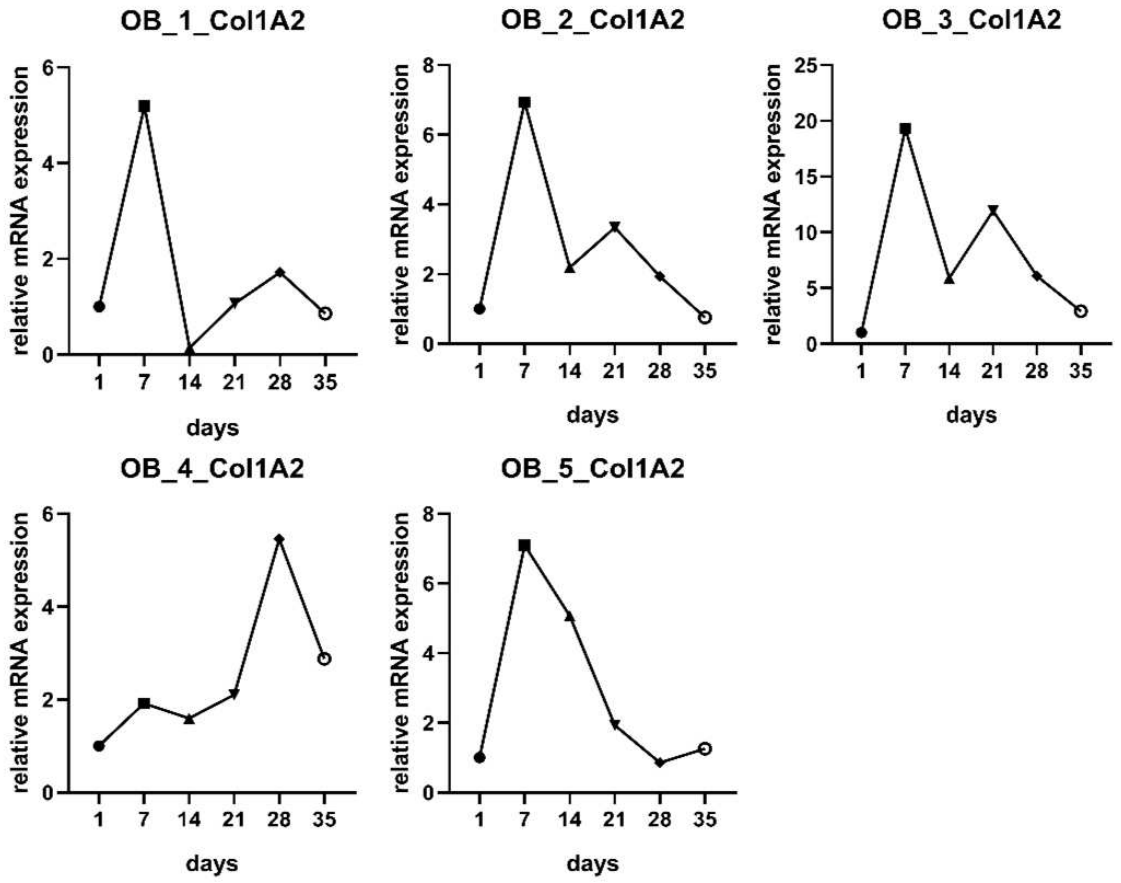

Figure 3.30: Individual evaluation of *Col1α2* mRNA expression across five different OBs during osteogenesis. The mRNA expression of the osteogenic differentiation marker *Col1α2* was determined by qPCR on days 1, 7, 14, 21, 28, and 35 of OIM-treated OBs (n = 5). Relative mRNA expression was calculated by the 2-ΔΔCt method and normalized to the control (day 1) of each experiment using the reference gene *TFRC*.

The mRNA expression of the marker *Runx2* displayed a consistent trend across the five donors during osteogenesis (Fig. 3.31). All OBs showed a steady increase in expression levels, with slight variations in the timing of peak expression. OB_1 reached its maximum on day 28, while OB_3 and OB_4 had the highest expression on day 21. In OB_2 and OB_5, the expression of Runx2 continued to rise, reaching the highest levels on day 35.

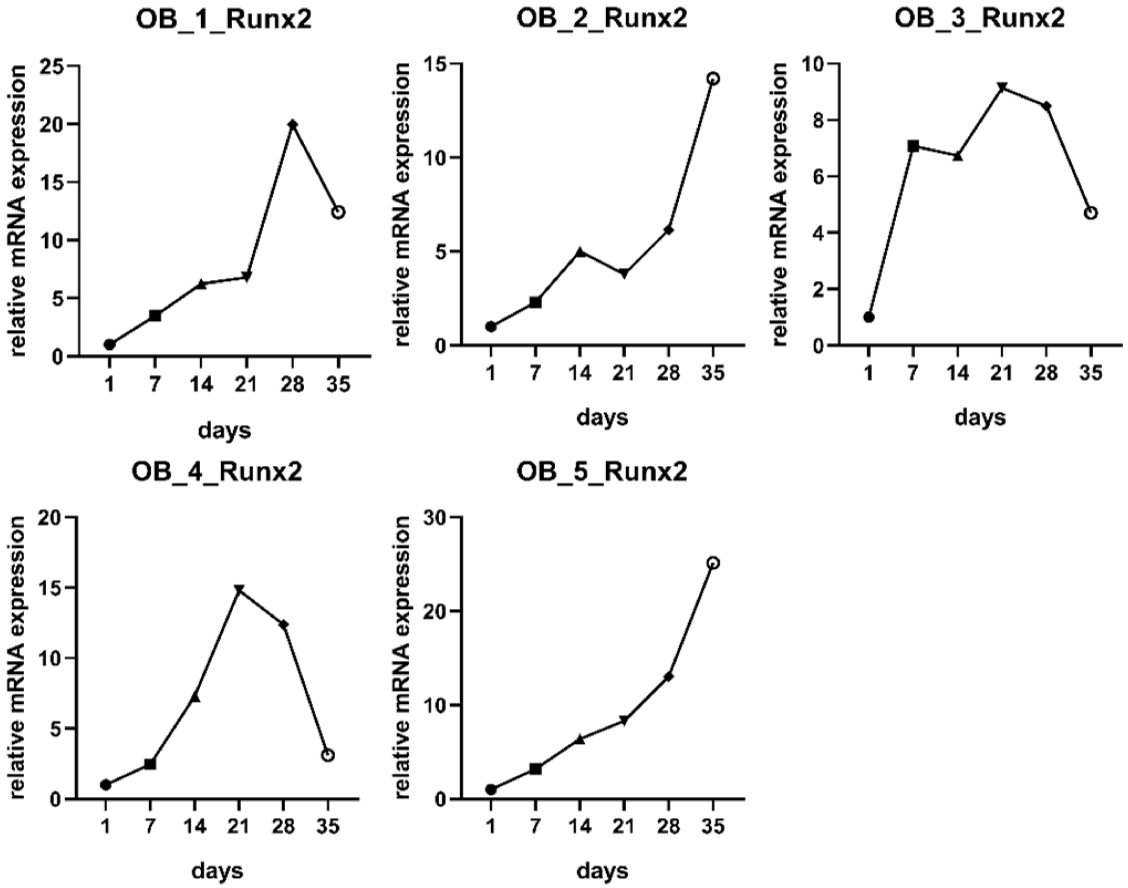

Figure 3.31: Individual evaluation of *Runx2* mRNA expression across five different OBs during osteogenesis. The mRNA expression of the osteogenic differentiation marker *Runx2* was determined by qPCR on days 1, 7, 14, 21, 28, and 35 of OIM-treated OBs (n = 5). Relative mRNA expression was calculated by the 2-ΔΔCt method and normalized to the control (day 1) of each experiment using the reference gene *TFRC*.

OPN gene expression had similarities across all five donor OBs during osteogenesis (Fig. 3.32). During the early stage of differentiation, only minor increases in *OPN*

expression were observed. However, from day 21 onwards, the expression levels markedly increased. In three donors (OB_1, OB_3, and OB_4), the maximum *OPN* expression was reached before day 35, while in OB_2 and OB_5, the highest levels were measured on day 35. Interestingly, OB_4 had a temporary drop in *OPN* expression on day 7 before the subsequent increase.

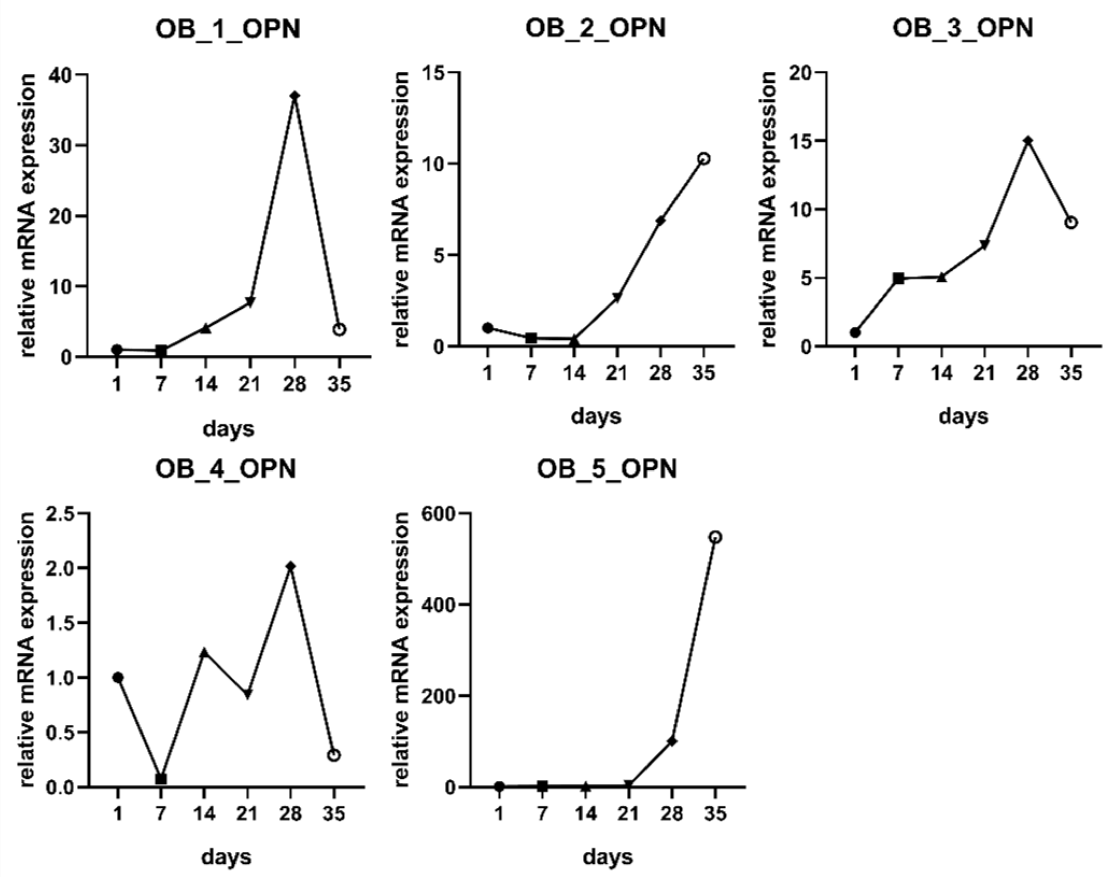

Figure 3.32: Individual evaluation of *OPN* mRNA expression across five different OBs during osteogenesis. The mRNA expression of the osteogenic differentiation marker *OPN* was determined by qPCR on days 1, 7, 14, 21, 28, and 35 of OIM-treated OBs (n = 5). Relative mRNA expression was calculated by the 2-ΔΔ Ct method and normalized to the control (day 1) of each experiment using the reference gene *TFRC*.

The expression pattern of *OCN* mRNA varied widely among the donor OBs (Fig. 3.33). OB_1 and OB_5 showed a single peak of high expression values, either on day 7 or day 14 of osteogenesis. In contrast, OB_2 had two distinct peaks on day 7 and later on day 28. OB_4 showed the highest expression level of *OCN* on day 1 in

undifferentiated OBs, with a drop on day 7 and minimal changes during the subsequent period. In OB_3, a consistent increase was observed from day 14 to 35.

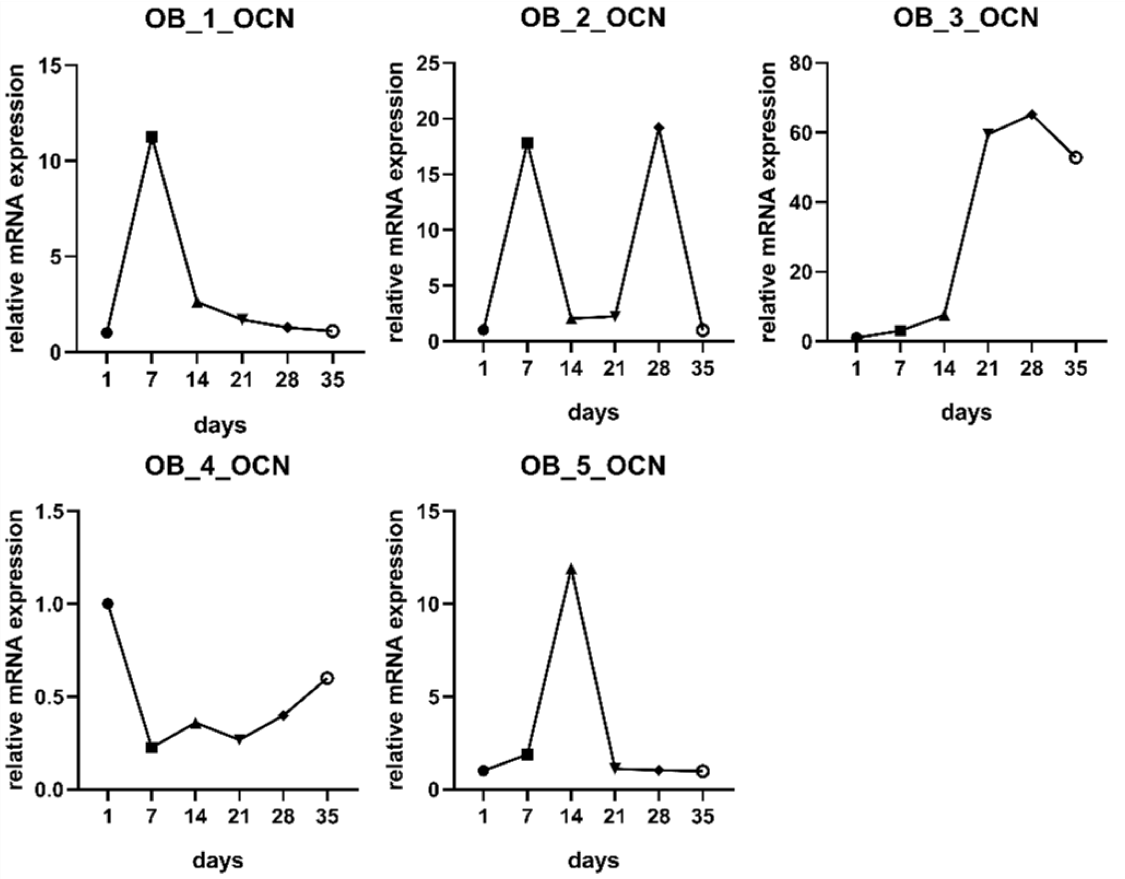

Figure 3.33: Individual evaluation of *OCN* mRNA expression across five different OBs during osteogenesis. The mRNA expression of the osteogenic differentiation marker *OCN* was determined by qPCR on days 1, 7, 14, 21, 28, and 35 of OIM-treated OBs (n = 5). Relative mRNA expression was calculated by the 2-ΔΔCt method and normalized to the control (day 1) of each experiment using the reference gene *TFRC*.

To further explore how cytokine treatments affect the expression of osteogenic differentiation markers in OBs, the mRNA expression levels of *ALP*, *Col1α2*, *Runx2*, *OPN*, and *OCN* were analyzed after 21-day treatment with IL-1β, IL-6, IL-8, TNF-α, and IFNγ.

IL-1β-treated OBs showed a tendency toward reduced mRNA expression of *Col1α2* and *Runx2* compared to the differentiated control without cytokines (Fig. 3.34). However, a slight upregulation of *ALP* and *OPN* expression was observed.

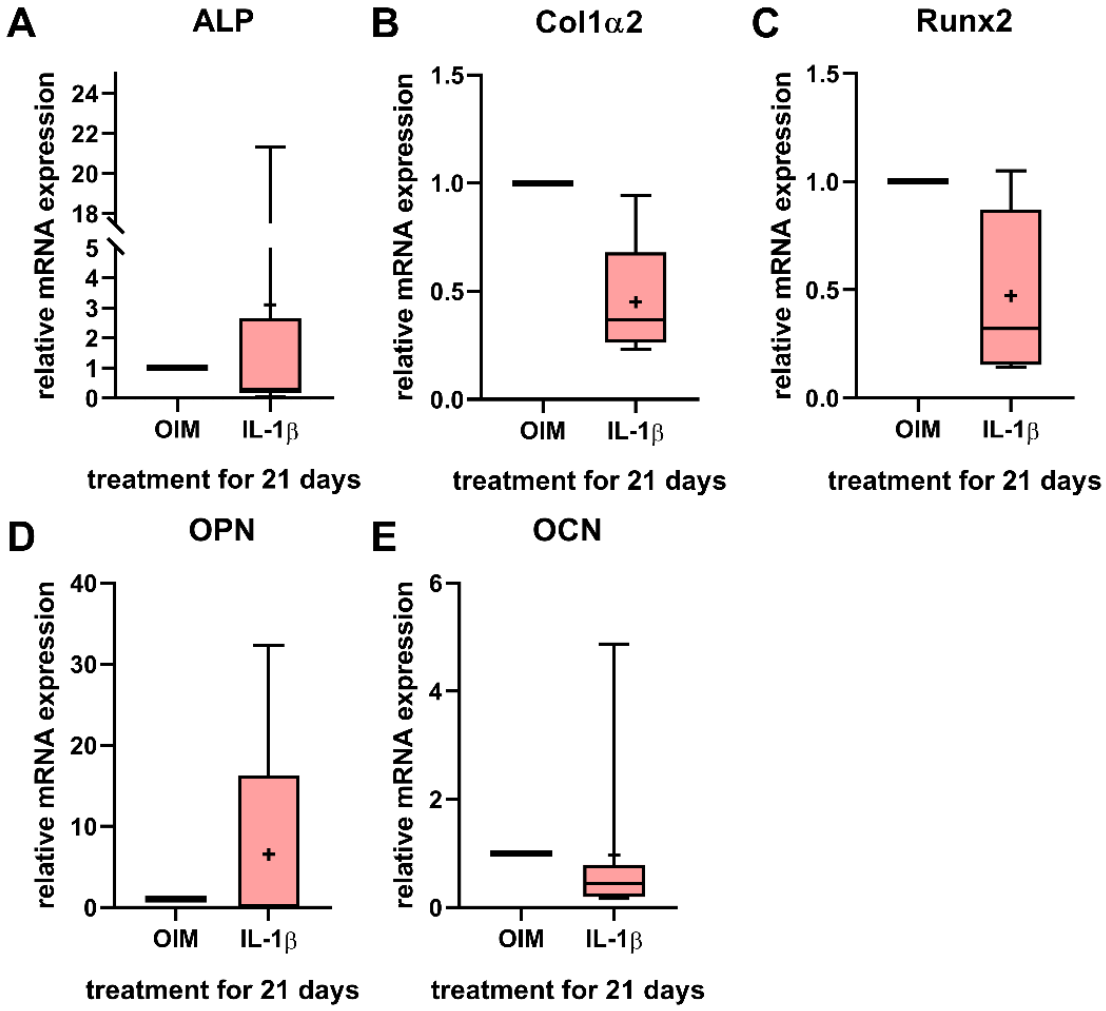

Figure 3.34: Impact of IL-1β treatment on osteogenic differentiation marker expression of OBs on day 21. The cells were treated with 250 units/mL of IL-1β in OIM for 21 days and the mRNA expression of the osteogenic differentiation markers (A) *ALP* (n = 9), (B) *Col1α2* (n = 5), (C) *Runx2* (n = 5), (D) *OPN* (n = 5), and (E) *OCN* (n = 8) were determined by qPCR. The relative mRNA expression was calculated by the 2-ΔΔ Ct method and normalized on the control (OIM) of each donor using the reference gene *TFRC*. Boxplot diagrams are shown and the significances were calculated by Wilcoxon signed rank test (ns).

Treatment with IL-6 resulted in a decrease in *Col1α2* expression, alongside an increase in *OPN* expression (Fig. 3.35). Meanwhile, *Runx2* and *ALP* tended to be expressed at lower levels compared to the control.

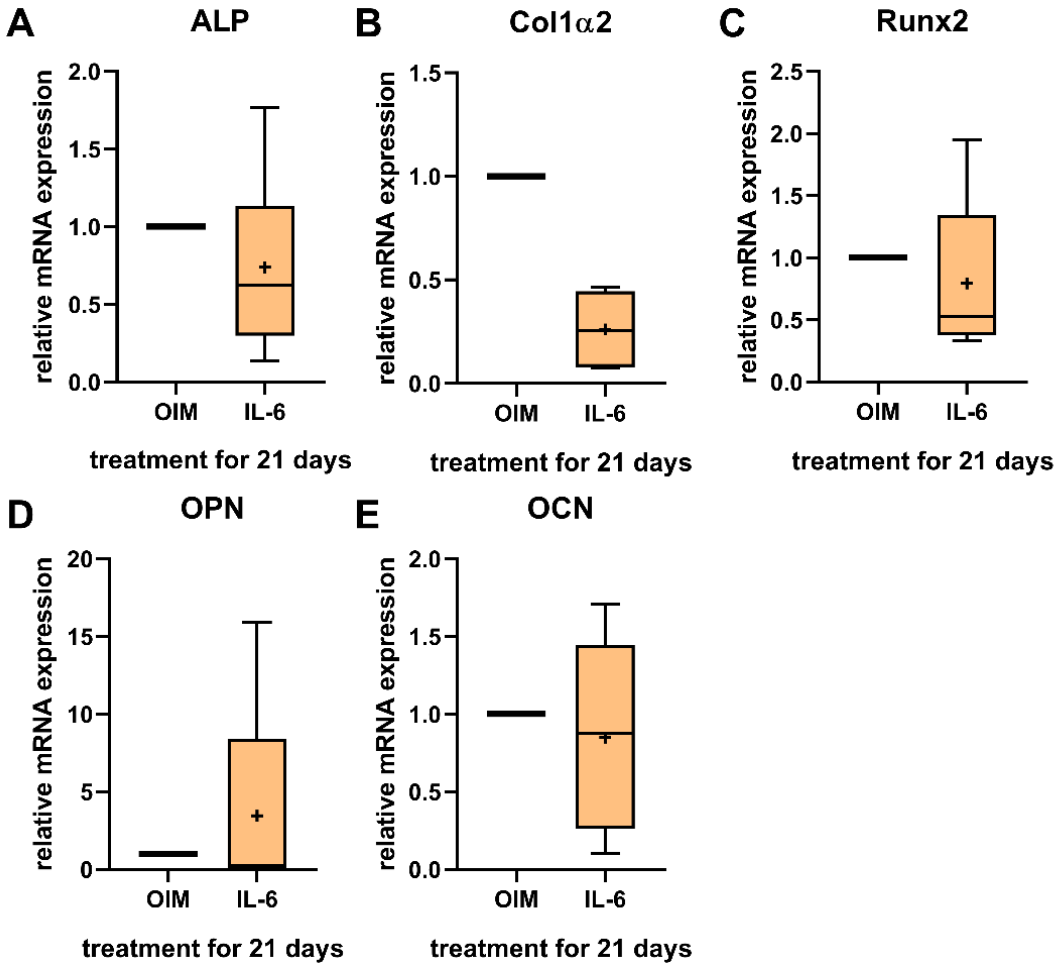

Figure 3.35: Impact of IL-6 treatment on osteogenic differentiation marker expression of OBs on day 21. The cells were treated with 12.5 units/mL of IL-6 in OIM for 21 days and the mRNA expression of the osteogenic differentiation markers (A) *ALP* (n = 6), (B) *Col1α2* (n = 5), (C) *Runx2* (n = 5), (D) *OPN* (n = 5), and (E) *OCN* (n = 7) were determined by qPCR. The relative mRNA expression was calculated by the 2-ΔΔ Ct method and normalized on the control (OIM) of each donor using the reference gene *TFRC*. Boxplot diagrams are shown and the significances were calculated by Wilcoxon signed rank test (ns).

A trend towards a reduction in *Runx2* expression and an increase in *OPN* expression was also measured with IL-8 treatment on day 21 of differentiation (Fig. 3.36). IL-8 had no consistent effect on the expression of *ALP*, *Col1α2*, and *OCN*.

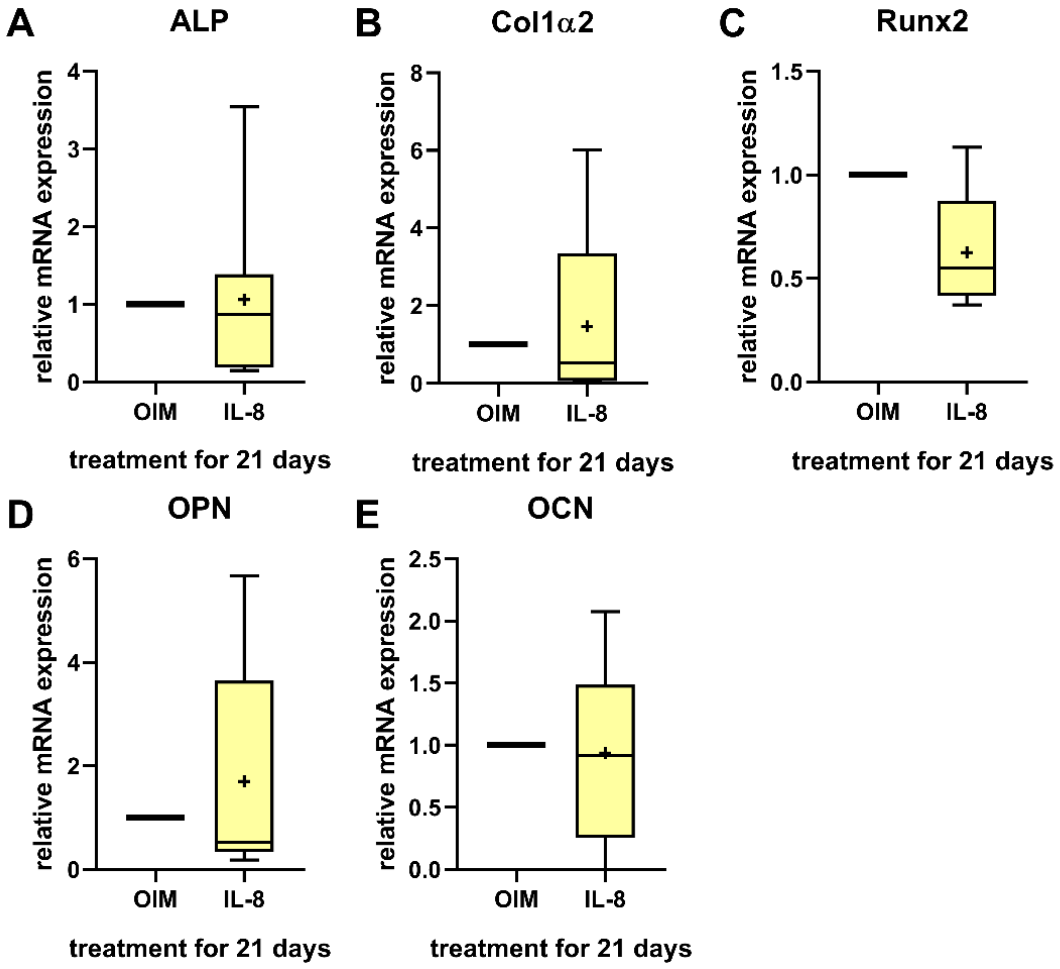

Figure 3.36: Impact of IL-8 treatment on osteogenic differentiation marker expression of OBs on day 21. The cells were treated with 12.5 units/mL of IL-8 in OIM for 21 days and the mRNA expression of the osteogenic differentiation markers (A) *ALP* (n = 8), (B) *Col1α2* (n = 5), (C) *Runx2* (n = 5), (D) *OPN* (n = 5), and (E) *OCN* (n = 8) were determined by qPCR. The relative mRNA expression was calculated by the 2-ΔΔ Ct method and normalized on the control (OIM) of each donor using the reference gene *TFRC*. Boxplot diagrams are shown and the significances were calculated by Wilcoxon signed rank test (ns).

Treatment with TNF-α led to a strong reduction in *OPN* and *OCN* mRNA expression (Fig. 3.37). Beside a trend towards a reduction in *Col1α2*, *ALP* and *Runx2* were not notably affected.

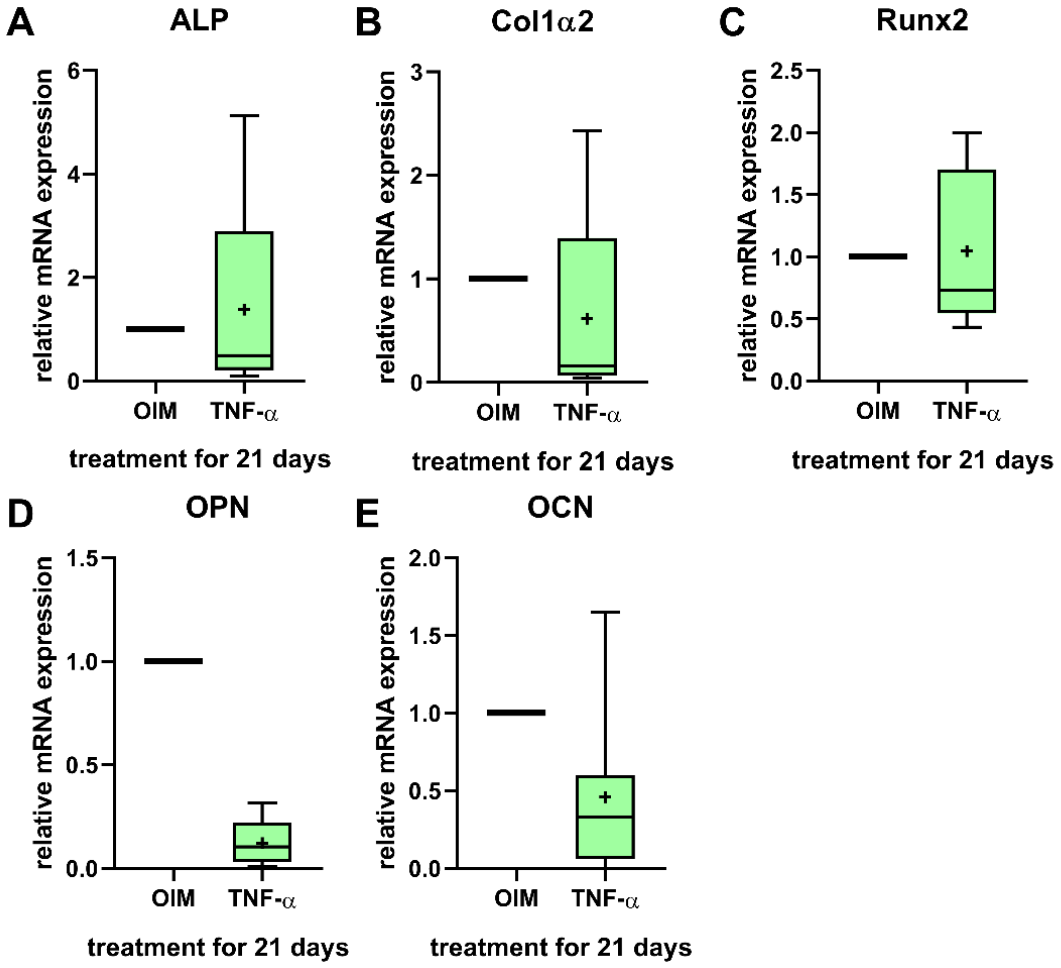

Figure 3.37: Impact of TNF-α treatment on osteogenic differentiation marker expression of OBs on day 21. The cells were treated with 250 units/mL of TNF-α in OIM for 21 days and the mRNA expression of the osteogenic differentiation markers (A) *ALP* (n = 8), (B) *Col1α2* (n = 5), (C) *Runx2* (n = 5), (D) *OPN* (n = 5), and (E) *OCN* (n = 8) were determined by qPCR. The relative mRNA expression was calculated by the 2-ΔΔ Ct method and normalized on the control (OIM) of each donor using the reference gene *TFRC*. Boxplot diagrams are shown and the significances were calculated by Wilcoxon signed rank test (ns).

IFNγ exposure slightly suppressed *OPN* and *Runx2* expression, while a minor increase in *OCN* expression was detected (Fig. 3.38). *ALP* and *Col1α2* levels remained largely unchanged.

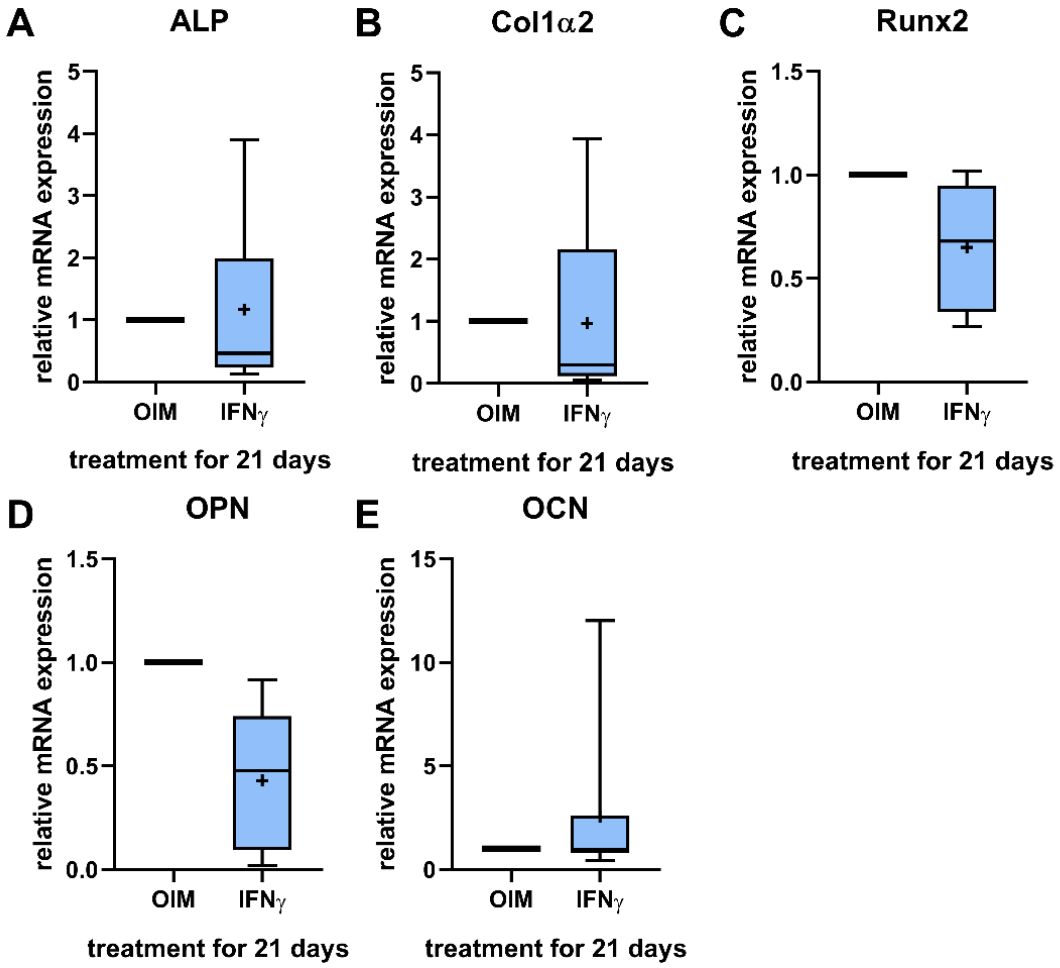

Figure 3.38: Impact of IFNγ treatment on osteogenic differentiation marker expression of OBs on day 21. The cells were treated with 3.125 units/mL of IFNγ in OIM for 21 days and the mRNA expression of the osteogenic differentiation markers (A) *ALP* (n = 8), (B) *Col1α2* (n = 5), (C) *Runx2* (n = 5), (D) *OPN* (n = 5), and (E) *OCN* (n = 8) were determined by qPCR. The relative mRNA expression was calculated by the 2-ΔΔ Ct method and normalized on the control (OIM) of each donor using the reference gene *TFRC*. Boxplot diagrams are shown and the significances were calculated by Wilcoxon signed rank test (ns).

3.2.3. Additional Analyses of the Differentiation of OBs

3.2.3.1. Analyses of Signaling Pathways

This study also aimed to investigate the role of the Wnt signaling pathway, which is essential for osteogenesis, and to evaluate how cytokines modulate its activity. Furthermore, the MAPK (mitogen-activated protein kinase) signaling pathway, which is documented to respond to cytokine stimulation, was analyzed.

3.2.3.1.1. Wnt Signaling – β-catenin Protein Expression

The protein expression of β-catenin varied among the donor cells during osteogenesis (Fig. 3.39). In OB_7, β-catenin levels showed a gradual increase throughout the 35 days of differentiation. For OB_8, the expression peaked on day 28 before declining by day 35. In contrast, OB_9 showed an early increase on day 7, followed by a reduction in expression until day 21, and subsequently returning to levels similar to day 1 by day 35.

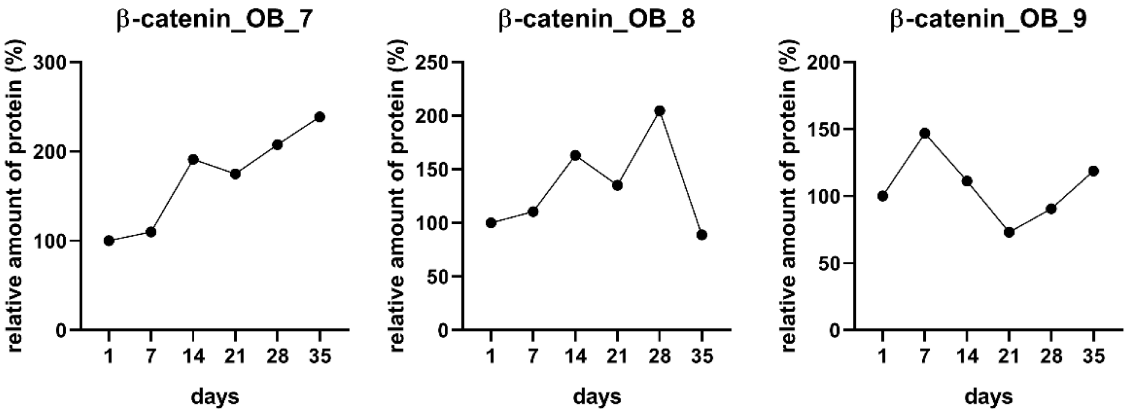

Figure 3.39: Protein expression of β-catenin in OBs during osteogenesis. The protein expression of β-catenin in OBs from three donors (OB_7, OB_8, and OB_9) treated with OIM for 35 days was determined weekly on days 1, 7, 14, 21, 28, and 35 by performing an SDS-PAGE (20 µg cell lysate) and subsequent Western blotting. The chemiluminescent images were quantified on total protein amount and the data were normalized to the control (day 1).

The impact of cytokine treatment on β-catenin expression on day 21 was assessed (Fig. 3.40). In the combined analysis across all donors, cytokine treatments did not

induce significant changes in β-catenin (Fig. 3.40, A). However, individual donor evaluation revealed considerable variability (Fig. 3.40, B). A trend towards reduced β-catenin expression following IL-1β and IL-6 treatments was observed in OB_1, OB_3, OB_4, OB_6, and OB_7. Conversely, these cytokines had no effect in OB_2 and increased β-catenin expression in OB_5 compared to the control (OIM). IL-8 treatment exhibited a tendency towards upregulation in the combined analysis, driven largely by elevated expression in OB_1 and OB_3, while other OBs showed either no change or even reduced expression. Similarly, IFNγ treatment resulted in high variability among donors, as reflected in the large whiskers in the combined data.

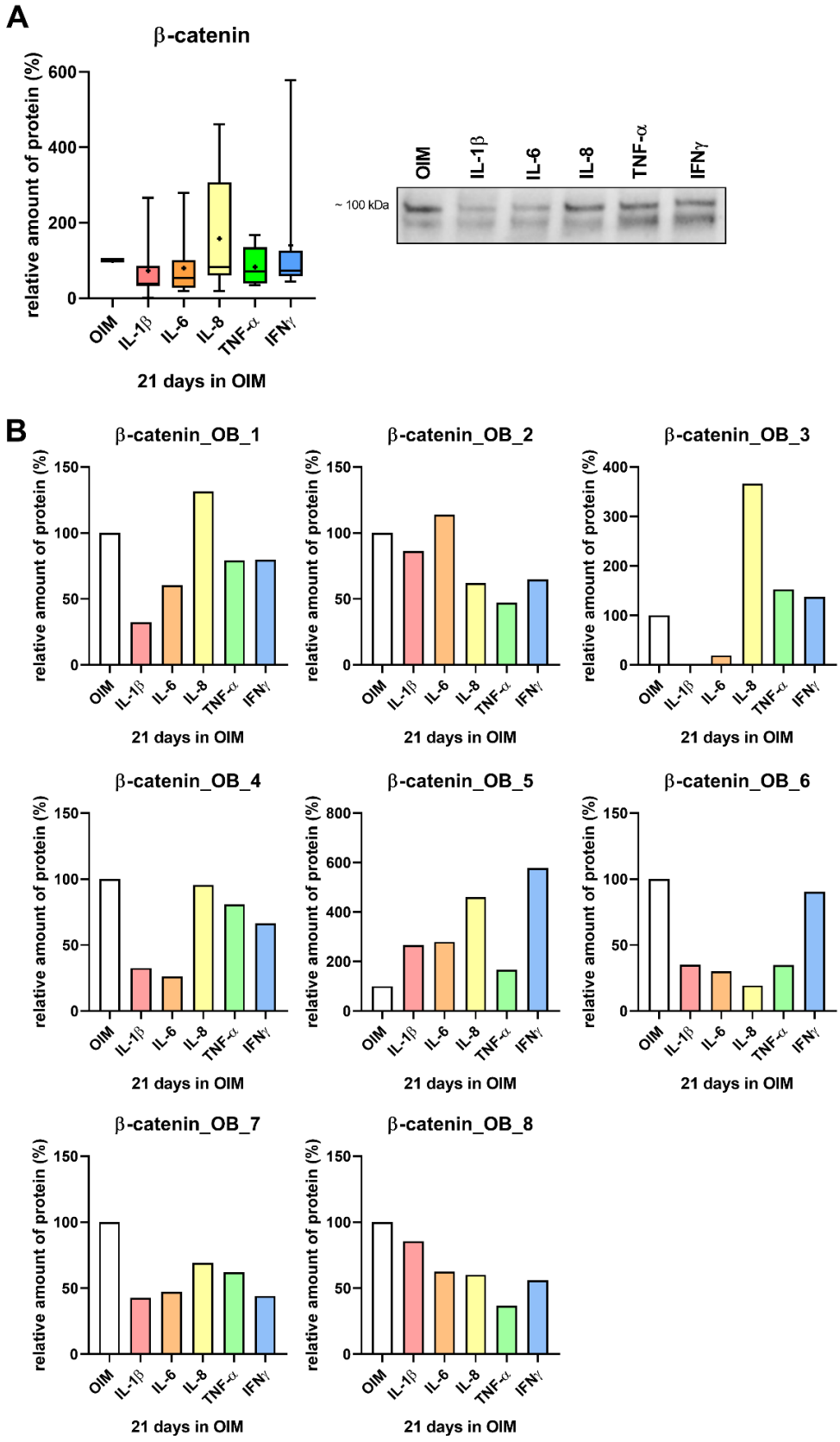

Figure 3.40: Effect of proinflammatory cytokines on β-catenin protein expression in OBs. β-catenin protein levels of OBs (n = 8) were assessed after 21-day treatment

with the cytokines IL-1β (250 units/mL), IL-6 (12.5 units/mL), IL-8 (12.5 units/mL), TNF-α (250 units/mL), or IFNγ (3.125 units/mL) in OIM. Protein expression was analyzed via SDS-PAGE (20 µg cell lysate) followed by Western blotting. (A) Combined evaluation with all donor OBs, and (B) individual results, both normalized to the control (OIM). The quantified chemiluminescent signals were normalized to total protein amount.

3.2.3.1.2. MAPK Signaling

To investigate the influence of cytokines on MAPK signaling during osteogenic differentiation, protein expression levels of MAPK and phosphorylated MAPK (p-MAPK) were analyzed.

On day 21 of treatment, the MAPK protein levels were significantly reduced in OBs treated with IL-1β and IL-6 (Fig. 3.41). TNF-α treatment also showed a trend towards decreased MAPK expression. In contrast, IL-8 and IFNγ treatments did not result in significant changes but demonstrated a tendency to enhance MAPK protein levels.

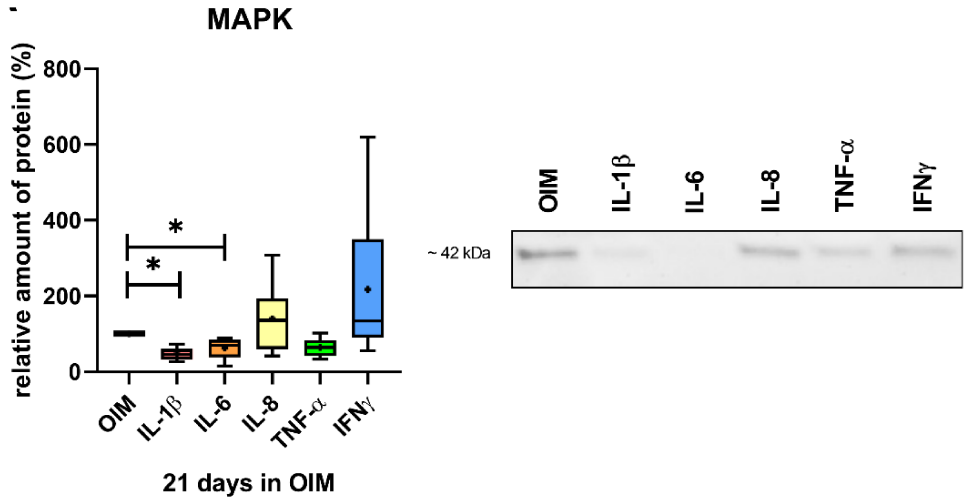

Figure 3.41: Effect of proinflammatory cytokines on p38-MAPK protein expression in OBs. The protein expression of p38-MAPK (mitogen-activated protein kinase) of OBs (n = 6), that were treated with the cytokines IL-1β (250 units/mL), IL-6 (12.5 units/mL), IL-8 (12.5 units/mL), TNF-α (250 units/mL), or IFNγ (3.125 units/mL) in OIM for 21 days was determined by performing an SDS-PAGE (20 µg cell lysate) and subsequent Western blotting. The quantified chemiluminescent

signals were normalized to total protein amount. The data was normalized to the control (OIM).

The protein levels of phospho-p38-MAPK varied significantly among OB donors following cytokine treatments, resulting in no significant changes in the combined analysis (Fig. 3.42, A). However, a trend was observed indicating that IL-8 treatment might increase p-p38-MAPK protein expression. This increase was particularly evident in OB_1, OB_3, and OB_4, while OB_2, OB_5, and OB_6 exhibited a decrease in p-MAPK levels following IL-8 treatment (Fig. 3.42, B). A similar variability was observed with IL-1β, IL-6, TNF-α, and IFNγ treatments, where both increases and decreases in p-38-MAPK protein expression were detected across different donors.

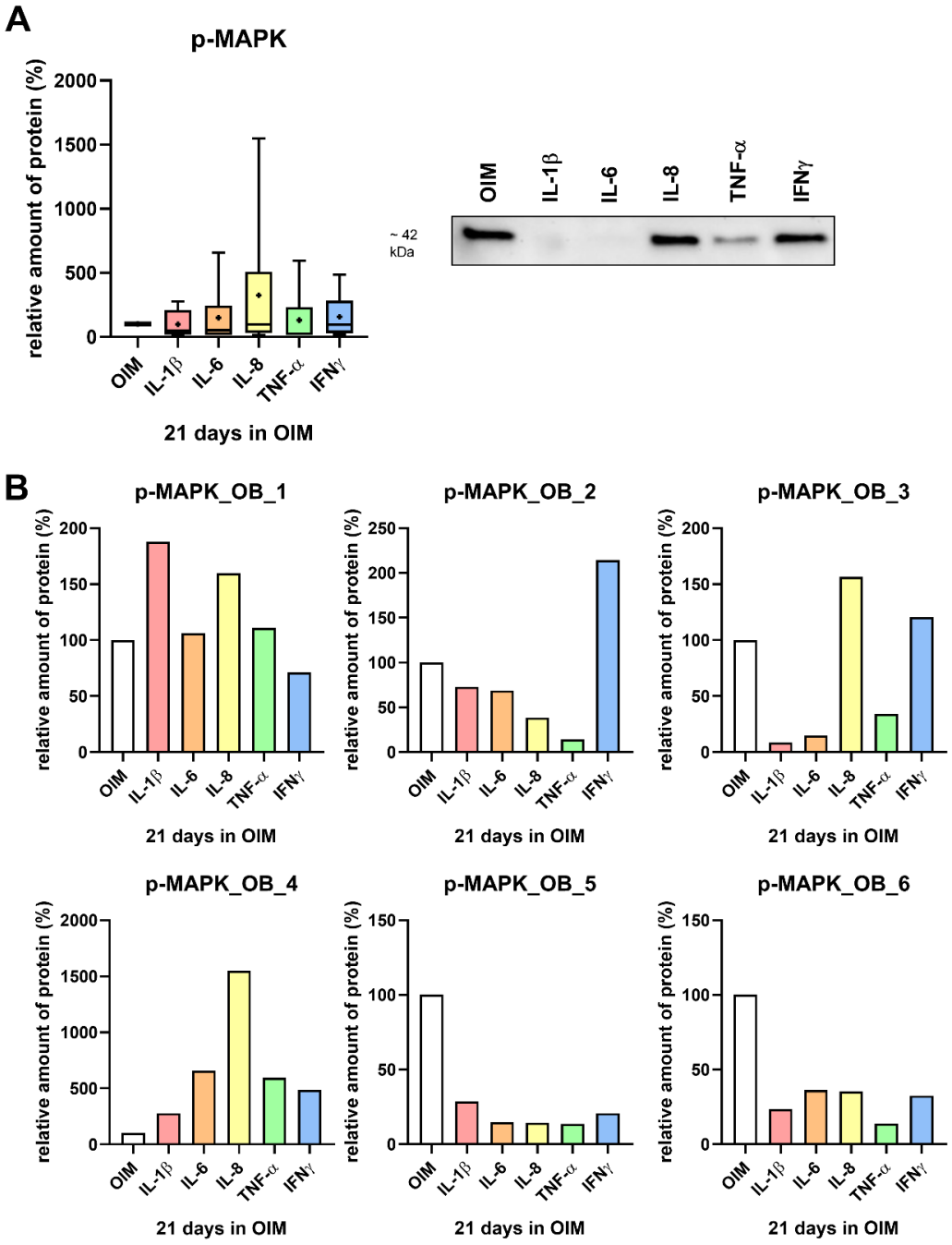

Figure 3.42: Effect of proinflammatory cytokines on phospho-p38-MAPK protein expression in OBs. The protein expression of p-MAPK (phospho-mitogen-activated protein kinase) of OBs (n = 6), that were treated with the cytokines IL-1β (250 units/mL), IL-6 (12.5 units/mL), IL-8 (12.5 units/mL), TNF-α (250 units/mL), or IFNγ (3.125 units/mL) in OIM for 21 days was determined by SDS-PAGE (20 µg cell lysate) and subsequent Western blotting. (A) Combined evaluation across all donors and (B) individual donor responses are shown. The quantified chemiluminescent signals were normalized to total protein amount and the data was normalized to the control (OIM).

3.2.3.2. Electron Microscopic Analysis of OBs

3.2.3.2.1. Surface Analysis with Scanning Electron Microscopy (SEM)

The cell surface of undifferentiated (day 1) and differentiated (day 21) OBs was visualized using scanning electron microscopy (SEM) at magnifications of 300 x and 3000 x (Fig. 3.43). At 300 x magnification on day 1, the outlines of individual cells are still visible, while on day 21, the cells appear more spread out with undefined cell boarders and a smoother, more uniform surface. At 3000 x magnification, prominent podocyte-like extensions with kind of rocky surface are visible from the undifferentiated cells. These features are also present on day 21 but appear as larger, hill-like structures. The surface on day 21 appears more layered, with fewer visible details compared to day 1.

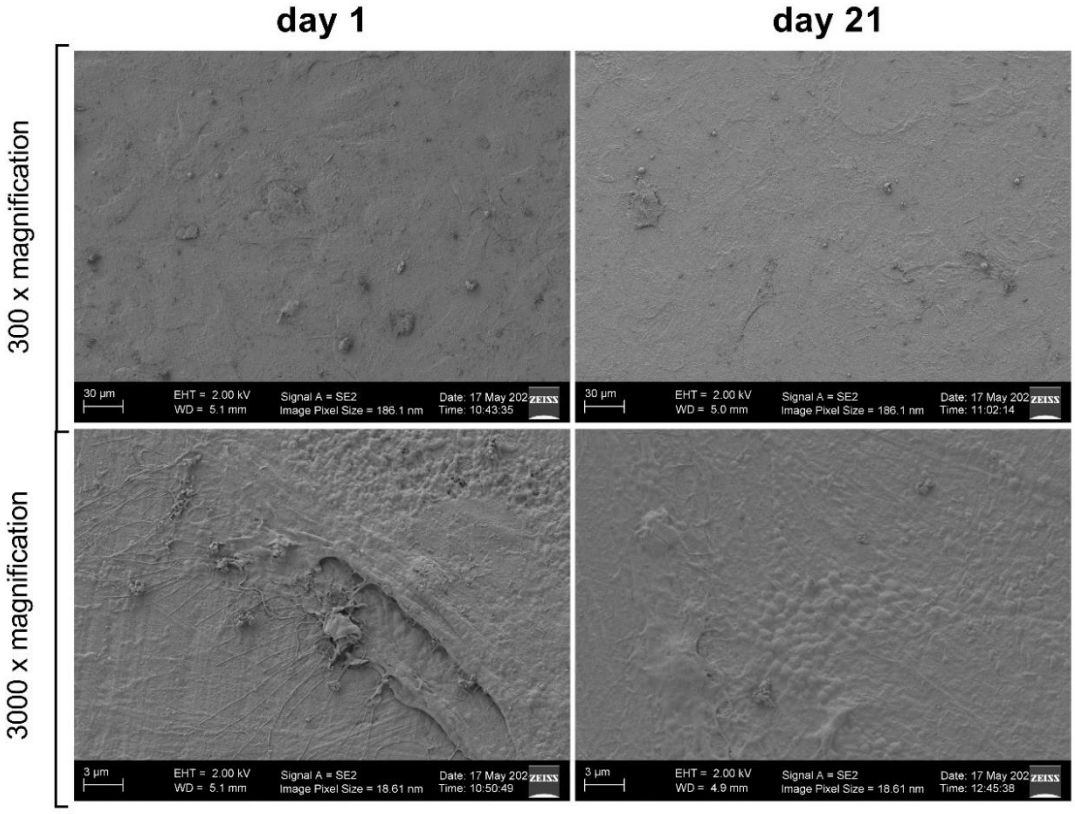

Figure 3.43: Scanning electron micrograph of the cell surface of undifferentiated and differentiated OBs. Using a scanning electron microscope (SEM), the surface of OBs that were confluent but undifferentiated (day 1) or differentiated in OIM for 21 days were imaged at 300 x (scale bar = 30 µm) or 3000 x (scale bar = 3 µm) magnification.

Additionally, the surface of OBs after treatment with IL-1β and IL-8 were also analyzed with SEM (Fig. 3.44). At 300 x magnification, the surface of cells differentiated in OIM for 21 days showed a smooth texture compared to the cells treated with IL-1β, which had a very rough surface with disruption of cellular material. Cells treated with IL-8 appear to have a smoother surface compared to IL-1β-treated cells, similar to the control cells in OIM, but with a slightly crumblier texture.

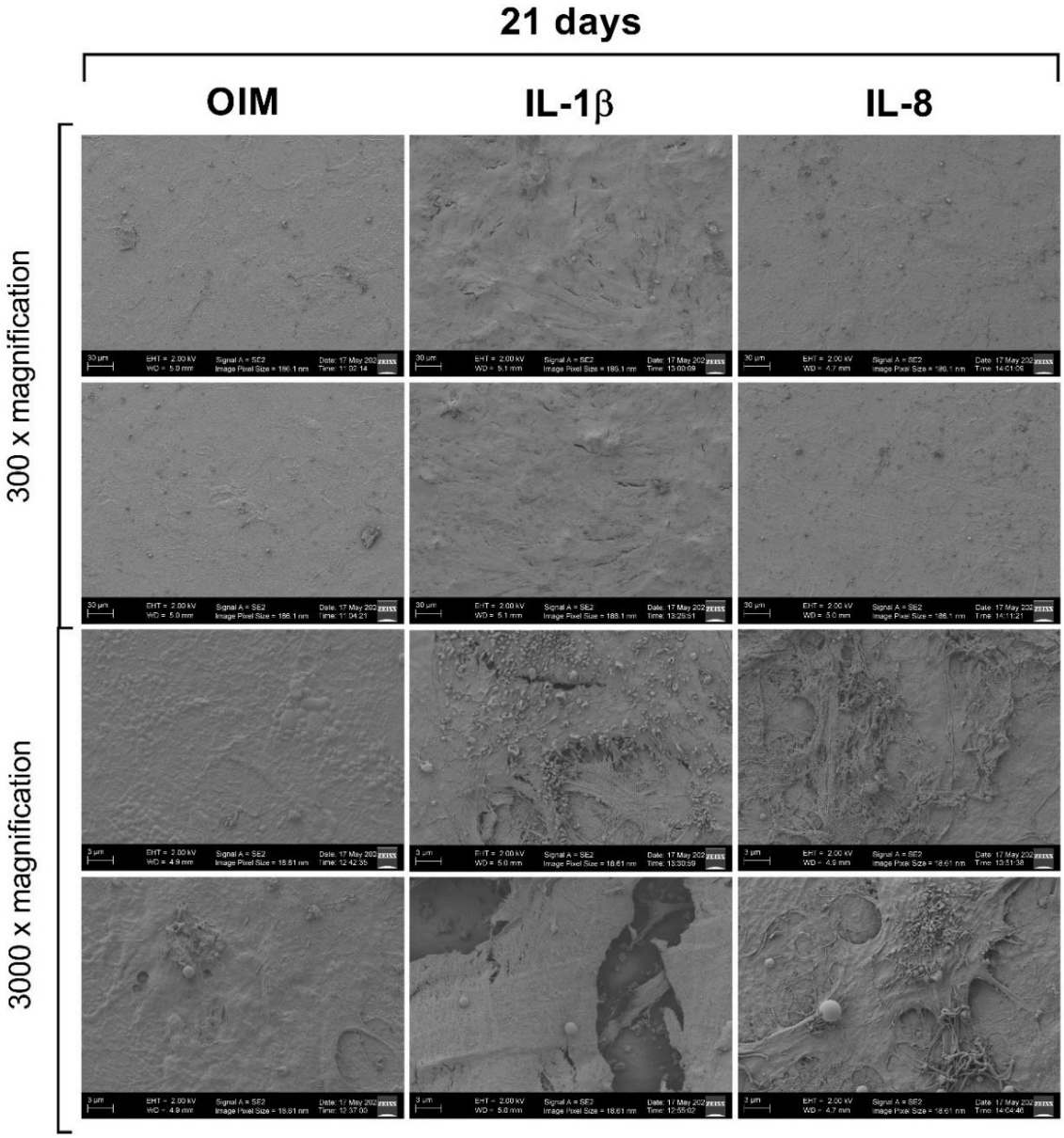

Figure 3.44: Scanning electron micrograph of the cell surface of differentiated OBs after IL-1β and IL-8 treatment. Using a scanning electron microscope (SEM), the surface of OBs differentiated in OIM without or with the cytokines IL-1β

(250 units/mL) and IL-8 (12.5 units/mL) for 21 days were imaged at 300 x (scale bar = 30 µm) or 3000 x (scale bar = 3 µm) magnification.

At 3000 x magnification, the differences become more visible. The OIM-treated cells show a relatively smooth surface with layered hill-like structures. IL-1β-treated cells reveal disrupted cell surfaces, revealing areas where the surface seemed to tear open. The cracks could also be an artefact of sample preparation. Beneath these openings, additional layers of cells are visible, suggesting the presence of multiple cellular layers in these regions. In contrast to the control, IL-8-treated OBs also seemed to exhibit increased crinkling and irregular folds, as already seen as the crumblier surface in 300 x magnification.

3.2.3.2.2. Analysis of Calcium Phosphate Structures with Transmission Electron Microscopy (TEM)

To validate that the mineralization observed in the differentiation experiments and stained with alizarin red S represents collagen-mediated calcium phosphate deposition, differentiated OBs were embedded in epoxy resin, sectioned, and analyzed using transmission electron microscopy (TEM).

TEM analysis revealed collagen fibers in the OB cell culture with their characteristic banding pattern (Fig. 3.45, A). In addition, collagen-associated hydroxyapatite crystals were identified, visible as dark structures due to the density, structured deposits along the collagen fibrils (Fig. 3.45, B). Interestingly, feather-like structures indicative of non-collagen associated hydroxyapatite were also observed in the OBs cultures (Fig. 3.45, C).

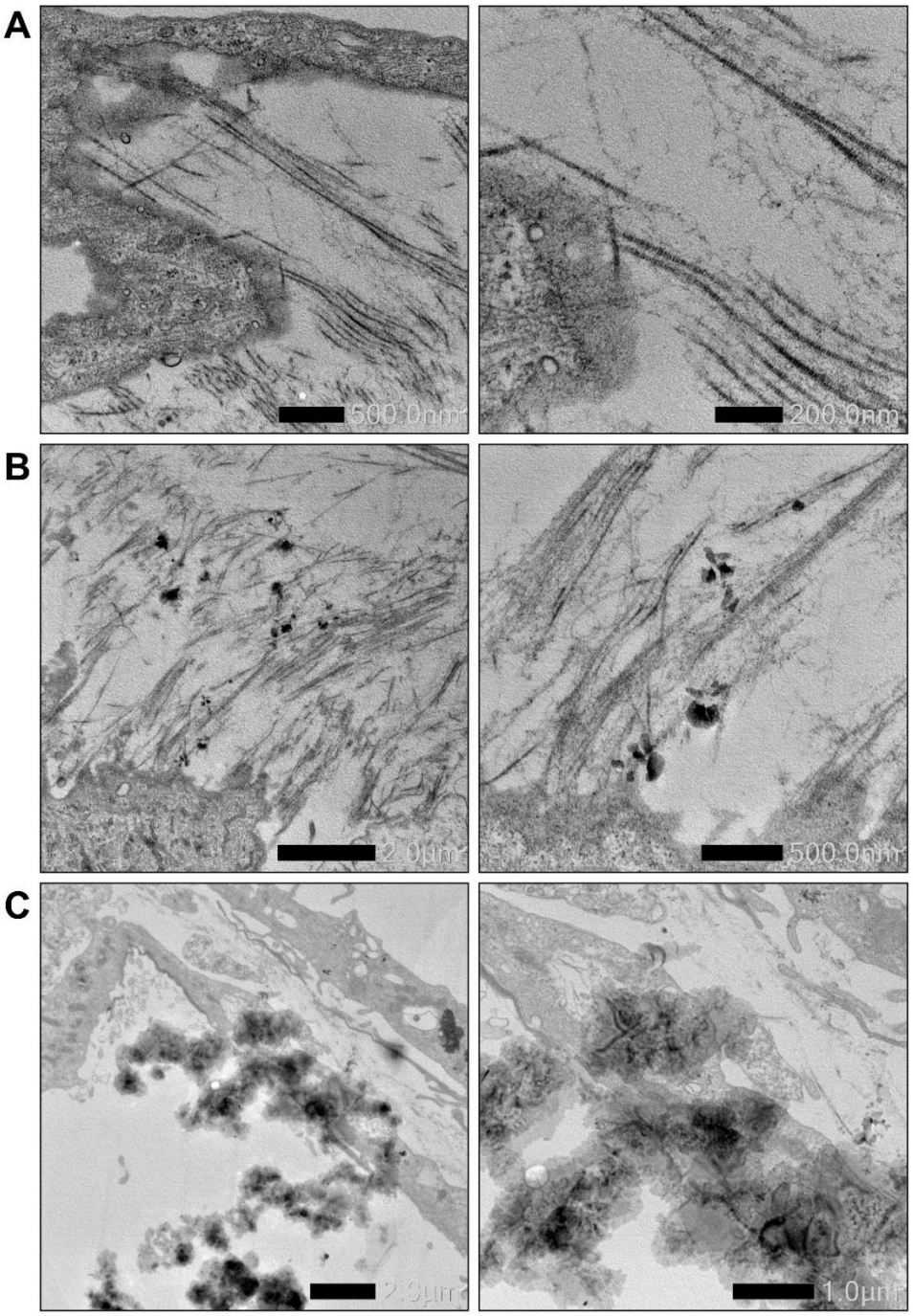

Figure 3.45: Transmission electron microscopy images of mineralized structures of differentiated OBs. Using a transmission electron microscope (TEM), slides of the mineralized structures of differentiated OBs (21-day incubation in OIM) were imaged, showing (A) collagen fibers, (B) collagen-associated hydroxyapatite, and (C) non-collagenous feather-like structured hydroxyapatite.

During the analysis of calcium phosphate, additional observations were made in the culture of differentiated OBs (Fig. 3.46). Multilamellar vesicles were frequently

detected, appearing in particularly high abundance (Fig. 3.46, A). Furthermore, rough endoplasmic reticulum with attached ribosomes was identified (Fig. 3.46, B) and large lipid bodies were observed within the cytoplasm of differentiated osteoblasts (Fig. 3.46, C).

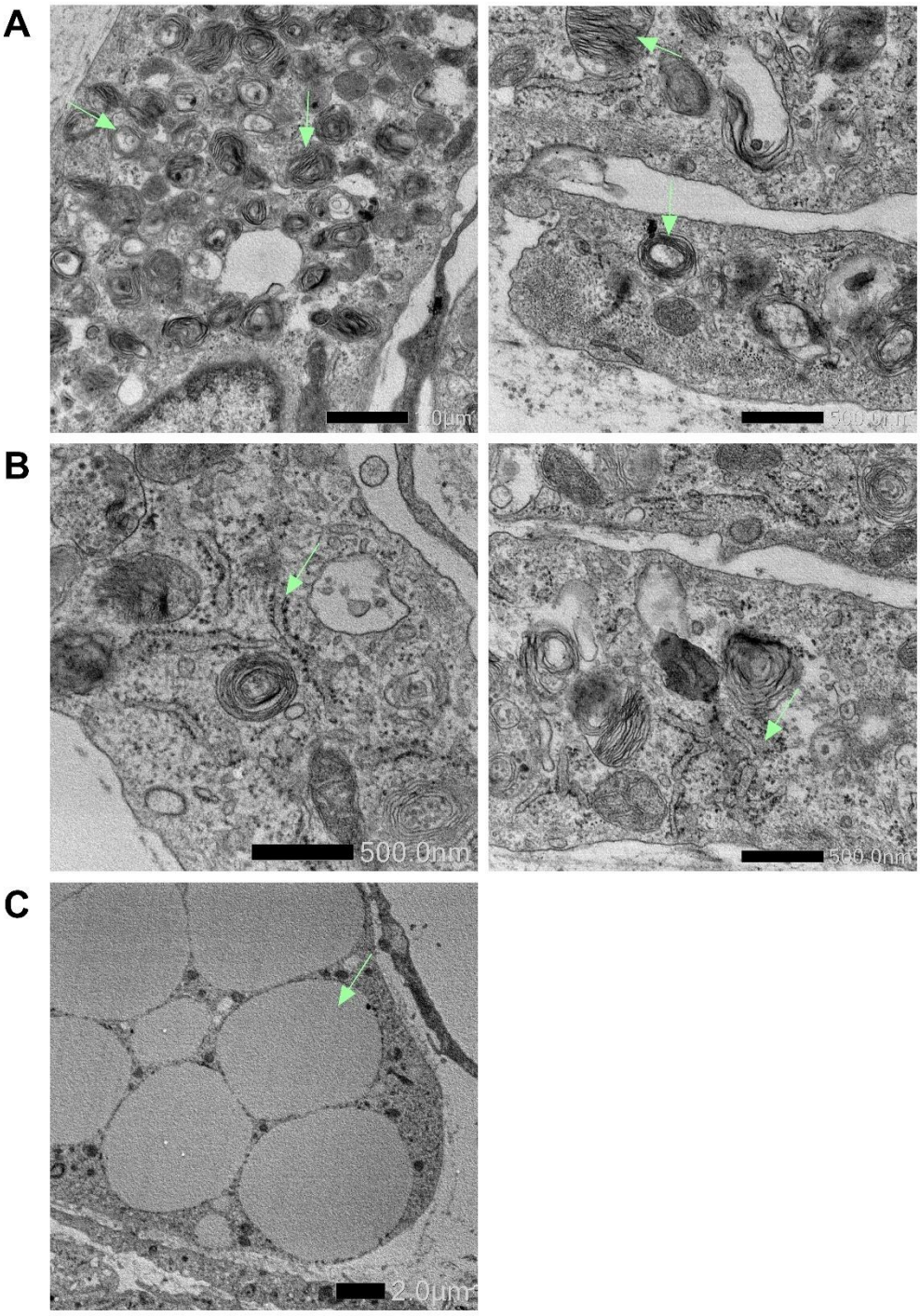

Figure 3.46: Transmission electron microscopy images of interesting structures in differentiated OB culture. Using a transmission electron microscope (TEM), slides

of the mineralized structures of differentiated OBs (21-day incubation in OIM) were imaged, showing (A) multilamellar vesicles, (B) endoplasmic reticulum with ribosomes, and (C) lipid bodies.

3.2.3.3. Further Investigations of the Influence of Cytokines on OBs Mineralization

To explore whether the mineralization-promoting effect of IL-1β treatment observed in OIM could also be replicated in GM, cells from a single donor were analyzed (Fig. 3.47). As shown in Fig. 3.47, A, mineralization in GM without osteogenic supplements (L-ascorbic acid, β-glycerophosphate, and dexamethasone) remained minimal, even with IL-1β treatment. While a slight increase in mineralization was observed between days 21 and 35 in both the control and IL-1β-treated groups, the absorption remained very low (about 0.05 on day 35) compared to those in OIM (about 7 – 10). IL-1β-treated cells showed a slightly elevated mineralization level compared to controls on days 14, 21, and 28; however, this difference did not indicate an induction of mineralization. In contrast, mineralization in OIM (Fig. 3.47, B) was significantly enhanced by IL-1β treatment, with levels more than twice as high as the control on day 14.

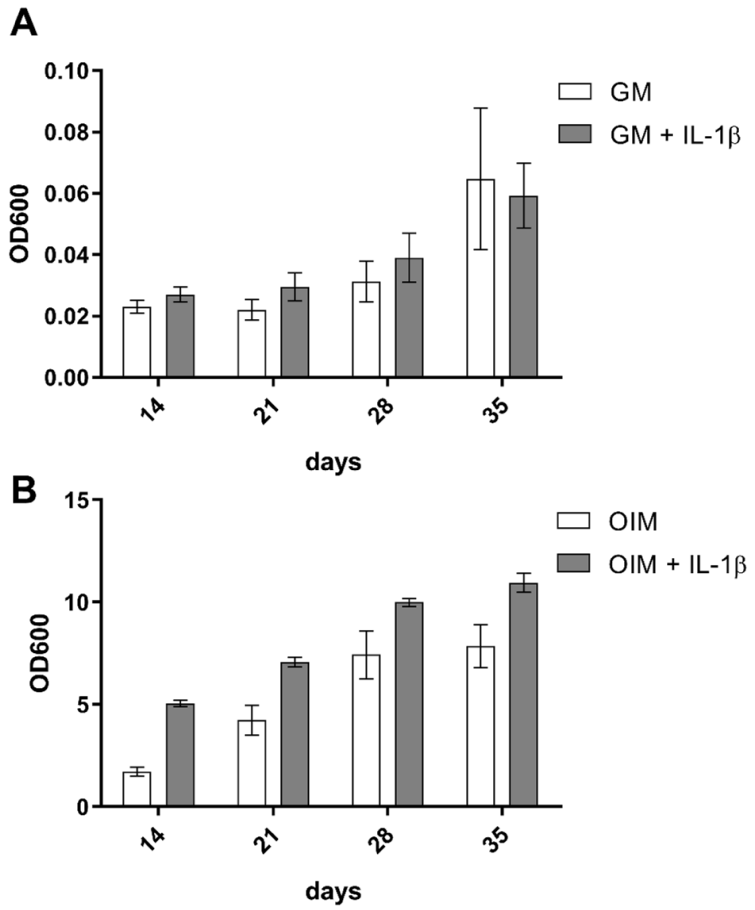

Figure 3.47: Mineralization assay of OBs treated with IL-1β in GM and OIM. The OBs mineralization from one donor (4 replicates) treated with 250 units/mL IL-1β (A) in GM without osteogenic additives, and (B) in OIM was quantified photometrically by alizarin red S staining (OD600) on days 14, 21, 28, and 35. The data is presented as mean ± SD.

Building on the previous findings, which demonstrated a strong mineralization-promoting effect of IL-1β in OIM, but not in GM, it was investigated whether this effect could also be observed in a GM after pre-incubation of OBs in OIM (Fig. 3.48). The mineralization of cells pre-incubated in OIM for short-term (48 h) and long-term (14 days), followed by 21 days of treatment with the cytokines IL-1β, IL-6, IL-8, TNF-α, and IFNγ in GM, was analyzed. Short-term OIM pre-incubation resulted in very low mineralization with absorption values about 0.05 (Fig. 3.48, A and B). Despite similar absorption values as in Fig. 3.48, A without pre-incubation in OIM, the treatment with IL-1β and TNF-α resulted in a slight increase in mineralization. IL-6, IL-8, and IFNγ had no measurable impact compared to the control. In contrast,

cells pre-incubated in OIM for a longer period of 14 days showed a markedly different response when subsequently incubated with cytokines in GM for 21 days (Fig. 3.48, C and D). Mineralization was notably increased under these conditions. IL-6 exhibited the strongest mineralization-promoting effect, while IL-1β, IL-8, and TNF-α also showed a comparable positive effect on mineralization. IFNγ treatment resulted only in a slight increase compared to the control.

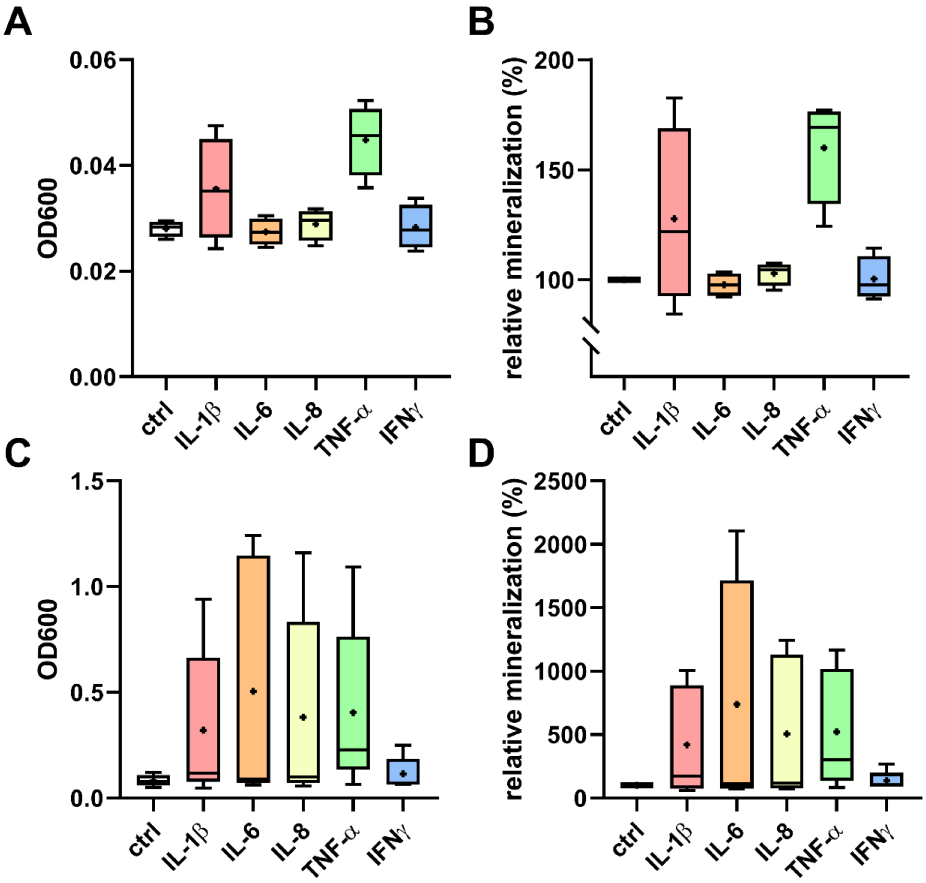

Figure 3.48: Effect of cytokines in GM after OIM pre-incubation on OBs mineralization. Mineralization of OBs with (A), (B) 48 h (n = 4) or (C), (D) 14 days (n = 5) OIM pre-incubation followed by 21 days cytokine incubation in GM with 250 units/mL IL-1β, 12.5 units/mL IL-6, 12.5 units/mL IL-8, 250 units/mL TNF-α, and 3.125 units/mL IFNγ. The boxplot diagrams in (B) and (D) show the values normalized to the untreated control (GM) of each donor.

Next, the impact of cytokine pre-incubation, either for a short (48 hours) or long (14 days) period, on subsequent mineralization in OIM was investigated (Fig. 3.49). The comparison between raw data (Fig. 3.49 A and C) and normalized data (Fig. 3.49, B and D) reveals that donor-specific variations significantly influenced the

results, presumably due to the extended incubation periods. In the normalized data of OBs pre-incubated with cytokines for 48 hours, IL-6, IL-8, TNF-α, and IFNγ demonstrated a positive effect on subsequent mineralization, with IL-8 and TNF-α having the strongest effects (Fig. 3.49, B). Interestingly, IL-1β showed no notable impact on mineralization under this condition. For OBs pre-incubated with cytokines for 14 days, both the control and treated cells had significantly enhanced mineralization compared to the 48-hour pre-incubation (Fig. 3.49, D). Notably, IL-1β treatment revealed a positive influence on mineralization under this condition. In contrast, pre-incubation with IL-6 and IL-8 tended to inhibit mineralization, while TNF-α and IFNγ showed no consistent effects and appeared to have large donor-dependent variability.

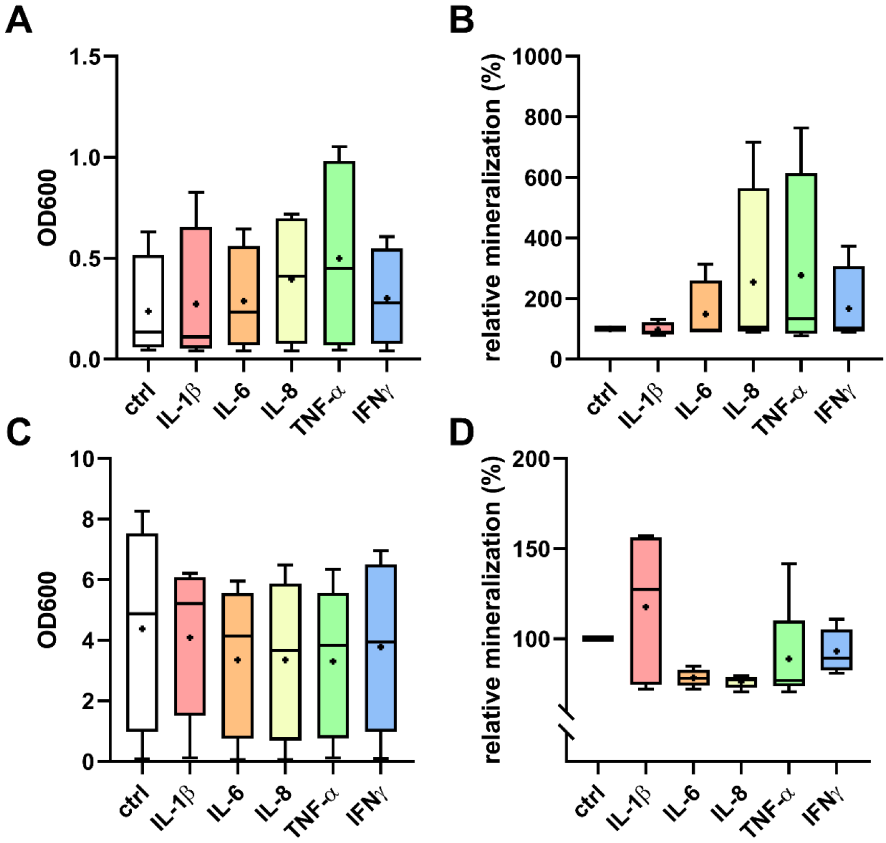

Figure 3.49: Impact of cytokine pre-incubation on OIM-induced mineralization of OBs. Mineralization of pre-incubated OBs (A), (B) for 48 h (n = 4) or (C), (D) for 14 days (n = 5) with 250 units/mL IL-1β, 12.5 units/mL IL-6, 12.5 units/mL IL-8, 250 units/mL TNF-α, or 3.125 units/mL IFNγ in GM with subsequent 21-day OIM incubation was determined by quantification of alizarin red S staining. The boxplots in (B) and (D) show the data normalized to the control of the respective donor.

4. Extended Discussion and Conclusion

4.1. Effects of Proinflammatory Cytokines on the Osteogenesis of Primary Human Osteoblasts

In the publication it was shown, contrary to initial expectations, that the cytokines IL-1β and TNF-α, as well as IL-6 and IL-8, significantly promoted the mineralization of primary osteoblasts (Fig. 3). IL-1β and TNF-α also had a positive effect on proliferation and increased the mRNA expression of *IL-6* and *IL-8* in the cells (Fig. 4 and 5). Both cytokines were secreted during osteogenesis, IL-6 at a relatively constant level and IL-8 only from day 14 with an increasing tendency (Fig. 2). Treatment with IL-1β also had promoting effects on glycolysis and non-glycolytic acidification, while TNF-α had a stimulating effect on OxPhos of the cells (Fig. 6 and 7).

Further analysis of the mRNA expression of osteogenic differentiation markers showed that the expression of *Col1α2* and *Runx2* was downregulated by IL-1β (Fig. 3.34). In contrast, the expression of *OPN*, a marker of late osteogenesis, was increased with IL-1β treatment. A similar observation was made with IL-6 treatment, leading to a significant reduction in *Col1α2* and increased *OPN* expression (Fig. 3.35). *Col1α2* and *Runx2* are expressed during early osteogenic differentiation in the production of ECM, whereas *OPN* is a rather late stage marker, which is involved in matrix mineralization together with *OCN* (Amarasekara et al., 2021; Zhang, 2010). These observations may indicate a later stage of differentiation of osteoblasts treated with IL-1β or IL-6, which is also consistent with the increased mineralization by these cytokines. Furthermore, the altered expression patterns of the matrix proteins OPN and Col1α2 could indicate an altered ECM composition. This, together with increased mineralization, may result in an altered mineral-to-matrix ratio, which in turn can strongly influence bone fragility (Naqvi et al., 2024; Unal et al., 2018). When secreted into the ECM, OPN binds to calcium ions, leading to an inhibition of hydroxyapatite formation (Hoac et al., 2017). Overexpression of *OPN* in MC3T3-E1 cells can also lead to a significant inhibition of mineralization *in*

vitro (Huang et al., 2004). Increased OPN production by cytokine-stimulated osteoblasts could also promote osteoclast adhesion to the bone matrix, thereby increasing bone resorption (Reinholt et al., 1990). OPN itself is a proinflammatory cytokine that is upregulated in the tissues of patients with osteoarthritis, and a correlation between elevated CRP and OPN levels has also been found in the synovial fluid of RA patients (Ohshima et al., 2002; Wang et al., 2017). This study shows that *OPN* expression, which plays an important role in inflammatory responses, was also upregulated by IL-1β and IL-6 *in vitro*. Interestingly, despite the mineralization-inhibiting function of OPN, treatment with these cytokines led to increased mineralization in primary osteoblasts. However, after treatment with TNF-α and IFNγ, a reduction in *OPN* expression was measured, which would be more consistent with the observed increase in mineralization (Fig. 3.37 and 3.38).

A significant reduction in p38-MAPK protein expression on day 21 of osteogenesis by IL-1β and IL-6 and a tendential reduction with TNF-α was measured (Fig. 3.41). Since increased MAPK activity is associated with the earlier differentiation stage and is also involved in the transcription of the early key osteogenic marker Runx2, the reduction by the cytokines could indicate a later differentiation stage (Xiao et al., 2000). However, p38-MAPK signaling also plays a role in later stages of mature osteoblasts and osteocytes (Rodríguez-Carballo et al., 2016). The expression of phosphorylated p38-MAPK was highly donor dependent and did not give a reliable result (Fig. 3.42). High donor variability was also observed in the expression of β-catenin, with a tendency towards inhibition by IL-1β und IL-6 (Fig. 3.40). β-catenin is an important marker for the activation of the canonical Wnt pathway, one of the most important signaling pathways for the regulation of osteogenic differentiation, which already serves as a target in osteoporosis therapy through the use of antibodies against the Wnt antagonist sclerostin (Bandeira et al., 2017). As the expression of osteogenic differentiation markers and signaling pathways only represent a snapshot of day 21 of osteogenesis, it is important to investigate how expression changes at different time points during osteogenesis.

Both short and long pre-differentiated osteoblasts were further enhanced in their mineralization by subsequent treatment with IL-1β without osteogenic additives (Fig. 3.48). Thus, IL-1β appears to activate signaling pathways that promote both early and late stages of osteogenesis, but it cannot induce mineralization on its own without the induction by osteogenic additives such as dexamethasone (Fig. 3.47). In contrast, IL-6 and IL-8 have no effect on the mineralization in early osteogenesis, but have a strong positive effect on osteoblasts in later stages (Fig. 3.48). On the other hand, pre-incubation with IL-6 or IL-8 for 14 days had an inhibitory effect, which was not seen with IL-1β, TNF-α, or IFNγ (Fig. 3.49). This suggests that, despite the positive effect of IL-6 and IL-8 on the differentiation during the induction of osteogenesis, the chronic inflammation may have long-term negative effects on osteogenesis. It is possible that acute inflammation and the increase of proinflammatory cytokine expression such as IL-1β, IL-6 and TNF-α may have a beneficial effect on bone repair, which could explain our findings in this work (Mountziaris & Mikos, 2008). IL-6 and IL-8 may be part of the negative effect of chronic inflammation leading to reduced bone density in chronic inflammatory diseases such as rheumatoid arthritis (Kareem et al., 2021).

In addition to IL-1β, IL-6, IL-8, and TNF-α, this study also investigates the influence of the proinflammatory cytokine IFNγ on primary osteoblasts, which is the only cytokine known to inhibit osteoclastogenesis, also induced by TNF-α (Amarasekara et al., 2018; Kohara et al., 2011). Treatment of OBs with IFNγ also resulted in increased mineralization of induced osteoblasts, comparable to IL-6 and IL-8 (Fig. 3.23). IFNγ had no significant effect on proliferation rate (Fig. 3.7 and 3.8) or energy metabolism (Fig. 3.11 and 3.12). A study utilizing MC3T3-E1 cells also showed a beneficial effect of IFNγ by upregulating the osteogenic markers ALP and OCN (Lai et al., 2022). In addition, IFNγ inhibits the adipogenic differentiation of MSCs in vitro (Vidal et al., 2012). The observations of this work confirm the literature showing that IFNγ has a beneficial effect on bone metabolism and may play an important role in the treatment of osteoporosis (S. Li et al., 2024).

Due to the high variability in the expression of osteogenic differentiation markers and signaling pathway markers in the primary osteoblast cultures (Fig. 3.28 – 3.33 and 3.39), no specific regulatory mechanism by which cytokines increase mineralization could be identified in this study. However, the results suggest a highly complex effect of cytokines on osteogenic differentiation, dependent on differentiation stage and time. Evidence of effects on proliferation and energy metabolism, as well as changes in individual osteogenic markers such as *OPN*, suggest possible signaling pathways targeted by the cytokines. It would be interesting to investigate these pathways and, in particular, the cytokine-mediated changes in the communication between osteoblasts and other bone cells such as osteoclasts.

4.1.1. Electron Microscopic Analysis of Osteoblast Differentiation

Comparison of undifferentiated and differentiated osteoblast cell cultures under the SEM showed that the differentiated cells covered the entire plate (Fig. 3.43). They also appeared to be covered by a layer as the cell borders were less clearly visible, presumably indicating the ECM produced by the cells. TEM showed more evidence of osteogenic differentiation. The cells were surrounded by collagen fibrils associated with electron-dense particles, namely hydroxyapatite crystals (Fig. 3.45, A and B). In addition, some dystrophic mineralization as described by Bonewald et al. (2003) was also observed (Fig. 3.45, C). Consistent with the collagen-associated mineralization, the cells showed abundant rough endoplasmic reticulum, which is known from matrix-producing osteoblasts (Fig. 3.46, B) (Marks Jr. & Popoff, 1988).

A noticeable large number of multilamellar organelles were found in the cells, which could have different functions. These are probably not matrix vesicles for the transport of calcium and phosphate ions, as the multilamellar organelles could only be observed intracellularly and matrix vesicles have bilamellar membranes (Shapiro et al., 2015). Based on the partially observed electron-dense structures in the center and an estimated size ranging from about 300 – 700 µm, they can be identified as multilamellar bodies (MLBs) (Hariri et al., 2000). They are associated

with various cellular processes, as the storage and secretion of lipids as well as the process of autophagy are involved in the biogenesis of MLBs (Hariri et al., 2000; Schmitz & Müller, 1991). This observation would be consistent with the increased autophagy process during mineralization (Nollet et al., 2014).

IL-1β treatment apparently induced the formation of multiple cell layers, which was visualized by disruption of the upper cell layer, revealing a lower layer beneath (Fig. 3.44). Consistent with this observation, a study by Hanna et al. (2018) using osteogenically differentiated human adipose mesenchymal stem cells showed the formation of four distinct cell layers. It is particularly interesting that the top layer of MSCs lost surface markers such as CD90 or CD44 faster than the lower layers (Hanna et al., 2018). The surface of untreated or IL-8-treated OBs was still intact, so it is not possible to say whether multiple cell layers were also formed. However, cells that had overgrown other cells were clearly visible in both cultures (Fig. 3.44).

4.2. Do Osteoblasts from Osteoporotic Donors Differ in Cell Activity *in vitro*?

4.2.1. Comparison of Basic Cellular Parameters Between OBs and oOBs

Since there are few studies on whether osteoblasts from osteoporotic and healthy individuals differ in their activity or physiology, we analyzed various cell parameters of oOBs and OBs *in vitro*. No significant differences were found for the basic parameters of proliferation, mineralization, ALP activity and cytokine secretion. Nevertheless, there were some observations that should be considered in further studies.

The mineralization of OBs and oOBs was very similar over a 28-day period and only decreased between day 28 and day 35 of differentiation, at a late time point, in oOBs in contrast to OBs (Fig. 3.2). A trend was also observed in IL-8 secretion during osteogenesis, with a tendency to lower levels in oOBs than in OBs between day 14 and day 35 (Fig. 3.3). The function and possible consequences of decreased IL-8 secretion in differentiating osteoblasts are not yet known and should be further

investigated. However, it has been shown that IL-8 increases the production of the protein RANKL in MC3T3-E1 cells and increases the formation of TRAP-positive multinuclear cells from PBMCs *in vitro* (Bendre et al., 2003). Therefore, contrary to expectations, the lower IL-8 secretion in oOBs may result in less activation of osteoclastogenesis. Conversely, due to its role as a chemokine and its function in neutrophil migration, less IL-8 could also lead to a reduced number of neutrophils at the fracture site in osteoporotic patients and thus to impaired bone healing (Bastian et al., 2016; Laterveer et al., 1995). To the best of my knowledge, the energy metabolism of osteoporotic osteoblasts has not been described in the literature. Again, no significant differences in OxPhos or glycolysis parameters were found between undifferentiated OBs and oOBs (Fig. 3.5 and 3.6). The proliferation of oOBs compared to OBs tended to be lower at all time points analyzed, but without reaching significance (Fig. 3.4).

The fact that the differences between osteoporotic and healthy cells are not significant is also confirmed by a comprehensive study in which BMSCs from the spine of osteoporotic patients were compared with cells from healthy donors in terms of their osteogenic differentiation potential (Haddouti et al., 2020). It was shown that the cells of these groups did not differ in their morphology, growth behavior and osteogenic, adipogenic, and chondrogenic differentiation potential. However, in contrast to our observations, differences between osteoporotic and healthy or osteoarthritic controls have been reported in the literature. In a study with BMSCs from osteoporotic patients, lower proliferation and ALP activity as well as calcium deposition during differentiation were measured after several days in culture compared to controls (Rodríguez et al., 1999). Osteoblasts from osteoporotic male donors also showed reduced proliferation and OCN production after vitamin D3 stimulation compared to osteoarthritis patients (Pernow et al., 2006). MSCs isolated from the blood of osteoporosis patients showed significantly lower expression levels of *Runx2*, *SP7*, *Col1α2*, and other bone-related genes during *in vitro* differentiation (Carbonare et al., 2009). BMSCs from osteoarthritic patients formed a more mineralized matrix with increased gene and protein levels *in vitro*, without significant differences in adipogenic differentiation compared to BMSCs from

osteoporotic patients (Z.-M. Zhang et al., 2009). However, in another study using human BMSCs, increased adipogenic potential was measured in osteoporotic cells compared to controls (Rodríguez et al., 2008). Another study confirmed these observations in osteoporotic MSCs, which showed a pro-adipogenic rather than osteogenic response compared to normal MSCs due to a disruption of BMP-2 signaling (Donoso et al., 2015).

In conclusion, differences were found in the literature that could not be supported by the findings on primary human osteoblasts in this study. The trends observed here should be further investigated, but with a larger number of samples, due to the complexity of osteoporosis as a disease.

4.2.2. Cytokine-Induced Effects on oOBs and OBs

Although some studies have investigated the role of cytokines in bone metabolism, often in cell lines or MSCs, no experimental work has been published about the influence of proinflammatory cytokines on human osteoporotic osteoblasts compared to a control. This research gap was addressed in the present study with the hypothesis that cells from an osteoporotic patient with an inflammatory milieu might have an altered response to cytokines *in vitro*.

The mineralization of oOBs, comparable to OBs, was promoted by the addition of the cytokines IL-1β, IL-6, IL-8, TNF-α, and IFNγ (Fig. 3.9). IL-1β and TNF-α also had an inducing effect on the proliferation of oOBs (Fig. 3.8). The oOBs tended to show different ALP activity compared to OBs, with less variability and a tendency for IL-1β to increase ALP activity on days 8 and 10 (Fig. 3.10). Treatment of oOBs with TNF-α resulted in an increase in OxPhos parameters, as in OBs. oOBs treated with IL-1β had higher basal respiration, ATP production, and proton leak than OBs, but without reaching significance compared to oOBs not treated with cytokines (Fig. 3.11). As in OBs, non-glycolytic acidification was increased in oOBs, with a trend toward increased glycolysis (Fig. 3.12).

It should be noted that the patients classified as osteoporotic in this study were diagnosed on the basis of a low T-score in DXA measurement, and therefore all patients with a high T-score belonged to the control group. The official diagnostic criteria for osteoporosis using DXA were defined by the WHO in 1994, with patients being diagnosed on the basis of their measured bone density (Kanis et al., 1994). However, osteoporosis is a multifactorial condition with a complex phenotype, influenced by factors such as age, hormonal status, and secondary causes. While low bone density is a key characteristic and risk factor, it represents only one aspect of the broader pathological changes seen in osteoporosis. The FRAX® tool, for example, incorporates these additional factors into its osteoporosis risk assessment (Kanis et al., 2008). This raises the question of whether "osteoporotic cells" truly exist or whether cellular changes observed in the literature are primarily due to the influence of the systemic environment of osteoporotic patients. If cells are cultured for an extended period after isolation, they may lose features associated with osteoporosis due to the absence of external signals such as cytokines or hormonal influences. Additionally, it should also be noted that the control cells were derived from patients with fractures or OA, conditions that also expose cells to a cytokine-rich environment (Molnar et al., 2021).

4.2.3. Future Analyses of OBs and oOBs

Although no significant differences in the cell parameters of OBs and oOBs were found in this study, it should be further investigated whether these cells have possible physiological differences. An important question is whether the cells change over time in culture, so that the previous conditions of osteoporotic bone tissue no longer affect their activity. It would be interesting to analyze the cells for protein and gene expression of osteogenic markers directly after isolation compared to a later stage of culture.

Neidlinger-Wilke et al. (1995) isolated osteoblasts from osteoporotic and normal patients and found no differences in proliferation, TGF-β secretion or ALP activity *in vitro*. The differences became apparent only after cyclic loading, as osteoblasts from

osteoporotic donors did not increase proliferation or TGF-β secretion compared to normal cells. Therefore, it would be interesting to investigate whether our oOBs would also show different behavior after shear stress compared to OBs. Perhaps these differences originate in a altered expression or activity of piezo ion channels, which are known to respond to mechanical stimuli and promote bone formation (X. Li et al., 2019). Furthermore it would be interesting to analyze the composition of the ECM of OBs and oOBs, as there is evidence that oOBs produce a lower proportion of type I collagen (Rodríguez et al., 2000). An alteration in the ECM and a decrease in type I collagen could explain the increased risk of fracture in osteoporotic patients.

Another important aspect would be to investigate the adipogenic differentiation potential of oOBs, as it has been shown several times that MSCs from osteoporotic donors show a pro-adipogenic response through increased peroxisome proliferator-activated receptor gamma (PPARγ) levels compared to controls (Donoso et al., 2015; Rodríguez et al., 2000, 2008). Several studies have also shown *in vivo* that the differentiation of MSCs in osteoporotic individuals is more adipocytic than osteogenic. *In vivo* experiments in osteoporotic mice with bilateral ovariectomy showed that their MSCs had increased expression of enhancer of Zeste homology 2 (EZH2), which in turn suppressed the Wnt pathway, causing the cells to differentiate in an adipogenic direction (Jing et al., 2016). The proportion of adipose tissue was significantly higher in iliac crest bone biopsies from osteoporotic patients with a lower proportion of trabecular bone compared to healthy individuals (Justesen et al., 2001). This observation has been confirmed several times, and an inverse correlation between BMD and bone marrow adipocytes has also been found in both younger and older men and women (Shen et al., 2012; Yeung et al., 2005). The cell fate decision of MSCs to differentiate into adipogenic or osteogenic lineage depends on several transcription factors. As mentioned above, Runx2 is the key transcription factor for osteogenic differentiation and simultaneously inhibits adipogenic and chondrogenic differentiation (Komori, 2006). Key transcription factors for adipogenic differentiation include PPARγ and CCAAT/enhancer binding protein alpha (C/EBPα), which act in a common signaling pathway (Hu et al., 2018;

Rosen et al., 2002). Therefore, it would be of particular interest to investigate whether freshly isolated osteoblasts show increased expression of adipogenic differentiation markers or whether they also show preferential adipogenic differentiation over osteogenic differentiation in cell culture. In addition, it should be examined whether proinflammatory cytokines influence the expression of adipogenic transcription factors. In hASCs, IL-1β and TNF-α have been shown to inhibit adipogenic differentiation, whereas IL-6 had no effect (Ma et al., 2020). Studies with primary human osteoblasts may help to understand the effect of inflammation in the context of increased adipogenesis and reduced osteogenesis in osteoporotic bone.

4.3. Comparison of Primary Human Osteoblasts with the hFOB 1.19 Cell Line

4.3.1. Opposing Effects of Proinflammatory Cytokines on the Mineralization of OBs and hFOB 1.19 Cells

Due to the high heterogeneity of primary human osteoblasts, they were compared to the immortalized human fetal osteoblast cell line hFOB 1.19 to determine whether the effect of proinflammatory cytokines observed in OBs could also be observed in the osteoblast cell line. The hFOB 1.19 cell line was developed by Harris et al. (1995) to study osteogenic differentiation in addition to primary human and rodent osteoblast cultures and osteosarcoma cell lines. This study confirms that hFOB 1.19 cells at 34 °C with osteogenic supplements (β-glycerophosphate, L-ascorbic acid, and dexamethasone) undergo osteogenic differentiation by increased mineralization (Fig. 3.16), increased ALP activity (Fig. 3.24), and expression of osteogenic differentiation markers (Fig. 3.26).

Comparison of the cell line and primary cells revealed that calcified nodules were visible microscopically in both between days 14 and 21 (Fig. 3.17 and Fig. 3.18). However, the morphologies of these nodules were different. While those of primary cells were more evenly distributed and reticular, the nodules of hFOB 1.19 cells were more speckled with uncolored intermediate areas. Overall, more

mineralization was measured in differentiated OBs (Fig. 3.16). Also in the undifferentiated state, there were clear differences between hFOB 1.19 cells and primary OBs (Fig. 3.13). The primary cells had a greater heterogeneity in size and shape with spindle-shaped and partially polygonal-shaped cells, while the hFOB 1.19 cells were more homogeneous and had a uniform spindle-shaped morphology.

The results regarding the influence of proinflammatory cytokines on the mineralization of hFOB 1.19 cells compared to primary osteoblasts were particularly interesting. All five cytokines tested – IL-1β, IL-6, IL-8, TNF-α, and IFNγ – showed the opposite effect in the cell line compared to primary cells. While treatment with IL-1β and TNF-α strongly promoted the mineralization of OBs in a dose-dependent manner, it significantly inhibited the mineralization of hFOB 1.19 cells at all concentrations (Fig. 3.19 and Fig. 3.22). Treatment with IL-6, IL-8, and IFNγ tended to promote or even significantly promote the mineralization of OBs at certain concentrations, but resulted in a significant inhibition of the mineralization of hFOB 1.19 cells, although less pronounced than IL-1β and TNF-α (Fig. 3.20, Fig. 3.21, and Fig. 3.23). In contrast to primary OBs, no increased mRNA expression of IL-6 and IL-8 could be detected in the cell line after treatment with IL-1β or TNF-α (Fig. 3.14). However, it was shown that IL-8 mRNA expression was also increased on day 14 of osteogenesis, while IL-6 expression was downregulated. ALP activity was also differentially affected by the cytokines. In OBs, cytokines had no significant effect on ALP activity (Fig. 3.10), whereas in hFOB 1.19 cells, low concentrations of IL-1β and TNF-α resulted in inhibition of ALP activity. In contrast, and despite the inhibitory effect on mineralization, IL-6, IL-8, and IFNγ did not affect the ALP activity of the cell line (Fig. 5.27). In addition, proliferation was not significantly altered after cytokine treatment in hFOB 1.19 cells (Fig. 3.25) compared to OBs, in which IL-1β and TNF-α treatment resulted in a higher proliferation rate (Fig. 5).

4.3.2. Effects of Proinflammatory Cytokines on the Expression of Osteogenic Differentiation Markers in hFOB 1.19 Cells

During differentiation of hFOB 1.19 cells, osteogenic differentiation markers were upregulated, including *ALP*, *Col1α2*, *Runx2*, *OPN*, *OCN*, *OSX*, and *TGFβ-RII* (Fig. 3.26). *Runx2*, *ALP*, *Col1α2*, and *TGFβ-RII*, which are considered early markers, showed increased expression between day 1 and day 14. Binding to TGFβ-RII can lead to activation of *Runx2* expression via Smad or p38-MAPK pathways (Chen et al., 2012; Lee et al., 2002). *OPN* expression also increased early with a maximum at day 14, whereas another important marker of mature osteoblasts, *OCN*, did not increase until after day 21 (Ponzetti & Rucci, 2021).

Notably, some osteogenic expression markers were up- or downregulated by cytokine treatments in hFOB 1.19 cells on day 21 of osteogenesis (Fig. 3.27). The expression of *OSX* was significantly downregulated by IL-8 and IFNγ, but also tended to be downregulated by IL-1β and TNF-α (Fig. 3.27, F). During osteogenesis of hFOB 1.19 cells, an increased expression of *OSX* was measured, together with *OPN*, *ALP*, *Runx2* and *TGFβ-RII* on day 14 and, interestingly, another peak later together with *OPN*, *ALP*, and *TGFβ-RII* on day 35 (Fig. 3.26). *OSX* is transcribed via BMP signaling or as a downstream signal via the activation of *Runx2*, so it is also mainly considered an early marker, but regulates later markers such as the expression of *OCN* (Liu et al., 2020). The downregulation of *OSX* by IL-8 and IFNγ correlated with a concomitant increase in *OPN* and *Runx2*. Together with the observed inhibition of mineralization, these results may indicate that cells are arrested in the state of ECM formation and the mineralization process is inhibited. Consistent with this, it was observed in *OSX*-inactivated adult mice that the expression of *Runx2*, *OPN* and *ALP* was increased, leading to an osteopenic phenotype *in vivo*, presumably due to an accumulation of immature osteoblasts (Baek et al., 2009). Activation of early osteogenic markers could be either directly mediated by cytokines or as a feedback mechanism in response to the inhibition of mineralization, possibly mediated by inhibition of *OSX*. Further analysis of possible matrix formation without

mineralization would be important and would show whether the proinflammatory cytokines inhibit cell differentiation or the process of matrix mineralization.

4.3.3. Evaluating the Suitability of Cell Lines as *in vitro* Models for Inflammatory Bone Diseases

Primary human or murine cells and various cell lines are mainly used as osteoblast models for *in vitro* studies. The most commonly used cell lines include the human cell lines hFOB 1.19, MG-63, and SAOs-2 and the murine cell line MC3T3-E1 (Czekanska et al., 2012). Cell lines have many advantages, including their ability to proliferate indefinitely and their homogeneity in function and activity, which greatly increases reproducibility compared to primary cells (Kaur & Dufour, 2012). However, genetic alterations in cell cultures can have a significant impact on their phenotype and physiology, reducing their comparability to primary cells (Czekanska et al., 2012).

In this work, it was shown that hFOB 1.19 cells, which are considered a suitable model for BMSCs in the literature, exhibit osteogenic properties such as ALP activity, mineralization, and expression of osteogenic markers, but also major serious differences from human primary osteoblasts (Marozin et al., 2021; Yen et al., 2007). The opposite response to proinflammatory cytokines therefore raises the question of whether this cell line should be used as a model to study inflammatory bone diseases. However, the reason why these cells showed an opposite result would be very interesting to investigate and may contribute to a better understanding of the effect of cytokines on osteogenic cells. These observations raise the question of whether studies in cell lines can be transferred to primary human cells or whether the immunological regulation of bone metabolism is too complex. The use of the MC3T3-E1 cell line, on which many previous studies on the influence of cytokines on osteoblasts were based, must also be questioned due to the species-divergent expression of osteogenic markers (Czekanska et al., 2014).

4.4. Conclusion and Future Perspectives

This study provides novel insights into the regulatory effects of proinflammatory cytokines on osteoblast function and their potential contribution to inflammation-associated bone diseases. By analyzing for the first time the effects of IL-1β, IL-6, IL-8, TNF-α, and IFNγ on the osteogenesis of primary human osteoblasts, this study provides a clinically relevant perspective on cytokine-mediated modulation of osteoblast activity. Contrary to many previous studies, proinflammatory cytokines significantly enhanced the mineralization by OBs. The observed increase in osteogenic differentiation and proliferation suggests that cytokines may have dual effects on bone formation, which may depend on the local inflammatory milieu and the duration of exposure. Furthermore, cytokine treatment induced metabolic adaptations in osteoblasts that may reflect a shift in cellular energy demands to support osteogenic differentiation under inflammatory conditions. The observed changes in early and late osteogenic marker expression indicate potential alterations in ECM composition and matrix-mineral ratios. These changes may have implications for bone quality and may affect osteoblast-osteoclast communication, resulting in an imbalance between bone resorption and formation.

Another key aspect of this work is the direct comparison of osteoblasts derived from individuals with normal and osteoporotic bone density. Despite the osteoporotic phenotype *in vivo*, no fundamental differences in baseline activity or cytokine responsiveness were observed between OBs and oOBs *in vitro*. This suggests that the impaired bone formation observed in osteoporosis may not be primarily due to intrinsic osteoblast dysfunction, but rather to altered microenvironmental factors such as inflammation. Future studies should investigate whether oOBs respond abnormally to prolonged exposure to inflammatory cytokines, whether the extracellular matrix composition is altered, or whether adipogenic differentiation potential contributes to the reduced bone formation capacity in osteoporotic patients. In addition, the discrepancies between hFOB 1.19 cells and primary osteoblasts in response to cytokine treatment underscore the limitations of using immortalized cell lines to study inflammation-related changes in bone remodeling.

These findings suggest that reliance on cell lines may lead to misleading conclusions regarding cytokine-mediated bone loss and emphasize the need to validate *in vitro* results in primary human models to ensure their translational relevance.

In conclusion, while proinflammatory cytokines enhance osteoblast mineralization, their broader impact on bone quality in acute and chronic inflammation remains to be fully understood. Future research should focus on elucidating the signaling pathways underlying the cytokine-induced stimulation of osteoblast mineralization and the long-term consequences of the metabolic adaptations on bone quality. Furthermore, the interplay between osteoblasts and osteoclasts in an inflammatory environment requires further investigation, especially in the context of chronic inflammatory diseases or inflamm-aging. These findings may contribute to the development of targeted therapeutic strategies that reduce cytokine-induced bone loss while preserving or even enhancing osteoblast function in bone metabolic diseases such as osteoporosis.

5. References

Amarasekara, D. S., Kim, S., & Rho, J. (2021). Regulation of Osteoblast Differentiation by Cytokine Networks. *International Journal of Molecular Sciences*, *22*(6), Article 6. https://doi.org/10.3390/ijms22062851

Amarasekara, D. S., Yun, H., Kim, S., Lee, N., Kim, H., & Rho, J. (2018). Regulation of Osteoclast Differentiation by Cytokine Networks. *Immune Network*, *18*(1), e8. https://doi.org/10.4110/in.2018.18.e8

Arponen, M., Jalava, N., Widjaja, N., & Ivaska, K. K. (2022). Glucose transporters GLUT1, GLUT3, and GLUT4 have different effects on osteoblast proliferation and metabolism. *Frontiers in Physiology*, *13*, 1035516. https://doi.org/10.3389/fphys.2022.1035516

Arron, J. R., & Choi, Y. (2000). Bone versus immune system. *Nature*, *408*(6812), 535–536. https://doi.org/10.1038/35046196

Azizieh, F., Raghupathy, R., Shehab, D., Al-Jarallah, K., & Gupta, R. (2017). Cytokine profiles in osteoporosis suggest a proresorptive bias. *Menopause (New York, N.Y.)*, *24*(9), 1057–1064. https://doi.org/10.1097/GME.0000000000000885

Baek, W., Lee, M., Jung, J. W., Kim, S., Akiyama, H., de Crombrugghe, B., & Kim, J. (2009). Positive Regulation of Adult Bone Formation by Osteoblast-Specific Transcription Factor Osterix. *Journal of Bone and Mineral Research*, *24*(6), 1055–1065. https://doi.org/10.1359/jbmr.081248

Baig, M. A., & Bacha, D. (2024). Histology, Bone. In *StatPearls*. StatPearls Publishing. http://www.ncbi.nlm.nih.gov/books/NBK541132/

Bandeira, L., Lewiecki, E. M., & Bilezikian, J. P. (2017). Romosozumab for the treatment of osteoporosis. *Expert Opinion on Biological Therapy*, *17*(2), 255–263. https://doi.org/10.1080/14712598.2017.1280455

Bastian, O. W., Koenderman, L., Alblas, J., Leenen, L. P. H., & Blokhuis, T. J. (2016). Neutrophils contribute to fracture healing by synthesizing fibronectin+ extracellular matrix rapidly after injury. *Clinical Immunology*, *164*, 78–84. https://doi.org/10.1016/j.clim.2016.02.001

Bastidas-Coral, A. P., Bakker, A. D., Zandieh-Doulabi, B., Kleverlaan, C. J., Bravenboer, N., Forouzanfar, T., & Klein-Nulend, J. (2016). Cytokines TNF-α, IL-6, IL-17F, and IL-4 Differentially Affect Osteogenic Differentiation of Human Adipose Stem Cells. *Stem Cells International*, *2016*, 1318256. https://doi.org/10.1155/2016/1318256

Bendre, M. S., Montague, D. C., Peery, T., Akel, N. S., Gaddy, D., & Suva, L. J. (2003). Interleukin-8 stimulation of osteoclastogenesis and bone resorption is a mechanism for the increased osteolysis of metastatic bone disease. *Bone*, *33*(1), 28–37. https://doi.org/10.1016/s8756-3282(03)00086-3

Bianco, P., Cao, X., Frenette, P. S., Mao, J. J., Robey, P. G., Simmons, P. J., & Wang, C.-Y. (2013). The meaning, the sense and the significance: Translating the science of mesenchymal stem cells into medicine. *Nature Medicine*, *19*(1), 35–42. https://doi.org/10.1038/nm.3028

Blanchard, F., Duplomb, L., Baud'huin, M., & Brounais, B. (2009). The dual role of IL-6-type cytokines on bone remodeling and bone tumors. *Cytokine & Growth*

Factor Reviews, *20*(1), 19–28. https://doi.org/10.1016/j.cytogfr.2008.11.004

Bonewald, L. F., Harris, S. E., Rosser, J., Dallas, M. R., Dallas, S. L., Camacho, N. P., Boyan, B., & Boskey, A. (2003). Von Kossa Staining Alone Is Not Sufficient to Confirm that Mineralization In Vitro Represents Bone Formation. *Calcified Tissue International*, *72*(5), 537–547. https://doi.org/10.1007/s00223-002-1057-y

Bonjour, J.-P., Ammann, P., & Rizzoli, R. (1999). Importance of Preclinical Studies in the Development of Drugs for Treatment of Osteoporosis: A Review Related to the 1998 WHO Guidelines. *Osteoporosis International*, *9*(5), 379–393. https://doi.org/10.1007/s001980050161

Borish, L. C., & Steinke, J. W. (2003). 2. Cytokines and chemokines. *Journal of Allergy and Clinical Immunology*, *111*(2), S460–S475. https://doi.org/10.1067/mai.2003.108

Boyce, B. F., Yao, Z., & Xing, L. (2009). Osteoclasts have Multiple Roles in Bone in Addition to Bone Resorption. *Critical reviews in eukaryotic gene expression*, *19*(3), 171–180.

Bresnihan, B., Newmark, R., Robbins, S., & Genant, H. K. (2004). Effects of anakinra monotherapy on joint damage in patients with rheumatoid arthritis. Extension of a 24-week randomized, placebo-controlled trial. *The Journal of Rheumatology*, *31*(6), 1103–1111.

Britannica, T. Editors of Encyclopaedia. (2010, Februar 16). Bone remodeling. *Encyclopedia Britannica*. https://www.britannica.com/science/bone-remodeling

Bruunsgaard, H. (2002). Effects of tumor necrosis factor-alpha and interleukin-6 in elderly populations. *European Cytokine Network*, *13*(4), 389–391.

Carbonare, L. D., Valenti, M. T., Zanatta, M., Donatelli, L., & Lo Cascio, V. (2009). Circulating mesenchymal stem cells with abnormal osteogenic differentiation in patients with osteoporosis. *Arthritis & Rheumatism*, *60*(11), 3356–3365. https://doi.org/10.1002/art.24884

Chang, B., & Liu, X. (2022). Osteon: Structure, Turnover, and Regeneration. *Tissue Engineering. Part B, Reviews*, *28*(2), 261–278. https://doi.org/10.1089/ten.teb.2020.0322

Chang, M. K., Raggatt, L.-J., Alexander, K. A., Kuliwaba, J. S., Fazzalari, N. L., Schroder, K., Maylin, E. R., Ripoll, V. M., Hume, D. A., & Pettit, A. R. (2008). Osteal Tissue Macrophages Are Intercalated throughout Human and Mouse Bone Lining Tissues and Regulate Osteoblast Function In Vitro and In Vivo1. *The Journal of Immunology*, *181*(2), 1232–1244. https://doi.org/10.4049/jimmunol.181.2.1232

Charatcharoenwitthaya, N., Khosla, S., Atkinson, E. J., McCready, L. K., & Riggs, B. L. (2007). Effect of blockade of TNF-alpha and interleukin-1 action on bone resorption in early postmenopausal women. *Journal of Bone and Mineral Research: The Official Journal of the American Society for Bone and Mineral Research*, *22*(5), 724–729. https://doi.org/10.1359/jbmr.070207

Chen, G., Deng, C., & Li, Y.-P. (2012). TGF-β and BMP Signaling in Osteoblast Differentiation and Bone Formation. *International Journal of Biological Sciences*, *8*(2), 272–288. https://doi.org/10.7150/ijbs.2929

Clarke, B. (2008). Normal Bone Anatomy and Physiology. *Clinical Journal of the American Society of Nephrology : CJASN*, *3*(Suppl 3), S131–S139. https://doi.org/10.2215/CJN.04151206

Clarke, B. L., & Khosla, S. (2010). Physiology of Bone Loss. *Radiologic clinics of North America*, *48*(3), 483–495. https://doi.org/10.1016/j.rcl.2010.02.014

Compston, J. (2018). Glucocorticoid-induced osteoporosis: An update. *Endocrine*, *61*(1), 7–16. https://doi.org/10.1007/s12020-018-1588-2

Czekanska, E. M., Stoddart, M. J., Ralphs, J. R., Richards, R. G., & Hayes, J. S. (2014). A phenotypic comparison of osteoblast cell lines versus human primary osteoblasts for biomaterials testing. *Journal of Biomedical Materials Research Part A*, *102*(8), 2636–2643. https://doi.org/10.1002/jbm.a.34937

Czekanska, E. M., Stoddart, M. J., Richards, R. G., & Hayes, J. S. (2012). In search of an osteoblast cell model for in vitro research. *European Cells & Materials*, *24*, 1–17. https://doi.org/10.22203/ecm.v024a01

Delaisse, J.-M. (2014). The reversal phase of the bone-remodeling cycle: Cellular prerequisites for coupling resorption and formation. *BoneKEy Reports*, *3*, 561. https://doi.org/10.1038/bonekey.2014.56

Dinarello, C. A., Simon, A., & Meer, J. W. M. van der. (2012). Treating inflammation by blocking interleukin-1 in a broad spectrum of diseases. *Nature Reviews. Drug Discovery*, *11*(8), 633. https://doi.org/10.1038/nrd3800

Dobbs, M. B., Buckwalter, J., & Saltzman, C. (1999). Osteoporosis. *The Iowa Orthopaedic Journal*, *19*, 43–52.

Donoso, O., Pino, A. M., Seitz, G., Osses, N., & Rodríguez, J. P. (2015). Osteoporosis-associated alteration in the signalling status of BMP-2 in human MSCs under adipogenic conditions. *Journal of Cellular Biochemistry*, *116*(7), 1267–1277. https://doi.org/10.1002/jcb.25082

Dr. Stashenko, P., Dewhirst, F. E., Rooney, M. L., Desjardins, L. A., & Heeley, J. D. (1987). Interleukin-1β is a potent inhibitor of bone formation in vitro. *Journal of Bone and Mineral Research*, *2*(6), 559–565. https://doi.org/10.1002/jbmr.5650020612

Duque, G., Huang, D. C., Macoritto, M., Rivas, D., Yang, X. F., Ste-Marie, L. G., & Kremer, R. (2009). Autocrine Regulation of Interferon γ in Mesenchymal Stem Cells Plays a Role in Early Osteoblastogenesis. *Stem Cells*, *27*(3), 550–558. https://doi.org/10.1634/stemcells.2008-0886

DVO Leitlinie Osteoporose. (2023). *Prophylaxe, Diagnostik und Therapie der OSTEOPOROSE - Leitlinie des Dachverbands der Deutschsprachigen Wissenschaftlichen Osteologischen Gesellschaften e.V.*

Dwek, J. R. (2010). The periosteum: What is it, where is it, and what mimics it in its absence? *Skeletal Radiology*, *39*(4), 319–323. https://doi.org/10.1007/s00256-009-0849-9

Eriksen, E. F. (2010). Cellular mechanisms of bone remodeling. *Reviews in Endocrine & Metabolic Disorders*, *11*(4), 219–227. https://doi.org/10.1007/s11154-010-9153-1

Esen, E., Chen, J., Karner, C. M., Okunade, A. L., Patterson, B. W., & Long, F. (2013). WNT-LRP5 signaling induces Warburg effect through mTORC2 activation during osteoblast differentiation. *Cell metabolism*, *17*(5), 745–755. https://doi.org/10.1016/j.cmet.2013.03.017

Esen, E., & Long, F. (2014). Aerobic Glycolysis in Osteoblasts. *Current osteoporosis reports*, *12*(4), 433–438. https://doi.org/10.1007/s11914-014-0235-y

Fardellone, P., Salawati, E., Le Monnier, L., & Goëb, V. (2020). Bone Loss, Osteoporosis, and Fractures in Patients with Rheumatoid Arthritis: A Review. *Journal of Clinical Medicine*, *9*(10), 3361. https://doi.org/10.3390/jcm9103361

Florencio-Silva, R., Sasso, G. R. da S., Sasso-Cerri, E., Simões, M. J., & Cerri, P. S. (2015). Biology of Bone Tissue: Structure, Function, and Factors That Influence Bone Cells. *BioMed Research International*, *2015*, 421746. https://doi.org/10.1155/2015/421746

Franceschi, C., Bonafè, M., Valensin, S., Olivieri, F., De Luca, M., Ottaviani, E., & De Benedictis, G. (2000). Inflamm-aging: An Evolutionary Perspective on Immunosenescence. *Annals of the New York Academy of Sciences*, *908*(1), 244–254. https://doi.org/10.1111/j.1749-6632.2000.tb06651.x

Franceschi, R. T., Xiao, G., Jiang, D., Gopalakrishnan, R., Yang, S., & Reith, E. (2003). Multiple Signaling Pathways Converge on the Cbfa1/Runx2 Transcription Factor to Regulate Osteoblast Differentiation. *Connective Tissue Research*, *44*(1), 109–116. https://doi.org/10.1080/03008200390152188

Ganesan, K., Jandu, J. S., Anastasopoulou, C., Ahsun, S., & Roane, D. (2024). Secondary Osteoporosis. In *StatPearls*. StatPearls Publishing. http://www.ncbi.nlm.nih.gov/books/NBK470166/

Garnero, P., Sornay-Rendu, E., Chapuy, M. C., & Delmas, P. D. (1996). Increased bone turnover in late postmenopausal women is a major determinant of osteoporosis. *Journal of Bone and Mineral Research: The Official Journal of the American Society for Bone and Mineral Research*, *11*(3), 337–349. https://doi.org/10.1002/jbmr.5650110307

Gibson, L. J. (1985). The mechanical behaviour of cancellous bone. *Journal of Biomechanics*, *18*(5), 317–328. https://doi.org/10.1016/0021-9290(85)90287-8

Gilbert, L., He, X., Farmer, P., Boden, S., Kozlowski, M., Rubin, J., & Nanes, M. S. (2000). Inhibition of osteoblast differentiation by tumor necrosis factor-alpha. *Endocrinology*, *141*(11), 3956–3964. https://doi.org/10.1210/endo.141.11.7739

Gilbert, L., He, X., Farmer, P., Rubin, J., Drissi, H., Wijnen, A. J. van, Lian, J. B., Stein, G. S., & Nanes, M. S. (2002). Expression of the Osteoblast Differentiation Factor RUNX2 (Cbfa1/AML3/Pebp2αA) Is Inhibited by Tumor Necrosis Factor-α *. *Journal of Biological Chemistry*, *277*(4), 2695–2701. https://doi.org/10.1074/jbc.M106339200

Ginaldi, L., Di Benedetto, M. C., & De Martinis, M. (2005). Osteoporosis, inflammation and ageing. *Immunity & ageing : I & A*, *2*, 14. https://doi.org/10.1186/1742-4933-2-14

Griffith, J. F. (2017). Age-Related Changes in the Bone Marrow. *Current Radiology Reports*, *5*(6), 24. https://doi.org/10.1007/s40134-017-0218-8

Guder, C., Gravius, S., Burger, C., Wirtz, D. C., & Schildberg, F. A. (2020). Osteoimmunology: A Current Update of the Interplay Between Bone and the Immune System. *Frontiers in Immunology*, *11*. https://doi.org/10.3389/fimmu.2020.00058

Guntur, A. R., Gerencser, A. A., Le, P. T., DeMambro, V. E., Bornstein, S. A., Mookerjee, S. A., Maridas, D. E., Clemmons, D. E., Brand, M. D., & Rosen, C. J. (2018). Osteoblast-like MC3T3-E1 Cells Prefer Glycolysis for ATP Production but Adipocyte-like 3T3-L1 Cells Prefer Oxidative Phosphorylation. *Journal of Bone and Mineral Research*, *33*(6), 1052–1065. https://doi.org/10.1002/jbmr.3390

Guntur, A. R., Le, P. T., Farber, C. R., & Rosen, C. J. (2014). Bioenergetics During Calvarial Osteoblast Differentiation Reflect Strain Differences in Bone Mass. *Endocrinology*, *155*(5), 1589–1595. https://doi.org/10.1210/en.2013-1974

Haddouti, E.-M., Randau, T., Hilgers, C., Masson, W., Pflugmacher, R., Burger, C., Gravius, S., & Schildberg, F. (2020). Vertebral Bone Marrow-Derived Mesenchymal Stromal Cells from Osteoporotic and Healthy Patients Possess Similar Differentiation Properties In Vitro. *International Journal of Molecular Sciences*, *21*. https://doi.org/10.3390/ijms21218309

Hadjidakis, D. J., & Androulakis, I. I. (2006). Bone remodeling. *Annals of the New York Academy of Sciences*, *1092*, 385–396. https://doi.org/10.1196/annals.1365.035

Hanna, H., Mir, L. M., & Andre, F. M. (2018). In vitro osteoblastic differentiation of mesenchymal stem cells generates cell layers with distinct properties. *Stem Cell Research & Therapy*, *9*(1), 203. https://doi.org/10.1186/s13287-018-0942-x

Hariri, M., Millane, G., Guimond, M.-P., Guay, G., Dennis, J. W., & Nabi, I. R. (2000). Biogenesis of Multilamellar Bodies via Autophagy. *Molecular Biology of the Cell*, *11*(1), 255–268.

Harris, S. A., Enger, R. J., Riggs, B. L., & Spelsberg, T. C. (1995). Development and characterization of a conditionally immortalized human fetal osteoblastic cell line. *Journal of Bone and Mineral Research: The Official Journal of the American Society for Bone and Mineral Research*, *10*(2), 178–186. https://doi.org/10.1002/jbmr.5650100203

Haugeberg, G., Helgetveit, K. B., Førre, Ø., Garen, T., Sommerseth, H., & Prøven, A. (2014). Generalized bone loss in early rheumatoid arthritis patients followed for ten years in the biologic treatment era. *BMC Musculoskeletal Disorders*, *15*, 289. https://doi.org/10.1186/1471-2474-15-289

Heino, T. J., Hentunen, T. A., & Väänänen, H. K. (2002). Osteocytes inhibit osteoclastic bone resorption through transforming growth factor-β: Enhancement by estrogen. *Journal of Cellular Biochemistry*, *85*(1), 185–197. https://doi.org/10.1002/jcb.10109

Hoac, B., Nelea, V., Jiang, W., Kaartinen, M. T., & McKee, M. D. (2017). Mineralization-inhibiting effects of transglutaminase-crosslinked polymeric osteopontin. *Bone*, *101*, 37–48. https://doi.org/10.1016/j.bone.2017.04.007

Hu, L., Yin, C., Zhao, F., Ali, A., Ma, J., & Qian, A. (2018). Mesenchymal Stem Cells: Cell Fate Decision to Osteoblast or Adipocyte and Application in Osteoporosis Treatment. *International Journal of Molecular Sciences*, *19*(2), 360. https://doi.org/10.3390/ijms19020360

Huang, W., Carlsen, B., Rudkin, G., Berry, M., Ishida, K., Yamaguchi, D. T., & Miller, T. A. (2004). Osteopontin is a negative regulator of proliferation and

differentiation in MC3T3-E1 pre-osteoblastic cells. *Bone*, *34*(5), 799–808. https://doi.org/10.1016/j.bone.2003.11.027

Huang, W., Yang, S., Shao, J., & Li, Y.-P. (2007). Signaling and transcriptional regulation in osteoblast commitment and differentiation. *Frontiers in bioscience : a journal and virtual library*, *12*, 3068–3092.

Infante, A., & Rodríguez, C. I. (2018). Osteogenesis and aging: Lessons from mesenchymal stem cells. *Stem Cell Research & Therapy*, *9*, 244. https://doi.org/10.1186/s13287-018-0995-x

Iwasaki, K., Komaki, M., Mimori, K., Leon, E., Izumi, Y., & Ishikawa, I. (2008). IL-6 Induces Osteoblastic Differentiation of Periodontal Ligament Cells. *Journal of Dental Research*, *87*(10), 937–942. https://doi.org/10.1177/154405910808701002

Jaiswal, N., Haynesworth, S. E., Caplan, A. I., & Bruder, S. P. (1997). Osteogenic differentiation of purified, culture-expanded human mesenchymal stem cells in vitro. *Journal of Cellular Biochemistry*, *64*(2), 295–312. https://doi.org/10.1002/(SICI)1097-4644(199702)64:2<295::AID-JCB12>3.0.CO;2-I

Jing, H., Liao, L., An, Y., Su, X., Liu, S., Shuai, Y., Zhang, X., & Jin, Y. (2016). Suppression of EZH2 Prevents the Shift of Osteoporotic MSC Fate to Adipocyte and Enhances Bone Formation During Osteoporosis. *Molecular Therapy*, *24*(2), 217–229. https://doi.org/10.1038/mt.2015.152

Justesen, J., Stenderup, K., Ebbesen, E. N., Mosekilde, L., Steiniche, T., & Kassem, M. (2001). Adipocyte tissue volume in bone marrow is increased with aging and in patients with osteoporosis. *Biogerontology*, *2*(3), 165–171. https://doi.org/10.1023/A:1011513223894

Kaneshiro, S., Ebina, K., Shi, K., Higuchi, C., Hirao, M., Okamoto, M., Koizumi, K., Morimoto, T., Yoshikawa, H., & Hashimoto, J. (2014). IL-6 negatively regulates osteoblast differentiation through the SHP2/MEK2 and SHP2/Akt2 pathways in vitro. *Journal of Bone and Mineral Metabolism*, *32*(4), 378–392. https://doi.org/10.1007/s00774-013-0514-1

Kanis, J. A., Cooper, C., Rizzoli, R., Reginster, J.-Y., & on behalf of the Scientific Advisory Board of the European Society for Clinical and Economic Aspects of Osteoporosis (ESCEO) and the Committees of Scientific Advisors and National Societies of the International Osteoporosis Foundation (IOF). (2019). European guidance for the diagnosis and management of osteoporosis in postmenopausal women. *Osteoporosis International*, *30*(1), 3–44. https://doi.org/10.1007/s00198-018-4704-5

Kanis, J. A., Johnell, O., Oden, A., Johansson, H., & McCloskey, E. (2008). FRAX and the assessment of fracture probability in men and women from the UK. *Osteoporosis International: A Journal Established as Result of Cooperation between the European Foundation for Osteoporosis and the National Osteoporosis Foundation of the USA*, *19*(4), 385–397. https://doi.org/10.1007/s00198-007-0543-5

Kanis, J. A., Melton III, L. J., Christiansen, C., Johnston, C. C., & Khaltaev, N. (1994). The diagnosis of osteoporosis. *Journal of Bone and Mineral Research*, *9*(8), 1137–1141. https://doi.org/10.1002/jbmr.5650090802

Kanis, J. A., Norton, N., Harvey, N. C., Jacobson, T., Johansson, H., Lorentzon, M., McCloskey, E. V., Willers, C., & Borgström, F. (2021). SCOPE 2021: A new scorecard for osteoporosis in Europe. *Archives of Osteoporosis*, *16*(1), 82. https://doi.org/10.1007/s11657-020-00871-9

Kareem, R., Botleroo, R. A., Bhandari, R., Ogeyingbo, O. D., Ahmed, R., Gyawali, M., Venkatesan, N., & Elshaikh, A. O. (o. J.). The Impact of Rheumatoid Arthritis on Bone Loss: Links to Osteoporosis and Osteopenia. *Cureus*, *13*(8), e17519. https://doi.org/10.7759/cureus.17519

Kareem, R., Botleroo, R. A., Bhandari, R., Ogeyingbo, O. D., Ahmed, R., Gyawali, M., Venkatesan, N., Elshaikh, A. O., Kareem, R., Botleroo, R. A., Bhandari, R., Ogeyingbo, O. D., Ahmed, R., Gyawali, M., Venkatesan, N., & Elshaikh, A. O. (2021). The Impact of Rheumatoid Arthritis on Bone Loss: Links to Osteoporosis and Osteopenia. *Cureus*, *13*(8). https://doi.org/10.7759/cureus.17519

Kim, J.-M., Lin, C., Stavre, Z., Greenblatt, M. B., & Shim, J.-H. (2020). Osteoblast-Osteoclast Communication and Bone Homeostasis. *Cells*, *9*(9), Article 9. https://doi.org/10.3390/cells9092073

Kohara, H., Kitaura, H., Fujimura, Y., Yoshimatsu, M., Morita, Y., Eguchi, T., Masuyama, R., & Yoshida, N. (2011). IFN-γ directly inhibits TNF-α-induced osteoclastogenesis *in vitro* and *in vivo* and induces apoptosis mediated by Fas/Fas ligand interactions. *Immunology Letters*, *137*(1), 53–61. https://doi.org/10.1016/j.imlet.2011.02.017

Komori, T. (2006). Regulation of osteoblast differentiation by transcription factors. *Journal of Cellular Biochemistry*, *99*(5), 1233–1239. https://doi.org/10.1002/jcb.20958

Kopesky, P., Tiedemann, K., Alkekhia, D., Zechner, C., Millard, B., Schoeberl, B., & Komarova, S. V. (2014). Autocrine signaling is a key regulatory element during osteoclastogenesis. *Biology Open*, *3*(8), 767–776. https://doi.org/10.1242/bio.20148128

Lacey, D. C., Simmons, P. J., Graves, S. E., & Hamilton, J. A. (2009). Proinflammatory cytokines inhibit osteogenic differentiation from stem cells: Implications for bone repair during inflammation. *Osteoarthritis and Cartilage*, *17*(6), 735–742. https://doi.org/10.1016/j.joca.2008.11.011

Lai, J.-H., Hsu, Y.-P., Yang, C.-H., Chen, Y.-H., Liu, C.-C., & Chen, S.-K. (2022). Interferon-gamma regulates the levels of bone formation effectors in a stage-dependent manner. *Molecular Biology Reports*, *49*(12), 12007–12015. https://doi.org/10.1007/s11033-022-07993-y

Langenbach, F., & Handschel, J. (2013). Effects of dexamethasone, ascorbic acid and β-glycerophosphate on the osteogenic differentiation of stem cells in vitro. *Stem Cell Research & Therapy*, *4*(5), 117. https://doi.org/10.1186/scrt328

Laterveer, L., Lindley, I., Hamilton, M., Willemze, R., & Fibbe, W. (1995). Interleukin-8 induces rapid mobilization of hematopoietic stem cells with radioprotective capacity and long-term myelolymphoid repopulating ability. *Blood*, *85*(8), 2269–2275. https://doi.org/10.1182/blood.V85.8.2269.bloodjournal8582269

Lee, K.-S., Hong, S.-H., & Bae, S.-C. (2002). Both the Smad and p38 MAPK pathways play a crucial role in Runx2 expression following induction by transforming

growth factor-β and bone morphogenetic protein. *Oncogene*, *21*(47), 7156–7163. https://doi.org/10.1038/sj.onc.1205937

Lencel, P., & Magne, D. (2011). Inflammaging: The driving force in osteoporosis? *Medical Hypotheses*, *76*(3), 317–321. https://doi.org/10.1016/j.mehy.2010.09.023

Li, S., Liu, G., & Hu, S. (2024). Osteoporosis: Interferon-gamma-mediated bone remodeling in osteoimmunology. *Frontiers in Immunology*, *15*, 1396122. https://doi.org/10.3389/fimmu.2024.1396122

Li, X., Han, L., Nookaew, I., Mannen, E., Silva, M. J., Almeida, M., & Xiong, J. (2019). Stimulation of Piezo1 by mechanical signals promotes bone anabolism. *eLife*, *8*, e49631. https://doi.org/10.7554/eLife.49631

Li, Z., Frey, J. L., Wong, G. W., Faugere, M.-C., Wolfgang, M. J., Kim, J. K., Riddle, R. C., & Clemens, T. L. (2016). Glucose Transporter-4 Facilitates Insulin-Stimulated Glucose Uptake in Osteoblasts. *Endocrinology*, *157*(11), 4094–4103. https://doi.org/10.1210/en.2016-1583

Liu, Q., Li, M., Wang, S., Xiao, Z., Xiong, Y., & Wang, G. (2020). Recent Advances of Osterix Transcription Factor in Osteoblast Differentiation and Bone Formation. *Frontiers in Cell and Developmental Biology*, *8*, 601224. https://doi.org/10.3389/fcell.2020.601224

Ma, H., Li, Y., Song, L., Liu, R., Li, X., Shang, Q., Wang, Y., Shao, C., & Shi, Y. (2020). Macrophages inhibit adipogenic differentiation of adipose tissue derived mesenchymal stem/stromal cells by producing pro-inflammatory cytokines. *Cell & Bioscience*, *10*(1), 88. https://doi.org/10.1186/s13578-020-00450-y

Malysheva, K., de Rooij, K., Löwik, C. W. G. M., Baeten, D. L., Rose-John, S., Stoika, R., & Korchynskyi, O. (2016). Interleukin 6/Wnt interactions in rheumatoid arthritis: Interleukin 6 inhibits Wnt signaling in synovial fibroblasts and osteoblasts. *Croatian Medical Journal*, *57*(2), 89–98. https://doi.org/10.3325/cmj.2016.57.89

Mao, C. -y, Wang, Y. -g, Zhang, X., Zheng, X. -y, Tang, T. -t, & Lu, E. -y. (2016). Double-edged-sword effect of IL-1β on the osteogenesis of periodontal ligament stem cells via crosstalk between the NF-κB, MAPK and BMP/Smad signaling pathways. *Cell Death & Disease*, *7*(7), e2296–e2296. https://doi.org/10.1038/cddis.2016.204

Marks Jr., S. C., & Popoff, S. N. (1988). Bone cell biology: The regulation of development, structure, and function in the skeleton. *American Journal of Anatomy*, *183*(1), 1–44. https://doi.org/10.1002/aja.1001830102

Martínez-Reyes, I., & Chandel, N. S. (2020). Mitochondrial TCA cycle metabolites control physiology and disease. *Nature Communications*, *11*(1), 102. https://doi.org/10.1038/s41467-019-13668-3

Molnar, V., Matišić, V., Kodvanj, I., Bjelica, R., Jeleč, Ž., Hudetz, D., Rod, E., Čukelj, F., Vrdoljak, T., Vidović, D., Starešinić, M., Sabalić, S., Dobričić, B., Petrović, T., Antičević, D., Borić, I., Košir, R., Zmrzljak, U. P., & Primorac, D. (2021). Cytokines and Chemokines Involved in Osteoarthritis Pathogenesis. *International Journal of Molecular Sciences*, *22*(17), 9208. https://doi.org/10.3390/ijms22179208

Motyl, K. J., Guntur, A. R., Carvalho, A. L., & Rosen, C. J. (2017). Energy Metabolism of Bone. *Toxicologic pathology*, *45*(7), 887–893. https://doi.org/10.1177/0192623317737065

Mountziaris, P. M., & Mikos, A. G. (2008). Modulation of the Inflammatory Response for Enhanced Bone Tissue Regeneration. *Tissue Engineering. Part B, Reviews*, *14*(2), 179–186. https://doi.org/10.1089/ten.teb.2008.0038

Nakashima, K., Zhou, X., Kunkel, G., Zhang, Z., Deng, J. M., Behringer, R. R., & de Crombrugghe, B. (2002). The novel zinc finger-containing transcription factor osterix is required for osteoblast differentiation and bone formation. *Cell*, *108*(1), 17–29. https://doi.org/10.1016/s0092-8674(01)00622-5

Naqvi, S. M., O'Sullivan, L. M., Allison, H., Casey, V. J., Schiavi-Tritz, J., & McNamara, L. M. (2024). Altered extracellular matrix and mechanotransduction gene expression in rat bone tissue following long-term estrogen deficiency. *JBMR Plus*, *8*(9), ziae098. https://doi.org/10.1093/jbmrpl/ziae098

Neidlinger-Wilke, C., Stalla, I., Claes, L., Brand, R., Hoellen, I., Rübenacker, S., Arand, M., & Kinzl, L. (1995). Human osteoblasts from younger normal and osteoporotic donors show differences in proliferation and TGF beta-release in response to cyclic strain. *Journal of Biomechanics*, *28*(12), 1411–1418. https://doi.org/10.1016/0021-9290(95)00089-5

Nolfi-Donegan, D., Braganza, A., & Shiva, S. (2020). Mitochondrial electron transport chain: Oxidative phosphorylation, oxidant production, and methods of measurement. *Redox Biology*, *37*, 101674. https://doi.org/10.1016/j.redox.2020.101674

Nollet, M., Santucci-Darmanin, S., Breuil, V., Al-Sahlanee, R., Cros, C., Topi, M., Momier, D., Samson, M., Pagnotta, S., Cailleteau, L., Battaglia, S., Farlay, D., Dacquin, R., Barois, N., Jurdic, P., Boivin, G., Heymann, D., Lafont, F., Lu, S. S., … Pierrefite-Carle, V. (2014). Autophagy in osteoblasts is involved in mineralization and bone homeostasis. *Autophagy*, *10*(11), 1965–1977. https://doi.org/10.4161/auto.36182

Oftadeh, R., Perez-Viloria, M., Villa-Camacho, J. C., Vaziri, A., & Nazarian, A. (2015). Biomechanics and Mechanobiology of Trabecular Bone: A Review. *Journal of Biomechanical Engineering*, *137*(1), 0108021–01080215. https://doi.org/10.1115/1.4029176

Ohshima, S., Yamaguchi, N., Nishioka, K., Mima, T., Ishii, T., Umeshita-Sasai, M., Kobayashi, H., Shimizu, M., Katada, Y., Wakitani, S., Murata, N., Nomura, S., Matsuno, H., Katayama, R., Kon, S., Inobe, M., Uede, T., Kawase, I., & Saeki, Y. (2002). Enhanced local production of osteopontin in rheumatoid joints. *The Journal of Rheumatology*, *29*(10), 2061–2067.

Osta, B., Benedetti, G., & Miossec, P. (2014). Classical and Paradoxical Effects of TNF-α on Bone Homeostasis. *Frontiers in Immunology*, *5*, 48. https://doi.org/10.3389/fimmu.2014.00048

Park, M. S., Kim, Y. H., Jung, Y., Kim, S. H., Park, J. C., Yoon, D. S., Kim, S.-H., & Lee, J. W. (2015). In Situ Recruitment of Human Bone Marrow-Derived Mesenchymal Stem Cells Using Chemokines for Articular Cartilage Regeneration. *Cell Transplantation*, *24*(6), 1067–1083. https://doi.org/10.3727/096368914X681018

Pernow, Y., Granberg, B., Sääf, M., & Weidenhielm, L. (2006). Osteoblast Dysfunction in Male Idiopathic Osteoporosis. *Calcified Tissue International*, *78*(2), 90–97. https://doi.org/10.1007/s00223-005-0158-9

Ponzetti, M., & Rucci, N. (2021). Osteoblast Differentiation and Signaling: Established Concepts and Emerging Topics. *International Journal of Molecular Sciences*, *22*(13), 6651. https://doi.org/10.3390/ijms22136651

Raggatt, L. J., & Partridge, N. C. (2010). Cellular and Molecular Mechanisms of Bone Remodeling*. *Journal of Biological Chemistry*, *285*(33), 25103–25108. https://doi.org/10.1074/jbc.R109.041087

Rauner, M., Sipos, W., & Pietschmann, P. (2007). Osteoimmunology. *International Archives of Allergy and Immunology*, *143*(1), 31–48. https://doi.org/10.1159/000098223

Reinholt, F. P., Hultenby, K., Oldberg, A., & Heinegård, D. (1990). Osteopontin—A possible anchor of osteoclasts to bone. *Proceedings of the National Academy of Sciences of the United States of America*, *87*(12), 4473–4475.

Remick, D. G. (2005). Interleukin-8. *Critical Care Medicine*, *33*(12), S466. https://doi.org/10.1097/01.CCM.0000186783.34908.18

Reynolds, E. S. (1963). The use of lead citrate at high pH as an electron-opaque stain in electron microscopy. *The Journal of Cell Biology*, *17*(1), 208–212. https://doi.org/10.1083/jcb.17.1.208

Riggs, B. L., & Melton, L. J. (1995). The worldwide problem of osteoporosis: Insights afforded by epidemiology. *Bone*, *17*(5 Suppl), 505S-511S. https://doi.org/10.1016/8756-3282(95)00258-4

Rodríguez, J. P., Astudillo, P., Ríos, S., & Pino, A. M. (2008). Involvement of adipogenic potential of human bone marrow mesenchymal stem cells (MSCs) in osteoporosis. *Current Stem Cell Research & Therapy*, *3*(3), 208–218. https://doi.org/10.2174/157488808785740325

Rodríguez, J. P., Garat, S., Gajardo, H., Pino, A. M., & Seitz, G. (1999). Abnormal osteogenesis in osteoporotic patients is reflected by altered mesenchymal stem cells dynamics. *Journal of Cellular Biochemistry*, *75*(3), 414–423. https://doi.org/10.1002/(SICI)1097-4644(19991201)75:3<414::AID-JCB7>3.0.CO;2-C

Rodríguez, J. P., Montecinos, L., Ríos, S., Reyes, P., & Martínez, J. (2000). Mesenchymal stem cells from osteoporotic patients produce a type I collagen-deficient extracellular matrix favoring adipogenic differentiation. *Journal of Cellular Biochemistry*, *79*(4), 557–565. https://doi.org/10.1002/1097-4644(20001215)79:4<557::AID-JCB40>3.0.CO;2-H

Rodríguez-Carballo, E., Gámez, B., & Ventura, F. (2016). P38 MAPK Signaling in Osteoblast Differentiation. *Frontiers in Cell and Developmental Biology*, *4*. https://doi.org/10.3389/fcell.2016.00040

Roggia, C., Gao, Y., Cenci, S., Weitzmann, M. N., Toraldo, G., Isaia, G., & Pacifici, R. (2001). Up-regulation of TNF-producing T cells in the bone marrow: A key mechanism by which estrogen deficiency induces bone loss in vivo. *Proceedings of the National Academy of Sciences of the United States of America*, *98*(24), 13960–13965. https://doi.org/10.1073/pnas.251534698

Rosen, E., Hsu, C.-H., Wang, X., Sakai, S., Freeman, M., Gonzalez, F., & Spiegelman, B. (2002). C/EBPα induces adipogenesis through PPARγ: A unified pathway. *Genes & development*, *16*, 22–26. https://doi.org/10.1101/gad.948702

Ruscitti, P., Cipriani, P., Carubbi, F., Liakouli, V., Zazzeroni, F., Di Benedetto, P., Berardicurti, O., Alesse, E., & Giacomelli, R. (2015). The Role of IL-1β in the Bone Loss during Rheumatic Diseases. *Mediators of Inflammation*, *2015*, 782382. https://doi.org/10.1155/2015/782382

Ryu, J., Kim, H. J., Chang, E., Huang, H., Banno, Y., & Kim, H. (2006). Sphingosine 1-phosphate as a regulator of osteoclast differentiation and osteoclast–osteoblast coupling. *The EMBO Journal*, *25*(24), 5840–5851. https://doi.org/10.1038/sj.emboj.7601430

Salamanna, F., Maglio, M., Sartori, M., Tschon, M., & Fini, M. (2020). Platelet Features and Derivatives in Osteoporosis: A Rational and Systematic Review on the Best Evidence. *International Journal of Molecular Sciences*, *21*(5), Article 5. https://doi.org/10.3390/ijms21051762

Schmitz, G., & Müller, G. (1991). Structure and function of lamellar bodies, lipid-protein complexes involved in storage and secretion of cellular lipids. *Journal of Lipid Research*, *32*(10), 1539–1570. https://doi.org/10.1016/S0022-2275(20)41642-6

Shapiro, I. M., Landis, W. J., & Risbud, M. V. (2015). Matrix vesicles: Are they anchored exosomes? *Bone*, *79*, 29–36. https://doi.org/10.1016/j.bone.2015.05.013

Shen, W., Chen, J., Gantz, M., Punyanitya, M., Heymsfield, S. B., Gallagher, D., Albu, J., Engelson, E., Kotler, D., Pi-Sunyer, X., & Gilsanz, V. (2012). MRI-measured pelvic bone marrow adipose tissue is inversely related to DXA-measured bone mineral in younger and older adults. *European Journal of Clinical Nutrition*, *66*(9), 983–988. https://doi.org/10.1038/ejcn.2012.35

Shum, L. C., White, N. S., Mills, B. N., de Mesy Bentley, K. L., & Eliseev, R. A. (2016). Energy Metabolism in Mesenchymal Stem Cells During Osteogenic Differentiation. *Stem Cells and Development*, *25*(2), 114–122. https://doi.org/10.1089/scd.2015.0193

Sonomoto, K., Yamaoka, K., Oshita, K., Fukuyo, S., Zhang, X., Nakano, K., Okada, Y., & Tanaka, Y. (2012). Interleukin-1β induces differentiation of human mesenchymal stem cells into osteoblasts via the Wnt-5a/receptor tyrosine kinase–like orphan receptor 2 pathway. *Arthritis & Rheumatism*, *64*(10), 3355–3363. https://doi.org/10.1002/art.34555

Sullivan, C. B., Porter, R. M., Evans, C. H., Ritter, T., Shaw, G., Barry, F., & Murphy, J. M. (2014). TNFα and IL-1β influence the differentiation and migration of murine MSCs independently of the NF-κB pathway. *Stem Cell Research & Therapy*, *5*(4), 104. https://doi.org/10.1186/scrt492

Syahrom, A., Januddi, M. A.-F. bin M. S., Harun, M. N., & Öchsner, A. (2017). *Cancellous Bone: Mechanical Characterization and Finite Element Simulation*. Springer.

Takayanagi, H., Ogasawara, K., Hida, S., Chiba, T., Murata, S., Sato, K., Takaoka, A., Yokochi, T., Oda, H., Tanaka, K., Nakamura, K., & Taniguchi, T. (2000). T-cell-mediated regulation of osteoclastogenesis by signalling cross-talk between RANKL and IFN-gamma. *Nature*, *408*(6812), 600–605. https://doi.org/10.1038/35046102

Tang, Y., Wu, X., Lei, W., Pang, L., Wan, C., Shi, Z., Zhao, L., Nagy, T. R., Peng, X., Hu, J., Feng, X., Van Hul, W., Wan, M., & Cao, X. (2009). TGF-β1–induced migration of bone mesenchymal stem cells couples bone resorption with formation. *Nature Medicine*, *15*(7), 757–765. https://doi.org/10.1038/nm.1979

Tsukasaki, M., & Takayanagi, H. (2019). Osteoimmunology: Evolving concepts in bone–immune interactions in health and disease. *Nature Reviews Immunology*, *19*(10), 626–642. https://doi.org/10.1038/s41577-019-0178-8

Turner, M. D., Nedjai, B., Hurst, T., & Pennington, D. J. (2014). Cytokines and chemokines: At the crossroads of cell signalling and inflammatory disease. *Biochimica et Biophysica Acta (BBA) - Molecular Cell Research*, *1843*(11), 2563–2582. https://doi.org/10.1016/j.bbamcr.2014.05.014

Udagawa, N., Takahashi, N., Katagiri, T., Tamura, T., Wada, S., Findlay, D. M., Martin, T. J., Hirota, H., Taga, T., Kishimoto, T., & Suda, T. (1995). Interleukin (IL)-6 induction of osteoclast differentiation depends on IL-6 receptors expressed on osteoblastic cells but not on osteoclast progenitors. *The Journal of Experimental Medicine*, *182*(5), 1461–1468. https://doi.org/10.1084/jem.182.5.1461

Unal, M., Creecy, A., & Nyman, J. S. (2018). The Role of Matrix Composition in the Mechanical Behavior of Bone. *Current Osteoporosis Reports*, *16*(3), 205–215. https://doi.org/10.1007/s11914-018-0433-0

van Bezooijen, R. L., Roelen, B. A. J., Visser, A., van der Wee-Pals, L., de Wilt, E., Karperien, M., Hamersma, H., Papapoulos, S. E., ten Dijke, P., & Löwik, C. W. G. M. (2004). Sclerostin Is an Osteocyte-expressed Negative Regulator of Bone Formation, But Not a Classical BMP Antagonist. *The Journal of Experimental Medicine*, *199*(6), 805–814. https://doi.org/10.1084/jem.20031454

Vidal, C., Bermeo, S., Li, W., Huang, D., Kremer, R., & Duque, G. (2012). Interferon Gamma Inhibits Adipogenesis In Vitro and Prevents Marrow Fat Infiltration in Oophorectomized Mice. *Stem Cells*, *30*(5), 1042–1048. https://doi.org/10.1002/stem.1063

Vlashi, R., Zhang, X., Wu, M., & Chen, G. (2023). Wnt signaling: Essential roles in osteoblast differentiation, bone metabolism and therapeutic implications for bone and skeletal disorders. *Genes & Diseases*, *10*(4), 1291–1317. https://doi.org/10.1016/j.gendis.2022.07.011

Wang, Q., Wang, W., Zhang, F., Deng, Y., & Long, Z. (2017). NEAT1/miR-181c Regulates Osteopontin (OPN)-Mediated Synoviocyte Proliferation in Osteoarthritis. *Journal of Cellular Biochemistry*, *118*(11), 3775–3784. https://doi.org/10.1002/jcb.26025

Wang, Z., Tan, J., Lei, L., Sun, W., Wu, Y., Ding, P., & Chen, L. (2018). The positive effects of secreting cytokines IL-17 and IFN-γ on the early-stage differentiation and negative effects on the calcification of primary osteoblasts in vitro. *International Immunopharmacology*, *57*, 1–10. https://doi.org/10.1016/j.intimp.2018.02.002

Wei, S., Kitaura, H., Zhou, P., Ross, F. P., & Teitelbaum, S. L. (2005). IL-1 mediates TNF-induced osteoclastogenesis. *Journal of Clinical Investigation*, *115*(2), 282–290. https://doi.org/10.1172/JCI200523394

Xian, L., Wu, X., Pang, L., Lou, M., Rosen, C. J., Qiu, T., Crane, J., Frassica, F., Zhang, L., Rodriguez, J. P., Jia, X., Yakar, S., Xuan, S., Efstratiadis, A., Wan, M., & Cao, X. (2012). Matrix IGF-1 maintains bone mass by activation of mTOR in mesenchymal stem cells. *Nature Medicine*, *18*(7), 1095–1101. https://doi.org/10.1038/nm.2793

Xiao, G., Jiang, D., Thomas, P., Benson, M. D., Guan, K., Karsenty, G., & Franceschi, R. T. (2000). MAPK Pathways Activate and Phosphorylate the Osteoblast-specific Transcription Factor, Cbfa1. *Journal of Biological Chemistry*, *275*(6), 4453–4459. https://doi.org/10.1074/jbc.275.6.4453

Xiao, G., Wang, D., Benson, M. D., Karsenty, G., & Franceschi, R. T. (1998). Role of the α2-Integrin in Osteoblast-specific Gene Expression and Activation of the Osf2 Transcription Factor *. *Journal of Biological Chemistry*, *273*(49), 32988–32994. https://doi.org/10.1074/jbc.273.49.32988

Xu, J., Yu, L., Liu, F., Wan, L., & Deng, Z. (2023). The effect of cytokines on osteoblasts and osteoclasts in bone remodeling in osteoporosis: A review. *Frontiers in Immunology*, *14*. https://doi.org/10.3389/fimmu.2023.1222129

Yang, A., Lu, Y., Xing, J., Li, Z., Yin, X., Dou, C., Dong, S., Luo, F., Xie, Z., Hou, T., & Xu, J. (2018). IL-8 Enhances Therapeutic Effects of BMSCs on Bone Regeneration via CXCR2-Mediated PI3k/Akt Signaling Pathway. *Cellular Physiology and Biochemistry: International Journal of Experimental Cellular Physiology, Biochemistry, and Pharmacology*, *48*(1), 361–370. https://doi.org/10.1159/000491742

Yasuda, H., Shima, N., Nakagawa, N., Yamaguchi, K., Kinosaki, M., Mochizuki, S., Tomoyasu, A., Yano, K., Goto, M., Murakami, A., Tsuda, E., Morinaga, T., Higashio, K., Udagawa, N., Takahashi, N., & Suda, T. (1998). Osteoclast differentiation factor is a ligand for osteoprotegerin/osteoclastogenesis-inhibitory factor and is identical to TRANCE/RANKL. *Proceedings of the National Academy of Sciences of the United States of America*, *95*(7), 3597–3602.

Yeung, D. K. W., Griffith, J. F., Antonio, G. E., Lee, F. K. H., Woo, J., & Leung, P. C. (2005). Osteoporosis is associated with increased marrow fat content and decreased marrow fat unsaturation: A proton MR spectroscopy study. *Journal of Magnetic Resonance Imaging*, *22*(2), 279–285. https://doi.org/10.1002/jmri.20367

Yoshitake, F., Itoh, S., Narita, H., Ishihara, K., & Ebisu, S. (2008). Interleukin-6 Directly Inhibits Osteoclast Differentiation by Suppressing Receptor Activator of NF-κB Signaling Pathways *. *Journal of Biological Chemistry*, *283*(17), 11535–11540. https://doi.org/10.1074/jbc.M607999200

Yu, Y., Zhang, G., Chen, Y., Bai, Q., Gao, C., Zeng, L., Li, Z., Cheng, Y., Chen, J., Sun, X., Guo, L., Xu, J., & Yan, Z. (2019). Selection of Reference Genes for qPCR Analyses of Gene Expression in Ramie Leaves and Roots across Eleven Abiotic/Biotic Treatments. *Scientific Reports*, *9*(1), 20004. https://doi.org/10.1038/s41598-019-56640-3

Zhang, C. (2010). Transcriptional regulation of bone formation by the osteoblast-specific transcription factor Osx. *Journal of Orthopaedic Surgery and Research*, *5*, 37. https://doi.org/10.1186/1749-799X-5-37

Zhang, J.-M., & An, J. (2007). Cytokines, Inflammation and Pain. *International anesthesiology clinics*, *45*(2), 27–37. https://doi.org/10.1097/AIA.0b013e318034194e

Zhang, Z.-M., Jiang, L.-S., Jiang, S.-D., & Dai, L.-Y. (2009). Osteogenic potential and responsiveness to leptin of mesenchymal stem cells between postmenopausal women with osteoarthritis and osteoporosis. *Journal of Orthopaedic Research*, *27*(8), 1067–1073. https://doi.org/10.1002/jor.20846

Zheng, S. X., Vrindts, Y., Lopez, M., De Groote, D., Zangerle, P. F., Collette, J., Franchimont, N., Geenen, V., Albert, A., & Reginster, J. Y. (1997). Increase in cytokine production (IL-1β, IL-6, TNF-α but not IFN-γ, GM-CSF or LIF) by stimulated whole blood cells in postmenopausal osteoporosis. *Maturitas*, *26*(1), 63–71. https://doi.org/10.1016/S0378-5122(96)01080-8

Zhu, S., Chen, W., Masson, A., & Li, Y.-P. (2024). Cell signaling and transcriptional regulation of osteoblast lineage commitment, differentiation, bone formation, and homeostasis. *Cell Discovery*, *10*(1), 1–39. https://doi.org/10.1038/s41421-024-00689-6

6. Scientific Contributions

Publication

1. Juliana Franziska Bousch, Christoph Beyersdorf, Katharina Schultz, Joachim Windolf, Christoph Viktor Suschek and Uwe Maus (**2024**): *Proinflammatory Cytokines Enhance the Mineralization, Proliferation, and Metabolic Activity of Primary Human Osteoblast-like Cells.* International Journal of Molecular Sciences, 25, 12358. https://doi.org/10.3390/ijms252212358

Poster

1. World Congress on Osteoporosis, Osteoarthritis and Musculoskeletal Diseases (WCO-IOF-ESCEO) (2023 – Barcelona, Spain): J.F.Bousch, C.Beyersdorf, K.Schultz, J.Windolf, C.V.Suschek, U.Maus: *Effect of proinflammatory cytokines on the mineralization of primary human osteoblasts in vitro.*
2. Kongress OSTEOLOGIE (2023 – Salzburg, Austria): J.F.Bousch, C.Beyersdorf, K.Schultz, J.Windolf, C.V.Suschek, U.Maus: *Einfluss der Zytokine IL-1β, IL-6 und TNF-α auf die osteogene Mineralisierung primärer Osteoblasten in vitro.*
3. Kongress OSTEOLOGIE (2023 – Salzburg, Austria): J.F.Bousch, C.Beyersdorf, K.Schultz, J.Windolf, C.V.Suschek, U.Maus: *Ein Vergleich der osteogenen Mineralisierung primärer osteoporotischer und nicht osteoporotischer Osteoblasten sowie BMSCs unter Einfluss von TNF-α, IL-8 und IFNγ in vitro.*
4. Kongress OSTEOLOGIE (2024 – Wiesbaden, Germany): J.F.Bousch, C.Beyersdorf, K.Schultz, M.Schnitker, J.Windolf, C.V.Suschek, U.Maus: *Die Rolle von IL-8 in der Osteogenese von primären humanen Osteoblasten in vitro.*
5. World Congress on Osteoporosis, Osteoarthritis and Musculoskeletal Diseases (WCO-IOF-ESCEO) (2024 – London, UK): J.F.Bousch, C.Beyersdorf, K.Schultz, J.Windolf, C.V.Suschek, U.Maus: *Characterization of the role of IL-6 and IL-8 in osteoblasts with normal or low bone density in vitro.*
6. Deutscher Kongress für Orthopädie und Unfallchirurgie (DKOU) (2024 – Berlin, Germany): J.F.Bousch, C.Beyersdorf, K.Schultz, J.Windolf, C.V.Suschek, U.Maus: *Einfluss proinflammatorischer Zytokine auf den Energiemetabolismus*

primärer humaner Osteoblasten während der Osteogenese in vitro. (awarded with a poster prize 2024)

7. Eidesstattliche Erklärung

Ich versichere an Eides Statt, dass die Dissertation von mir selbstständig und ohne unzulässige fremde Hilfe unter Beachtung der "Grundsätze zur Sicherung guter wissenschaftlicher Praxis an der Heinrich-Heine-Universität Düsseldorf" erstellt worden ist.

Juliana Franziska Bousch

Date _____ Signature _____